Isolation, Structure Elucidation and Biological Investigation of Active Compounds in *Cordia americana* and *Brugmansia suaveolens*

Dissertation

der Mathematisch-Naturwissenschaftlichen Fakultät
der Eberhard Karls Universität Tübingen
zur Erlangung des Grades eines
Doktors der Naturwissenschaften
(Dr. rer. nat.)

vorgelegt von
Fabiana Cristina Geller
aus Santa Cruz do Sul - Brasilien

Tübingen
2010

The research work described herein, was conducted under the supervision of Prof. Dr. Stefan Laufer in the Department of Pharmaceutical and Medicinal Chemistry, Institute of Pharmacy, University of Tübingen from 01.01.07 to 31.08.10.

Tag der mündlichen Qualifikation:	10. November 2010
Dekan:	Prof. Dr. Wolfgang Rosenstiel
1. Berichterstatter:	Prof. Dr. Stefan Laufer
2. Berichterstatter:	Prof. Dr. Irmgard Merfort (Albert-Ludwigs-Universität Freiburg)

“Jesus said to them, I am the bread of life; whoever comes to me shall not hunger, and whoever believes in me shall never thirst”. John 6:35

“O segredo não é correr atrás das borboletas, mas sim, cultivar o seu jardim para que elas venham até você.” (Mário Quintana)

Mama, Papa (in memoriam) and Djones for your love, patience and support at all times.

Acknowledgments

The following is my appreciation to those people that in the past and present gave me the spirit and encouragement to start, conduct and complete this thesis, as well to those people who made me feel at home in Germany. My thanks go to my family, colleagues, cooperation partners and friends who accompanied me during this work, in particular ...

- I am very grateful to my supervisor, **Prof. Dr. Stefan Laufer** for his comprehensive support in all phases of this work and for the excellent opportunity of being a PhD. student in his department during my doctoral studies, in the last three years. For his insights and efforts to construct this bridge between South Brazil, Freiburg and Tübingen. Also for the financial support allowing me the participation in conferences and academic activities in Europe and in Brazil. His attention and motivation contributed to my personal and professional improvement. "Prof. Laufer, vielen herzlichen Dank!".

- I am specially thankful to **Prof. Dr. Irmgard Merfort**, Freiburg, and her group. Thanks for your dedication concerning the cooperation project Brazil-Germany and for the generous support allowing the execution of phytochemical and biological analysis in your department. Also for your valuable advices and improvements concerning my work and for teaching me a lot of things about Pharmacognosy.

- the members of my defense committee **Prof. Dr. Rolf Daniels** and **Prof. Dr. Peter Ruth**, for their time to go through my dissertation and taking part of my final exam.

- "muchas gracias tambien al profesor del Costa Rica", **Prof. Dr. Renato Murillo**, for introducing me the complicated NMR topic in a very patient and uncomplicated form. Your suggestions and discussion regarding the elucidation of the flavonol glycosides were indispensable.

- "um grande muito obrigado" to **Prof. Dr. Berta Heinzmann**, from Santa Maria, Brazil. Thank you for introducing me to the plant world and for the profitable afternoons during the collection of plants. I will always remember the nice time with you and your group.

- **Prof. Dr. Érico Flores**, who always supported our cooperation project, specially during the extraction of the plant material at the Department of Chemistry, at the Federal University of Santa Maria, Brazil.

- **Prof. Dr. Oliver Werz** and his group, for the good living, the gatherings and the use of his laboratories and equipment. Specially, I would like to thank **Bianca Jazzar** and **Daniela Müller** for providing me technical assistance in the 5-lipoxygenase assays.

- "ein grosses Dankeschön" to **Prof. Dr. Wolf Engels** (Brasilien-Zentrum), who along with Prof. Dr. Stefan Laufer made efforts to acquire financial support from the Ministry of Science, Research and the Arts of Baden-Württemberg for the project involving Brazil and Germany.

- "ein grosses Dankeschön" to **Dr. Rainer Radtke** for the great time that we spent together in Tübingen. Thanks for reading my dissertation and for your suggestions and improvements.

- the botanists **Dr. Solon Longhi** and **Dr. Gilberto Zanetti** for the collection of the plants *Cordia americana* and *Brugmansia suaveolens*.

- **Márcio Fronza** and **Cléber Schmidt** from the Department of Pharmaceutical Biology and Biotechnology, University of Freiburg, for carrying out the scratch and NF-κB assays. **Catiguria**, many thanks for the nice chats from time to time about research and also other things. Thanks for reading my dissertation and for your suggestions. I am sure that we became good friends. I appreciated that I had the chance to meet you here in Germany!

- "ein super Dankeschön für" **Stef** , for your very sweet Swabian sentence "Fabi, es wird scho". **Stef** , many thanks for reading my dissertation, for your suggestions involving NMR spectra, as well as for the chocolates and "Gummibärchen" time! I hope that you will come to visit me in Brazil.

- "ein grosses Dankeschön" to **Lisa Steinhauser** for supporting me with the NMR spectra and also for organizing the NMR measurements.

- **Sabine** for enjoying with me the rare sunshine time during the breaks at the university. **Joe** and **Mohamed** thanks for the patience during the first steps with the flash chromatography. **Maissa** thanks for your big smile. Thanks also for the nice time in the lab and also for the friendship.

- **Claudi** and **Frank** for their time to perform the LC-MS measurements and for the nice chat during the "Mittagspause" in the "Mensa".

- **Verena Schattel** for conducting the molecular modeling studies and for providing the docking pictures.

- **Márcia Goettert** and **Katharina Bauer** for carrying out the biological assays on p38α, JNK3 and TNFα.

- our secretary **Karin Ward** for all solutions concerning the bureaucratic problems.

- all my **colleagues** and the **employees** from our department who contributed to the realization of my dissertation.

- "meu amor e meu alemão preferido" **Djones**; how can I thank you? You are the best thing, the best person that Tübingen brought me! Thanks for your love, patience, encouragement and support.

- my lovely, wonderful and big **Geller family**, specially meine **Mutti**, for her love, for the unconditionally support, even many times feeling the distance ... a thousand thanks for everything!

- my **parents-in-law** for holding me up in many moments.

- my family and friends in Germany: **Walter** for the very nice time in München and in the"Bayerische Wald", **Pedro**, **Sandra** and **Jorge**, **Birkner s** thanks for the nice celebrations together. Also for the forever Brazilian friends that Tübingen brought me: **Melissa**, **Lissi**, **Ana Carolina**, **Karina**, for sure we will see us in Brazil and will miss the nice time in Tübingen.

- my friends in Brazil, **Julie**, **Ana Paula** e **Andressa**. The friendship that keeps us together is one of the greatest thing that ever happened to me.

- the **Eberhard Karls University of Tübingen** and the **Pharmacy Institute** in Tübingen for supporting the necessary conditions for the development of this research work and also for the opportunity to attend German courses in order to improve my language skills.

- the **Goverment of Baden-Württemberg** (Zukunftsoffensive IV "Innovation und Exzellenz", Förderung von internationalen Kooperationen zwischen den Hochschulen) for the financial support that was indispensable for the development of this work.

Fabiana Cristina Geller

Abstract

In Brazil, medicinal plants have been widely used for the treatment of diseases in folk medicine. However, the effective compounds responsible for the biological effects are often unknown. Extracts prepared from traditional medicinal plants from South Brazil were screened for their anti-inflammatory and wound healing activities. The Boraginaceae *Cordia americana*, locally known as "Guajuvira", and the Solanaceae *Brugmansia suaveolens*, generically recognized as "Trombeteira", presented interesting activity in the biological screening. Thus, the objective of this dissertation was the investigation of the ethanolic extracts prepared from the leaves of both plants and the characterization of potential effective compounds, focusing on: firstly, the isolation of the plant constituents using chromatographic methods; secondly, structural elucidation by means of spectroscopy experiments; and finally, biological investigation of the plant extracts and their respective compounds targeting different aspects of inflammation and wound healing processes.

From the ethanolic extract of *Cordia americana*, flavonols (rutin and quercitrin), phenolic compounds (rosmarinic acid, rosmarinic acid ethyl ester and 3-(3,4-dihydroxyphenyl)-2-hydroxypropanoic acid), phytosterols (campesterol and β-sistosterol) and triterpenoids (α- and β-amyrin) were characterized. Quantification analysis of the plant extract showed rosmarinic acid as the major constituent with an amount of 8.44%. The ethanolic extract exhibited higher inhibition (i.e., pro-inflammatory mediators p38α and JNK3, TNFα and 5-LO as well as on scratch assay) in comparison with the predominant and other isolated compounds, however, evidences were provided for a crucial role of rosmarinic acid as the major key player.

Regarding the ethanolic extract of *Brugmansia suaveolens*, four new flavonol glycosides kaempferol 3-O-β-D-glucopyranosyl-(1$'''\rightarrow$2$''$)-O-α-L-arabinopyranoside-7-O-β-D-glucopyranoside, kaempferol 3-O-β-D-[6$'''$-O-(3,4-dihydroxy-cinnamoyl)]-glucopyranosyl-(1$'''\rightarrow$2$''$)-O-α-L-arabinopyranoside-7-O-β-D-glucopyranoside, kaempferol 3-O-β-D-[2$'''$-O-(3,4-dihydroxy-cinnamoyl)]-glucopyranosyl-(1$'''\rightarrow$2$''$)-O-α-L-arabinopyranoside-7-O-β-D-glucopyranoside, and kaempferol 3-O-β-D-glucopyranosyl-(1$'''\rightarrow$ 2$''$)-O-α-L-arabinopyranoside were isolated. Concerning the biological effects of the ethanolic extract, the kaempferol aglycone as well as further non-isolated secondary metabolites might contribute to the plant activity.

In summary, this dissertation increases the phytochemical and pharmacological knowledge about *Cordia americana* and *Brugmansia suaveolens*, which support their use in traditional medicine.

Zusammenfassung

In Brasilien werden in der Volksmedizin Heilpflanzen häufig für die Behandlung von Krankheiten verwendet. Die wirksamen Verbindungen, verantwortlich für die biologischen Wirkungen, sind aber in der Regel unbekannt. Extrakte aus traditionellen Heilpflanzen aus Süd-Brasilien wurden auf ihre entzündungshemmenden und wundheilenden Eigenschaften untersucht. Die Boraginaceae *Cordia americana*, lokal bekannt als "Guajuvira", und die Solanaceae *Brugmansia suaveolens*, allgemein bekannt als "Trombeteira", präsentierten interessante biologische Aktivitäten in den ersten Screening-Versuchen. So war das Ziel dieser Dissertation die Untersuchung der ethanolischen Extrakte aus den Blättern der beiden Pflanzen und die Charakterisierung von potentiell wirksamen Verbindungen. Hierbei erfolgte die Isolierung der pflanzlichen Inhaltstoffe mit chromatographischen Methoden, die Strukturaufklärung mittels NMR- und MS-Spektroskopie, und die biologische Untersuchung der Pflanzenextrakte und ihrer jeweiligen Inhaltstoffe in Testsystemen, die die Untersuchung verschiedener Aspekte der Entzündung und Wundheilung möglich machen.

Von dem ethanolischen Extrakt von *Cordia americana* wurden die Flavonoide (Rutin und Quercitrin), Phenolische Verbindungen (Rosmarinsäure, Rosmarinsäure Ethylester und 3-(3,4 dihydroxyphenyl)-2-Hydroxypropansäure), Phytosterine (Campesterin und β-Sitosterol) und Triterpenoide (α-und β-Amyrin) charakterisiert. Die Quantifizierung des pflanzlichen Extrakts zeigte Rosmarinsäure als Hauptbestandteil mit einer Konzentration von 8,44%. Der ethanolische Extrakt zeigte eine nennenswerte Hemmung von proinflammatorischen Mediatoren wie p38α, JNK3, TNFα und 5-LO sowie im Scratch assay (als Modelle für Wundheilung), im Vergleich zu den Hauptbestandteilen und anderen isolierten Verbindungen. Rosmarinsäure kommt eine Schlüsselrolle für diese Wirkung zu.

Hinsichtlich des ethanolischen Extrakts von *Brugmansia suaveolens*, konnten vier neue Flavonolglykoside isolierter werden: Kaempferol 3-O-β-D-glucopyranosyl-(1$'''\rightarrow$2$''$)-O-α-L-arabinopyranoside-7-O-β-D-glucopyranoside, Kaempferol 3-O-β-D-[6$'''$-O-(3,4-dihydroxy-cinnamoyl)]-glucopyranosyl-(1$'''\rightarrow$2$''$)-O-α-L-arabinopyranoside-7-O-β-D-glucopyranoside, Kaempferol 3-O-β-D-[2$'''$-O-(3,4-dihydroxy-cinnamoyl)]-glucopyranosyl-(1$'''\rightarrow$2$''$)-O-α-L-arabinopyranoside-7-O-β-D-glucopyranoside, and Kaempferol 3-O-β-D-glucopyranosyl-(1$'''\rightarrow$2$''$)-O-α-L-arabinopyranoside. Bezüglich der biologischen Effekte des ethanolischen Extrakts könnten das Kaempferol Aglykon sowie weitere nicht isolierte Sekundärmetaboliten zur Aktivität des Extrakts beitragen.

Damit trägt dieser Dissertation zur Ausweitung der phytochemischen und pharmakologischen Kenntnisse über *Cordia americana* und *Brugmansia suaveolens*.

List of Publications and Presentations

Full Papers

- Geller F., Schmidt C., Goettert M., Fronza M., Schattel V., Heinzmann B., Werz O., Flores E.M.M., Merfort I., Laufer S. Identification of rosmarinic acid as the major active constituent in *Cordia americana*. Journal of Ethnopharmacology, 128, 561-566, 2010.

- Geller F., Murillo R., Steinhauser L., Heinzmann B., Flores E., Albert K., Merfort I., Laufer S. Flavonol glycosides from the leaves of *Brugmansia suaveolens*. In preparation.

- Schmidt C., Fronza M., Goettert M., Geller F., Luik S., Flores E.M.M., Bittencourt C.F., Zanetti G.D., Heinzmann B.M., Laufer S., Merfort I. Biological studies on Brazilian plants used in wound healing. Journal of Ethnopharmacology, 122, 523-532, 2009.

Oral Presentations

- Geller, F., Schmidt, C., Goettert, M., Fronza, M., Heinzmann, B., Werz, O., Merfort, I., Laufer, S. Rosmarinic acid as the effective compound in *Cordia americana*. Deutsch-Brasilianisches Jahr 2010/11, Drugs from Natural Sources: The Potential of Brazilian Plants used in Traditional Medicine, São Paulo, Brazil, 22.09.2010.

- Geller F., Heinzmann B., Goettert M., Werz O., Merfort I., Laufer S. Isolation and identification of natural compounds with anti-inflammatory activity from *Cordia americana*. IV Simpósio Brasil Alemanha: Desenvolvimento Sustentável, Curitiba, Brazil, 05-07.10.2009.

Presentations

- Geller F., Schmidt C., Goettert M., Fronza M., Heinzmann B., Werz O., Merfort I., Laufer S. Rosmarinic acid as the effective compound in *Cordia americana*. 58^{th} International Congress and Annual Meeting of the Society for Medicinal Plant and Natural Product Research, Berlin, 29.08-02.09.2010.

- Geller F., Goettert M., Fronza M., Schmidt C., Schattel V., Heinzmann B., Flores E., Merfort I., Laufer S. Phytochemical and biological investigation on the ethanolic extract of *Cordia americana*. 6^{th} Status Seminar Chemical Biology, Frankfurt, 30.11-1.12.2009.

- Geller F., Heinzmann B., Schattel V., Goettert M., Werz O., Merfort I., Laufer S.. Identification of the main effective compound in the ethanolic extract from *Cordia americana*. IV Deutsch-Brasilianisches Symposium, Curitiba - Paraná, Brasilien, 05-10.10.2009

- Geller F., Heinzmann B., Goettert M., Schattel V., Werz O., E. Flores, Merfort I., Laufer S. Phytochemical and anti-inflammatory investigation on the ethanolic extract of *Cordia americana*. Jahrestagung der Deutschen Pharmazeutischen Gesellschaft, Jena, 28.09-1.10.2009.

- Fronza M., Heinzmann B., Geller F., Laufer S., Merfort I. An improved scratch assay for studying the wound healing effects of medicinal plants. IV Simpósio Brasil Alemanha: Desenvolvimento Sustentável, Curitiba, Brazil, 05-07.10.2009.

- Goettert M., Luik S., Fronza M., Schmdit C., Geller F., Heinzmann B., Merfort I., Laufer S. Structural features and biological evaluation of flavonoids as p38α MAPK inhibitors. IV Simpósio Brasil Alemanha: Desenvolvimento Sustentável, Curitiba, Brazil, 05-07.10.2009.

- Goettert M., Luik S., Fronza M., Schmidt C., Geller F., Heinzmann B., Merfort I., Laufer S. Effect of natural phenolic compounds on p38α MAPK activity IV Deutsch-Brasilianisches Symposium, Curitiba - Paraná, Brasilien, 05-10.10.2009.

- Goettert M., Luik S., Fronza M., Schmidt C., Geller F., Merfort I., Laufer S. Natural phenolic compounds as inhibitors of p38α MAPK. Drug Discovery and Delivery Membrane Proteins and Natural Product Research, Freiburg, 16-17.04.2009.

- Goettert M., Luik S., Fronza M., Geller F., Schmidt C., Merfort I. , Laufer S. Biological testing of bioactive compounds that inhibit p38α MAPK. 5^{th} Status Seminar Chemical Biology, ChemBioNnet, Frankfurt, 08.12.2008.

- Fronza M., Geller F., Bittencourt C., Flores E., Heinzmann B., Laufer S., Merfort I. The scratch assay: A suitable in vitro tool for studying wound healing effects. 7^{th} Joint Meeting of AFERP, ASP, GA, PSE, SIF, Athens, Greece, August 2008.

- Geller F., Goettert M., Heinzmann B., Laufer S. Identification, structural elucidation and biological testing of active principles of Brazilian medicinal plants. Naturräume Brasiliens: Im Spannungsfeld zwischen biologischer Vielfalt und industrieller Entwicklung. Austellung Universitätsbibliothek Tübingen, 05.6.2008.

- Merfort I., Heinzmann B., Flores E., Bittencourt C., Schmidt C., Geller F., Goettert M., Laufer S. Biological active compounds from Brazilian traditional medicinal plants. III Deutsch-Brasilianisches Symposium, Freiburg, 23-27.07.2007.

Contents

List of Figures

List of Tables

List of Abbreviations

μ	micro
4-NPP	4-nitrophenylphosphate
5-LO	5-Lipoxygenase
E. coli	*Escherichia coli*
AA	Arachidonic Acid
ACN	Acetonitrile
ADAM	A Disintegrin and Metalloprotease
Asp	Asparagine
ATF-2	Activation Transcription Factor-2
ATP	Adenosine-5 -triphosphate
AU	Adenosine/Uridine
B.C.	Before Christ
BAFF	B-cell Activating Factor
br	broad
BSA	Bovine Serum Albumin
CC	Column Chromatography
CDK	Cyclin Dependent Kinase
cm	centimeter
COSY	Correlation Spectroscopy
COX	Cyclooxygenase
COX-2	Cyclooxygenase-2
d	doublet

Da	Dalton
DAD	Diode Array Detector
DAPI	4 ,6-diamino-2-phenylindole
DEPT	Distortionless Enhancement by Polarization Transfer
DMEM	Dulbecco s modified Eagle s medium
DMSO	Dimethylsulfoxide
DMSO-d_6	Deuterated Dimethylsulfoxide
DNA	Deoxyribonucleic Acid
ECM	Extracellular Matrix
EET	Epoxyeicosatrienoic
EGF	Epidermal Growth Factor
EI-MS	Electron Ionization Mass Spectrometry
ELISA	Enzyme-Linked Immunosorbent Assay
EMSA	Electrophoretic Mobility Shift Assay
ERK	Extracellular Signal Regulated Protein Kinase
ESI-MS	Electrospray Ionisation Mass Spectrometry
EtOH	Ethanol
FA	Formic Acid
FBS	Fetal Bovine Serum
FGF	Fibroblast Growth Factor
FT-ICR-MS	Fourier-Transform-Ion Cyclotron Resonance-Mass Spectrometry
FT-IR	Fourier Transform-Infrared Spectroscopy
g	gram
GC-MS	Gas Chromatography Mass Spectrometry
Gln	Glutamine
Glu	Glutamate

Glu	Glutamic Acid
Gly	Glycine
h	Hour
H_2O	Water
HETE	Hydroxy-Eicosatetraenoic Acid
His	Histidine
HIV	Human Immunodeficiency Virus
HMBC	Heteronuclear Multiple Bond Coherence
HPETE	Hydroperoxyeicosatetraenoic Acid
HPLC	High Pressure Liquid Chromatography
HSQC	Heteronuclear Single Quantum Coherence
Hz	Hertz
I/R	Ischemia/Reperfusion
IC_{50}	Half Maximal Inhibitory Concentration
IFN	Interferon
IKK	IκB Kinase
IL	Interleukin
iNOS	Inducible Nitric Oxide Synthase
IUPAC	International Union of Pure and Applied Chemistry
J	J-coupling
JNK	c-Jun-N-terminal Protein Kinase
K	Kilo
KB	Kinase Buffer
L	Liter
LC	Liquid Chromatography
Leu	Leucine

LO	Lipoxygenase
LPS	Lipopolysaccharide
LT	Leukotriene
Lys	Lysine
M	Mega
m	meter, mili or multiplet
m/z	mass-to-charge ratio
MAPK	Mitogen Activated Protein Kinase
MAPKAPK2	MAP Kinase Activated Protein Kinase 2
MAPKK	MAP2K, MEK, MKK, MAP Kinase Kinase
MAPKKK	MAP3K, MEKK, MKKK, MAP Kinase Kinase Kinase
MAPKKKK	MAP4K, MKKKK, MAPKKK Kinase
MEF 2C	Myocyte Enhancer Factor 2C
MEK	Message Encryption Key or MAP/ERK Kinase
MeOH	Methanol
MeOH-d_4	Deuterated Methanol
Met	Methionine
min	minutes
mm	millimeter
mRNA	Messenger RNA
MS	Mass Spectrometry
MSK	Mitogen- and Stress-activated Protein Kinase
MTT	3-(4,5-Dimethylthiazol-2-yl)-2,5-diphenyltetrazolium bromide
Mult.	Multiplet
NEMO	NF-κB-Essential Modulator
NF-κB	Nuclear Factor-κB

NIK	NF-κB Inducing Kinase
NLS	Nuclear Localization Sequence
nm	nanometer
NMR	Nuclear Magnetic Resonance
NSB	Non Specific Binding
OC	Open Column Chromatography
PDB	Protein Data Bank
PDGF	Platelet-Derived Growth Factor
PG	Protaglandin
Phe	Phenylalanine
PKC	Protein Kinase C
PMNL	Polymorphonuclear Leukocytes
ppm	parts per million
Pro	Proline
Pyridine-d_5	Deuterated Pyridine
q	quartet
R_f	Retention Factor
RA	Rheumatoid Arthritis
RHD	Rel-Homology Domain
RNA	Ribonucleic Acid
RP	Reverse Phase
RT	Room Temperature
s	singlet
SAPK	Stress-Activated Protein Kinase
SAR	Structure Activity Relationship
SEM	Standard Error of the Mean

Ser	Serine
T	Transmittance
t	triplet
t_R	Retention time
TACE	TNFα Converting Enzyme
TBS	Tris Buffered Saline
TGY	Thr-Gly-Tyr
Thr	Threonine
TLC	Thin Layer Chromatography
TMB	3,3 ,5,5 -tetramethylbenzidine
TNF	Tumor Necrosis Factor
TNFα	Tumor Necrosis Factor α
TX	Tromboxano
Tyr	Threonine
UV	Ultraviolet
UV/VIS	Ultraviolet-Visible Spectrophotometry
v:v	volume to volume
WHO	World Health Organization

1 Introduction

This chapter outlines, firstly, the importance of the ethnopharmacological research. Secondly, it briefly introduces the Brazil-Germany cooperation project and the selected plants that were investigated, namely, *Cordia americana* and *Brugmansia suaveolens*. Finally, the objectives of this study and the scientific contributions are presented.

1.1 The Importance of Medicinal Plants in Drug Discovery

Medicinal herbs were used to treat wounds and inflammations during the history of many civilizations. In Egypt (1,500 years B.C.), the papyrus "Ebers" related 800 remedies based on 150 plants. In India (600 years B.C.), the text "Susruta-samhita" described 700 medicinal plants. Dioscorides in Greece (1^{st} Century) wrote the "Materia Medica", which is considered as a precursor to all modern pharmacopeias and it gave the knowledge about herbs and remedies used by the Greeks, Romans, and other cultures in the antiquity [198]. Between 18^{th} and 20^{th} centuries, the formation of the modern pharmaceutical industry was stimulated by essential natural drugs, such as digoxin from *Digitalis purpurea* (1785), morphine from *Papaver somniferum* (1806), aspirin from salicylic acid in *Salix* species (1897) and penicillin from *Penicillium chrysogenum* (1928) [260].

Nowadays, the herbal medicines are still widely used in conventional as well as alternative medical practices in developed and developing countries as a complementary medicine [37]. However,

the irrational use of therapies, such as inaccurate dosage, lack of proof of safety and efficacy, and interaction risk with other drugs, may lead to health hazards [166]. Additionally, the search for new or alternative agents is an important factor to replace drugs with side effects [208], for example, such as pancreatitis and peptic ulcer due to high-dose or prolonged *Glucocorticoide* therapy [257]. Therefore, the systematic investigation of medicinal plants plays a key role in the understanding of its active principles and mode of action.

Still today, natural products including those from plants play an important role in the therapy of diseases. "*A study of the 25 best-selling pharmaceutical drugs in 1997 found that 11 of them (42%) were biologicals, natural products or entities derived from natural products, with a total value of US$ 17.5 billion*" [232]. So far, about 25% of all drugs prescribed worldwide originate from plants. Moreover, from 252 drugs considered as basic and essential by the World Health Organization (WHO), 11% are exclusively from plants and there is a significant number of drugs that were obtained by molecular modification of natural products [256].

Brazil is considered to belong to the leading country in biodiversity, with 15 to 20% of the total number of species on the planet. The country has the most diverse flora in the world, resulting in more than 55 thousand described species [307]. Due to this large species diversity, there is a higher chance to identify new substances with pharmacological potentials and to discover new biological targets. The "Farmacopia Brasileira" [14] contains 42 medicinal plants which have been extensively described, and since 2005, it is recognized by the European Union [13].

Since the ancient civilizations of Brazil, medicinal plants have been used in folk medicine, however, the compounds responsible for the biological effect are often unknown. For a safe use, it is necessary to increase the knowledge on their effects and side effects by intensive phytochemical and pharmacological studies [177, 209]. Therefore, a cooperation project between Brazil-Germany was undertaken in order to investigate medicinal plants that have been used in South Brazil as traditional medicine. The objective of this project and the investigated plants are presented in the next section.

1.2 Project Overview

A cooperation network between the institutes Federal University of Santa Maria in South Brazil, Albert-Ludwigs University of Freiburg as well as Eberhard-Karls University of Tübingen was undertaken in order to increase the knowledge on Brazilian medicinal plants. The project has started in January 2007 and was financially supported by the government of Baden-Württemberg [177, 209].

The Brazilian plants studied in this project focused on their anti-inflammatory, antitumoral, antimicrobial and wound healing effects.

1.2.1 Screening

The plants used in the screening phase[1] (see Table 1.1) were collected in autumn-winter season (between March and July) in the region of Santa Maria, South Brazil. Both hexanic and ethanolic extracts were prepared by means of soxhlet and ultrasonic extraction resulting in four different extracts for each plant (see Section 5.5, Experimental Part).

As aforementioned, the screening of the plant extracts were based on bioassays targeting anti-inflammatory, cytotoxic, antimicrobial and wound healing activity in order to identify the most interesting extracts. Ethanolic extracts from *Cordia americana* and *Brugmansia suaveolens* were selected for further investigation in the Eberhard-Karls University of Tübingen, since both hydrophilic extracts exhibited significantly inhibition effects on p38α MAPK (Mitogen-activated Protein Kinase), TNFα release (Tumor Necrosis Factor α) and NF-κB assays (Nuclear Factor-κB), and on fibroblast scratch assay [277, 113]. The selected plants are introduced in the following sections.

[1] Leaves, aerial parts and flowers from the plants were collected and extracted by the doctoral candidate Fabiana Geller with support of Dr. Klaus Gasser and Cleber Schmidt under coordination of Prof. Dr. Berta Heinzmann. The plants were authenticated by the botanist Dr. Gilberto Zanetti.

Table 1.1: Plants selected for the biological screening phase

Species	Popular name	Part used
Sida rhombifolia	Guanchuma	Roots
Cecropia catarinensis	Embaúba	Leaves
Echinodorus grandi orus	Chapéu-de-couro	Leaves
Cordia americana	Guajuvira	Leaves
Erythroxylum argentinum	Cocção	Leaves
Myrocarpus frondosus	Cabreúva	Bark
Bauhinia for cata	Pata-de-vaca	Leaves
Caesalpina ferrea	Pau-ferro	Bark
Peltodon longipes	Baicurú-amarelo	Roots
Luhea divaricata	Acoita-cavalo	Leaves
Parapiptadenia rigida	Angico-vermelho	Bark
Petiveria alliaceae	Guiné	Leaves
Brugmansia suaveolens	Trombeteira	Leaves
Schinus mole	Aroeira-mansa	Leaves
Gochnatia polymorpha	Cambará-do-mato	Leaves and bark
Adiantopsis chlorophylla	Samambaia-do-talo-roxo	Leaves
Dodonae viscosa	Vassoura-vermelha	Leaves
Stachytarpheta cayennensis	Gervão	Leaves
Vermonia tweediana Baker	Assa-peixe	Leaves
Mirabilis jalapa	Maravilha	Leaves and flower
Xanthium cavallinesii	Carrapicho	Leaves
Piper gaudichaudianum	Pariparobão	Roots
Pluchea sagitalis	Erva-lucera	Leaves
Alternanthera coidea	Rabo-de-gato	Aerial parts
Phrygillanthus acutifolius	Erva-de-passarinho	Leaves
Leonorus sibiricus	Erva-de-macae	Aerial parts
Leonotis nepetafolia	Cordao-de-frade	Flower
Irisinea herbstii	Irisinea/Mussurú	Aerial parts
Eupatorium laevigatum	Erva-de-santana	Leaves
Coleus barbatus	Boldo africano	Leaves
Eubrachyon ambiguum	Erva-de-passarinho	Aerial parts
Waltheria douradinha	Douradinha	Total plant with flowers
Kalanchöe tubi ora	Bálsamo-brasileiro	Leaves
Jaranda micrantha	Caroba	Bark
Galinsoga parvi ora	Picao-branco	Aerial parts
Hedychium coronarium	Falso-gengibre	Root hairs
Piper regnelli	Paribaroba	Leaves
Dichorisandra thyrssi ora	Cana-de-macaco	Aerial parts

1.2.2 *Cordia americana*

Cordia americana (Linaeus) Gottschling & J.S.Mill. (syn. *Patagonula americana*) belongs to the Boraginaceae family, subfamily Cordioideae.

The Boraginaceae family consists of about 2,700 species which are distributed in tropical, subtropical and warmer regions around the world [117]. It is composed of about 130 genera and six subfamilies: Boraginoideae, Cordioideae, Ehretioideae, Heliotropioideae, Hydrophylloideae, and Lennooideae. Some well-known species that can be found in the Boraginaceae family and used as medicinal plants are: *Symphytum of cinale* (Comfrey), *Borago of cinalis* (Borage) and *Echium amoenum* (Echium).

The subfamily Cordioideae contains the genus *Cordia*, which is comprised of evergreen trees and shrubs [308]. About 300 species of *Cordia* have been identified worldwide. In Brazil, the genus *Cordia* is represented by approximately 65 species [306]. In this genus, some well-known species are: *Cordia dichotona*, *Cordia myxa*, *Cordia obliqua*, *Cordia verbenacea*, *Cordia martinicensis*, *Cordia salicifolia*, *Cordia spinescens*, *Cordia latifolia* and *Cordia ulmifolia*, which have been used as cicatrizant, astringent, anti-inflammatory, antihelmintic, antimalarial remedy, and in the treatment of urinary infections and lung diseases [308]. For example, studies with *Cordia verbenacea* revealed that α-humulen was the main compound responsible for the anti-inflammatory properties of this plant [36]. Thus, the product *Ache an*, manufactured by Brazilian Aché Laboratories, was developed based on the extract of *Cordia verbenacea* and it is used in the treatment of chronic tendinitis and muscle pains.

Since 2003, *Cordia americana*, which was previously classified as *Patagonula americana*, was included in the Cordioideae subfamily due to its molecular and morphology characteristics [117].

1.2.2.1 Localization

The subfamily Cordioideae is distributed worldwide mainly in warmer regions. The majority of the species grow in the American continent (i.e., more than 250 species) and the remaining species are distributed in Africa, Asian and Oceania continents (i.e., more than 50 species) [117].

Cordia americana is commonly located in South Brazil, but can be found also in Argentina, Uruguay, Paraguay and Bolivia (see Figure 1.1). In Brazil, usually it is located in regions with 20 up to 900 m of altitude. In Bolivia, it can be found up to 1,200 m of altitude [74]. Concerning its etymology, *Cordia americana* (i.e., *Patagonula americana*) comes originally from "Patagonia", Southern and semi-arid regions of Argentina [74]. This tree has different local names like "guajuvira" in South Brazil, "guajayvi" in Paraguay, "guayaibi" in Argentina, and "guayubira" in Uruguay.

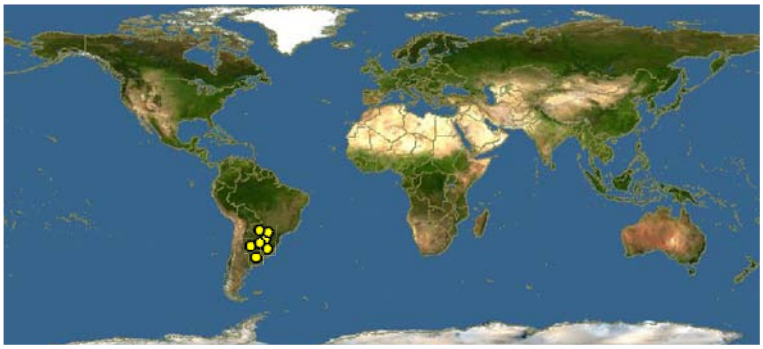

Figure 1.1: Distribution of *Cordia americana* [241]

1.2.2.2 Botany

Cordia americana is described by the following botanical features [194, 74, 117]:

- Regarding its **morphologic characteristics**, *Cordia americana* is a semicaducifolia[2] tree, with 10 to 15 m height and with 20 to 40 cm diameter at breast height[3] (see Figure 1.2). In adulthood, it can reach up to 30 m height and 100 cm diameter at breast height.

[2]Semicaducifolia means that part of the tree leaves falls in winter.
[3]Diameter at breast height is a standard method of expressing the diameter of a tree trunk.

- The **leaves** (see Figure 1.3) of *Cordia americana* are simple, alternate, elongated elliptical shape, with the edges in half gently to the apex and grouped together on the branches, with 3 up to 10 cm length and with 1 up to 3 cm wide.

Figure 1.2: Tree of *Cordia americana*

Figure 1.3: Leaf of *Cordia americana*

- The **owers** (see Figure 1.4) are fragrant, white or beige, with 5 mm in length, grouped in terminal panicles. Its flowering period is from September to November, during the development of new leaves.

- The **fruit** is drupe[4] subglobose (i.e., prolate spheroidal), with acute apex formed by the persistent cup base, with 4 up to 6 mm length. The base is persistent and similar to a propeller with petals, which facilitates to be spread by the wind, as seen in Figure 1.5. Its maturation period is from November until December.

- The **seed** is spherical with up to 3 mm in diameter and 5 mm in length, dark-brown and with an extension pointed at the apex. Its germination occurs in 15-20 days and is generally abundant. It prefers deep soils and moist, but not waterlogged, as typically found in the valleys. Its occurrence is rare in the steep slopes or in arid areas.

[4]Drupe is a fruit in which an outer fleshy part surrounds a shell of hardened endocarp with a seed inside.

Figure 1.4: Flower of *Cordia americana*

Figure 1.5: Fruit of *Cordia americana* [117]

- The **trunk** is rarely cylindrical, often tortuous and irregular. Its bole is usually short and irregular when the species grows alone, but in the forest, it reaches up to 10 m length. Usually, it presents branches sprouting from the trunk.

- The **shell** has a thickness of up to 8 mm. The outer shell is generally grizzly, rarely dark, slightly cracks in the longitudinal direction, forming rectangular plaques. The inner bark is white to yellowish and with fibrous striations.

- The **branch** is typically raceme (i.e., unbranched and indeterminated). Its top is crown narrow, elongated, ascending and densely branched.

1.2.2.3 Economical Importance and Traditional Medicine

The wood of *Cordia americana* has economical value due to its elasticity, flexibility and durability. Because of its flexible heartwood, it is widely applied to handwork, as for example by the *Caingangue* Indians in the manufacture of bows for hunting. The heartwood has normally a dark color. For this reason, the name given by German immigrants in South Brazil was "*schwarz-herz*" (i.e., black heartwood) [164]. Nowadays, the wood is still utilized in building construction, manufacture of doors, windows, and luxe furniture [74]. Furthermore, this tree is applied in landscaping and it is appropriated for heterogeneous reforestation of degraded areas.

In folks medicine, a decoction prepared from its leaves is used in order to wash wounds and to treat inflammatory diseases [297, 164]. The cataplasm from the leaves is also externally applied on wounds [294, 59, 164]. Additionally, this plant is known for the treatment of ulcers, because of its suggested astringent and mucilaginous properties [207].

1.2.2.4 Chemical Constituents

The genus *Cordia* has been demonstrated to be a potential producer of diverse secondary metabolites including flavonoids, phenolic acids, triterpenes, sesquiterpenes, saponins, hydroquinones, chromenes, terpenoid naphthoquinones and benzoquinones. Table 1.2 presents the state-of-the-art concerning the studied secondary metabolites of the genus *Cordia* and its biological activities.

Regarding the investigation of secondary metabolites in *Cordia americana*, so far only few phytochemical investigations have been done. Two quinones (cordiachrome G and leucocordiachrome H) and one phenolic aldehyde known as patagonaldehyde were isolated from its heartwood [213, 214]. From the bark coumarin [266] and tannins [131] have been reported. From its leaves, only tannins have been identified [294, 131] and no pyrrolizidine alkaloids were identified in *Cordia americana* [251]. None of the previous studies considered the biological investigation, therefore, this plant has not been extensively investigated.

Table 1.2: Chemical constituents and biological investigations of the genus *Cordia*

Species	Part used	Constituents	Activity	Reference
Cordia cylindrostachya Roem. & Schult.	-	α-pinene, amphene, tricylene	Antibacterial, anti-inflammatory	[101]
Cordia dichotoma G. Forst	Fruits	Flavonoids	Wound healing	[168]
Cordia francisci Ten.	Leaves	-	Analgesic, anti-inflammatory	[253]
Cordia martinicensis (Jacq.) Roem. & Schult.	Leaves	-	Analgesic, anti-inflammatory	[253]
Cordia myxa L.	Leaves and fruits	Robinin, rutin, datiscoside, hesperidin, dihydrorobinetin, chlorogenic, caffeic acid, quercitrin, carotenoids, oleic acid, β-sitosterol	Anti-inflammatory, anti-arthritic	[253, 7, 93, 106, 4, 212]
Cordia obliqua Willd.	Seeds	α-amyrin, betulin, octacosanol, lupeol-3-rhamnoside, β-sitosterol, β-sitosterol-3-glucoside, hentricontanol, hentricontane, taxifolin-3, 5-dirhamnoside, hesperetin-7-rhamnoside	Anti-inflammatory	[5]
Cordia serratifolia Kunth.	Leaves	-	Analgesic, anti-inflammatory	[253]
Cordia ulmifolia Juss.	Leaves	Pyrrolizidine alkaloids	Hepatotoxic, anti-inflammatory	[254]
Cordia curassavica (Jacq.) Roem. & Schult. (syn. *Cordia verbenacea* D.C.)	Leaves, areal parts	α-pinene, α-humulene, trans-caryophyllene, aloaromadendrene, cordialin A, cordialin B, rosmarinic acid, flavonols-artemetin	Anti-edematogenic, analgesic, anti-inflammatory, anti-rheumatic	[204, 26, 290, 73, 320, 310]
Cordia dentata Poir.	Flowers	Rosmarinic acid, quercetin-3-o-rutinoside	-	[90]
Cordia dichotoma Forst.	Leaves	Quercetin, quercitrin	-	[324]
Cordia globosa Jacq.	Roots	Meroterpenoid benzoquinone	Anti-cancer	[76]
Cordia linnaei Stearn.	Roots	Meroterpenoid naphthoquinones, naphthoxirene	Antifungal, larvicidal	[143]
Cordia latifolia Roxb.	Fruits	-	Anti-ulcer, anti-histaminic	[6]
Cordia spinescens L.	Leaves	Triterpenes	Anti-viral	[221, 201]
Cordia americana	Leaves	Tannins	-	[294, 131]
	Heartwood	Quinones, phenolic aldehyde	-	[213, 214]

1.2.3 *Brugmansia suaveolens*

Brugmansia suaveolens (Humb. & Bonpl. ex Willd.) Bercht. & C. Presl (syn. *Datura suaveolens* Humb. & Bonpl. ex Willd.) belongs to the Solanaceae family.

The family Solanaceae consists of about 2,700 species and of about 98 genera [226] and contains flowering plants which have a large number of important agricultural as well as toxic species. They are extensively used by humans as an important source of food, spice and medicine. However, some Solanaceae species are often rich in alkaloids, whose toxicity ranges from mildly irritating to fatal for humans as well as for animals. Some well-known species in this family include: *Datura stramonium* (Jimson weed), *Solanum tuberosum* (Potatoes), *Solanum lycopersicum* (Tomato), *Nicotiana tabacum* (Tobacco) and the genus *Capsicum* (Chili pepper). The greatest diversity of species can be found in South and in Central America. The origin of the name "Solanaceae" might come from the Latin "Solanum" meaning the "nightshade" plant, or it might be originated from the Latin verb "solari" meaning "to soothe", because of its soothing pharmacological properties of some psychoactive species in this family.

Brugmansia is a genus of the flowering species in the family Solanaceae. It is known as "angel s trumpets", sharing this name with the genus *Datura*, which is closely related. *Brugmansia* is perennial and woody [246]. *Brugmansia* species consist of large shrubs and small trees reaching heights of 3 up to 11 m. The name "angel s trumpets" refers to the large pendulous flowers that may be 14-50 cm long and 35 cm wide. This flower might have white, yellow, pink, orange or red colours. In this genus, some of well-known species include: *Brugmansia arborea*, *Brugmansia aurea*, *Brugmansia sanguinea*, *Brugmansia suaveolens*, and *Brugmansia versicolor*, which have been used to treat rheumatic and arthritic pains, swelling, scalds, inflammations, skin rashes, hemorrhoids and wounds. Their extracts exhibit spasmolytic, antiasthmatic, anticholinergic, narcotic and anesthetic properties [350]. The "*Brugmansia*" name is honored to Sebald J. Brugmans (1763-1819), a Dutch botanist, physician and professor of natural sciences. The "*suaveolens*" name means "fragrant", which is a characteristic of this plant due to its intense smell in the evening period [246].

Brugmansia suaveolens was firstly described by Willdenow in 1809 as *Datura suaveolens* and discovered by Humboldt and Bonpland on their expeditions in North America. Since 1823, it was reclassified into the genus *Brugmansia* [246]. In Brazil, this species is locally known as "trombeteira" (i.e., trumpeter) and it can be found in various regions of the country. Due this plant is popular as a drug (i.e., hallucinogenic tea from the flowers) its commercialization is controlled by the Ministry of Health in Brazil [43].

1.2.3.1 Localization

The genus *Brugmansia* is native in subtropical regions of South America mainly along the Andes (from Colombia to Northern Chile) and in the Southeast Brazil.

Brugmansia suaveolens has its origins in the coastal regions of the rainforest of Southeast Brazil. It grows in regions with altitude lower than 1,000 meters, mostly near to forest or along the river banks, where high humidity can be found. As a consequence of its ornamental value, *Brugmansia suaveolens* has been cultivated and nowadays it can also be located in Mexico and on the Caribbean Islands (see Figure 1.6) [246]. This plant has different local names, such as "trombeteira" or "saia-branca" in Brazil, "borrachero" in Colombia, "misha colambo" in Peru, and "campanita" in Venezuela.

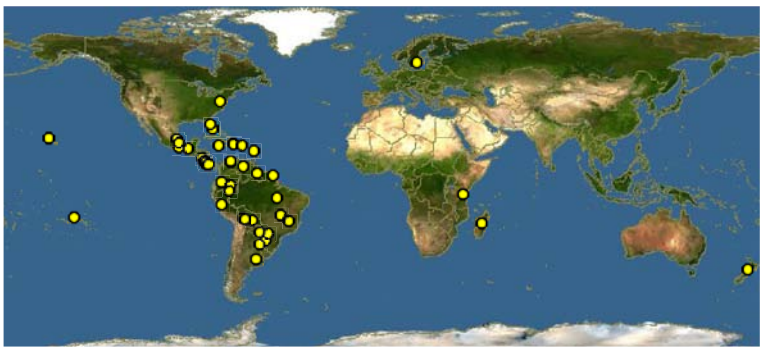

Figure 1.6: Distribution of *Brugmansia suaveolens* [241]

1.2.3.2 Botany

Concerning its botany aspects, *Brugmansia suaveolens* has the following properties [246]:

- Regarding its **morphologic characteristics**, *Brugmansia suaveolens* (see Figure 1.7) is a perennial and semi-woody plant. In its natural habitat, it grows as a shrub, and sometimes as a small tree, up to a height of 3 to 5 m.
- The **leaves** (see Figure 1.8) are oval to elliptical in shape and they have rarely hairs.

Figure 1.7: Shrub of *Brugmansia suaveolens*

Figure 1.8: Leaf of *Brugmansia suaveolens*

- The **owers** (see Figure 1.9) have five peaks on the edge. Each of these is supported by three prominent flower vein, which produces a corolla funnel-shape. The flower corollas are 24-32 cm long, as it can be observed in Figure 1.10. This species has two flowering phase, namely strong-flowering and weak-flowering, however, it is never completely without flowers. This plant requires normal light conditions and the temperatures should be between 12 and 18 °C.
- The elongated **fruit** has a shape like spindles with 10-22 cm long. They have numerous uneven covers and grooves. Its fruits dry out while still on the tree so that the seed is released only after the outer skin has tanned.

- The **seed** is tiny about 8 mm in size and is naturally spread by wind or flowing water. Seeds can number from as few as 40 to more than 150 per pod.

Figure 1.9: Flower form

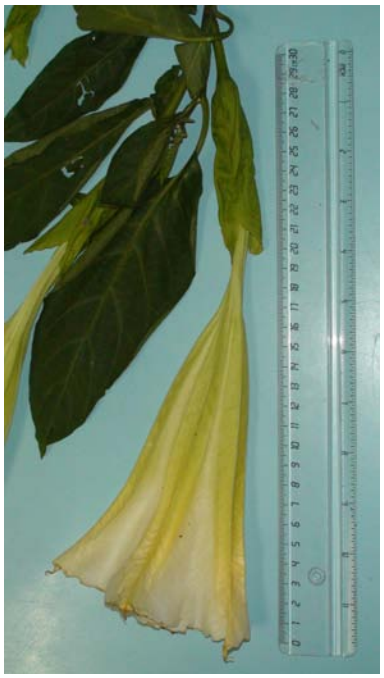

Figure 1.10: Flower length

1.2.3.3 Economical Importance and Traditional Medicine

Brugmansia is economically important as a flowering plant species. Its constant flowering increases its ornamental value, thus, it is also located in gardens around the world [246].

Brugmansia was used by the South American Indians to induce change in consciousness (i.e., trance) "allowing" the contact with their gods. However, the ancient civilizations did not only used this plant in sacred rituals, but also as a therapeutic [224].

Concerning the ethnopharmacological usage of *Brugmansia suaveolens*, the leaves of this species have been used for the treatment of wounds [283]. Feo, (2003) [89] described its traditional application of

> *... the leaves, whole or shredded, sometimes mixed with tobacco leaves ("Tabaco" = Nicotiana tabacum L.; Tabaco cimarrón = Nicotiana paniculata L.), are used in the healing of wounds. The leaf decoction (approximately 100 g in 1 L of water, boiled for*

30 min. until the preparation becomes green) is used externally in cataplasms as an anti-in ammatory on traumatized body parts. The vapors of this decoction are used as a vaginal cleanser (antiseptic) in cases of dysmenhorrea and white secretions. The plant is claimed to be toxic if ingested.

Havelius and Asman, (2002) [129] and Oliveira *et al.*, (2003) [225] described intoxication occurrences due to the ingestion of leaves, flowers and/or fruit by children. The contact of the sap with the eyes caused mydriasis. Moreover, a study is presented based on patients with anticholinergic poisoning by *Brugmansia suaveolens* between July 1990 and June 2000 in Australia. The main clinical effects were mydriasis, dried mouth, delirium, flushed skin, aggressiveness, visual hallucinations, tachycardia, urinary retention and fever [144]. In more severe cases, the patients may have neurological, cardiovascular and respiratory disorders, leading to death [225].

1.2.3.4 Chemical Constituents

The genus *Brugmansia* has been demonstrated to be a potential producer of alkaloids. As can be observed in Table 1.3, the main alkaloids are: scopolamine, hyoscyamine and atropine. Most of the studies did not consider the pharmacological activities, with exception of [40], which demonstrated anticholinergic effects for this plant.

Table 1.3: Chemical constituents and biological activity of the genus *Brugmansia* without *B. suaveolens*

Species	Part used	Constituents	Activity	Reference
Brugmansia arborea (L.) Lagerheim	Leaf, flower	Atropine, scopolamine, nor-hyoscine	-	[38, 211]
Brugmansia aurea Saff.	Nectar, pollen	Saponins, cardiac glycosides, cyanogenic glycosid	-	[79]
Brugmansia candida Pers.	Hairy roots	Scopolamine, hyoscyamine; cadaverine, polyamines, putrescine, spermidine, spermine, anisodamine	-	[242, 42, 39]
Brugmansia candida Pers.	Flower	6β-hydroxyhyoscyamine	Anticholinergic	[40]
Brugmansia sanguinea Ruiz & Pav.	-	Humic acid	-	[69]
	Leaf, root	Meteloidine, oscine, littorine	-	[85]
Brugmansia versicolor Lagerheim	Whole plant	Scopolamine	-	[29]

Concerning the investigation of secondary metabolites in *Brugmansia suaveolens*, Table 1.4 presents the state-of-the-art about the chemical constituents and biological activities. In *Brugmansia suaveolens*, the tropane alkaloids scopolamine, hyoscyamine and atropine are the mainly investigated compounds. Young leaves, flowers, and unripe fruits with seeds have higher scopolamine concentrations than other tissues. Leaves of this species increase their content of scopolamine after artificial damage, which might be used by the plant as chemical defense. However, the lowest concentration of scopolamine was detected in the matured leaves [10]. Thus, the alkaloid formation is not static, but it is dependent on the regulation of internal and external factors. Additionally, there are few studies on the isolation of other compounds such as flavonols [27] and essential oils [12].

Table 1.4: Chemical constituents and biological investigations of *Brugmansia suaveolens*

Reference	Part used	Constituents	Activity
[231]	Flower	-	Antinociceptive
[350]	Root cultures	Tropine, pseudotropine, scopoline, scopine, 3α-acetoxy tropane, 3-acetoxy-6-hydroxytropane, 3α-tigloyloxytropane, cuscohygrine, 3-hydroxy-6-(2-methyl butyryloxy)-tropane, 3-tigloyloxy-6-hydroxytropane, 3-hydroxy-6-tigloyloxytropane, apoatropine, 3-tigloyloxy-6-(2-methylbutyryloxy)-tropane, aposcopolamine, hyoscyamine, 3α,6β-ditigloyloxytropane, 7β-hydroxyhyoscyamine, 6β-hydroxyhyoscyamine	-
[10]	Leaf	Scopolamine	Defense theory
[97]	Leaf	Hyoscyamine, norscopolamine, scopolamine	Defense theory
[84]	Aerial	Hyoscine, apohyoscine, norhyoscine, atropine, noratropine, 3α,6β-ditigloyloxytropan-7β-ol,6β-tigloyloxytropan-3α,7β-diol, 3α-tigloyloxytropan-6β,7β-dio	-
[84]	Roots	Hyoscine, meteloidine, atropine, littorine, 3α-acetoxytropane, 6β-(α-methylbutyryloxy)-3αutigloyloxytropane, 3α,6β-ditigloyloxytropan-7β-ol, 3α-tigloyloxytropan-6β-ol, tropine, cuscohygrine	-
[84]	Flower	Norhyoscine	-
[12]	Flower	1,8-Cineole, (E)-nerolidol, α-terpineol, phenethyl alcohol, heptanal, nonanal, terpinen-4-ol, megastigmatrienone	-
[112]	Pollen	Pectin, callose	-
[27]	Leaf	Kaempferol 3-O-α-L-arabinopyranosyl-7-O-β-D-glucopyranoside, kaempferol 3-O-α-L-arabinopyranoside, 3-phenyl lactic acid, 3-(3-indolyl) lactic acid, physalindicanol A, physalindicanol B	-

1.3 Objectives of this Dissertation

In Brazil, *Cordia americana* and *Brugmansia suaveolens* have been used for the treatment of anti-inflammatory diseases in the folk medicine. However, the effective compounds responsible for the biological effects are widely unknown. Thus, the general objective of this dissertation was the investigation of the anti-inflammatory and wound healing properties of the ethanolic extracts from the leaves of both medicinal plants.

More specifically, this dissertation focused on:

- Bioguide fractionation of the plant extracts based on p38α.
- Isolation of the plants constituents using chromatographic methods.
- Structural elucidation by means of spectroscopic methods such as UV/VIS, mass spectrometry and nuclear magnetic resonance spectroscopy.
- Biological investigation of the ethanolic extracts and their isolated compounds in the p38α, JNK3, TNFα release, 5-lipoxygenase, NF-κB activation, and fibroblast scratch assay.

2 Inflammatory and Wound Healing Processes

This chapter presents an overview about inflammatory and wound healing processes. More specifically, it describes in details the biological targets p38α, JNK3, TNFα, 5-lipoxygenase, NF-κB and fibroblasts scratch assay.

2.1 Inflammatory and Wound Healing Processes

Inflammation is a biological response of the immune system against challenges originating from the surrounding environment. Challenge of host tissues due to traumatic, infectious or toxic injury or lesions lead to a complex series of vascular and cellular events carried out by the organism to remove the injury and to initiate the healing process, resulting in the release of different biochemical mediators. These events[1] causes redness, heat, swelling, pain and loss of function [289]. Vasodilatation, increased blood flow, enhanced permeability of blood vessels and peripheral nervous tissue stimulation are further events. Depending on the extent of insult, prolonged inflammation can lead to a chronic condition and eventually to loss of function [293].

The inflammation comprises of a large and complex regulated number of biochemical events including cellular, molecular and physiological changes in response to the stimuli. It involves

[1] Based on visual observation, the ancients characterized inflammation by five cardinal signs, namely redness (*rubor*), swelling (*tumour*), heat (*calor*, only applicable to the body extremities), pain (*dolor*) and loss of function (*functio laesa*). The first four of these signs were named by Celsus in ancient Rome (30-38 B.C.) and the last by Galen (A.D. 130-200) [289].

the immune system, the local vascular system and cells resident within the injured tissue. These cells produce multiple inflammatory mediators like cytokines (e.g., interleukin 1 and TNF (Tumor Necrosis Factor)), plasma proteins (thrombin), histamine and bioactive lipids. These events enable the successive recruitment of neutrophils, monocytes/macrophages and lymphocytes from the blood, which in turn release further pro-inflammatory mediators [223, 293].

Wounds are physical injuries that result in an opening or break of the skin. Healing is a complex and intricate process, initiated by a response to an injury, that restores the function and integrity of damaged tissues [277]. Wound healing involves inflammation as well as the formation and remodeling of new tissue [100].

Thus, more targets are necessary to study how the plant extracts and isolated compounds can modulate or inhibit inflammatory responses, and increase or accelerate the wound healing process [277]. Among several mediators, which are responsible to induce or maintain the inflammation, this dissertation focuses on the following biological targets: p38α and JNK3 (c-Jun N-terminal Protein Kinase 3) MAPK, TNFα, 5-lipoxygenase, NF-κB and fibroblasts scratch assay. These biological targets are explained in more details in the following sections.

2.2 Mitogen-Activated Protein Kinases (MAPKs)

Mitogen-activated protein kinase (MAPK) pathways regulate diverse processes ranging from proliferation and differentiation to apoptosis. Activated by an enormous array of stimuli, they phosphorylate numerous proteins, including transcription factors, cytoskeletal proteins and other enzymes. MAPKs have greatly influence on gene expression, metabolism, cell division, cell morphology and cell survival [248, 48].

Each MAPK pathway contains a three-tiered kinase cascade comprising a MAP kinase kinase kinase (MAPKKK, MAP3K, MEKK or MKKK), a MAP kinase kinase (MAPKK, MAP2K, MEK or MKK) and a MAP kinase [91, 248]. Normally, a MAPKKK kinase (MAPKKKK, MAP4K or MKKKK) activates the MAPKKK. The MAPKKKK or MAPKKK can be linked to the plasma membrane, for example, through association with a small GTPase or lipid (i.e., MAPKKKKs and

Raf MAPKKKs) [248].

MAPKs are dual specific serine-threonine kinases that phosphorylate both threonine (Thr) and tyrosine (Tyr) residues in their MAPK substrate [233, 284, 60, 165, 341, 17, 48]. All MAPKs share the amino-acid sequence Thr-Xxx-Tyr, in which X differs depending on the MAPK isoform. The amino-acid X is glutamic acid (Glu), proline (Pro) and glycine (Gly) for ERK (Extracellular-signal Regulated Kinase), JNK and p38 MAPK, respectively (see Table 2.1) [338, 326]. The Thr-Xxx-Tyr phosphorylation motif is localized in an activation loop near the ATP (adenosine-5 -triphosphate) and substrate binding sites [30, 48]. The length of the activation loop also differs between the three MAPK families [120]. Phosphorylation occurs by an ordered addition of phosphate to the tyrosine, followed by the threonine [122].

Table 2.1: Sequence alignment of the ATP binding pocket region of some MAPK isoforms with the amino acid X highlighted in the Thr-Xxx-Tyr phosphorylation motif [1]

MAPK isoform	**ATP binding pocket**	**Phosphorylation site**
p38α	Thr106-His107-Leu108-Met109	Thr180-**Gly**181-Tyr182
p38β	Thr106-Thr107-Leu108-Met109	
p38γ	Met109-Pro110-Phe111-Met112	Thr183-**Gly**184-Tyr185
p38δ	Met107-Pro108-Phe109-Met110	
JNK1/2	Met108-Glu109-Leu110-Met111	Thr183-**Pro**184-Tyr185
JNK3	Met146-Glu147-Leu148-Met149	Thr221-**Pro**222-Tyr223
ERK1	Gln122-Asp123-Leu124-Met125	Thr202-**Glu**203-Tyr204
ERK2	Gln103-Asp104-Leu105-Met106	Thr183-**Glu**183-Tyr185

Once activated (see Figure 2.1), MAPKs can phosphorylate and activate other kinases or nuclear proteins such as transcription factors in the cytoplasm or the nucleus. This event occurs by a rapid sequential mechanism, whereby the protein or peptide binds first into the substrate pocket (peptide-binding channel) of p38 MAPK, followed by ATP binding into the ATP pocket [134]. Then the substrate and ATP interact each other ensuring firm binding [192]. This leads to an increase or decrease in the expression of certain target genes, resulting in a biological response. The variation in specificity within a pathway suggests that different extracellular signals can produce stimulus and tissue specific responses by activating one or more MAPKs pathways [353, 248, 56, 183].

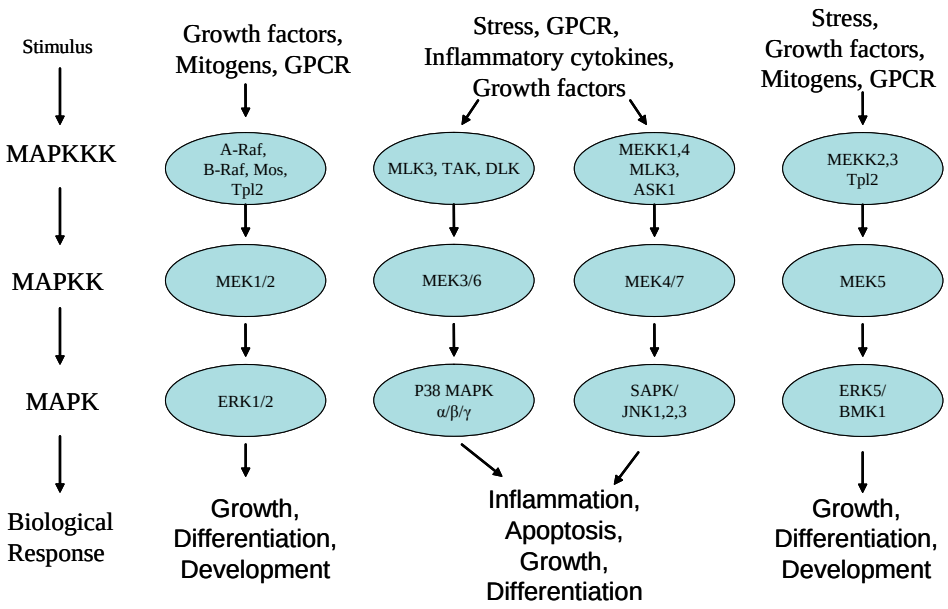

Figure 2.1: Illustration of the general MAPK signaling cascades [44]

There are at least three MAPKs that differ in the sequence and size of the activation loop: the extracellular signal-regulated kinases (ERK1 and ERK2), the c-Jun N-terminals kinases (JNK1, JNK2, JNK3) and the p38 kinase isozymes (p38α, p38β, p38γ, p38δ) [70, 48, 46, 149, 261, 183, 248]. They are activated by various stress-associated stimulus like high osmolarity, ultraviolet light, toxins, xenobiotics, heat, as well as mitogens and growth factors [65].

2.2.1 The ERK Signaling Pathway

The subfamily of ERK (extracellular-signal regulated kinase) was the first MAPK to be cloned and characterized in detail. ERKs are expressed in all tissues, including terminally differentiated cells [32, 30]. Thus, they are involved in many fundamental cellular processes, such as proliferation, differentiation, apoptosis and metabolism [248]. They are activated by mitogenic stimuli such as growth factors and cytokines which activate a variety of receptors and G proteins [99, 157, 82, 18, 34, 30].

ERK1 and ERK2 have 43 and 41 kDa and are activated by MEK1 and MEK2 (message encryption key), respectively. In fibroblasts, they are activated strongly by growth factors, serum, esters and also to a lesser degree by ligands of G protein-coupled receptors, cytokines, trans-

forming growth factors and osmotic stress. In differentiated cells, they are often activated by the primary stimuli that regulate tissue specific functions, like glucose in islets or transmitters in brain [48, 99, 157, 18]. ERK1 is important for T cell responses, whereas ERK2 plays a role in mesoderm differentiation and placenta formation [248].

Blocking of ERK activity could be a great benefit for the treatment of metastatic cancer, because they are involved in the control of proliferation, differentiation and apoptosis. Therefore, the ERK pathway is also explored for the therapy of viral diseases including HIV [215], influenza [243] as well as neurodegenerative syndromes such as Alzheimer [255] or cardiovascular diseases [55].

2.2.2 The JNK Signaling Pathway

The c-Jun N-terminal protein kinases (JNK) consist of at least ten protein isoforms that are generated through alternative splicing of three closely related genes, such as JNK1, JNK2 and JNK3. The JNKs along p38 are also called as stress-activated protein kinases (SAPK). JNK1 and JNK2 are expressed ubiquitously in all tissues. In contrast, the JNK3 has more limited pattern of expression and is largely restricted to the nervous system, but also detected in heart and testis [227, 30].

JNKs are involved in a wide range of cell signaling, including cell death apoptosis [78, 172, 123, 83, 344, 195, 295] and neurodegenerative diseases [316, 33, 111, 343, 319], brain, heart [325, 130] and renal ischemia [108], epilepsy and inflammatory disorders (multiple sclerosis, rheumatoid arthritis (RA), asthma, inflammatory bowel diseases and psoriasis) [126, 262, 58, 259, 258, 15, 222].

Along with p38 MAPK, JNK pathways are triggered by a variety of cellular stresses, inflammatory cytokines, UV light and peroxides [24, 248]. The major JNK activators are MKK4 and MKK7 [335]. Both protein kinases can activate JNK by dual phosphorylation of the motif Thr-Pro-Tyr, located in the activation loop [78]. While MKK4 phosphorylates preferentially JNK on tyrosine, MKK7 phosphorylates JNK on threonine [181, 313, 322, 35].

So far, most of the reported JNK inhibitors come from synthetic efforts to design p38 compounds. The p38 inhibitors SB203580 and SB202190 also block JNK activity at concentrations above those, which are necessary to block p38. One of the first compounds discovered as inhibitor of JNK pathway without effect on p38 was CEP-1347 and further the SP600125 inhibitor [125]. These last two inhibitors also reduced the symptoms of adjuvant induced arthritis in rat [180], indicating that JNK inhibitors could be a potential therapy for rheumatoid arthritis.

2.2.3 The p38 MAPK

The p38 MAPK is the largest subfamily of the mitogen activated protein kinase, characterized in mamallian cells. The p38 are serine/threonine kinases that play a central role in the regulation of a variety of inflammatory responses like expression of pro-inflammatory mediators, such as TNFα, IL-1β and IL-6 (interleukin), leucocyte adhesion, chemotaxis and oxidative burst [270, 336, 116]. However, as aforementioned p38 MAPK is not the only signaling route leading to these cellular responses, that is, ERK, JNK and NF-κB can also be involved. Interaction between these pathways very often determines the final biological response [134].

Four isoforms of p38 have been characterized and are distributed in different tissues (see Table 2.2). A detailed understanding of the role of each isoform remains unclear, once the majority of investigation are focused into the p38α and β isoforms [65, 116]. Analysis of differential tissues from patients with rheumatoid arthritis suggested that the p38α isoform is over activated within the inflamed tissue and may be a preferential target for intervention in the disease [122, 163, 274, 116].

Table 2.2: p38 isoforms expression in tissues and cells of the immune system and endothelium [122, 275, 30]

p38 isoforms	**Tissues expression**	**Cellular expression**
p38α	Ubiquitous mainly: spleen, bone, marrow, heart, brain, pancreas, liver, skeletal muscle, kidney, placenta, lung	All cell types mainly: pheripheral leucocytes
p38β	Ubiquitous mainly: brain and heart	Endothelial cells, T cells
p38δ	Lung, kidney, endocrine organs, small intestine, salivary, pituitary, adrenal glands, prostate, testes, pancreas	Macrophages, neutrophils, T cells, monocytes
p38γ	Skeletal muscle and cardiac muscle	Little or no expression in immune system

The main activation route for p38 MAPK is through phosphorylation of MKK3 and MKK6 [171, 272, 35]. MKK3 shows a selective activation of p38α and p38γ, while MKK6 activates all four isoforms [115, 62]. MKK4 activates both p38 and JNK [148, 183].

Like all the other kinase cascades, p38 is also activated in response to the pro-inflammatory cytokines, like TNFα and IL-1, and by cellular stress such as ultraviolet light, heat shock and cigarette smoke [28]. The p38 MAP kinase is activated through dual phosphorylation at threonine and tyrosine by a specificity cascade of kinase (MAPKK). The Thr-Gly-Tyr (TGY) motif of p38 is located in the activation loop. By phosphorylation, this loop takes an altered conformation, so that ATP can bind at the catalytic center [28].

The phosphorylation promotes the enzymatic activity of MAP kinase and also their dimerization. Only the dimeric form of the enzyme reaches the nucleus, where the MAPK activates a number of transcription factors such as ATF-1 and 2 (activation transcription factor-1 and 2) and the MEF 2C (myocyte enhancer factor 2C) [267]. In addition, downstream kinases, for example, the MAP kinase-dependent protein kinases and MSK-1 (mitogen-and stress-activated protein kinase-1) are also activated by phosphorylation. The activated MAPKAPK2 (MAP kinase-activated protein kinase 2) binds to the adenosine/uridine (AU)-rich region of mRNA (messenger RNA), resulting in a stabilization of AU-rich mRNA. Moreover, the translation is directly influenced by AU-binding proteins that regulate the protein to be activated. Finally, the activation of p38 MAPK pathway is mainly responsible for the biosynthesis of TNFα [167]. The complete pathway of p38 MAPK is shown in Figure 2.2. p38 MAPK is considered to be the most physiologically relevante kinase involved in the inflammatory response.

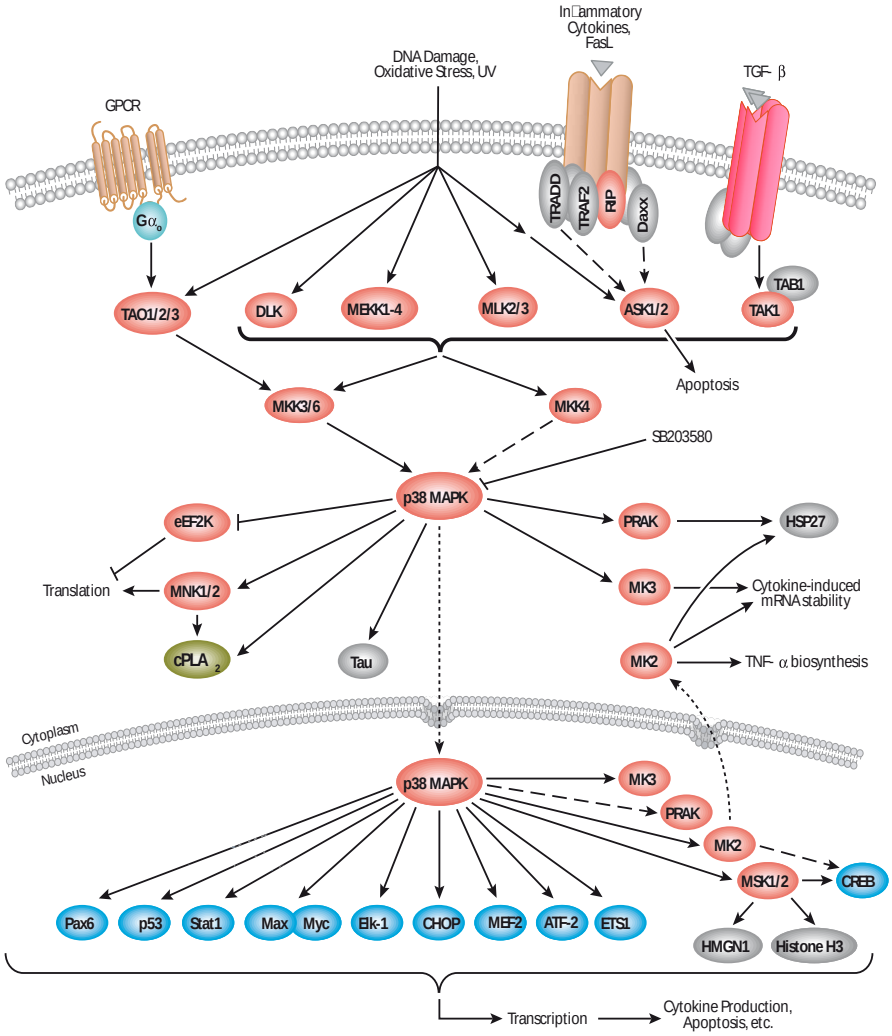

Figure 2.2: p38 MAPK signaling pathway [44]

2.2.4 Structure of Protein Kinase

The genome is composed of 518 genes that encode for protein kinases with similar tertiary structure and ATP binding sites. Protein kinases catalyze the same chemical reaction, namely the phosphorylation of other proteins. Each kinase presents its own structural and dynamic characteristics. MAPKs share between 50% and 80% sequence identity [268]. Most protein kinases have a common fold of two domains, the N-terminal lobe consisting of five antiparallel β-strands and one α-helix, and the C-terminal lobe, which is composed predominantly of α-helix. The two structural subunits are linked together via a hinge region that allows the rotation of the two lobes [114].

Hanks and Hunter, (1995) [127] divide the protein kinase in 11 subdomains, as shown in Figure 2.3. In the gap between the two domains (i.e., N and C-terminal lobe), the ATP binding site is lying. In position 53 of the subdomain two, the conserved lysine residue is located, which is involved in the phosphate transfer. In the subdomains eight and nine the activation loop of kinase is situated. In this region the TGY motif can be found with the amino acids Thr 180 (T180) and Tyr 182 (Y182) that are phosphorylated by a MAP kinase kinase and thus lead to the activation of the enzyme. The subdomains six and eight are involved in the substrate binding [137].

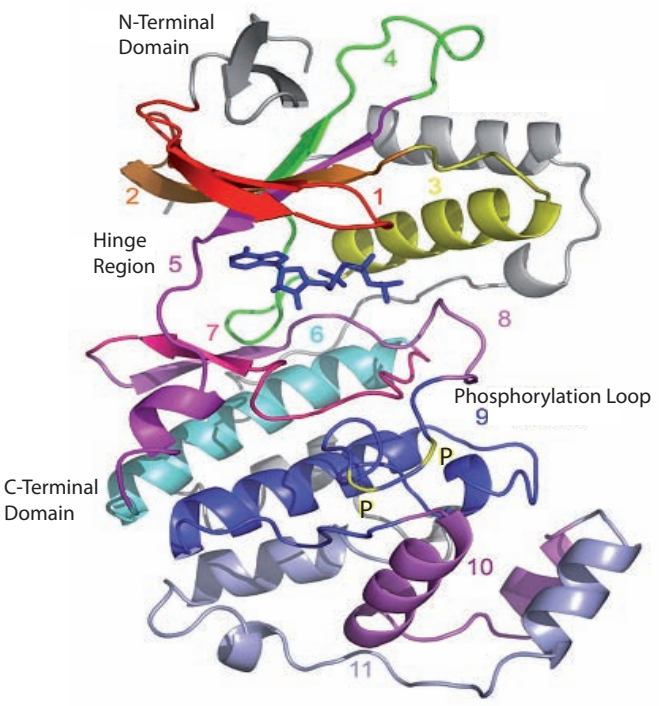

Figure 2.3: Representation of the structure of p38 MAPK (PDB ID: 1A9U) [137, 127])

Research concerning protein kinases is concentrated on the development of ATP-competitive inhibitors which can be exploited for gaining potency as well as selectivity. In the ATP binding pocket, inhibitors can bind (competitive or in allosteric mode) instead of ATP and thus inhibit the enzyme. The ATP binding site consists of a front and back side. The front side contains the ATP-binding pocket and the back side important elements needed for the regulation of catalysis of kinases [187]. Between these two regions a gateway is formed, that is, the so-called gatekeeper residue. This gatekeeper regulates the access of the back side from the binding pocket, the so-called

hydrophobic pocket I. If the gatekeeper is a small amino acid such as threonine or alanine, than the access to hydrophobic region I is granted. A large amino acid at this position (e.g., phenylalanine) leucine or methionine prevented however, the interaction between the inhibitor and this region [187]. The gatekeeper residues for p38α and JNK3 consist Thr106 and Met146, respectively.

Based on cristallographic structural data, Manning *et al.*, (2002) [199, 314] proposed to divide the ATP-binding site of kinases into five sub regions (see Figure 2.4), as following:

- Adenine-binding region (Purin-binding region): The predominantly hydrophobic character of this region permits that ATP as well as the inhibitors interact through van der Walls forces with this pocket. This observation is confirmed by the linear correlation between completed or occupied surface and binding affinity of ATP-competitive ligands. The position of H-bond donors and acceptors in this area allows important interactions with the hinge region.

- Hydrophobic backpocket (Hydrophobic pocket I, selectivity pocket): The hydrophobic region I is similar to a cavity (gap), whose dimension is determined through the gatekeeper residue Thr 106 in case of p38. This region is located orthogonal behind the adenin in the ATP binding region.

- Hydrophobic region II (Hydrophobic pocket II): This region is a kind of groove located in front of the ATP binding site. This area has predominantly a hydrophobic character in contact to the solvent. This region as well as the hydrophobic pocket I are not occupied by ATP and they can be used for the development of selective inhibitors.

- Phosphate-binding region (Glycin-rich loop): The phosphate binding region is the roof of the ATP-binding pocket and consists of a glycine rich sequence that is mainly exposed to the solvent. The glycine residues make the loop flexible and thus allows the opening and closing of the ATP binding site during catalysis. It is a highly conserved region, since amino acid residues play an important role in this region in the catalytic process and in the binding of

the triphosphate. Only a few inhibitors use this region, because this area is highly conserved and it cannot contribute to selectivity.

- Ribose-binding pocket: In this region, hydrophilic and hydrophobic interactions are possible. The ribose-binding pocket is highly conserved, therefore, it is often exploited to improve hydrophilicity as well as selectivity by introducing solubilizing moieties.

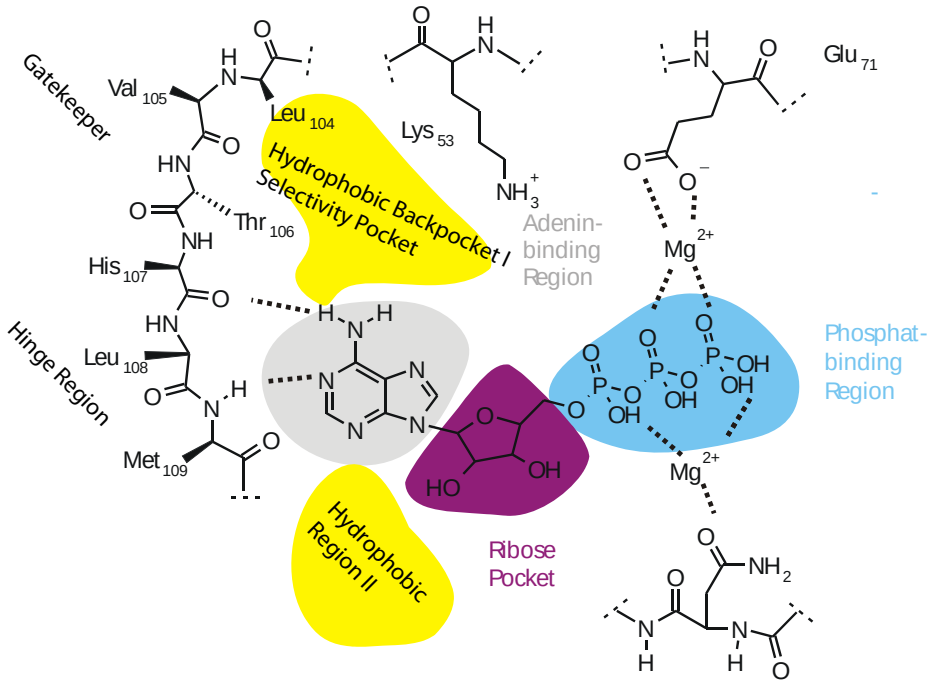

Figure 2.4: Representation of the ATP-binding site of protein kinases bound to the ATP cofator [314]

The discovery of the pyridinylimidazole SB203580 as potent inhibitor of p38 MAPK by competitive binding in the ATP pocket [183] and its further use in several animal models of inflammation, validated this kinase as an important anti-inflammatory therapeutic target [311, 339]. Analog to SB203580, alternate structural types of compounds continue to be developed as anti-inflammatory agents, like SB210313 and ML3163 [178].

An example of a natural compound as kinase inhibitor is the synthetic flavopiridol. This flavone has been reported as first cyclin-dependent kinase (CDK) inhibitor in phase II clinical trials for cancer and has also been investigated for the treatment of arthritis [86, 288, 31].

2.2.5 Diseases Associated with MAPKs

A signal transduction, which is initiated by receptor activation, is a complex set of cascading networks involving significant crosstalk, intracellular trafficking, scaffold modules, and feedback loops. The net cellular response is dependent on a large number of parameters like signal strength, amplification, and duration, protein expression levels, and the numbers and types of concurrent extracellular signals [276]. There are many studies in stroke suggesting the involvement of the three families of MAPKs (ERK, JNKs, and p38 MAPKs) in inflammations. They are attractive targets for new therapies and development of more selective inhibitors against inflammatory diseases.

The most studies concerning p38 MAPK are focused on their function in inflammatory processes. Several groups have reported that specific and selective p38α/β MAPK inhibitors block the production of IL-1, TNF and IL-6 *in vitro* and *in vivo*. In addition, the p38 MAPK pathway is involved in the induction of several other inflammatory molecules, such as COX-2 (Cyclooxygenase-2) and inducible nitric oxide synthase (iNOS). Moreover, p38α-dependent histone H3 phosphorylation has been shown to mark and recruit NF-κB to other promoters resulting in increased expression of several inflammatory cytokines and chemokines [263].

Concerning the diseases associated with MAPKs, rheumatoid arthritis is a chronic autoimmune inflammatory disease which affects about 1% of the adult population worldwide [275, 276] and is characterized by inflammation of the synovial joints and production of pro-inflammatory mediators by immune cells that infiltrate in the synovium. This provokes proliferation of synovial fibroblasts, further release of inflammatory molecules and formation of pannus tissue that eventually degrades cartilage and subchondral bone, leading to joint destruction, pain and loss of physical function. Arthritis results from dysregulation of pro-inflammatory cytokines (e.g., IL-1 and TNFα) and pro-inflammatory enzymes that mediate the production of prostaglandins (e.g., COX-2) and leukotrienes (e.g., lipoxygenase) together with the expression of adhesion molecules and matrix metalloproteinases, and hyperproliferation of synovial fibroblasts. All of these factors are regulated by the activation of NF-κB [167, 156]. Anti-cytokine biotherapeutic approaches, such as etanercept

(tumor necrosis factor receptor-p-75 Fc fusion protein), infliximab (chimeric anti-human TNFα monoclonal antibody) and adalimumab (recombinant human anti-human TNFα monoclonal antibody) bind to TNF-α and prevent the binding to cell-surface receptors [167, 276, 275]. Agents that suppress the expression of TNFα, IL-1β, COX-2, lipoxygenase, matrix metalloproteinases or adhesion molecules, or suppress the activation of NF-κB, have all potential for the treatment of arthritis. Compounds derived from plants like curcumin (from tumeric), resveratrol (red grapes, cranberries and peanuts), tea polyphenols, genistein (soy), quercetin (onions), silymarin (artichoke), boswellic acid and anolides can also suppress these cell signaling intermediates [156].

Increasing tissue levels of inflammatory cytokines (i.e., IL- 1, IL-6, TNFα) have also been observed in patients suffering from inflammatory Crohns diseases which is characterized by a chronic inflammation in the gastrointestinal tract. Therapy with anti-TNF-α agents have been showing clinically efficacious [276, 66].

MAPKs and NF-κB activation have been also identified in the pathogenesis of chronic inflammatory bowel diseases. Immunohistochemical analysis of inflamed mucosal biopsies revealed that expression of p38α was abundant in activated macrophages and neutrophils infiltrating bowel mucosa. The treatment with SB203580 improves the clinical score, ameliorates the histological alterations, and reduces mRNA levels of pro-inflammatory cytokines [151].

JNKs and p38 MAPKs are also activated by ischemia/reperfusion (I/R) [171, 245]. Evidences from studies conducted on mice have suggested that JNKs might be a potential therapeutic target for obesity and type 2-diabetes [135, 68].

The MAPK pathway is also investigated in connection with cancer. The pathway is activated by mitogens that promote mitosis, however, unregulated activation of this pathway has been linked to be a cause of cancer [184, 167].

2.3 Cytokines

Cytokines are glycoproteins produced by different cell types that bind to specific high-affinity receptors. They consist of 100-200 amino acids and have molecular weights around 10-25 kDa and are high active in a concentration range of pg to ng [54]. Cytokines regulate intercellular communication and are directly implicated in many immune processes [16, 203]. They act only in short distances (except TNFα) differently from hormones [23].

There are two different classes of cytokines (inflammatory /pro-inflammatory and anti-inflammatory cytokines). The pro-inflammatory cytokines (TNFα, IFNg, IL-1, IL-2, IL-6, IL-12) ensure that in case of penetration of one pathogen, for example, the immune cells are attracted to the site of infection and activated. However, anti-inflammatory cytokines (IL-4, IL-10, IL-13) should be a successful fight against the infectious agent, so that the resulting inflammation may be counteracted quickly. Because of their biological function, cytokines can be classified in interferon (IFN), interleukins (IL-1 to IL-23), tumor necrosis factor (TNF), growth factors (EGF, FGF, PDGF) and chemokines [193].

IL-1 is a 17 kDa protein that is mostly produced by monocytes and macrophages but also by endothelial cells, B cells, and activated T cells. IL-1 includes two different cytokine agonists, termed as IL-1α and IL-1β. Both IL-1 forms differ very slightly in their physiological and pathophysiological function [175]. IL-1β is a crucial mediator of the inflammatory response that plays an important role in the development of chronic inflammation, especially joint damage causing arthritis [54].

IL-4 is produced by CD4 type-2 helper T cells and participates in the differentiation and growth of B cells [145]. *In vitro*, IL-4 inhibits the activation of type-1 helper T cells, and this, in turn, decreases the production of IL-1 and TNFα and inhibits cartilage damage. In rheumatoid arthritis, this anti-inflammatory cytokine inhibits the production of IL-1 and increases the expression of IL-1 receptor antagonist, and both actions should decrease inflammation [52].

IL-6 is an inflammatory cytokine produced by T cells, monocytes, macrophages and synovial

fibroblasts. This interleukin is involved in diverse biological processes, such as activation of T cells, the induction of acute-phase response, the stimulation of the growth and differentiation of hematopoietic precursor cells and proliferation of synovial fibroblasts [54].

IL-8 is produced by monocytes, T lymphocytes, neutrophils, fibroblasts, epithelial, endothelial and tumor cells. It is hardly found in healthy tissues, but its production is increased from five to one hundred times after stimulation by cytokines such as TNFα and IL-1, LPS (lipopolysaccharide), viral products, and cellular stress. The uncontrolled production of IL-8 is related to diseases such as rheumatoid arthritis, lung disease, skin, viral infections, tumor growth, sclerosis and arteriosclerosis [189]. The expression of IL-8 may be regulated by treatment with immunosuppressive agents, but polyphenols isolated from green tea and genistein from soy also inhibit the production of this cytokine [315] and many other compounds.

IL-10 belongs to the anti-inflammatory cytokine group and is produced by monocytes, macrophages, B-cells and T-cells. It inhibits the production of several cytokines, including IL-1 and TNFα and the proliferation of T-cells *in vitro*. The IL-10 is also found in synovial fluid of patients with rheumatoid arthritis, but the amount is insufficient to suppress inflammation [54].

2.3.1 Tumor Necrosis Factor α (TNFα)

Tumor necrosis factor (TNF) is a non glycosylated polypeptide that belongs to the group of multifunctional pro-inflammatory cytotoxins. It exists in an α and β-form, which are only 30% homologus [175]. Normal quantities of circulating TNFα are between 10 and 80 pg/mL [190]. TNFα plays an important role in chronic inflammation, cell proliferation, differentiation and apoptosis [229, 25]. It is predominantly detected during the early stages of diseases and its dysregulation of expression and/or signaling is involved in many pathologies, including Crohns diseases, rheumatoid arthritis and neurophatologies such as stroke, multiple sclerosis and Alzheimer s disease [72, 21].

TNFα is produced in macrophages, monocytes, T-cells and NK cells but also in endothelial cells

and fibroblasts by stimulation of lipopolysaccharide (LPS), for example [291, 184]. Initially, TNF is produced as a membrane-associated precursor protein with a molecular weight of 26 kDa and is accumulated in the intracellular space. By means of TACE (TNFα converting enzyme), pro-TNFα is transformed in the active 17 kDa form and released from the cells. TACE is a membrane-bound metalloproteinase, which belongs to the group of ADAM (a disintegrin and metalloprotease) protein family [218].

The biological responses to TNFα are mediated through two structurally distinct receptors: type 1 (TNFR1) and type 2 (TNFR2). Both receptors are transmembrane-glycoproteins with multiple cysteine-rich regions in the extracellular N-terminal domains. Although their extracellular domains share structural and functional homology, their intracellular domains are distinct and transduce their signals through both overlapping and different pathways. The primary characteristic property that distinguishes the intracellular domains of TNFR1 and TNFR2, is the presence of a death domain in TNFR1, which is not present in TNFR2. The death domain is a sequence of approximately 70 amino acids and is pivotal to the ability of TNFα to trigger cellular apoptosis [229].

Under physiological conditions, signaling through TNFR1 seems to be primarily responsible for the pro-inflammatory and shock producing properties of TNFα. It means that the biological responses to TNFα seem to be dependent on signaling through both receptors. Both TNFα receptors can be cleaved from the cell surface by members of the matrix metalloproteinase family in response to inflammatory signals, such as TNFα receptor binding. The extracellular domains of the receptors retain their ability to bind TNFα. Therefore, these domains have either endogenous inhibitors or facilitators of the biological activity of TNFα [351], which are dependent on their concentrations and ligands [229].

Exposure of cells to TNFα can result in an activation of a caspase cascade leading to apoptosis [45]. However, more commonly, the binding of TNFα to its receptors causes activation of two major transcription factors, AP-1 and NF-κB, that in turn induce genes involved in chronic and acute inflammatory responses. Furthermore, some of these genes act to suppress TNFα induced apoptosis, thereby explaining why the apoptotic response to TNFα is usually dependent on inhi-

bition of RNA or protein synthesis. The suppression of apoptosis is mostly dependent on NF-κB, which increases the inflammatory response to TNFα [25].

2.4 Nuclear Factor-κB (NF-κB)

The nuclear factor (NF)-κB plays a crucial role in the regulation of numerous genes involved in diverse cellular processes like cell growth, apoptosis, differentiation, inflammation by regulating the transcription of genes encoding for cytokines, COX-2, nitric oxide synthase, immunoreceptor molecules of adhesion and hematopoietic growth factors [110, 197]. Dysregulation of NF-κB pathway is associated with a variety of human diseases, like atherosclerosis, asthma, rheumatoid arthritis, cancer, inflammatory bowel disease, type 1 diabetes mellitus, and psoriasis [20, 170].

NF-κB is a dimeric protein, which can be differently composed. Five NF-κB members have been found in mammal cells: NF-κB1 (p105/50), NF-κB2 (p100/52), RelA (p65), RelB and RelC. All NF-κB proteins share the RHD (Rel-homology domain) in their N-terminal region, which is required for dimerization, DNA binding, interaction with the inhibitory protein IκB, as well as the nuclear localization sequence (NLS) [152, 153, 352].

In inactive cells, NF-κB resides in the cytoplasm bound to the inhibitory IκB subunit. The IκB family of proteins include IκB-α, IκB-β, IκB-γ, IκB-ϵ, Bcl-3 and the precursor proteins p105 and p100. Activation of p105 and p100 give the subunits p52 and p50, respectively. IκB proteins interact with the RHD of NF-κB, thereby inhibiting its transport to the nucleus and binding of NF-κB to the DNA [109].

The major activation route of NF-κB (canonical pathway) occurs through the activation of the IκB kinase complex (IKK). The substances that induce the activation of the IκB-kinase complex are LPS, cytokines, viruses, physical and physiological stress such as UV and gamma radiation, and several chemical agents. The activation of IKK leads to phosphorylation of serine in IκB-α. Phosphorylated IκB undergoes ubiquitination and subsequent proteosomal degradation [152, 352]. The degradation of IκB allows the transport of NF-κB into the nucleus and its DNA binding [109, 352].

The IKK complex contains two catalytic sites, the IKK-α and IKK-β and a regulatory unit known as NEMO (NF-κB-essential modulator). Generally, in the canonical pathway stimuli such as LPS and cytokines activate IKK-β and leads to NF-κB dimer composed of RelA, RelC and p50. Another route of activation, much less common, is activated by BAFF (B-cell activating factor), which promotes activation of NIK (NF-κB inducing kinase) and involves the activation of p100 by IKK-α. This route also called non-canonical or alternative pathway leads to dimers with p52 and RelB [109, 352]. Figure 2.5 shows a simplified scheme of the canonical and the non-canonical pathway.

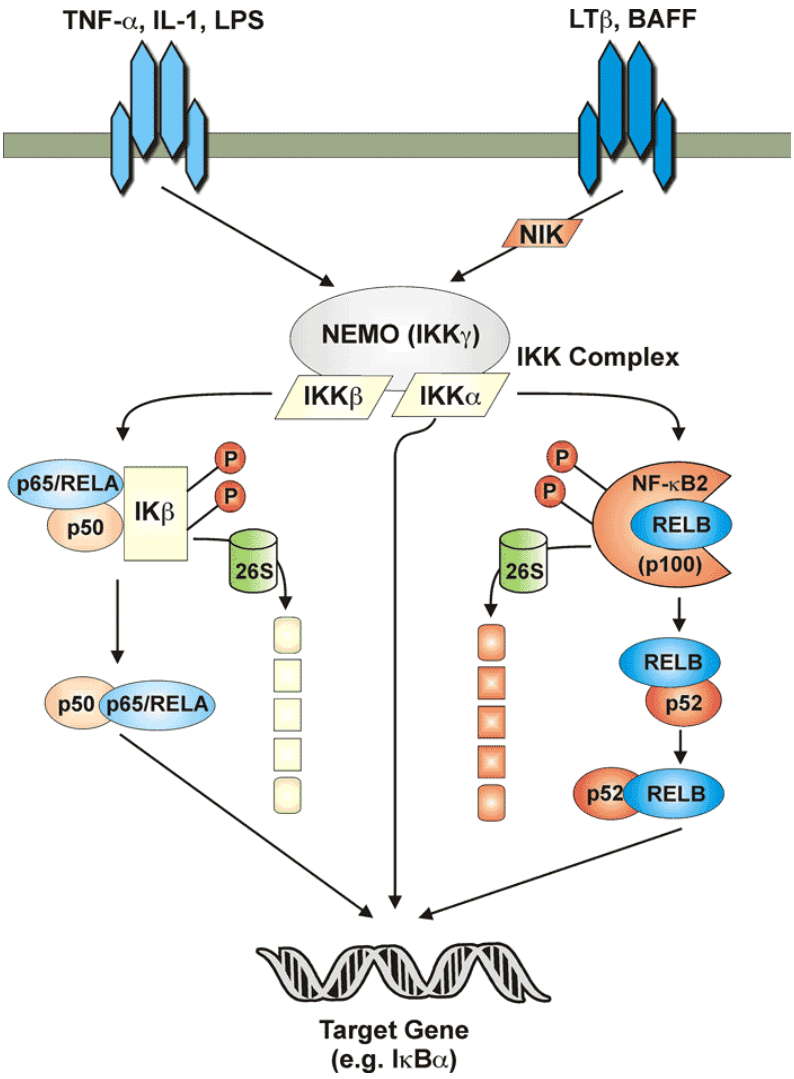

Figure 2.5: Activation pathways of the transcription factor NF-κB [279]

A large number of natural compounds have been shown to interfere with the cascade leading to NF-κB activation and gene transcription. Sodium-salicilate and its semi-synthetic derivative aspirin were the first plant-derived compounds reported to modulate NF-κB activity [162, 75]. The compounds kamebakaurin, a kaurane diteperne from *Isodon japonicus* and acanthoic acid, a diterpene from *Acanthopanax koreanum* were reported to inhibit NF-κB too [185, 141]. Sesquiterpene lactones can also interfere with NF-κB, presumably directly targeting subunit p65. For example, helenalin, a lactone isolated from medicinal plant *Arnica montana*, has been suggested to selectively alkylate the p65 subunit of NF-κB [159]. On the other hand, parthenolide, from the medicinal herb *Tanacetum parthenium* is reported to bind also directly to IκB kinase-β (IKK-β) [229].

2.5 Arachidonic Acid Cascade

The metabolism of arachidonic acid (AA) can be catalyzed by one of the two enzyme families: cyclooxygenases and lipoxygenases. The metabolites of arachidonic acid are involved in the development and regulation of pain and inflammatory diseases, such as asthma, arthritis and psoriasis.

Arachidonic acid is a carboxylic acid with a 20-carbon chain and four cis-configured double bonds (all-cis 5, 8, 11, 14-eicosatetraenoic acid). The first double bound is located at the sixth carbon from the omega end (20:4;ω-6). The polyunsaturated AA is abundantly incorporated in an esterified form (sn-2) into membranous phospholipids. Cellular activation by an appropriated stimulus (e.g., platelet activation with thrombin, IL-1 and TNF in leukocytes) induces release of AA from cellular membrane phospholipids via the activity of the enzyme phospholipase A2 (PLA2). Once liberated, free AA functions as second messenger itself [155] ans is re-incorporated into phospholipids, or serves as the primary precursor of eicosanoid biosynthesis in mammalian cells. The conversion of AA into eicosanoids is governed by three classes of enzymes [298] (see Figure 2.6), which initially incorporate oxygen at different positions of the substrate:

- Cyclooxygenases (COXs), which initiate the synthesis of prostaglandins (PGs) and trom-

boxanos (TXs), altogether termed as prostanoids.

- Lipoxygenases (LOs), such as 5-LO, which catalyzes the formation of leukotrienes (LT) as well as 12- and 15-LOs yielding hydroxy-eicosatetraenoic acids (HETEs).
- A class of CYP 450 enzymes which form epoxyeicosatrienoic acids (EETs).

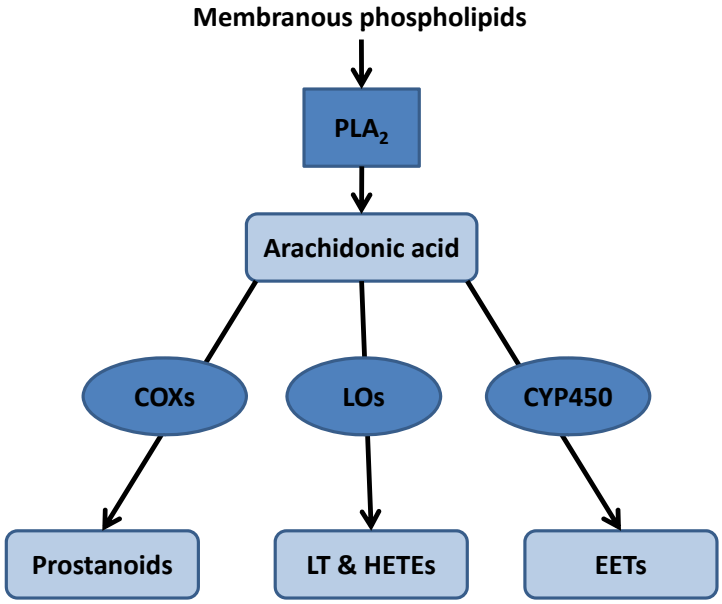

Figure 2.6: Arachidonic acid cascade

2.5.1 5-Lipoxygenase

Lipoxygenases are a family of structurally related non-heme iron-containing enzymes that insert molecular oxygen into polyunsaturated fatty acids with cis, cis-1,4-pentadiene. Depending on the position of oxygen insertion into arachidonic acid, mammalian lipoxygensases are classified as 5-, 12- and 15-hydroperoxyeicosatetraenoic acids (HPETEs), which are reduced to the corresponding hydroxyeicosatetraenoic acids (HETEs) or converted into various other types of eicosanoids such as leukotrienes [278, 299].

Leukotrienes (LTs) are bioactive mediators mainly produced and released from activated leukocytes, but also in granulocytes, monocytes/macrophages, mast cells, dendritic cells and B lympho-

cytes. Platelets, endothelial cells, T-cells and erythrocytes do not express them [300, 102]. Elevated levels of lipoxygenase metabolites, particularly 5-LO, have been also found in lung, prostate, breast, colon and skin cancer cells, as well as in cells from patients with acute leukemias [299]. The antagonists of leukotrienes pathway have been used in the treatment of bronchial asthma, arteriosclerosis, cardiovascular diseases and cancer [299, 250, 330, 236].

The conversion of arachidonic acid in leukotrienes by 5-lipoxygenase is shown in Figure 2.7. The initial step in LT biosynthesis is the dioxygenation of free AA by 5-LO yielding 5(S)-hydroperoxyeicosatetraenoic acid (5-HPETE) which is further metabolized by 5-LO to the instable epoxide LTA_4. In neutrophils and monocytes, LTA_4 can be converted to LTB_4 by LTA_4 hydrolase, whereas in mast cells and eosinophils, LTC_4 synthase or membrane-associated proteins can conjugate LTA_4 with glutathione, yielding the cysteinyl-LT which can be cleaved in the extracellular environment yielding LTD_4 and then LTE_4 [330, 299].

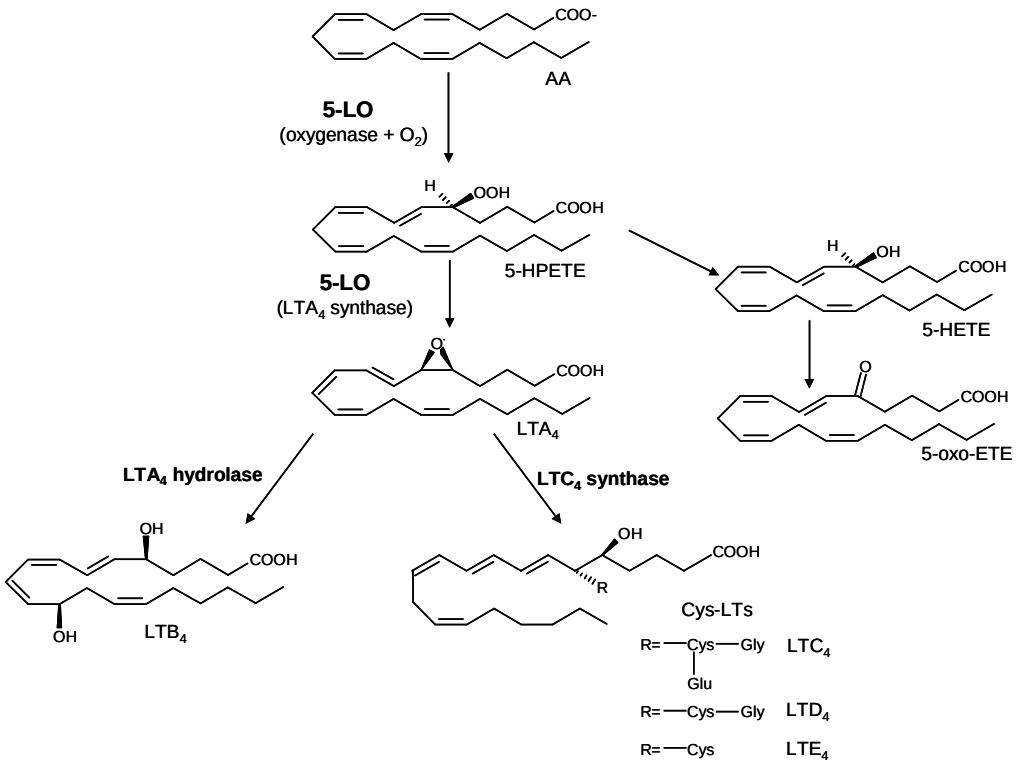

Figure 2.7: Conversion of arachidonic acid in leukotrienes by 5-Lipoxygenase [330]

2.5.2 Structure and Regulation of 5-LO

So far, the 3D structure of 5-LO has not been resolved. However, practicable computational models of 5-LO based on the structure of 15-LO from rabbit have been used to explain the interactions between compounds and the enzyme [334, 124]. The structure of 5-LO is composed of two domains: C-terminal and N-terminal domain. The catalytic C-terminal domain is mainly helical and contains iron. The smaller N-terminal domain is a C2-like β sandwich with typical ligand-binding loops [124, 133]. The C-terminal domain contains a non-heme iron in the active site, essential for their catalytic activity. This iron acts as an electron acceptor or donor during catalyses. In the inactive form, the iron is presented in the ferrous state (Fe^{2+}), whereas the catalytic active 5-LO requires conversion to the ferric (Fe^{3+}) iron [9].

5-LO is phosphorylated by MAP kinase kinase and traffics through the nuclear pore, possibly in association with NF-κB [298, 332]. During cell activation, for example, by the intracellular increase of Ca^{2+}, both cytosolic and nuclear soluble 5-LO can translocate to the nuclear envelope, leading to colocalization with cytosolic phospholipase A2 and lipoxygenase activating protein. This migration of 5-LO ist probably important for its activity and regulation [250].

2.5.3 5-LO Inhibitors

The most inhibitors, synthetic and as well as from natural sources (e.g., polyphenols, coumarins and quinones) act at the catalytic domain by reducing or chelating the active-site iron or simply by scavenging electrons participating in the redox cycle of iron [329, 333]. Until now, no pharmacological data demonstrate inhibition of 5-LO interfering with the C-2-like domain [330]. Compounds that interfere with cellular 5-LO traffic will cause a suppression of LT formation. For example, natural compounds that interfere with Ca^{2+} prevent the activation of 5-LO without inhibiting the enzyme directly [330].

Redox-active 5-LO inhibitors comprise lipophilic reducing agents, and among those, there are many plant derived classes like flavonoids, coumarins, quinones, lignans and other polyphenols.

These drugs act by keeping the active site iron in the ferrous state, thereby uncoupling the catalytic cycle of the enzyme. They are highly efficient inhibitors of 5-LO product formation *in vitro* and partially also *in vivo*. Iron ligand inhibitors chelate the active site iron via a hydroxamic acid or an N-hydroxyurea moiety and also exert weak reducing properties. BWA4C, a hydroxamic acid belongs to this class of potent orally-active 5-LO inhibitor [330].

Examples of natural compounds that inhibit the 5-LO pathway are the constituents of *Boswellia serrata* [264, 265], hyperforin, the main ingredient of the extracts of *Hypericum perforatum* [8] and myrtucommulon, a acylphloroglycinol from the leaves of *Myrtus communis* [88]. Licofelone is also an example of an anti-inflammatory natural drug that inhibits 5-LO and COX pathway and is currently undergoing in the phase III trials for osteoarthritis [160].

2.6 Wound Healing Process: Scratch and Elastase

A complex series of cellular and molecular events including inflammation, cellular proliferation and migration, angiogenesis and matrix remodeling are involved in wound healing. This process requires the coordinate involvement of different cell types, such as keratinocytes, fibroblasts, endothelial and inflammatory cells. These cells proliferate into the wound area, synthesize new extracellular matrix (ECM), as well as express thick actin bundles as myofibroblasts [252].

Wound healing involves continuous cell-cell and cell-matrix interactions that allow the process to occur in three overlapping phases: inflammation (0-3 days), cellular proliferation (3-12 days) and remodeling (3-6 months) [277]. These processes are mediated by molecular signals, involving cytokines and growth factors, which stimulate and modulate the main cellular activities that underscore the healing process [328].

Extracellular and cytosolic concentration of calcium plays a central role in the remodeling of tissue during wound healing, particularly in epidermal cell migration [174, 49]. Moreover, other components of cell signaling are known to be involved in wound healing such as MAPK [186, 57].

The scratch assay has been used to obtain first insights how plant preparations and their isolated

compounds can positively influence the formation of new tissues and repair them. Through this assay, it is possible to evaluate the proliferation and migration of fibroblast to the wounded area [100]. One example of plant formulation that stimulates the wound reepithelialization is eupolin ointment, prepared from the leaves of *Chromolaena odorata* [239]. Fronza *et al.*, (2009) [100] also showed potential wound healing effects for *Calendula of cinalis*.

Another important target involved in wound healing is the serinprotease elastase, which is mainly secreted by neutrophils, and also to a lesser extent by keratinocytes and fibroblasts. Secreted elastase can degrade local extracellular matrix proteins, modulate the function of other inflammatory cells, such as lymphocyte activation, as well as the influx of neutrophils into the site of inflammation. Studies have being shown that uncontrolled elastase activity may be implicated in delayed wound healing and in a decrease of skin elasticity [292].

3 Results and Discussion

In this chapter, the phytochemical results and discussion from the bioguided fractionation, isolation and structural elucidation of the compounds from *Cordia americana* and *Brugmansia suaveolens* are presented. In the second part, the results and discussion about the biological investigations of the plant extracts and their corresponding characterized compounds are reported.

3.1 Phytochemical Investigation

3.1.1 *Cordia americana*

3.1.1.1 Bioguided Fractionation based on p38α MAPK Assay

The ethanolic extract from *Cordia americana* was fractionated by Sephadex®LH-20 open column chromatography and methanol as mobile phase (see Section 5.6.1, Experimental Part). The fraction sets were analysed by using the p38α assay (see Table 5.12, Experimental Part) and the active fractions with higher output yields (see criteria in Section 5.6.1, Experimental Part), such as fractions E, F, G, H, I and K were further investigated in order to characterize the compounds which may be responsible for the biological activity. In fraction E, the compounds CA6, CA7 as well as CA8 and CA9 were identified using GC-MS by comparison of the experimental data with the data from a natural compound in the library (see Section 5.4.7.1, Experimental Part). CA5 was identified from fraction I by LC-ESI-MS. Parts of the fractions F, G, H and K were subfractionated by flash chromatography over a RP-18 column and a mixture of methanol and water as eluent (further details see Section 5.6.1, Experimental Part). The following compounds were isolated from

the fractions: CA3 from fraction F; CA4 from fraction G; CA1 from fraction K; and CA2 from fraction H.

The ethanolic extract from the leaves of *Cordia americana* as well as the isolated compounds were evaluated for their inhibition acitivity for p38α, JNK3, TNFα release, 5-lipoxygenase, NF-κB activation and in the fibroblast scratch assay.

3.1.1.2 Identi cation and Structural Elucidation

Phytochemical studies (i.e., MS and NMR analysis, see Section 5.4, Experimental Part) resulted in the identification of compounds in *Cordia americana*, which are described in the following sections. The absolute configuration of all characterized compounds were not studied. All chemical structures are in accordance with their literature.

3.1.1.2.1 CA3: 3-(3,4-dihydroxyphenyl)-2-hydroxypropanoic acid

The subfractionation of fraction F was performed by flash chromatography over a RP-18 column using methanol and water as mobile phase (see Section 5.6.1.1, Experimental Part) and resulted in 5 mg of 3-(3,4-dihydroxyphenyl)-2-hydroxypropanoic acid (syn., danshensu). This compound was isolated as a light gray powder and its chemical structure is shown in Figure 3.1. This structure was confirmed by MS and NMR spectroscopic data.

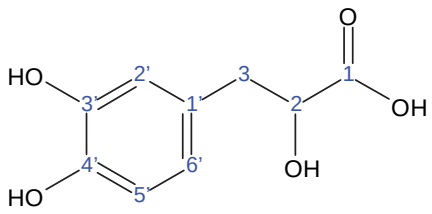

Figure 3.1: Chemical structure of CA3

Useful structural information was supplied by mass spectrometry. The EI mass spectrometry (see Figure 3.2) showed a molecular ion peak[1] at *m/z* 198.1 [M] (11), and further peaks at *m/z*: 123.1 [$C_7H_7O_2$] (100) (i.e., base peak); 77.1 [C_6H_5] (11). Based on the molecular mass at *m/z* =

[1] In brackets, the relative intensity in % of the ion peaks is shown.

198.1 and on the structural information obtained by NMR analysis, the molecular formula $C_9H_{10}O_5$ was attributed to compound CA3.

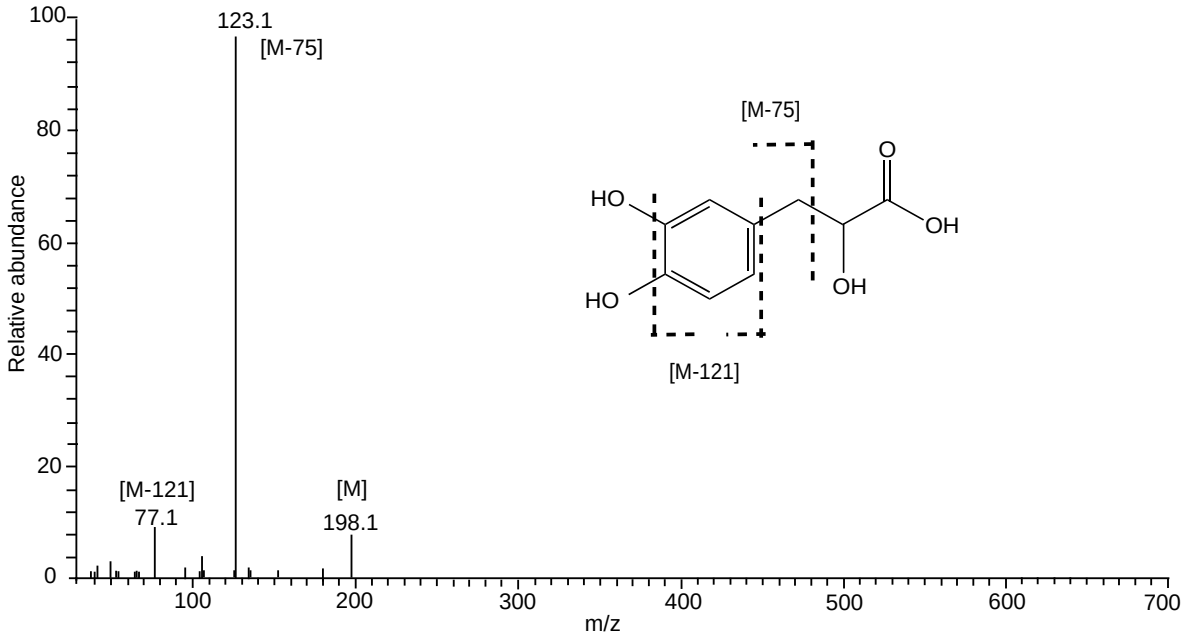

Figure 3.2: EI-MS of CA3

The ^{1}H-NMR spectrum shows 6 signals (see Figure 3.3). The methylene group corresponding to the two protons at C-3 gave two signals with chemical shifts at δ = 2.72 ppm and 2.93 ppm, as a result of the non-equivalence of these two protons caused by the asymmetry center at the C-2 position. The three protons of the aromatic ring, that is C-2′, C-5′ and C-6′, have chemical shifts at δ = 6.71 ppm, δ = 6.56 ppm and δ = 6.66 ppm, respectively.

The ^{13}C-NMR spectrum (see Figure 3.4) shows 9 signals, which correspond to 9 carbons. The peaks between δ = 116.16 ppm and δ = 145.91 ppm are located in the aromatic region. The signal at δ = 177.44 ppm is located in the carbonyl region and can be assigned to the COOH group of the compound. The signal at δ = 40.72 ppm correlates with the methylene group and is confirmed by the negative signal from CH_2 in the DEPT-135 spectrum (see Figure 3.5).

The H-H-COSY spectrum (see Figure 3.6) shows a coupling between the protons δ = 4.25 ppm, δ = 2.72 ppm and δ = 2.93 ppm with coupling constant J = 12.5 Hz and J = 7.5 Hz. Additionally, a coupling between the protons δ = 6.56 ppm and δ = 6.66 ppm is exhibited.

Based on the MS, 1D- and 2D-NMR analysis, 3-(3,4-dihydroxyphenyl)-2-hydroxypropanoic acid (syn. danshensu) was identified as the compound CA3 and compared to the literature [136], as shown in Table 3.1.

Table 3.1: Chemical shifts of CA3 and literature

Atom numbers	^{13}**C*** δ**/ppm**	^{13}**C**** δ**/ppm**	^{1}**H*** δ**/ppm (Mult., J(Hz), H)**	^{1}**H**** δ**/ppm (Mult., J(Hz), H)**	^{1}**H - ^{1}H*** **COSY**
1	177.4	177.15	-	-	-
2	73.1	72.15	4.25 (s, 1H)	4.32 (s, 1H)	3
3	41.0	39.95	2.72 (dd, 12.52, 7.5 Hz, 1H); 2.93 (d, 12.9 Hz,1H)	2.73 (dd, 1H); 2.98 (d, 1H)	2, 3
$1'$	130.3	129.75	-	-	-
$2'$	116.2	116.70	6.71 (brs, 1H)	6.79 (s, 1H)	-
$3'$	144.9	144.30	-	-	-
$4'$	145.9	144.35	-	-	-
$5'$	117.2	116.95	6.56 (d, 7.8 Hz, 1H)	6.72 (d, 1H)	$6'$
$6'$	121.9	121.85	6.66 (m, 1H)	6.60 (dd, 1H)	$5'$

* In MeOH-d_4. ** Data from the literature [136].

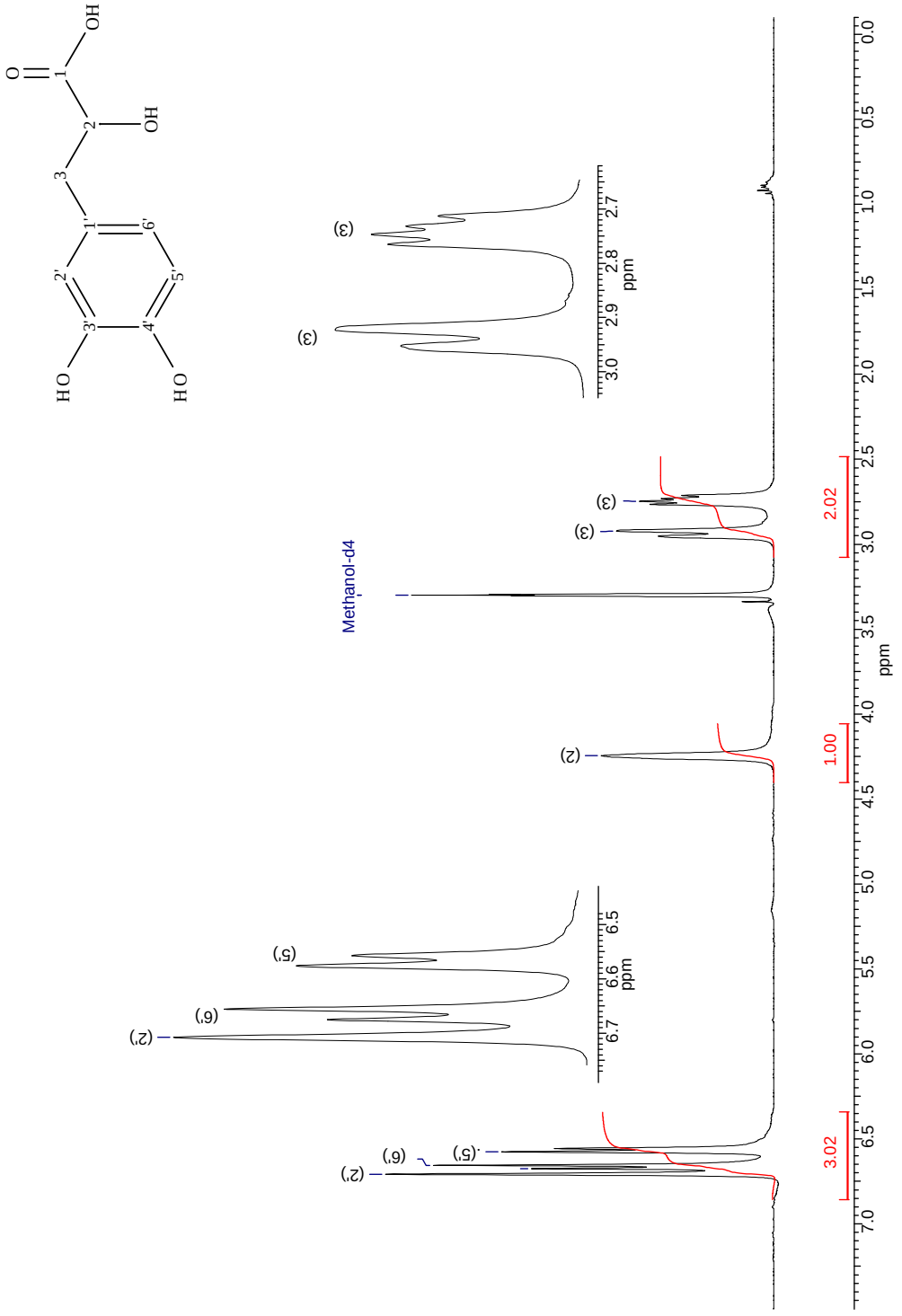

Figure 3.3: ^{1}H-NMR of CA3 (400 MHz, MeOH-d_4)

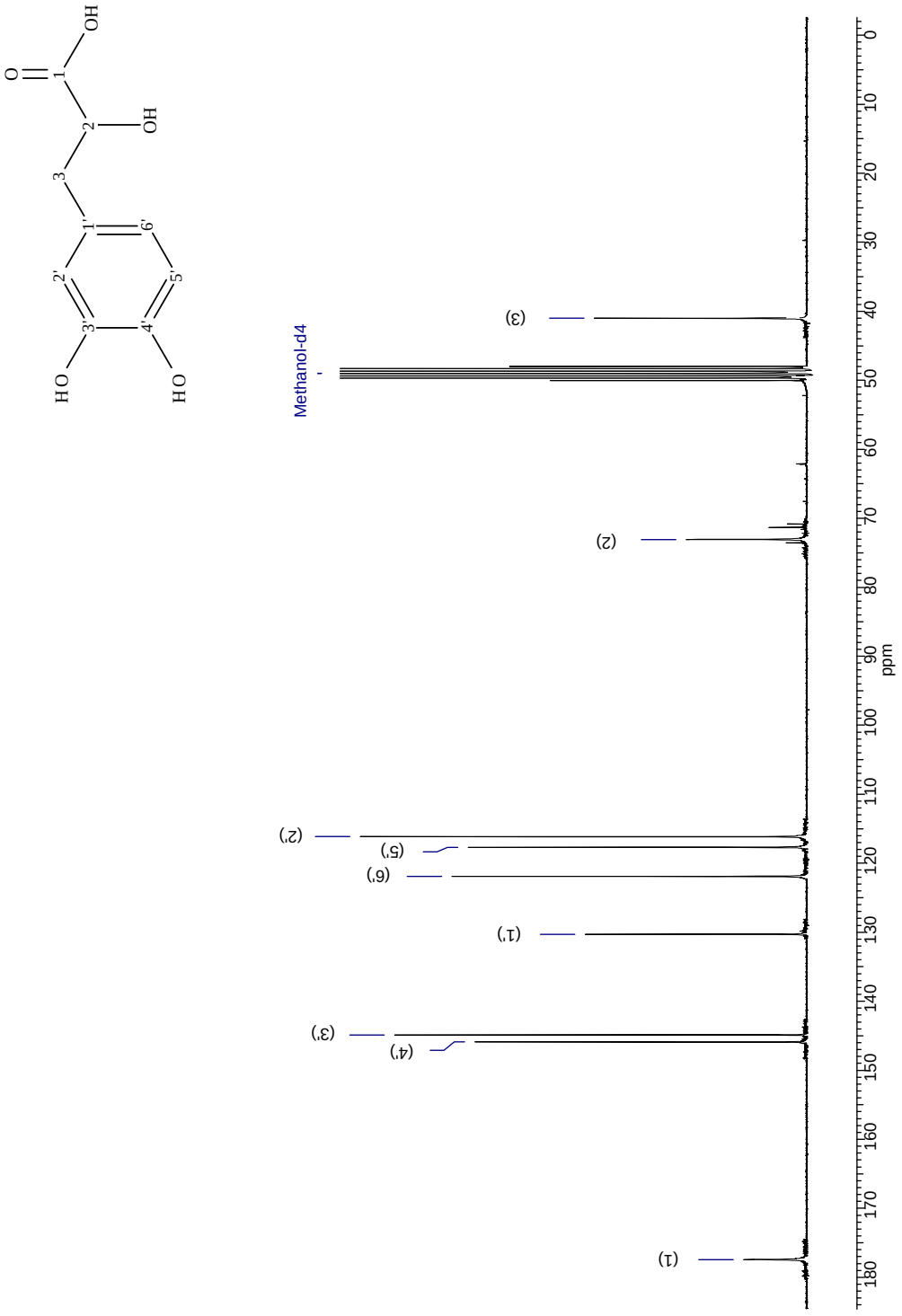

Figure 3.4: ^{13}C-NMR of CA3 (100 MHz, MeOH-d_4)

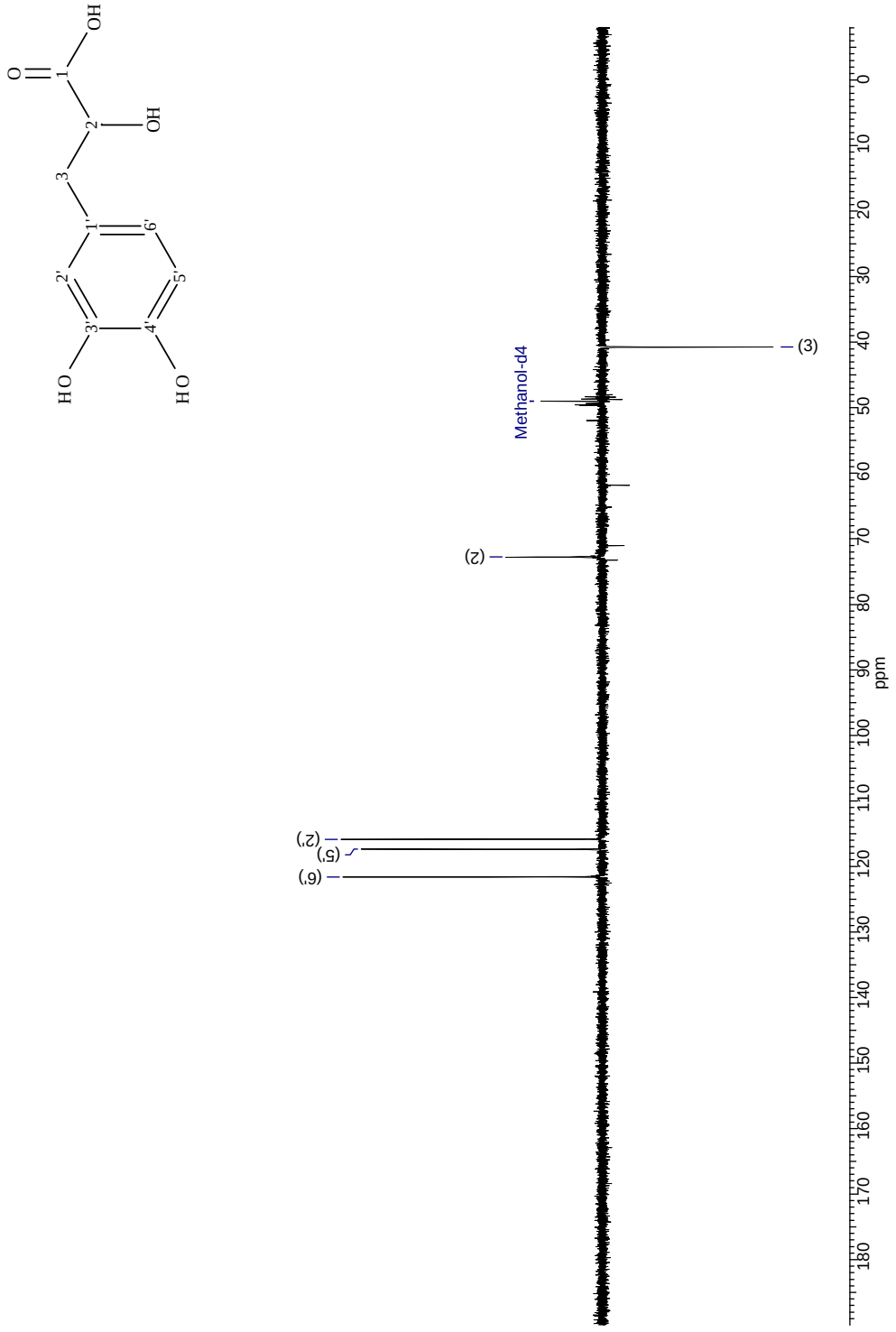

Figure 3.5: DEPT-135 of CA3 (100 MHz, MeOH-d_4)

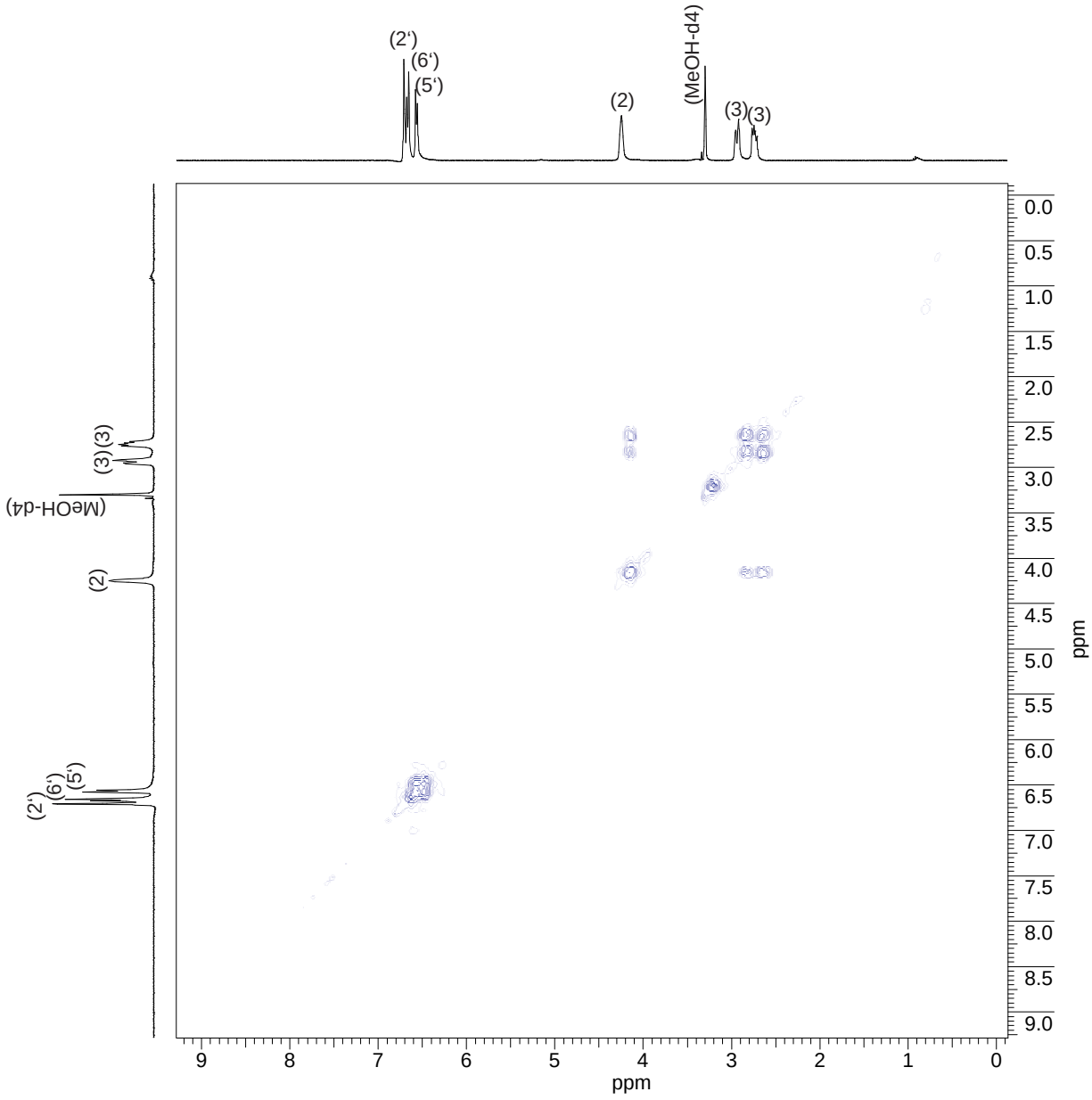

Figure 3.6: H-H-COSY of CA3 (400 MHz, MeOH-d_4)

3.1.1.2.2 CA1: Rosmarinic Acid

The subfractionation of fraction K was separated by flash chromatography over a RP-18 column using methanol and water as mobile phase (see Section 5.6.1.1, Experimental Part) and resulted in 12 mg of rosmarinic acid[2]. This compound was isolated as a light gray colored powder and its chemical structure can be observed in Figure 3.7. This structure was established on the basis of UV, IR, MS and NMR spectroscopic data.

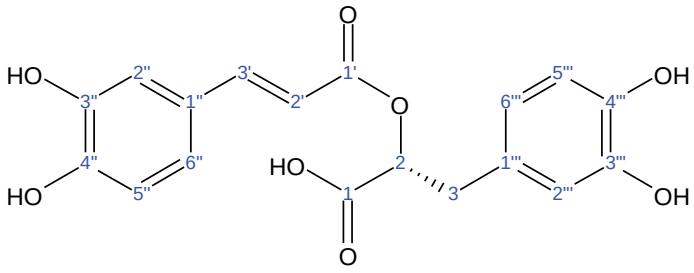

Figure 3.7: Chemical structure of CA1

The UV spectrum of CA1 (see Figure 3.8) exhibited two absorption maxima (in MeOH) at λ = 290 and 330 nm. The FTIR spectrum (see Figure 3.9) showed distinguishable absorption bands at: 3165.4, 1707.2, 1617.4, 1515.6, 1348.7, 1285.1, 1260.4, 1231.5, 1200.5, 1154.0, 1113.4, 1075.9, 972.3, 851.7, 818.8, 781.4 cm^{-1}.

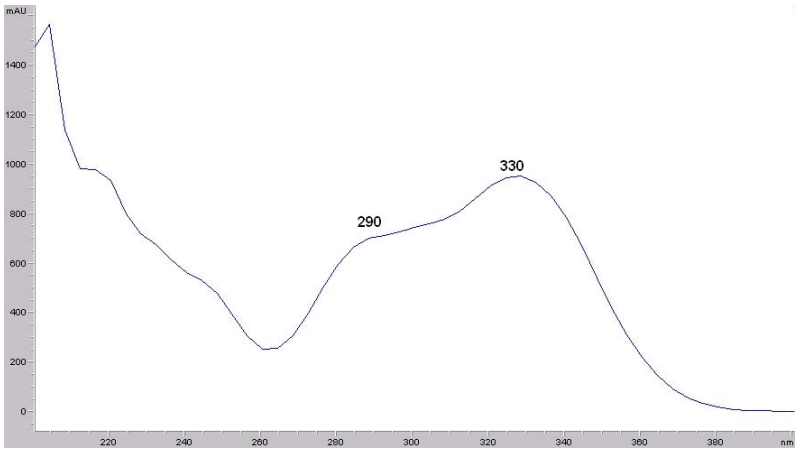

Figure 3.8: UV spectrum of CA1

[2]IUPAC name: (2R)-3-(3,4-dihydroxyphenyl)-2-[(E)-3-(3,4-dihydroxyphenyl)prop-2-enoyl]oxypropanoic acid

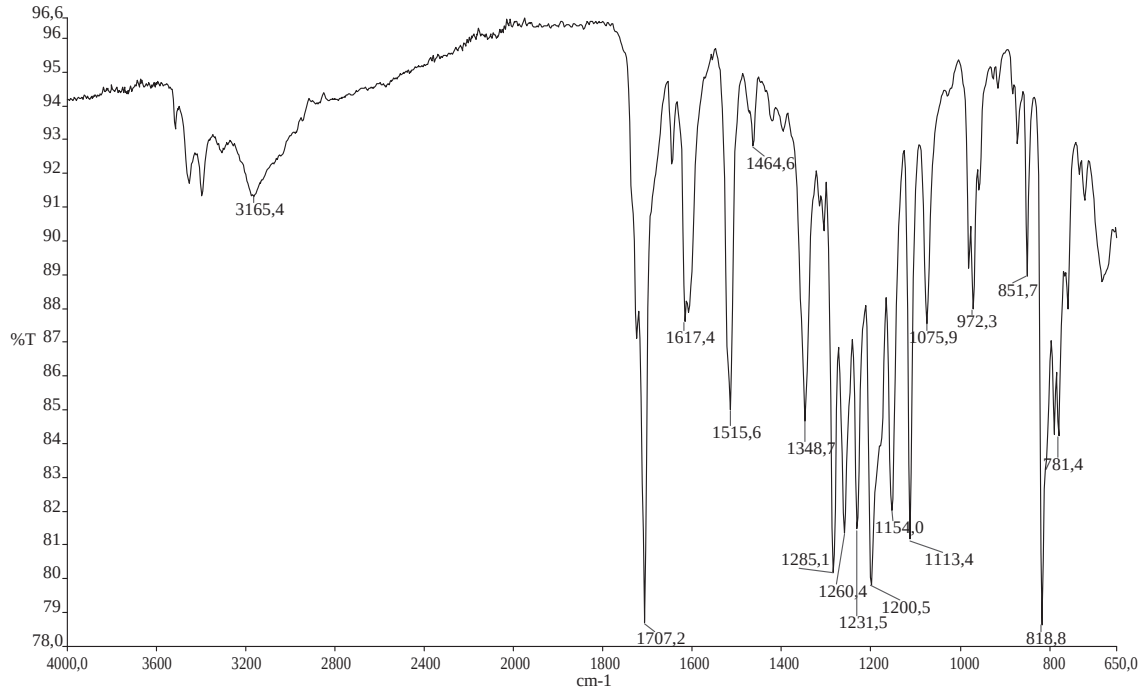

Figure 3.9: IR spectrum of CA1

The ESI-MS (negative mode) (see Figure 3.10) revealed the a quasimolecular peak[3] $[M - H]^-$ at *m/z* = 359.0 (100) (i.e., base peak). Further ions at *m/z* = 197.0 (10) and *m/z* = 161.1 (36) resulted from the loss of caffeic acid (163) and of 3-(3,4-dihydroxyphenyl)-2-hydroxypropanoic acid (197). On the basis of the molecular mass at *m/z* = 360.1 and the structural information obtained by NMR analysis, the molecular formula $C_{18}H_{16}O_8$ was attributed to compound CA1. This molecular mass was confirmed by the high resolution FT-ICR-MS for $[M - H]^-$ at *m/z* = 359.076450 (calculated mass for $C_{18}H_{16}O_8$ was 359.07614).

[3]In brackets, the relative intensity in % of the ion peaks is shown.

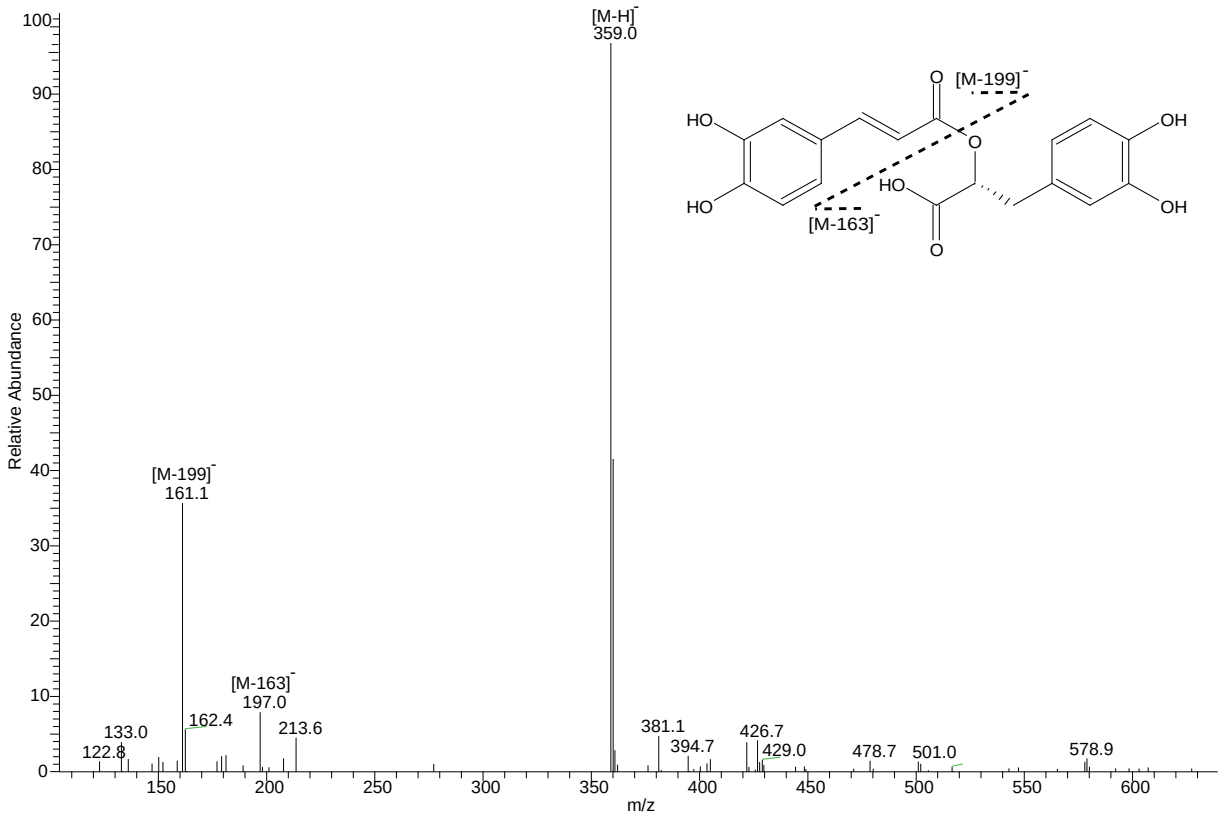

Figure 3.10: ESI-MS (negative mode) of CA1

The NMR analysis of CA1 showed similarities to that of compound CA3 (see Section 3.1.1.2.1). The ^{1}H-NMR spectrum shows 11 signals (see Figure 3.11). The aliphatic region has two signals with chemical shifts at δ = 2.92 ppm and δ = 3.08 ppm and can also be assigned to the methylene group of the 3-(3,4-dihydroxyphenyl)-2-hydroxypropanoic acid structural unit. The six protons of the two aromatic rings have the chemical shifts between δ = 6.65 ppm and δ = 7.02 ppm. The H-H-COSY spectrum (see Figure 3.14) shows similar couplings compared to the compound CA3. Additionally, the protons H-2$'$ and H-3$'$ of the double bond in the caffeic acid and appear as two doublets (δ = 6.26 ppm and δ = 7.49 ppm) in the ^{1}H-NMR spectrum.

The ^{13}C-NMR spectrum (see Figure 3.12) shows 18 signals for 18 carbons. The peaks between δ = 114.09 ppm and δ = 149.12 ppm are located in the aromatic region, corresponding to two aromatic rings. The two signals δ = 177.41 ppm and δ = 168.88 ppm in the carbonyl region are defined through the both carbonyl groups of the acid and ester functions in the molecule CA1.

Figure 3.13 depicts the negative signal δ = 38.66 ppm, which represents a CH_2 in the DEPT-135 spectrum. The other signals are visualized in ^{13}C-NMR spectrum.

Based on the MS, 1D- and 2D-NMR analysis, the chemical-shift values of the protons and carbons were in agreement with those of the rosmarinic acid, which was compared to the literature [340] as shown in Table 3.2.

Table 3.2: Chemical shifts of CA1 and literature

Atom numbers	^{13}**C*** δ**/ppm**	^{13}**C**** δ**/ppm**	^{1}**H*** **δ/ppm (Mult., J(Hz), H)**	^{1}**H**** **δ/ppm (Mult., J(Hz), H)**	(^{1}**H** - ^{1}**H**)* **COSY**
1	177.41	177.67	-	-	-
2	77.61	77.79	5.07 (dd; 9.9, 3.3 Hz; 1H)	5.09 (dd; 10.0, 3.5 Hz; 1H)	3
3	38.66	38.93	3.08 (dd; 9.9, 3.3 Hz; 1H); 2.92 (dd; 14.31, 9.9 Hz; 1H)	3.10 (dd; 14.5, 3.5 Hz; 1H); 2.94 (dd; 14.5, 10.0 Hz; 1H)	2, 3
$1'$	168.88	169.24	-	-	-
$2'$	115.56	115.77	6.26 (d; 15.8 Hz; 1H)	6.27 (d; 15.5 Hz; 1H)	$3'$
$3'$	146.51	146.79	7.49 (d; 15.8 Hz; 1H)	7.51 (d; 15.5 Hz; 1H)	$2'$
$1''$	127.84	128.12	-	-	-
$2''$	114.90	115.27	7.02 (d; 1.8 Hz; 1H)	7.03 (d; 2.0 Hz; 1H)	$6''$
$3''$	145.75	146.85	-	8.75 (s; OH)	-
$4''$	149.12	149.50	-	9.20 (s; OH)	-
$5''$	116.25	116.60	6.75 (d; 7.9 Hz; 1H)	6.77 (dd; 8.0, 2.0 Hz; 1H)	$6''$
$6''$	122.66	123.04	6.91 (dd, 8.36, 1.8 Hz, 1H)	6.91 (dd; 8.0, 2.0 Hz; 1H)	$5''$, $2''$
$1'''$	131.09	131.29	-	-	-
$2'''$	117.28	117.63	6.67 (brs; 1H)	6.77 (d; 2.0 Hz; 1H)	$6'''$
$3'''$	146.31	146.08	-	8.81 (s; OH)	-
$4'''$	144.58	144.93	-	9.68 (s; OH)	-
$5'''$	115.98	116.60	6.62 (d; 7.5 Hz; 1H)	6.68 (d; 8.0 Hz; 1H)	$6'''$
$6'''$	121.54	121.89	6.65 (m; 1H)	6.63 (dd; 8.0, 2.0 Hz; 1H)	$2'''$

* In MeOH-d_4. ** Data from the literature [340] in CD_3OD.

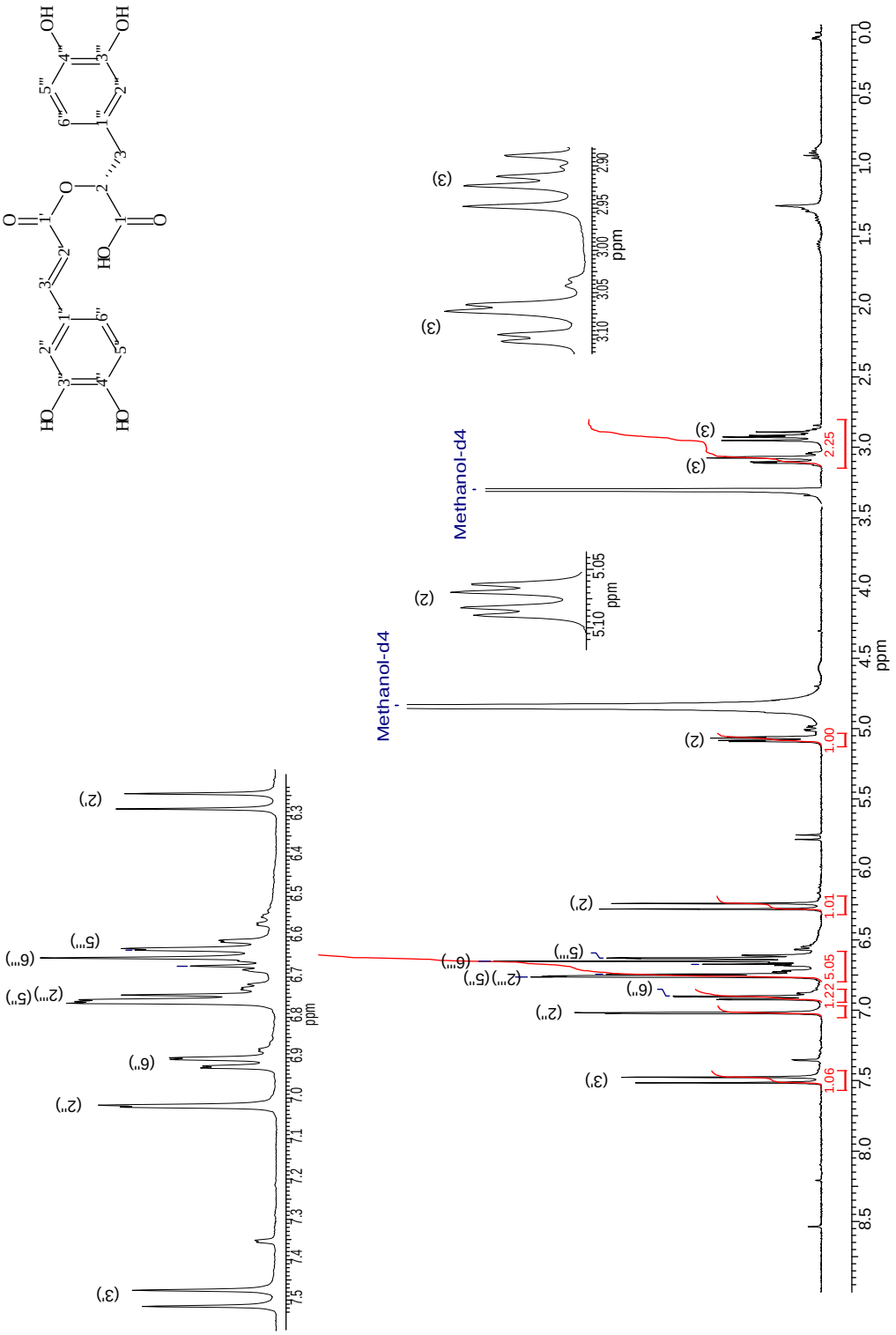

Figure 3.11: ^{1}H-NMR of CA1 (400 MHz, MeOH-d_4)

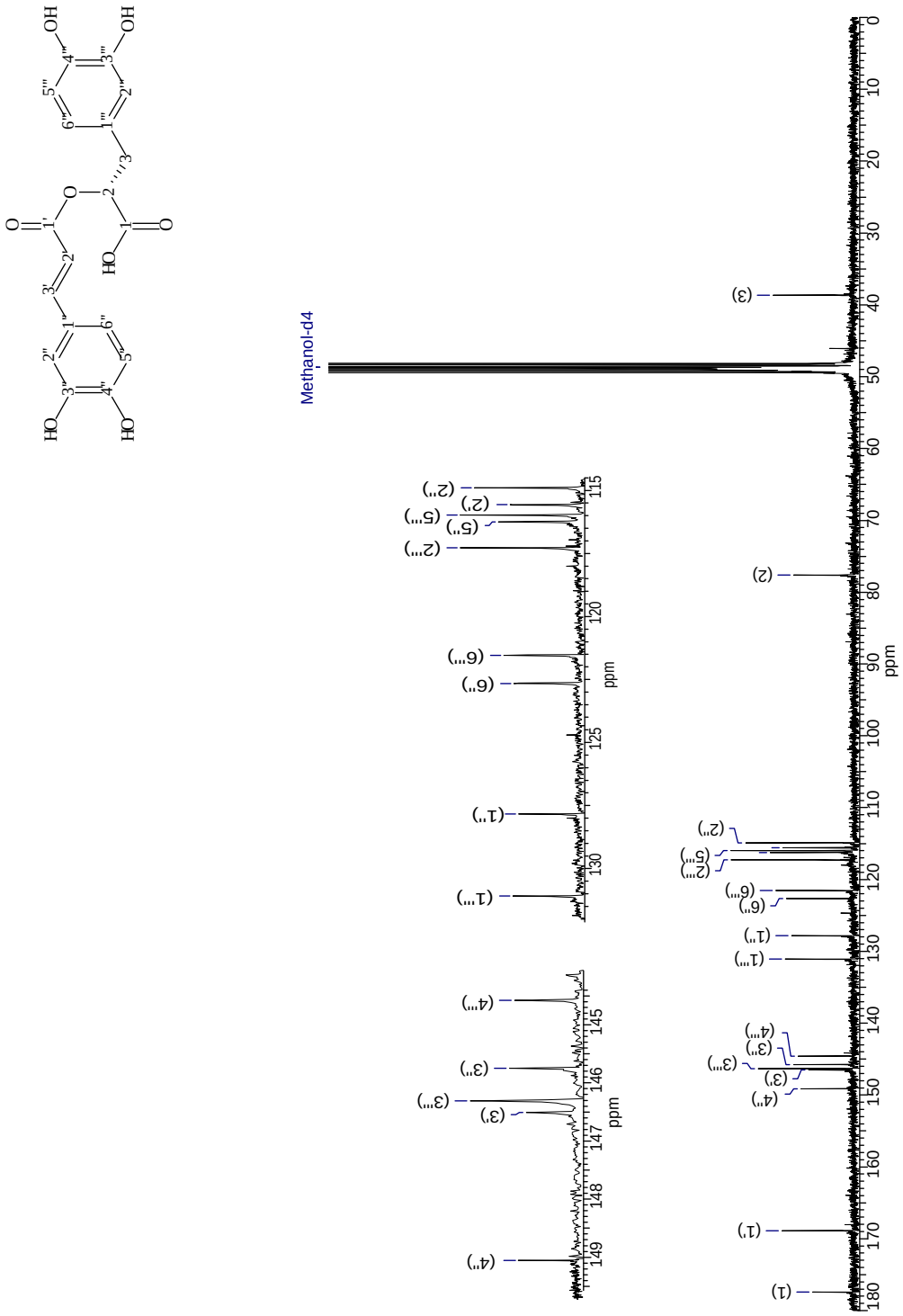

Figure 3.12: ^{13}C-NMR of CA1 (100 MHz, MeOH-d_4)

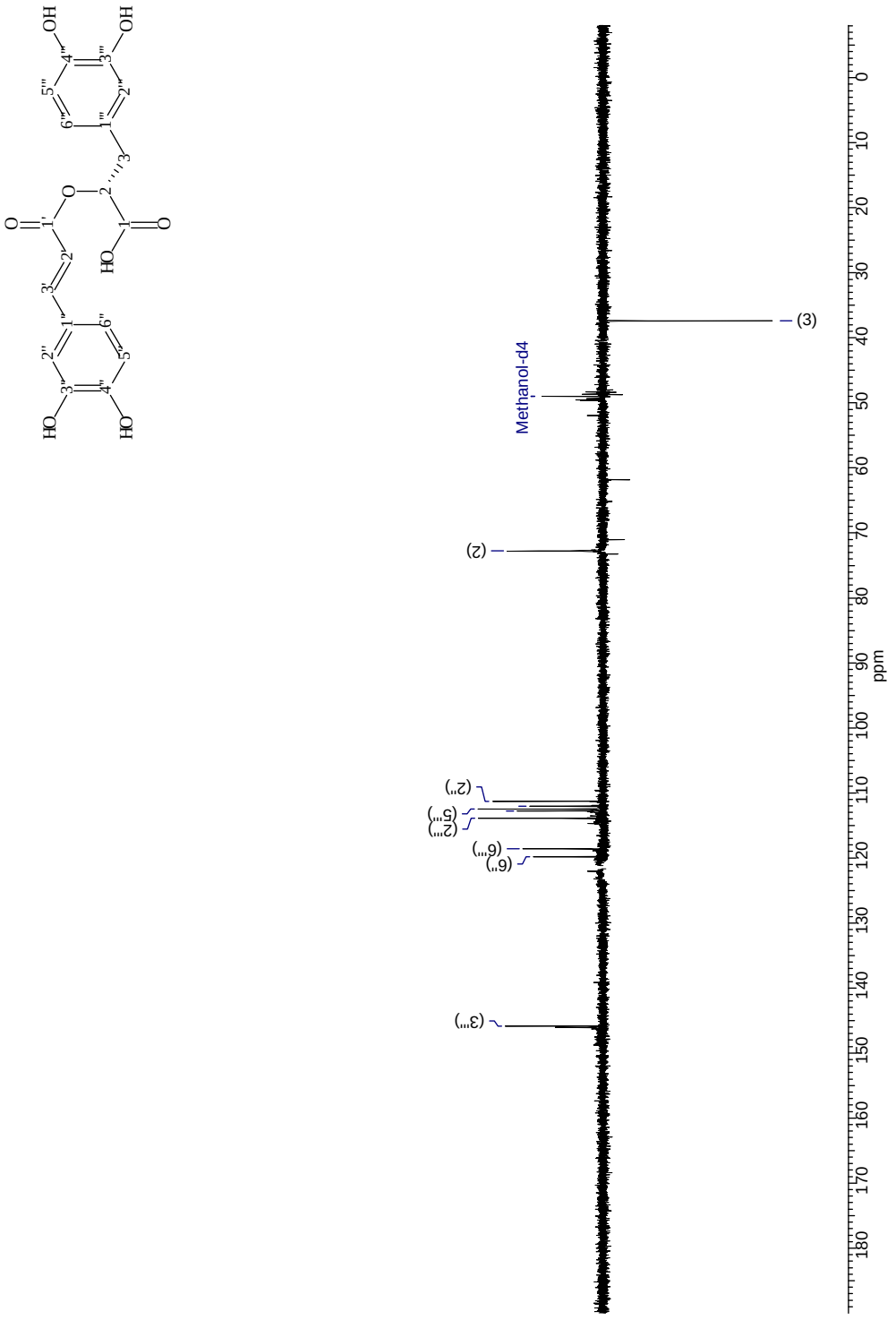

Figure 3.13: DEPT-135 of CA1 (100 MHz, MeOH-d_4)

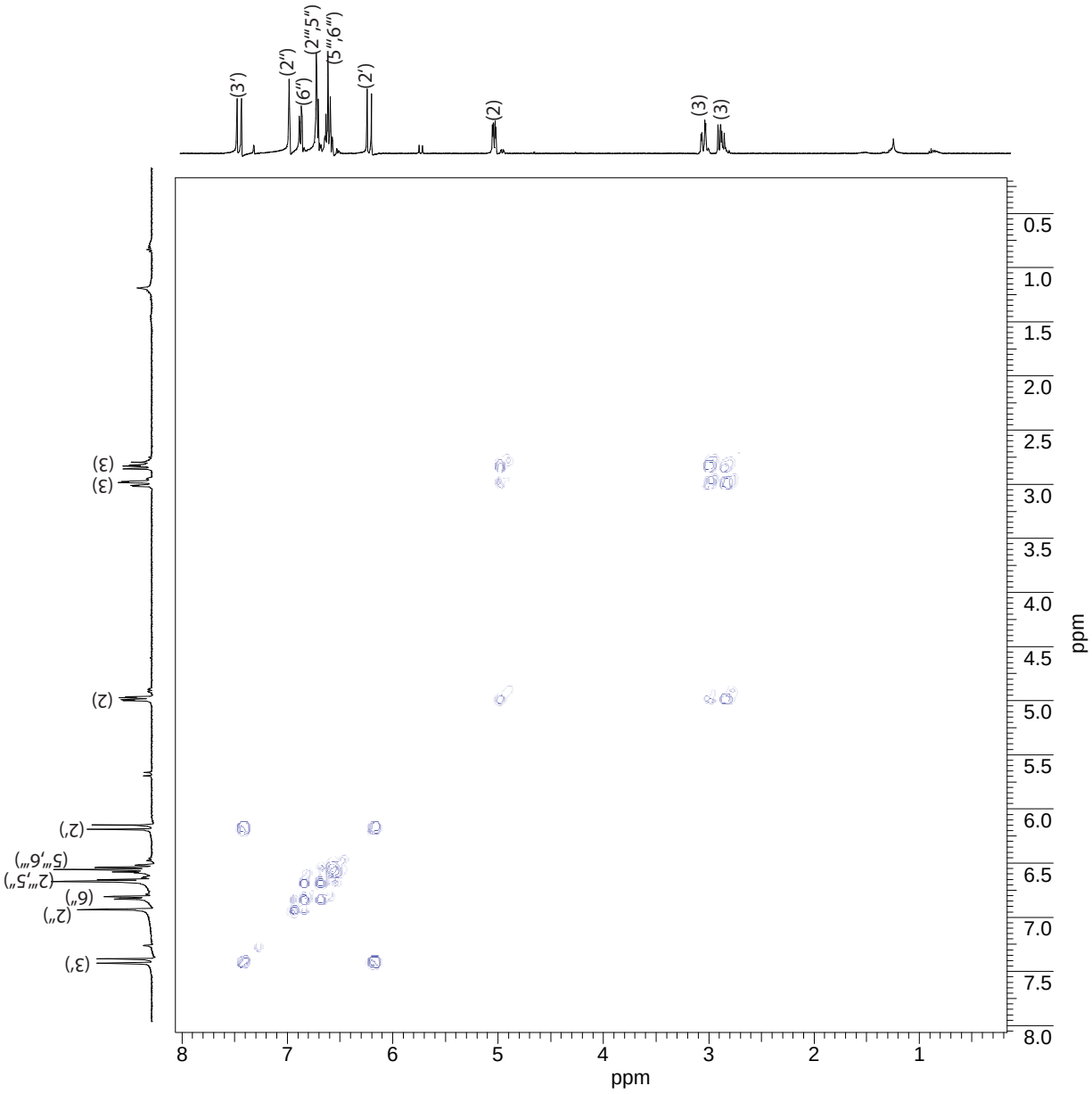

Figure 3.14: H-H-COSY of CA1 (400 MHz, MeOH-d_4)

3.1.1.2.3 CA2: Rosmarinic Acid Ethyl Ester

The subfractionation of fraction H was separated by flash chromatography over a RP-18 column using methanol and water as mobile phase (see Section 5.6.1.1, Experimental Part) followed by a further purification in an analytical HPLC system resulting in 3.3 mg of rosmarinic acid ethyl ester[4]. This compound was isolated as a light gray amorphous powder and its chemical structure is represented in Figure 3.15. This structure was established on the basis of MS and NMR spectroscopic data.

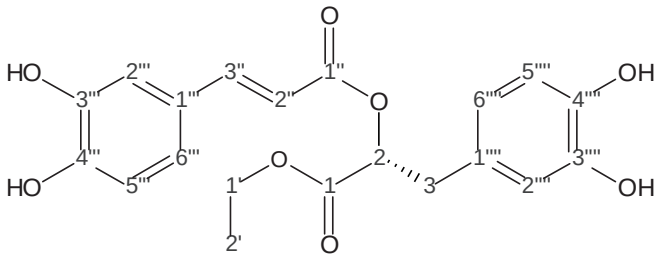

Figure 3.15: Chemical structure of CA2

The ESI mass spectrometry (negative mode) (see Figure 3.16) showed a quasimolecular ion peak[5] at *m/z* = 388.7 $[M]^-$ (24) and further peaks at *m/z*: 387.5 $[M - H]^-$ (100) (i.e., base peak); 207.3 $[M - 179]^-$ (2); 179.3 $[M - 209]^-$ (19); 161.2 $[M - 225]^-$ (4); 135.3 $[M - 253]^-$ (17). Based on the molecular mass at *m/z* = 388.7 and the structural information obtained by NMR analysis, a molecular formula $C_{20}H_{20}O_8$ was assigned to compound CA2. This molecular mass was confirmed by the high resolution FT-ICR-MS for $[M + Na]^+$ at *m/z* = 411.105329 (calculated mass for $C_{20}H_{20}O_8Na$ was 411.10504).

[4]IUPAC name: (1R)-1-(3,4-dihydroxybenzyl)-2-ethoxy-2-oxoethyl (2E)-3-(3,4-dihydroxyphenyl)acrylate
[5]In brackets, the relative intensity in % of the ion peaks is shown.

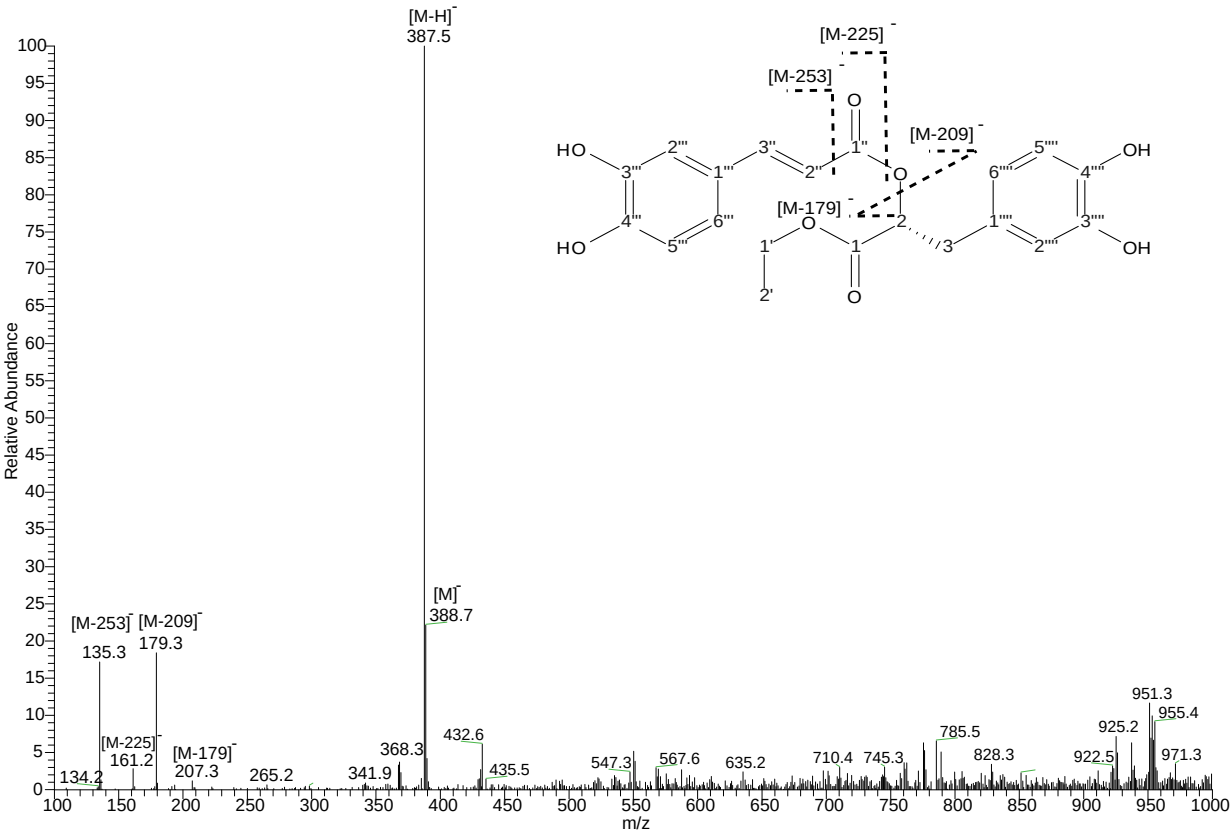

Figure 3.16: ESI-MS (negative mode) of CA2

The NMR analysis showed high similarities with compound CA1 (see Section 3.1.1.2.5). The ^{1}H-NMR spectrum shows 12 signals, which correspond in total to 20 protons (see Figure 3.17). Additionally, signals for five protons occurred δ = 4.17 ppm and δ = 1.30 ppm, which gave a quartet and a triplet in the NMR spectrum, respectively. These protons can be assigned to a methylene and a methyl groups, which correspond to an ethyl ester moiety.

The ^{13}C-NMR spectrum (see Figure 3.18) shows 20 signals for 20 carbons. The peaks between δ = 114.2 ppm and 149.8 ppm are located in the aromatic region, corresponding to two aromatic rings. Comparing with the signal at δ = 177.4 ppm of CA1 located in the carbonyl region, the signal δ = 171.7 ppm in CA2 is shifted to the highfield indicating that the carbonyl group is bound to other group. Figure 3.19 shows the negative signals at δ = 62.4 ppm and δ = 37.9 ppm, which represents two CH_2 groups in the DEPT-135 spectroscopy. The two positive signals at δ = 74.8 ppm and δ = 14.4 ppm in the aliphatic region of the DEPT-135 spectrum are generated by the CH

group of the propanoic acid unit as well as by the CH_3 group of the ethyl ester function. The signal at δ = 37.9 ppm has already been characterized for both compounds CA3 and CA1. Based on the MS, 1D- and 2D-NMR analysis, the chemical-shift values of the protons and carbons were in agreement with those of the rosmarinic acid ethyl ester, which was compared to the literature [340] as shown in Table 3.3.

Table 3.3: Chemical shifts of CA2 and literature

Atom numbers	^{13}**C*** δ**/ppm**	^{13}**C**** δ**/ppm**	^{1}**H*** δ**/ppm (Mult., J(Hz), H)**	^{1}**H**** δ**/ppm (Mult., J(Hz), H)**	(^{1}**H -** ^{1}**H**)* **COSY**
1	171.7	171.91	-	-	-
2	74.8	74.95	5.15 (m; 1H)	5.15 (dd; 7.5, 6.0 Hz; 1H)	3
3	37.9	38.07	3.05 (dd; 13.0, 5.0 Hz; 1H); 2.99 (dd; 13.0, 7.6 Hz; 1H)	3.31 (dd; 14.0, 4.8 Hz; 1H); 3.03 (dd; 14.0, 6.6 Hz; 1H)	2
$1'$	62.4	62.57	4.17 (q; 7.2 Hz: 2H)	4.15 (q; 7.5 Hz; 2H)	$2'$
$2'$	14.4	14.52	1.30 (t; 7.9 Hz; 3H)	1.21 (t; 7.5 Hz; 3H)	$1'$
$1''$	168.4	168.54	-	-	-
$2''$	115.3	114.29	6.29 (d; 15.1 Hz; 1H)	6.27 (d; 16.0 Hz; 1H)	$3''$
$3''$	147.9	148.09	7.58 (d; 15.9 Hz; 1H)	7.56 (d; 16.0 Hz; 1H)	$2''$
$1'''$	127.6	127.70	-	-	-
$2'''$	114.2	115.36	7.07 (d; 2.1 Hz; 1H)	7.05 (d; 2.0 Hz; 1H)	$5'''$
$3'''$	146.9	147.03	-	-	-
$4'''$	149.8	150.07	-	-	-
$5'''$	116.6	116.66	6.81 (d; 8.8 Hz; 1H)	6.78 (d; 8.0 Hz; 1H)	$6'''$
$6'''$	123.2	123.37	6.98 (dd; 8.3 Hz, 1.9 Hz; 1H)	6.96 (dd; 8.0, 2.0 Hz; 1H)	$5'''$
$1''''$	128.8	128.87	-	-	-
$2''''$	117.6	117.75	6.73 (d; 2.01 Hz; 1H)	6.72 (d; 2.0 Hz; 1H)	$6''''$
$3''''$	146.2	146.37	-	-	-
$4''''$	145.4	145.56	-	-	-
$5''''$	116.3	116.44	6.68 (d; 8.0 Hz; 1H)	6.70 (d; 8.0 Hz; 1H)	$6''''$
$6''''$	121.9	121.99	6.71 (dd; 8.7 Hz, 3.09 Hz; 1H)	6.58 (dd; 8.0, 2.0 Hz; 1H)	$5''''$

* In MeOH-d_4. ** Data from literature [340] in CD_3OD.

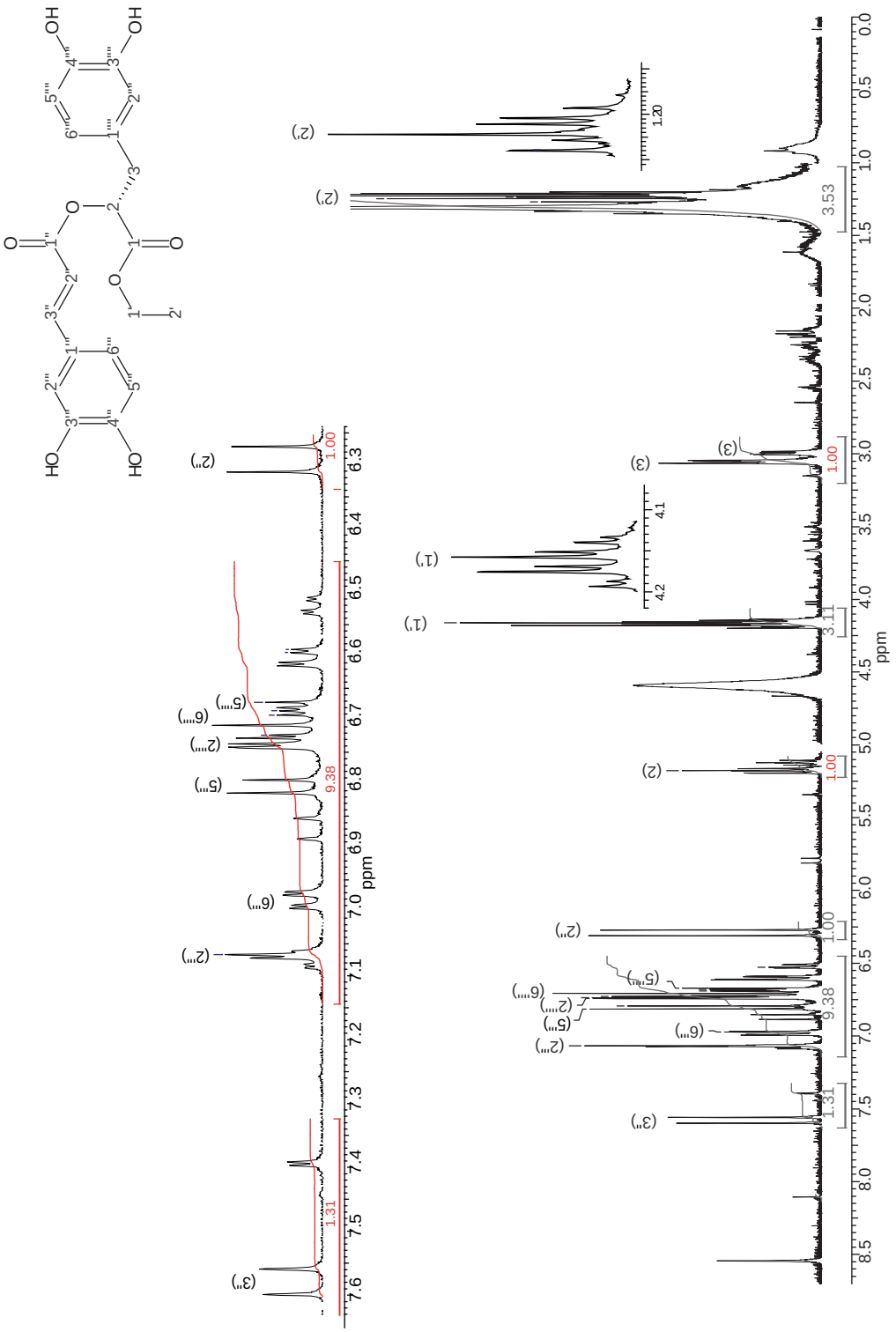

Figure 3.17: ^{1}H-NMR of CA2 (400 MHz, MeOH-d_4)

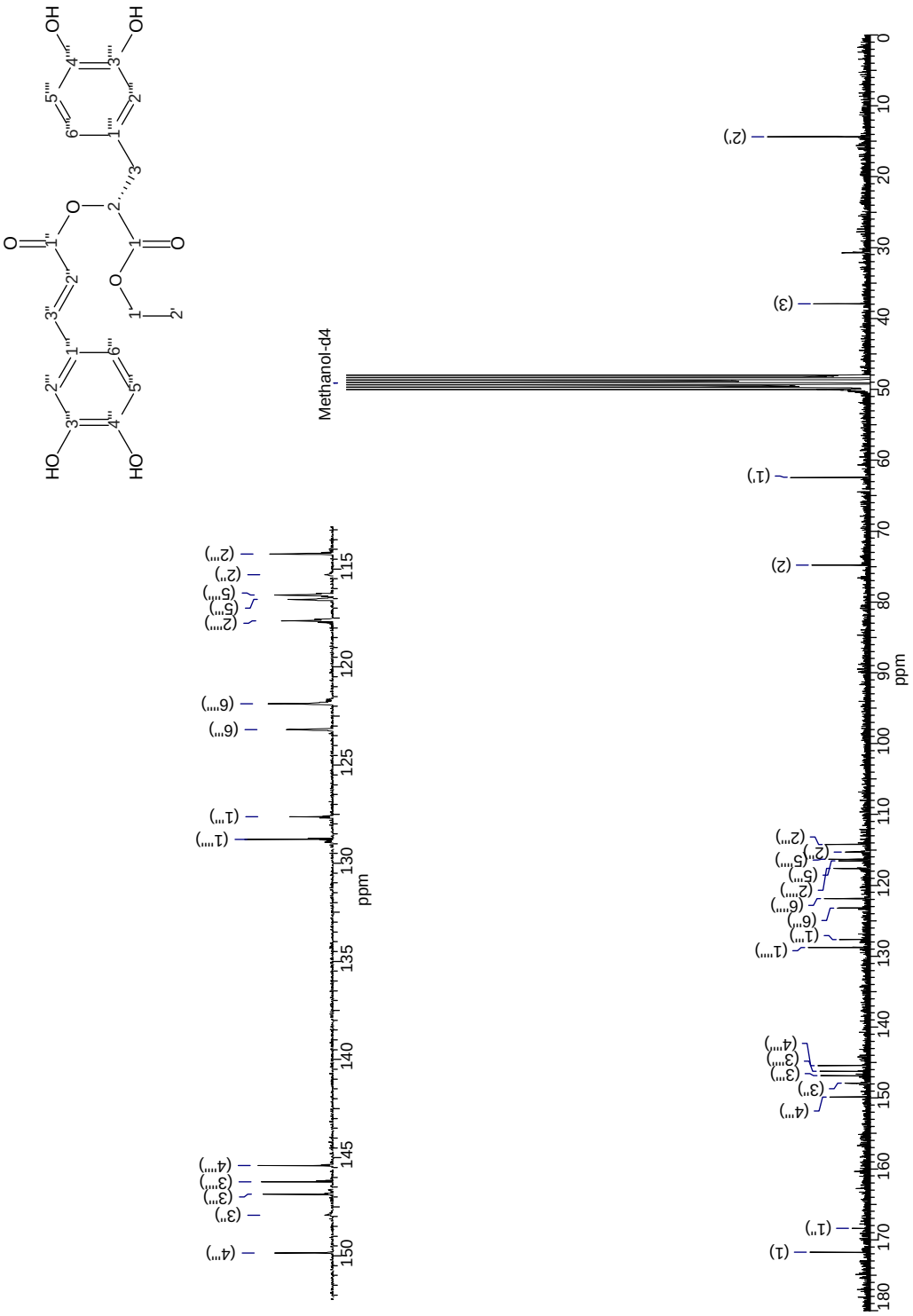

Figure 3.18: ^{13}C-NMR of CA2 (100 MHz, MeOH-d_4)

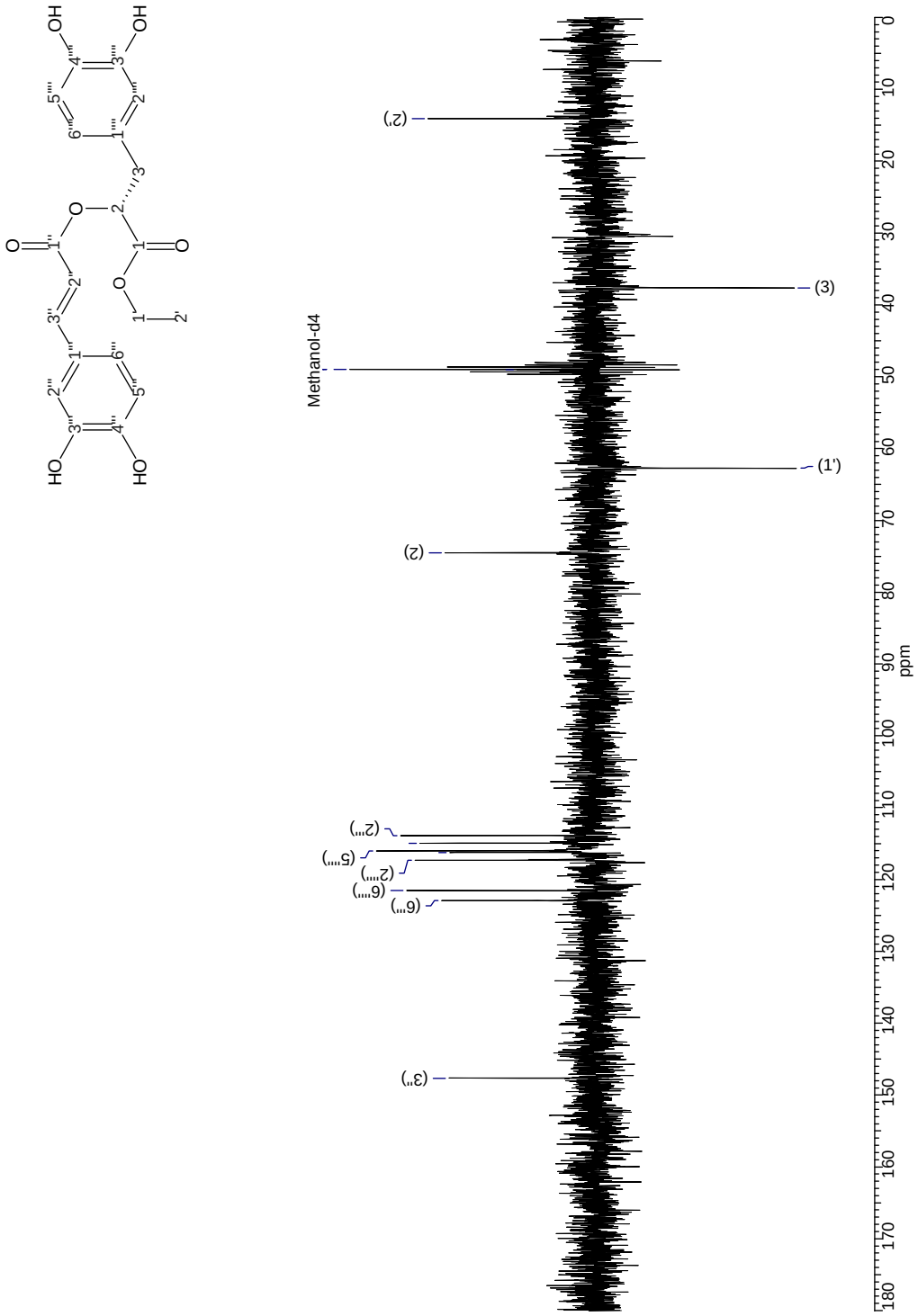

Figure 3.19: DEPT-135 of CA2 (100 MHz, MeOH-d_4)

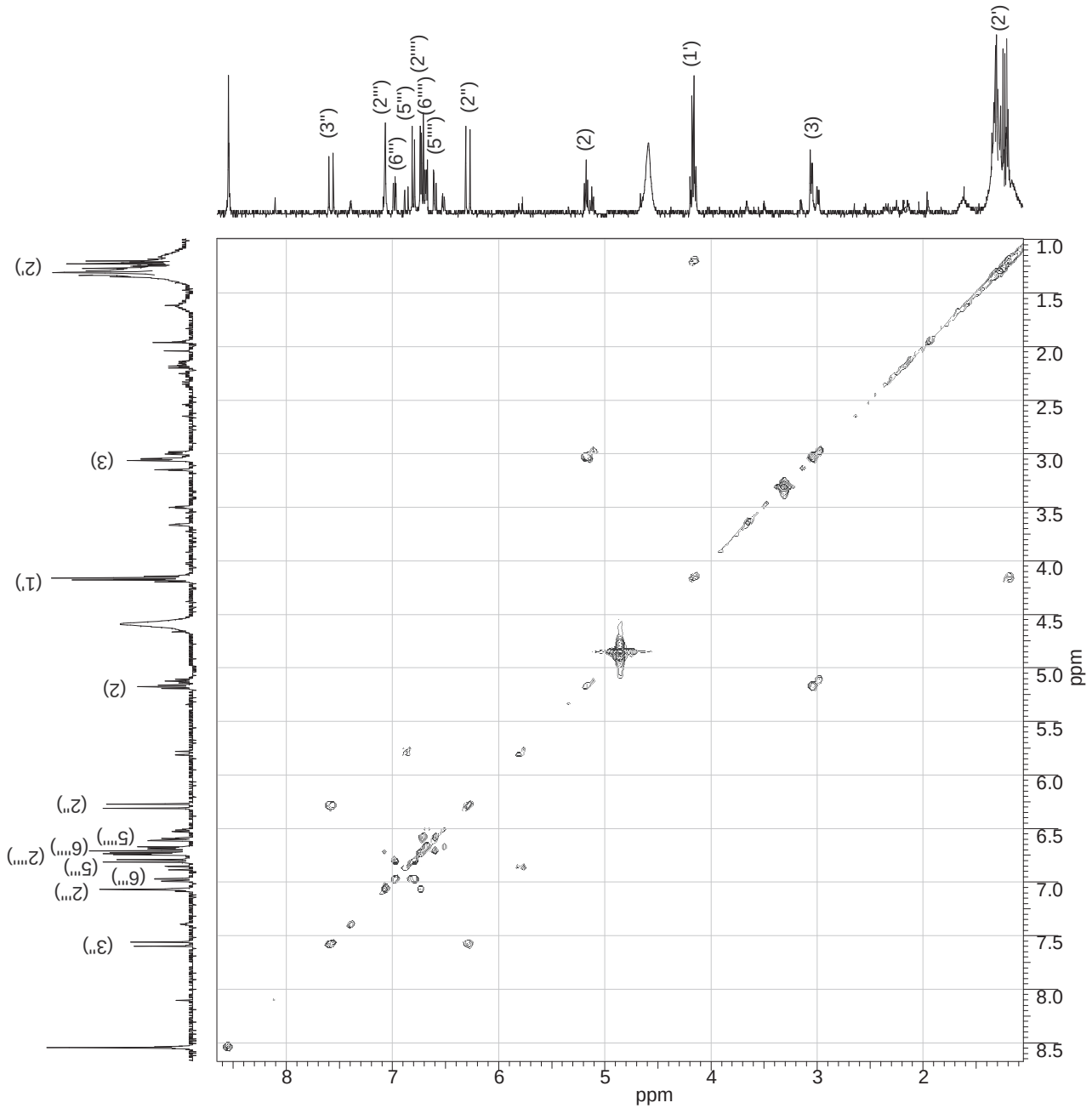

Figure 3.20: H-H-COSY of CA2 (400 MHz, MeOH-d_4)

3.1.1.2.4 CA4: Rutin

The subfractionation of fraction G was performed by flash chromatography over a RP-18 column using methanol and water as eluent (see Section 5.6.1.1, Experimental Part) and resulted in 15 mg of rutin[6]. This compound is a yellow powder and its chemical structure can be observed in Figure 3.21. This structure was also established based on UV, IR, MS and NMR spectroscopic data.

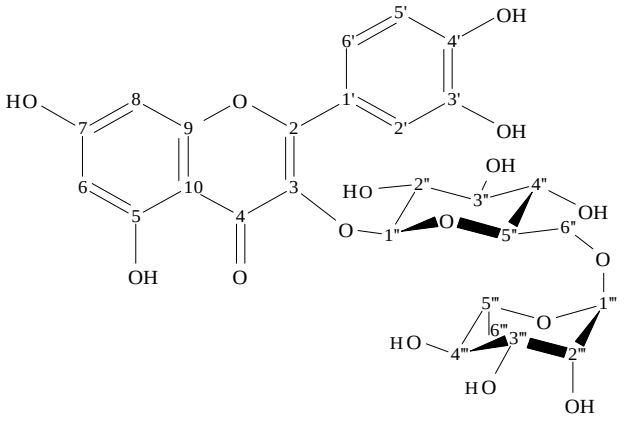

Figure 3.21: Chemical structure of CA4

The UV spectrum of CA4 (see Figure 3.22) exhibited two absorption maxima (in MeOH) at λ = 257 and 354 nm, which indicated the presence of a flavonol structure [196]. The FTIR spectrum (see Figure 3.23) showed the absorption bands at: 3329.6, 1653.9, 1596.1, 1501.0, 1455.7, 1358.9, 1296.4, 1203.3, 1172.2, 1062.9, 1041.9, 1014.5, 1001.2, 967.7, 944.5, 808.0, 707.2, 686.6 cm^{-1}.

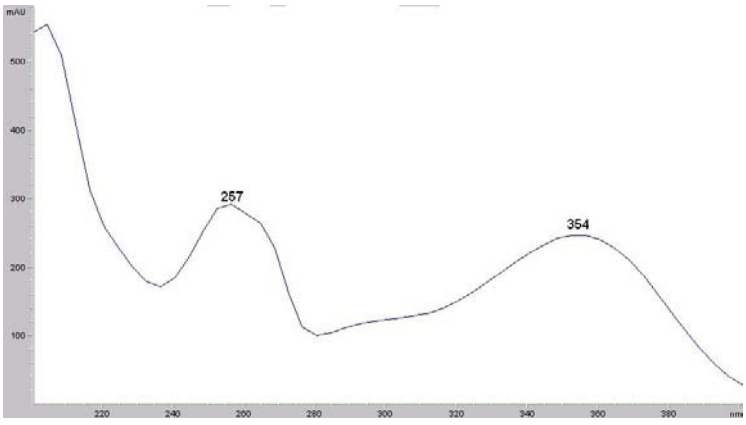

Figure 3.22: UV of CA4

[6]IUPAC name: 2-(3,4-dihydroxyphenyl)-5,7-dihydroxy-3-[(2S,3R,4S,5S,6R) -3,4,5-trihydroxy-6-[[(2R,3R,4R,5R,6S)-3,4,5-trihydroxy-6-methyloxan-2-yl]oxymethyl]oxan-2-yl]oxychromen-4-one

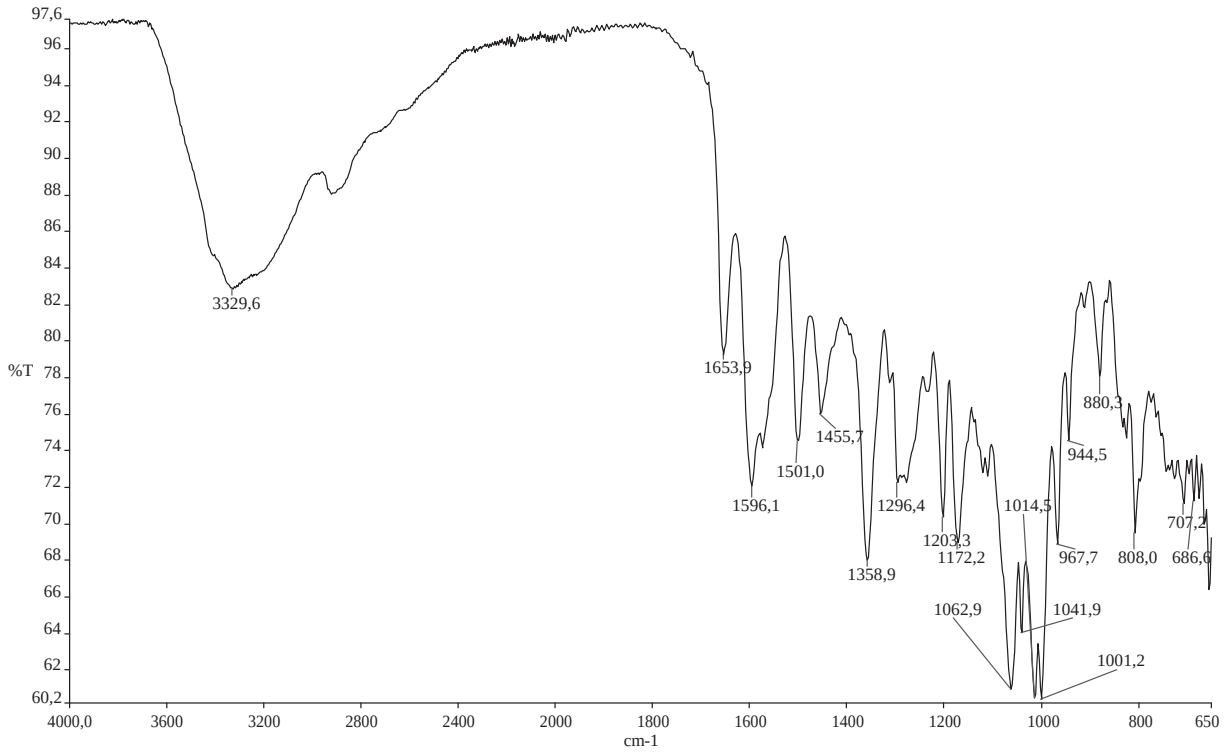

Figure 3.23: IR spectrum of CA4

The ESI-MS (see Figure 3.24) revealed the positive ions[7] at *m/z*: 611.1 $[M + H]^+$ (10) and 633.1 $[M + Na]^+$ (100) (i.e., base peak). Further ions at *m/z* = 303.2 (16) and *m/z* = 464.9 (13) are the fragment ions $[AH_2]^+$ and $[F_1H_2]^+$, respectively. The latter ions are formed by the loss of one sugar (146) and two sugar moieties (146 + 162) Crow *et al.*, (1986) [61] and Stobiecki *et al.*, (1999) [302]. On the basis of the molecular mass at *m/z* = 610.1 and the structural information obtained by NMR analysis, a molecular formula of $C_{27}H_{30}O_{16}$ was assigned to compound CA4. This molecular mass was confirmed by the high resolution FT-ICR-MS for $[M + Na]^+$ at *m/z* = 633.142547 (calculated mass for $C_{27}H_{30}O_{16}Na$ was 633.1426).

[7]In brackets, the relative intensity in % of the ion peaks is shown.

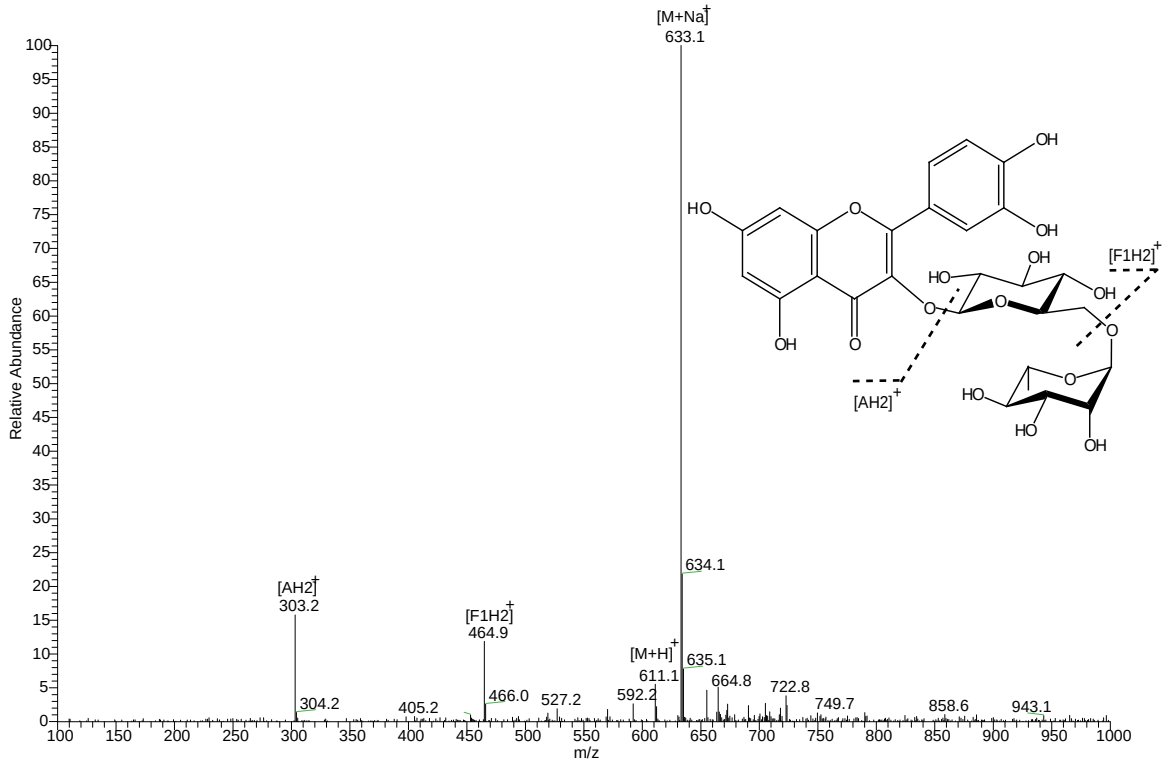

Figure 3.24: ESI-MS (positive mode) of CA4

The aromatic region of the ^{1}H-NMR spectrum (see Figure 3.25 and Table 3.4) showed two doublet signals at δ = 6.83 ppm and δ = 7.53 ppm and three singlets at δ = 7.52 ppm, δ = 6.38 ppm and δ = 6.19 ppm (last two are broadly), which refer to three isolated aromatic protons in a A-B system. In the upfield region, there are two anomeric signals of two sugar units at δ = 5.33 ppm and δ = 4.37 ppm. Further nine protons have been identified due to the sugar units, that is, between δ = 3.0 ppm and δ = 3.8 ppm.

The ^{13}C-NMR spectrum (see Figure 3.26 and Table 3.4) showed 27 signals for 27 carbons. The two signals at δ = 101.3 and δ = 100.9 ppm correspond to the anomeric signals of the sugar units. In the aromatic region, additional 10 tetrasubstituted carbons are represented. The DEPT experiment (see Figure 3.27) showed a CH_2 group at δ = 67.1. Further 15 CH groups and one CH_3 groups were identified. The chemical shifts of the aromatic signals of both the ^{1}H- and ^{13}C-NMR spectra suggested the presence of quercetin as aglycone with two sugar units.

The HSQC experiment (see Figure 3.29) exhibited that the proton signals at δ = 6.38 ppm (H-8)

and 6.19 ppm (H-6) are related to signals at δ_{C8} = 93.7 ppm and δ_{C6} = 98.8 ppm, respectively. Additionally, the carbon signals at $\delta_{C2'}$ = 116.4 ppm, $\delta_{C5'}$ = 115.4 ppm, and $\delta_{C6'}$ =121.7 ppm are correlated to the proton signals at δ = 7.52 ppm (H-2), 6.83 ppm (H-5), and 7.53 ppm (H-6). The HH-COSY spectrum (see Figure 3.28 and Table 3.4) showed two couplings, between δ = 6.19 ppm (H-6) and 6.38 ppm (H-8), and between δ = 6.83 ppm (H-5") and 7.53 ppm (H-6").

The coupling constant of the anomeric proton (H-1") of the sugar (J = 6.7 Hz) was in accordance with that of the β-glucosyl, while the coupling constant of the anomeric proton (H-1") of the sugar (J = 2 Hz) was in accordance with an α-rhamnosyl, as compared to the literature [87] in Table 3.4. The HH-COSY experiment showed additionally the ^{1}H correlations for the β-glucosyl: between H-1" and H-2"; between H-4" and H-5"; between H-5" and H-6". The α-rhamnosyl showed correlations between H-5" and H-6" .

Based on the MS, 1D- and 2D-NMR analysis, the chemical-shift values of the protons and carbons of the sugar units were in agreement with those of the rutin [quercetin 3-O-β-(6$''$-O-α-rhamnosyl glucoside)], which was characterized as the compound CA4 and compared to the literature [87] as shown in Table 3.4.

Table 3.4: Chemical shifts of CA4 and literature

Atom numbers	^{13}**C*** δ**/ppm**	^{13}**C**** δ**/ppm**	^{1}**H*** δ**/ppm (Mult., J(Hz), H)**	^{1}**H**** δ**/ppm (Mult., J(Hz), H)**	^{1}**H - ^{1}H*** **COSY**
2	156.5	157.3	-	-	-
3	133.4	134.1	-	-	-
4	177.5	178.2	-	-	-
5	156.8	157.5	-	(-OH) 12.62 (s; 1H)	-
6	98.8	99.5	6.19 (brs; 1H)	6.21 (d; 2 Hz; 1H)	8
7	164.2	164.9	-	(-OH) 10.86 (s; 1H)	-
8	93.7	94.5	6.38 (brs; 1H)	6.40 (d; 2 Hz; 1H)	6
9	161.3	162.1	-	-	-
10	104.1	104.8	-	-	-
$1'$	121.3	122.5	-	-	-
$2'$	116.4	116.1	7.52 (s; 1H)	7.55 (d; 2.1 Hz; 1H)	-
$3'$	144.8	145.6	-	(-OH) 9.21 (s; 1H)	-
$4'$	148.5	149.3	-	(-OH) 9.71 (s; 1H)	-
$5'$	115.4	117.1	6.83 (d; 8.9 Hz; 1H)	6.86 (d; 9.0 Hz; 1H)	$6'$
$6'$	121.7	122.0	7.53 (m; 1H)	7.56 (dd; 9.0, 2.1 Hz; 1H)	$5'$
$1''$	101.3	101.6	5.33 (d; 6.7 Hz; 1H)	5.35 (d; 7.4 Hz; 1H)	$2''$
$2''$	74.2	74.9	3.23 (m; 1H)	-	$1''$
$3''$	76.5	77.3	3.23 (m; 1H)	-	$4''$
$4''$	71.9	72.7	3.08 (m; 1H)	-	$5''$
$5''$	76.0	76.7	3.23 (m; 1H)	-	$6''$, $5''$
$6''$	67.1	67.9	3.69 (d; 10.5 Hz; 2H)		$5''$
$1'''$	100.9	102.2	4.37 (d; 2.1 Hz; 1H)	-	-
$2'''$	70.1	70.8	3.07 (d; 9.4 Hz; 1H)	-	-
$3'''$	70.5	71.2	3.39 (m; 1H)	-	-
$4'''$	70.7	71.4	3.29 (m; 1H)	-	-
$5'''$	68.4	69.1	3.27 (m; 1H)	-	$6'''$
$6'''$	17.8	18.6	0.99 (d; 6.1 Hz; 3H)	1.00 (d; 6.1 Hz; 3H)	$5'''$

[*] In DMSO-d_6. [**] Data from the literature [87] in DMSO-d_6.

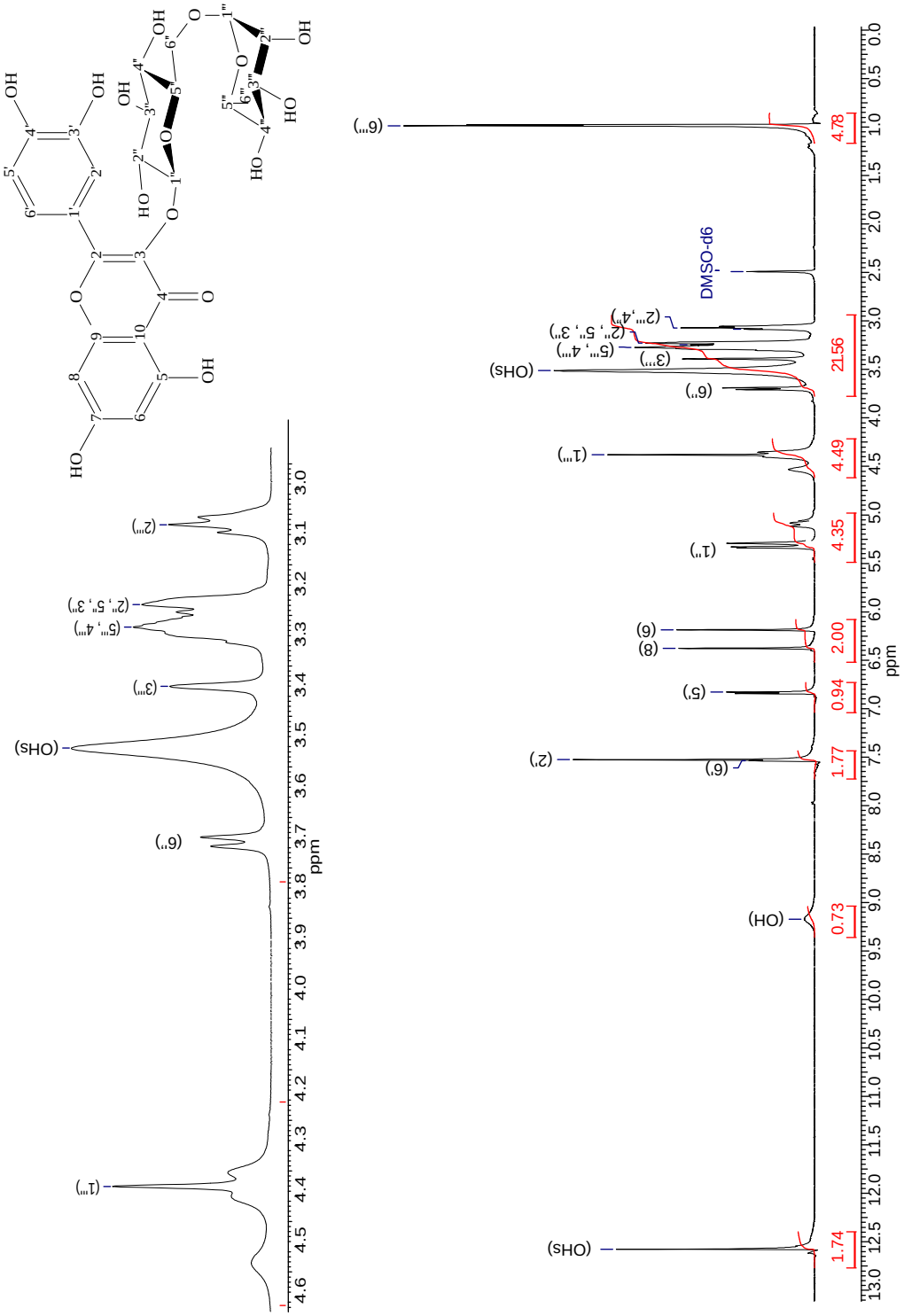

Figure 3.25: ^{1}H-NMR of CA4 (400 MHz, DMSO-d_6)

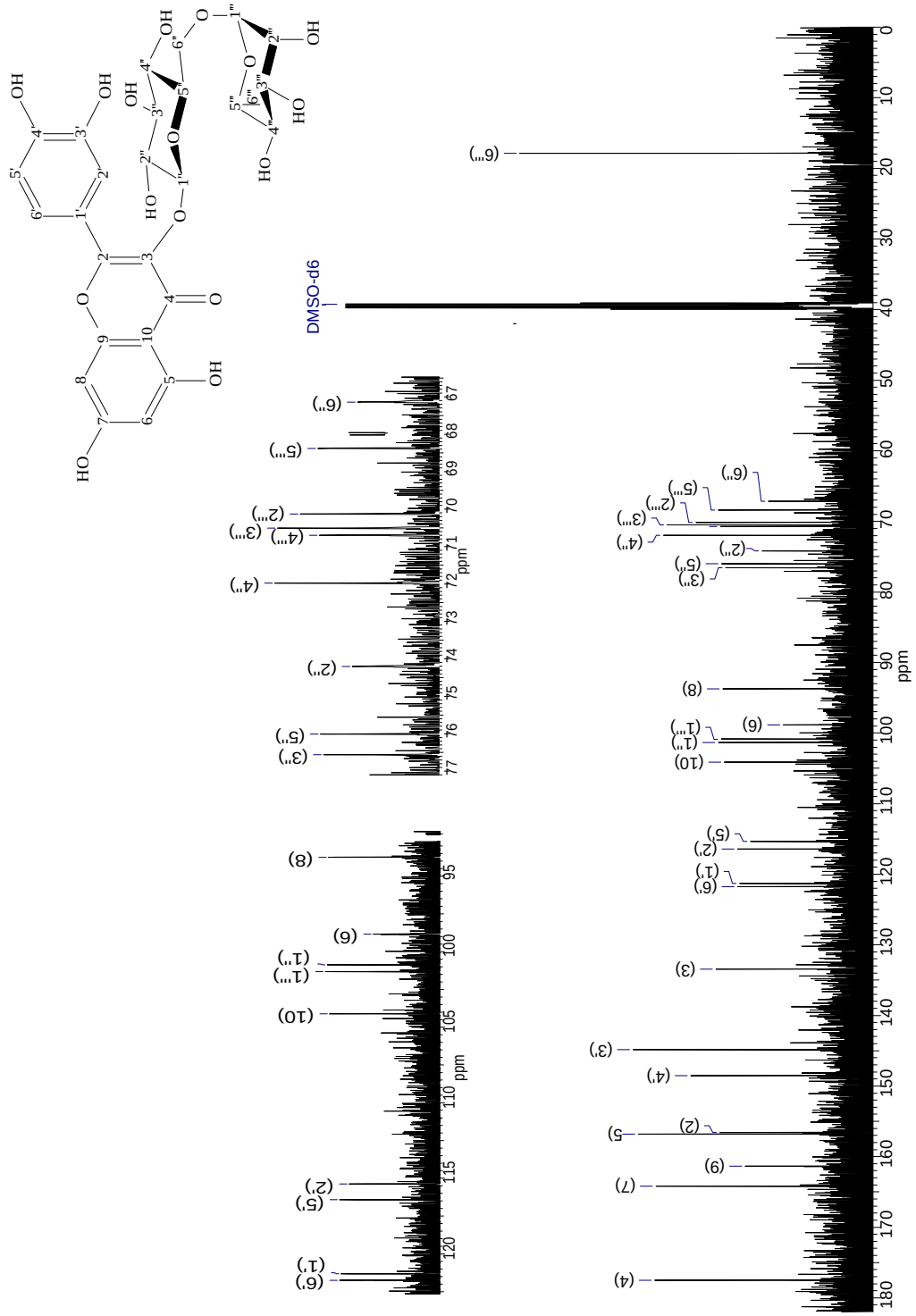

Figure 3.26: ^{13}C-NMR of CA4 (100 MHz, DMSO-d_6)

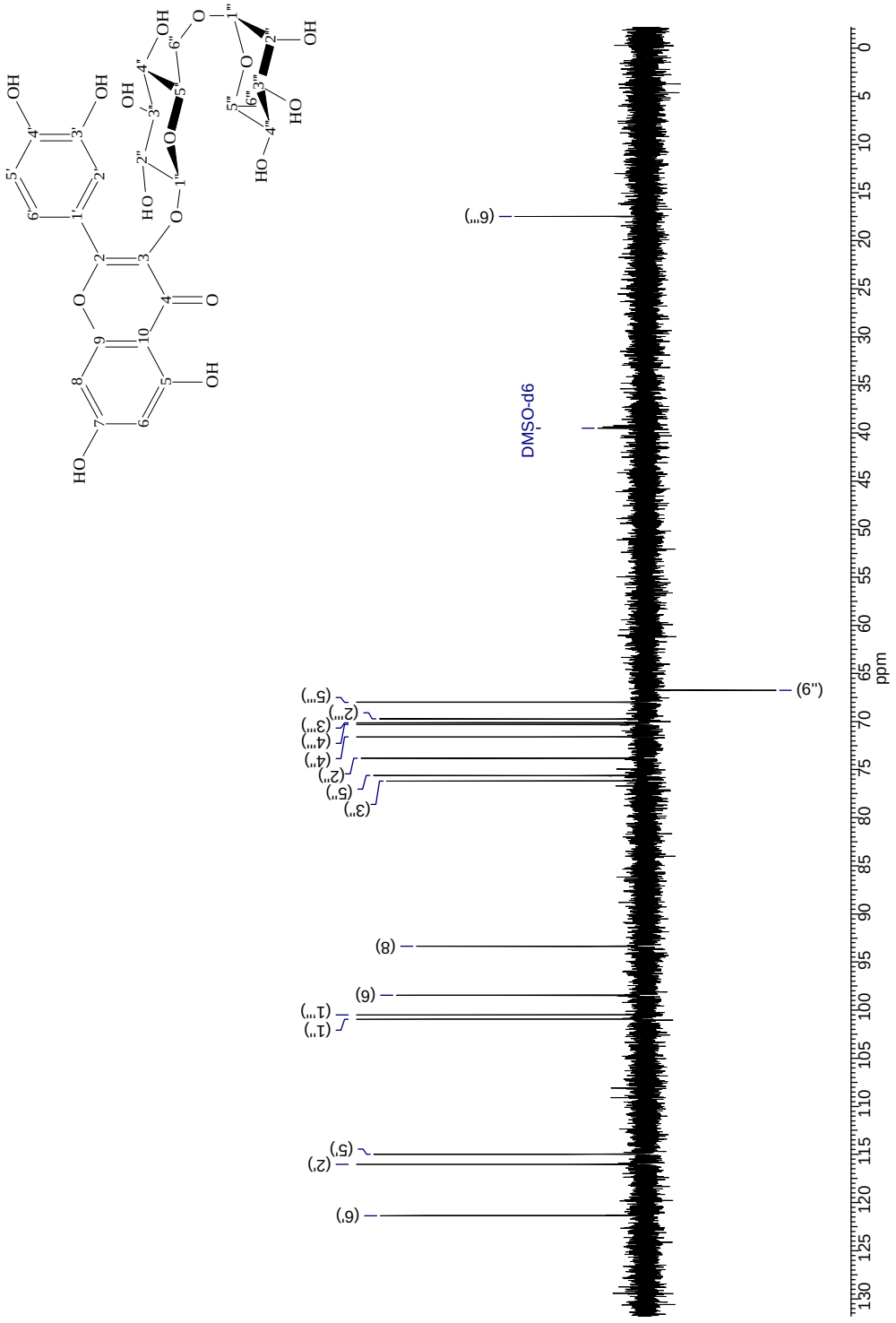

Figure 3.27: DEPT-135 of CA4 (100 MHz, DMSO-d_6)

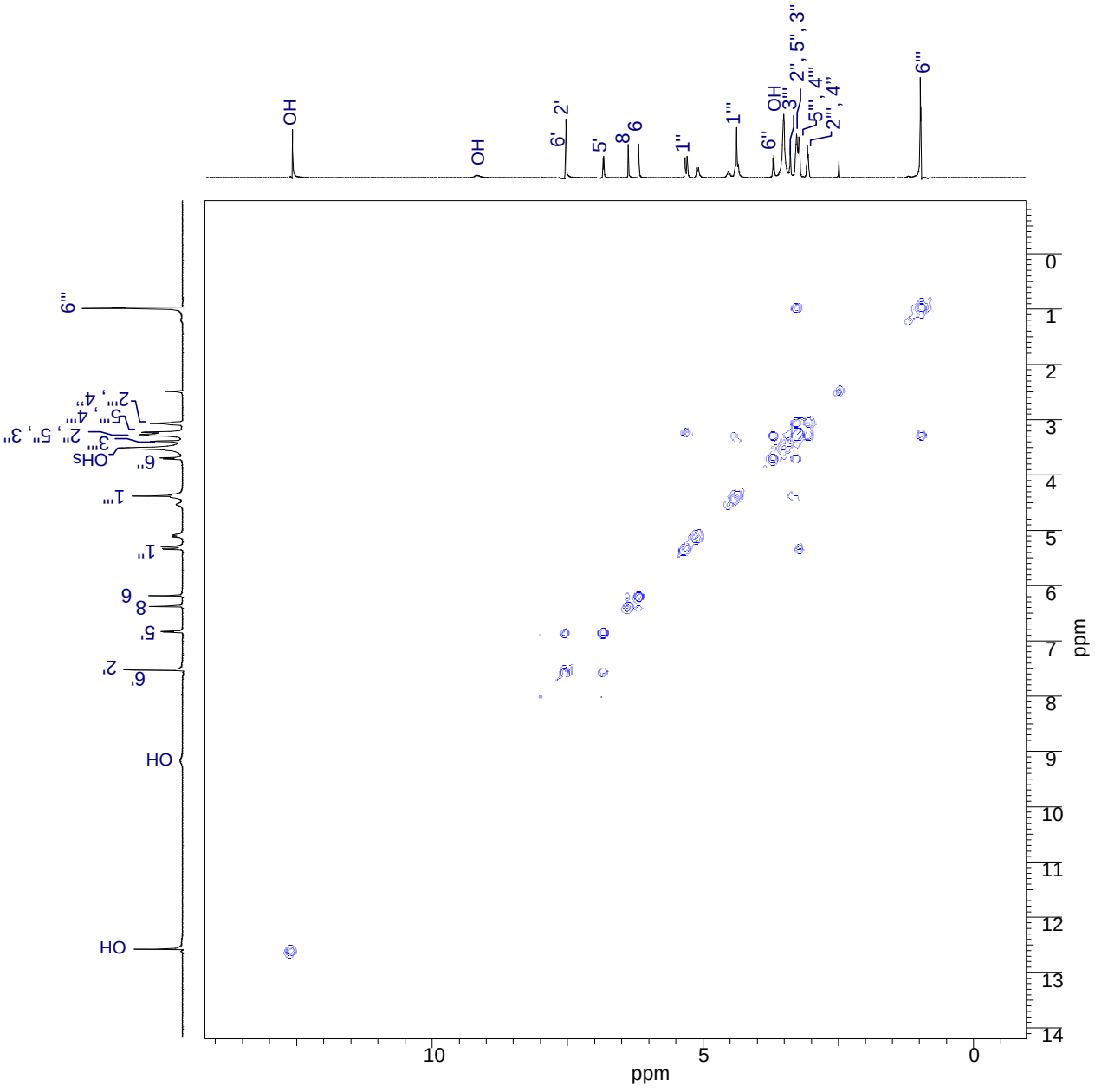

Figure 3.28: H-H-COSY of CA4 (400 MHz, DMSO-d_6)

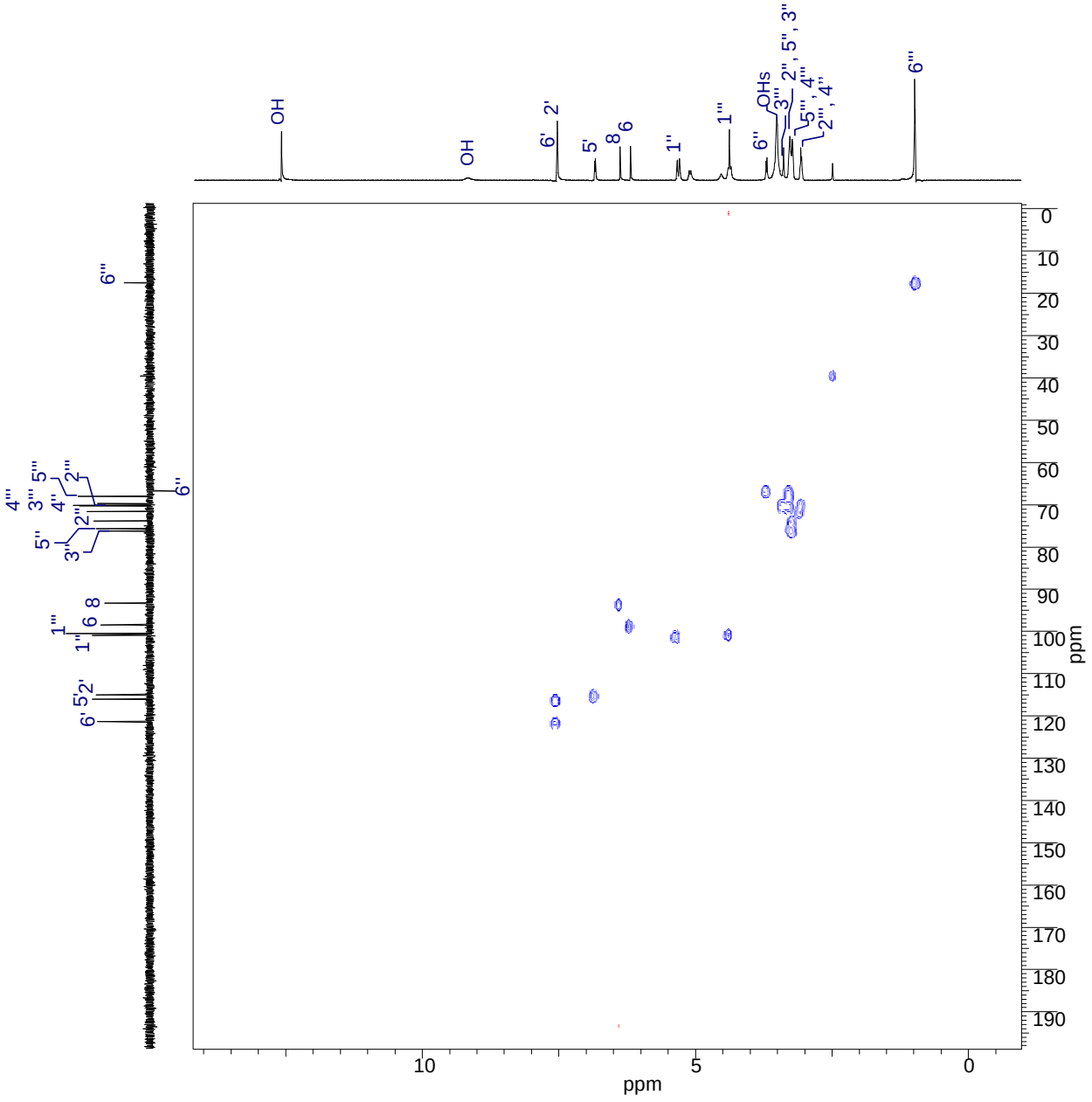

Figure 3.29: HSQC of CA4 (400 MHz, DMSO-d_6)

3.1.1.2.5 CA5: Quercitrin

Fraction I was analyzed by LC-ESI-MS spectrometry (see Section 5.6.1.2, Experimental Part). This fraction was compared with the retention time and mass fragmentation of standards. This analysis showed the presence of quercitrin[8], which chemical structure is represented in Figure 3.30.

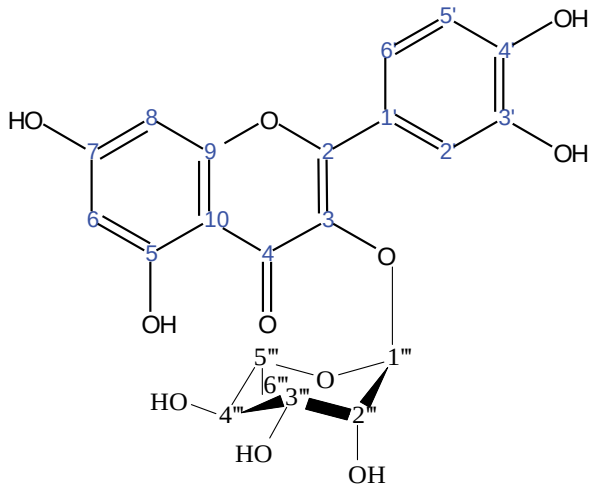

Figure 3.30: Chemical structure of CA5

Figure 3.31 compares the chromatogram (Method LC-DAD, see Section 5.4.7.3) with retention times between the fraction I and the quercitrin standard. As it can be observed, the peak Q with retention time t_R = 12.90 min. in fraction I has a similar retention time t_R = 12.39 min. compared to the standard. The MS data (negative mode) of the peak Q and the standard are depicted in Figure 3.32. The peak Q has a quasimolecular negative ion peak[9] at *m/z* = 448.2 (15) $[M]^-$ and further peaks at at *m/z*: 447.1 (100) $[M - H]^-$ and 300.4 (10) $[M - rha]^-$. The MS fragmentation (negative mode) of the quercitrin standard has ion peaks at *m/z*: 448.1 (17) $[M]^-$; 447.1 (100) $[M - H]^-$; and 300.1 (15) $[M - rha]^-$.

Therefore, both retention time and the MS data of the peak *Q* agreed with those from the quercetrin standard.

[8]IUPAC name: 2-(3,4-dihydroxyphenyl)-5,7-dihydroxy-3-[(2S,3R,4R,5R,6S) -3,4,5-trihydroxy-6-methyloxan-2-yl]oxychromen-4-one

[9]In brackets, the relative intensity in % of the ion peaks is shown.

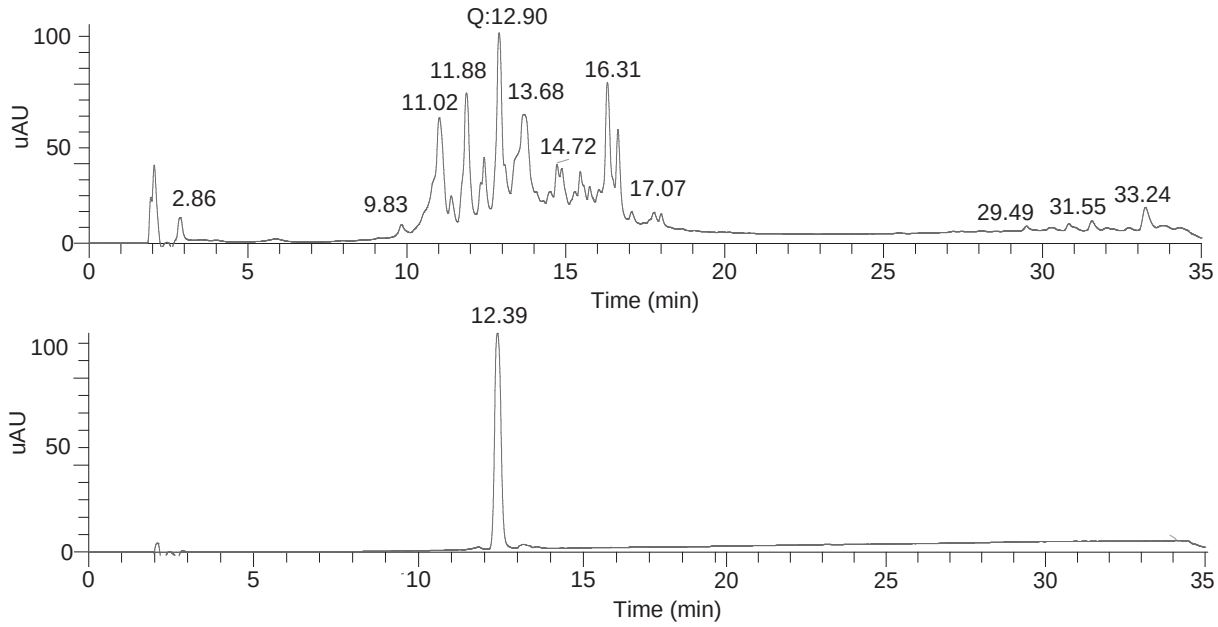

Figure 3.31: Comparison between the chromatogram of the fraction I and quercitrin standard (Method LC-DAD)

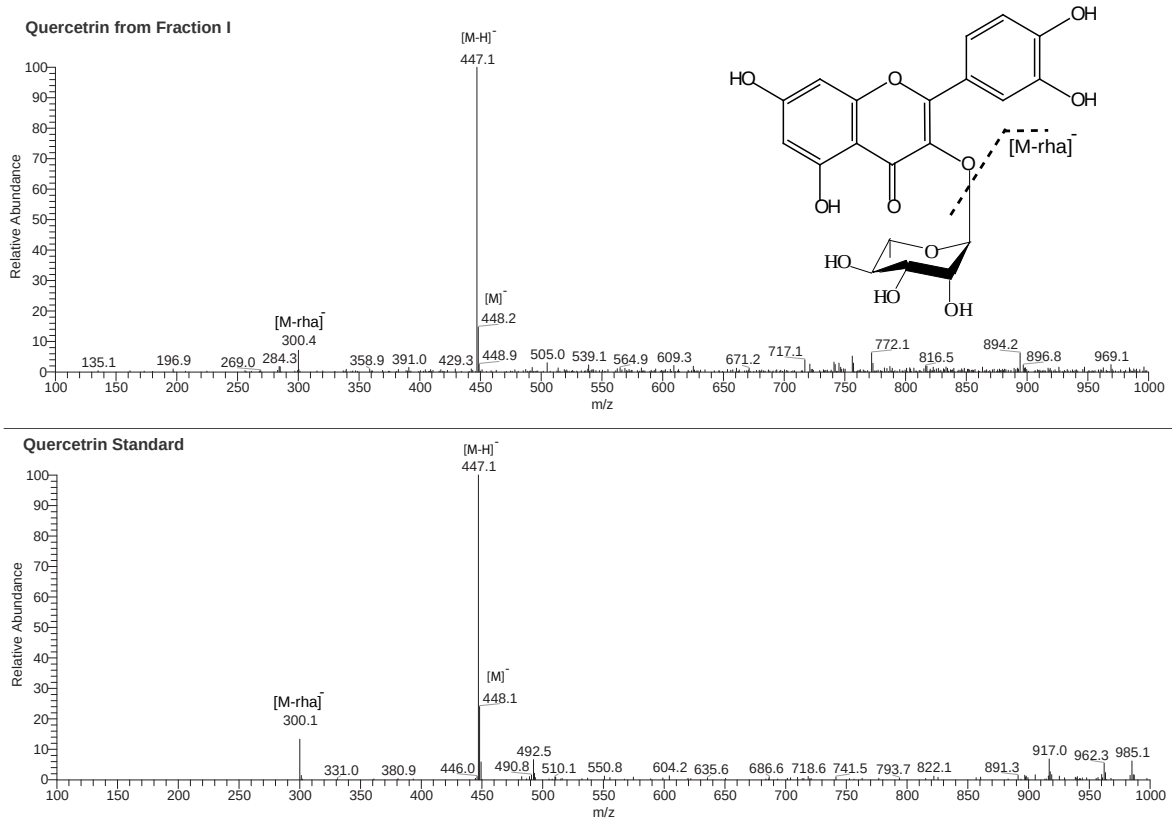

Figure 3.32: Comparison of the MS data of quercetrin from fraction I and the standard

3.1.1.2.6 CA6: β-Sitosterol

Fraction E was analyzed using GC-MS[10] (see Section 5.4.7.1, Experimental Part) by comparison of the spectrum of the fraction E and the respective standard. Both spectra were compared with the data from a natural compound library. It was possible to determine the presence of β-sitosterol[11], whose chemical structure can be observed in Figure 3.33.

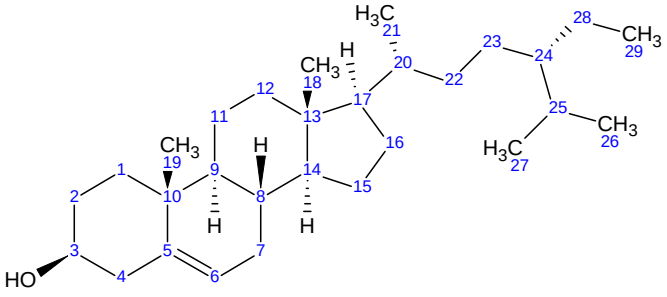

Figure 3.33: Chemical structure of CA6

Figure 5.1 (see Section 5.4.7.1, Experimental Part) exhibited a peak GC-CA6 with a retention time t_R = 16.7 min in the fraction E. Figure 3.34.(A) shows the MS spectrum of peak GC-CA6. The search analysis in the digital library indicated the compound β-sitosterol. In order to confirm this result, the respective standard (Figure 3.34.(B)) was also analyzed by GC-MS and compared to the data from the natural compound library (see Section 5.4.7.1, Experimental Part). These results confirmed the presence of β-sitosterol in *Cordia americana*.

[10]The GC-MS analysis were performed by C. Schmidt at the Department of Pharmaceutical Biology and Biotechnology, University of Freiburg.

[11]IUPAC name: (3S,8S,9S,10R,13R,14S,17R)-17-[(2R,5R)-5-ethyl-6-methylheptan-2-yl] -10,13-dimethyl-2,3,4,7,8,9,11,12,14,15,16,17-dodecahydro-1H-cyclopenta[a]phenanthren-3-ol

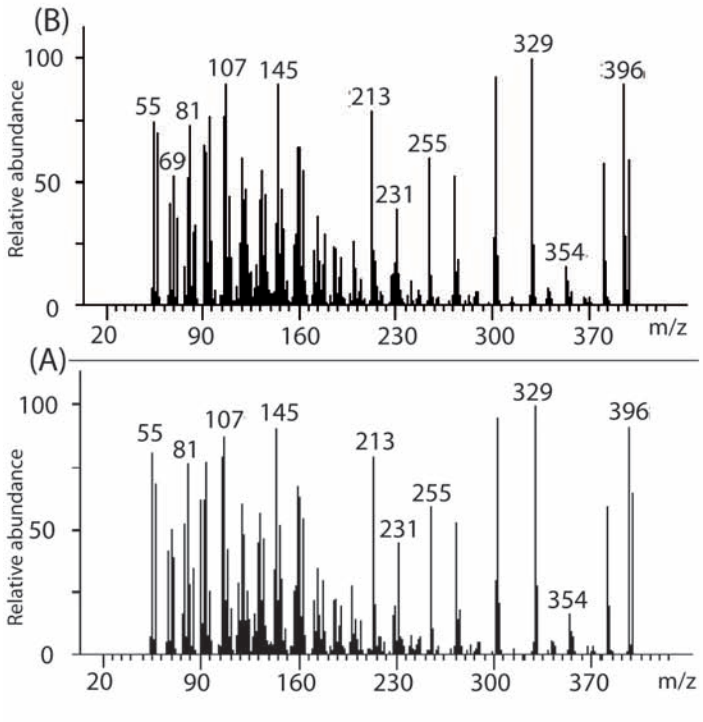

Figure 3.34: Comparison of the MS data between peak GC-CA6 (A) and respective standard (B)

3.1.1.2.7 CA7: Campesterol

Fraction E was analyzed by GC mass spectrometry (see Section 5.4.7.1, Experimental Part) by comparison of the spectrum of the fraction E with the respective standard. Both spectra were compared to the data from a natural compound library. It was possible to determine the presence of campesterol[12], whose chemical structure can be observed in Figure 3.35.

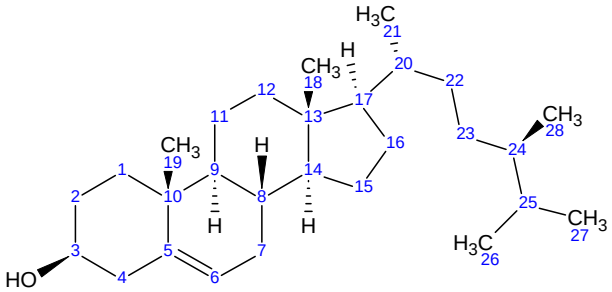

Figure 3.35: Chemical structure of CA7

[12]IUPAC name: (3S,8S,9S,10R,13R,14S,17R)-17-[(2R,5R)-5,6-dimethylheptan-2-yl] -10,13-dimethyl-2,3,4,7,8,9,11,12,14,15,16,17-dodecahydro-1H-cyclopenta[a]phenanthren-3-ol

Figure 5.1 (see Section 5.4.7.1, Experimental Part) exhibited a peak GC-CA7 with a retention time t_R = 34.8 min in the fraction E. Figure 3.36.(A) shows the MS spectrum of peak GC-CA7. The search analysis in the digital library indicated the compound campesterol. In order to confirm this result, the respective standard (Figure 3.36.(B)) was also analyzed by GC-MS and compared to the data from the natural compound library (see Section 5.4.7.1, Experimental Part). These results confirmed the presence of campesterol in *Cordia americana*.

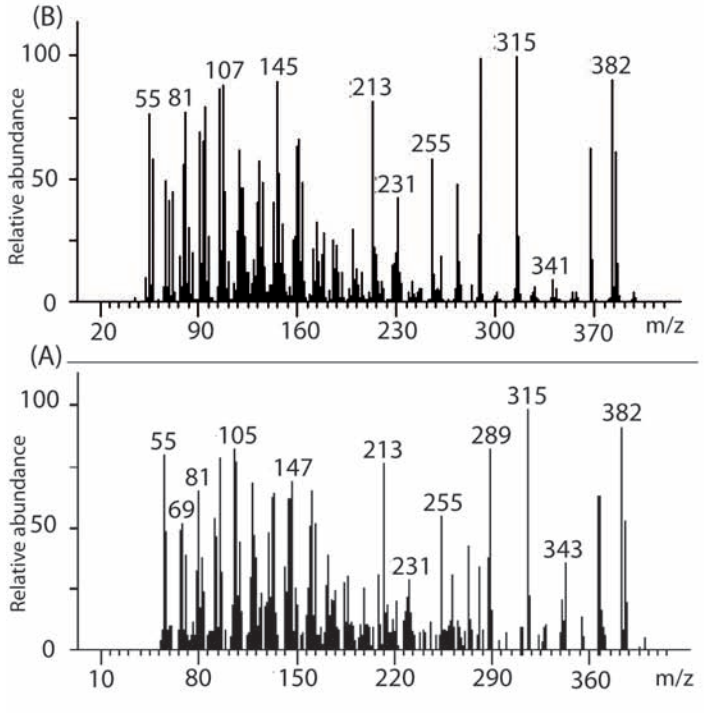

Figure 3.36: Comparison of the MS data between peak GC-CA7 (A) and respective standard (B)

3.1.1.2.8 CA8: α-Amyrin

The mass spectrum of fraction E was analyzed by means of GC-MS (see Section 5.4.7.1, Experimental Part) using computer searches in the natural compound library. It was possible to determine the presence of α-amyrin[13], whose chemical structure can be observed in Figure 3.37.

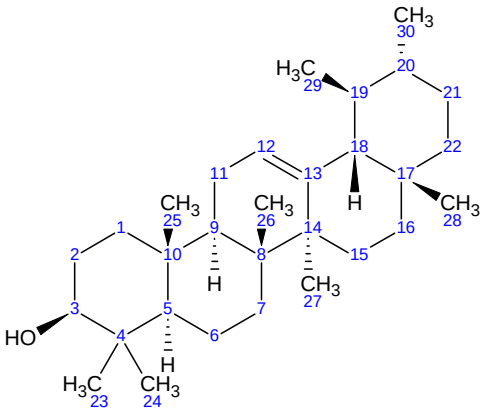

Figure 3.37: Chemical structure of CA8

Figure 5.1 (see Section 5.4.7.1, Experimental Part) exhibited a peak GC-CA8 with a retention time of 22.2 min in the fraction E. Figure 3.38.(A) shows the comparison between the MS fragmentation of peak GC-CA8 and data from a natural compound library (see Section 5.4.7.1, Experimental Part) (Figure 3.38.(B)). The search analysis in the digital library indicated that the pentacyclic triterpene α-amyrin is present in the fraction E from *Cordia americana*.

[13] IUPAC name: (3S,4aR,6aR,6bS,8aR,11R,12S,12aR,14aR,14bR)-4,4,6a,6b,8a,11,12,14b-octamethyl-2,3,4a,5,6,7,8,9,10,11,12,12a,14,14a-tetradecahydro-1H-picen-3-ol

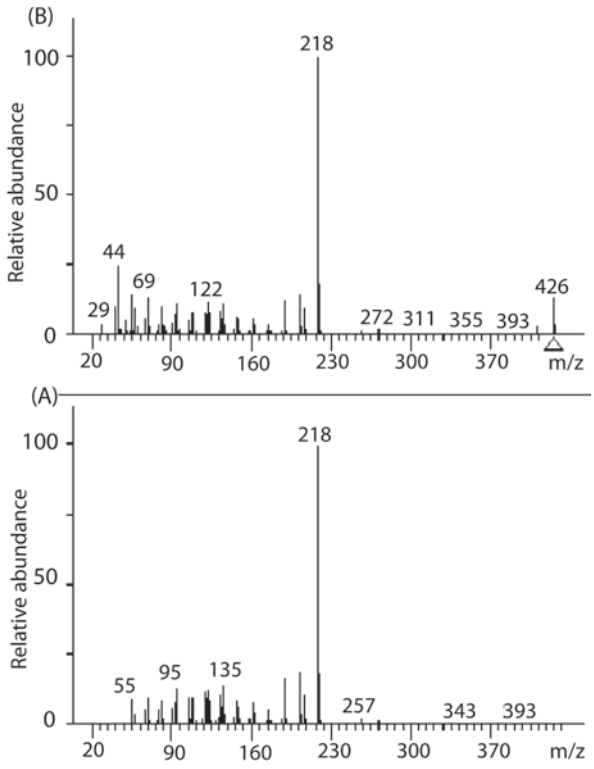

Figure 3.38: Comparison of the MS fragmentation between peak GC-CA8 (A) and data from the natural compound library (B)

3.1.1.2.9 CA9: β-Amyrin

The fraction E was analyzed by GC-MS (see Section 5.6.1.2, Experimental Part) using computer searches in the natural compound library. It was possible to determine the presence of β-amyrin [14], whose chemical structure can be observed in Figure 3.39.

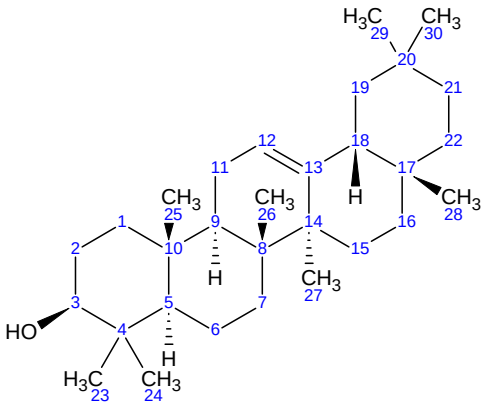

Figure 3.39: Chemical structure of CA9

[14] IUPAC name: (3β)-olean-12-en-3-ol

Figure 5.1 (see Section 5.4.7.1, Experimental Part) exhibited a peak GC-CA9 with a retention time of 18.7 min in the fraction E. Figure 3.39.(A) shows the comparison between the MS fragmentation of peak GC-CA9 and data from the natural compound library (see Section 5.4.7.1, Experimental Part) (Figure 3.39.(B)). The search analysis in the digital library indicated that the pentacyclic triterpene β-amyrin is present in the fraction E from *Cordia americana*.

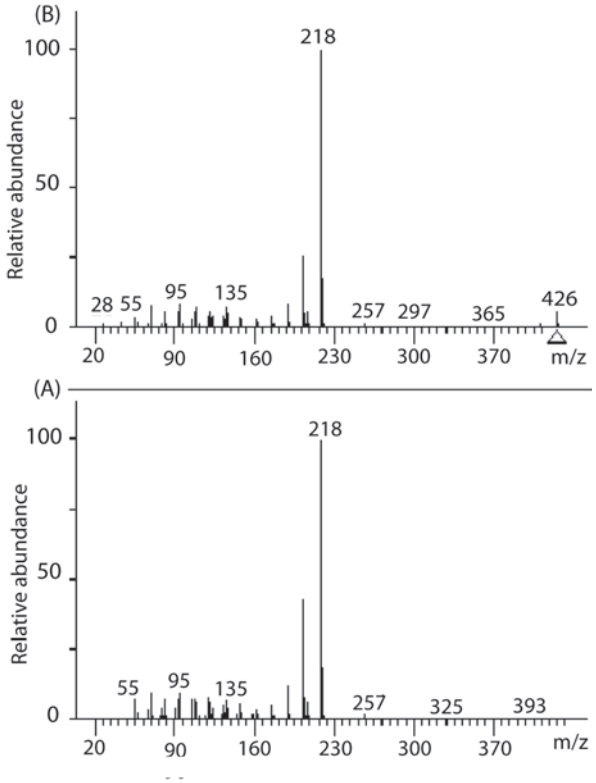

Figure 3.40: Comparison of the MS fragmentation between peak GC-CA9 (A) and data from the natural compound library (B)

3.1.1.3 Discussion

As presented in the previous sections, the phytochemical studies (i.e., MS, 1D and 2D NMR) revealed the presence of

- flavonols: rutin and quercitrin;
- phytosterols: campesterol and β-sitosterol;
- triterpenoids: α- and β-amyrin;
- phenolic acids: 3-(3,4-dihydroxyphenyl)-2-hydroxypropanoic acid, rosmarinic acid and rosmarinic acid ethyl ester in the ethanolic extract from the leaves of *Cordia americana*.

Figure 3.41 illustrate the DAD-HPLC chromatogram of the ethanolic extract of *Cordia americana* and its characterized compounds. As it can be observed, the ethanolic extract contains rosmarinic acid (CA1) as the major compound. Additionally, further HPLC analysis (Method LC-DAD, see Section 5.4.7.3, Experimental Part) (see Figure 5.5, Experimental Part) revealed compound CA1 as the major compound in the ethanolic extract of *Cordia americana* at different wavelengths (220, 250, 280, 330, 350 nm).

Rosmarinic acid, an ester of caffeic acid with 3,4-dihydroxyphenylpropionic acid, is a characteristic constituent in members of the Lamiaceae and the Boraginaceae where it occurs in higher amounts [318]. CA1 was also found in the leaves of Lemon balm (*Melissa of cinalis*, Lamiaceae) in a concentration of 3.91% [312]. In *Rosmarinus of cinalis* (Lamiaceae), CA1 can be detected in leaves, flowers, stems and roots, but the highest amount of 2.5% was found during the first stages of leaf growth [22]. In the crude extract of *Borago of cinalis* (Boraginaceae), 2.5% of CA1 was quantified [337]. However, quantification analysis (see Section 5.6.1.3, Experimental Part) in the ethanolic extract from the leaves of *Cordia americana* showed the concentration of 8.44% of CA1, which is so far the highest concentration found in a species of the Boraginaceae family.

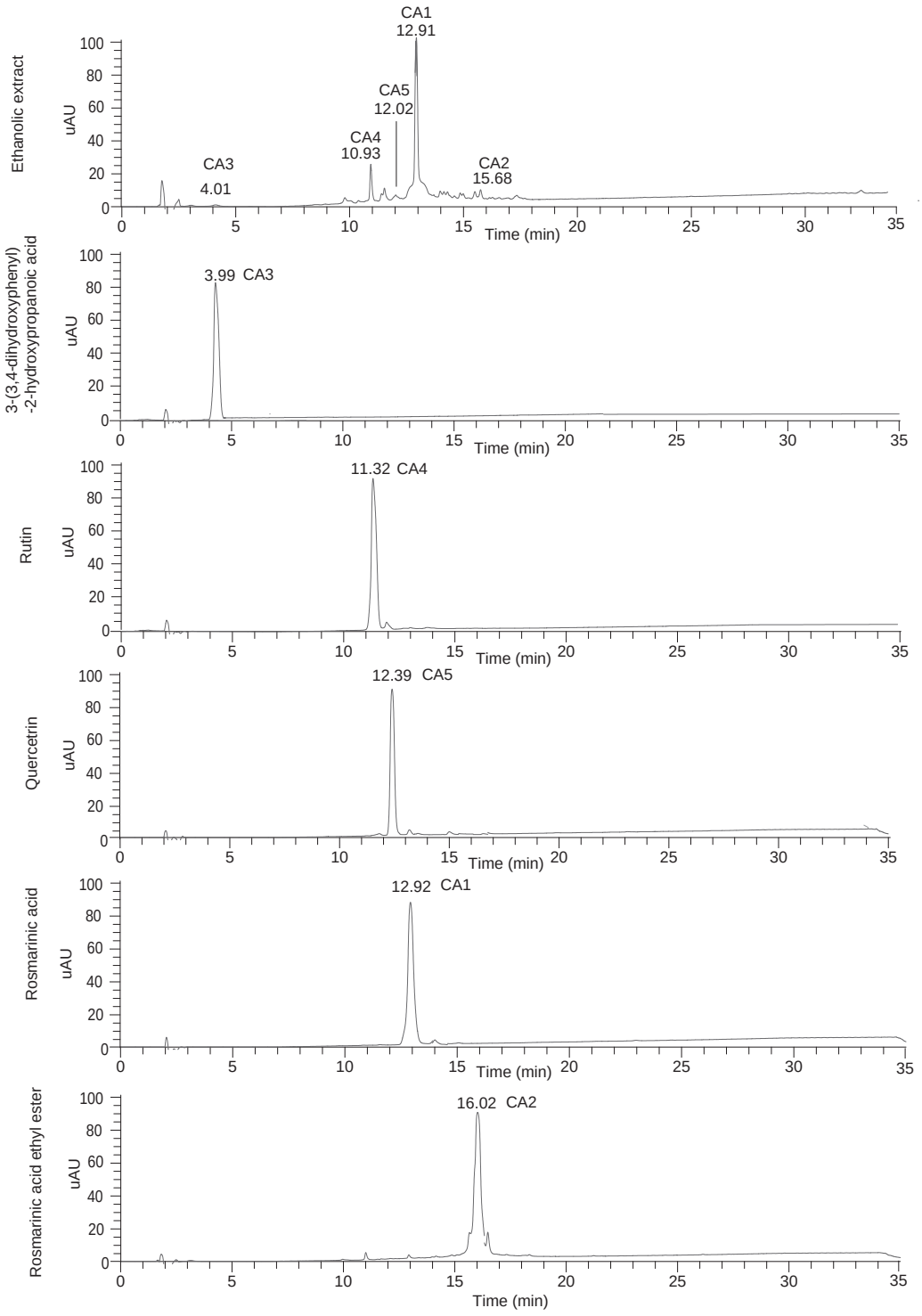

Figure 3.41: Representative HPLC chromatogram of the ethanolic extract of *Cordia americana* and its characterized compounds. Rosmarinic acid (CA1), rosmarinic acid ethyl ester (CA2), 3-(3,4-dihydroxyphenyl)-2-hydroxypropanoic acid (CA3), rutin (CA4), and quercitrin (CA5) (Method LC-DAD, with wavelength λ = 254 nm).

Research concerning the identification of rosmarinic acid started around 1950, when it was isolated from *Rosmarinus of cinalis* (Lamiaceae) by Scarpati and Oriente, (1958) [269]. Up to now, CA1 has already been isolated in some species of the genus *Cordia*, for example from flowers of *Cordia dentata* Poir [90] and from the leaves of *Cordia verbenacea* [310]. Nevertheless, this was the first report about the presence of CA1 in *Cordia americana*. CA1 is widely found in the plant kingdom and presumably accumulated as a defense compound [237]. In order to identify and quantify CA1, there are several analytical methods described in the literature concerning Lamiaceae species, including UV-VIS spectrophotometry, HPLC and GC [318, 312].

So far, the compound rosmarinic acid ethyl ester (CA2) has not been isolated for the genus *Cordia*. However in the Boraginaceae family, it has been isolated from *Lindelo a sylosa* [53]. Additionally, CA2 has previously been identified in *Lycopus lucidus* (Lamiaceae) [340, 217], in *Prunella vulgaris* L. (Labiatae) [327], and in *Nepeta prattii* (Lamiaceae). However, this compound might be also an artifact that was originated during the extraction process.

3-(3,4-dihydroxyphenyl)-2-hydroxypropanoic acid (CA3) has been isolated from the water extract of Chinese herb *Salvia miltiorrhiza* Bunge [249] from the Lamiaceae family. However, no reports have been made for the genus *Cordia* as well as for the Boraginaceae family. Therefore, it can be assumed that this was the first time to describe the isolation of CA3 in the genus *Cordia* as well as in the Boraginaceae family.

Rutin (CA4), a quercetin-3-rutinoside, has been previous identified in the leaves of *Cordia myxa* L. [106] and in the flowers of *Cordia dentata* Poir [90]. Additionally, CA4 has been isolated from *Fagopyrum sculentum* (Polygonaceae), *Sophora japonica* (Fabaceae), and *Ruta graveolens* (Rutaceae) [87] and many other plant species. Some methods have been described for the determination of rutin in different plants extracts, these include HPLC, capillary electrophoresis and spectrophotometry [3]. CA4 has also been used as a coloring agent, food additive in various food preparations and drinks, and for various purposes in cosmetics [87].

Concerning the phytochemical studies of quercitrin (CA5), it has been isolated from the leaves of *Cordia dichotoma* Forst. [324], from leaves and fruits of *Cordia myxa* L. [324] and from *Cordia*

globosa [64]. Additionally, the plants *Bauhinia microstachya* (Leguminosae)[103], *Kalanchoe pinnata* (Crassulaceae) and *Polygonum hydropiper* L. (Polygonaceae) are reported to contain CA5 [219] and in many other plant species. It belongs together with rutin to the ubiquitous flavonol glycosides.

β-sitosterol (CA6) has been isolated in the genus *Cordia* from heart wood of *Cordia trichotoma* [206] and from the seeds of *Cordia obliqua* [5].

Campesterol (CA7) is one of the most common plant sterols in nature along β-sitosterol and stigmasterol [142]. This compound is abundant in seeds, nuts, cereals, beans, legumes and vegetable oils [240]. CA7 for example, is one of the most common sterols in *Chrysanthemum coronarium* (Asteraceae) [51], in *Euphorbia pulcherimma* (Euphorbiaceae) [285] and in tomato shoots [347].

α-amyrin (CA8) and β-amyrin (CA9) are pentacyclic triterpenes found in various plants. α-amyrin has been isolated from the seeds of *Cordia obliqua* [5]. Both of these compounds were isolated from *Brazilian red propolis* [317] and from *Protium kleinii* (Burseraceae), both medicinal plants used in Brazil [228].

As presented in Section 1.2.2.4, only a few compounds such as two quinones, one phenolic aldehyde, one coumarin and tannins has been studied for *Cordia americana*. Thus, all the aforementioned compounds were isolated and identified for the first time in *Cordia americana*.

3.1.2 *Brugmansia suaveolens*

3.1.2.1 Bioguided Fractionation based on p38α MAPK Assay

The ethanolic extract from *Brugmansia suaveolens* was fractionated by means of Sephadex®LH-20 open column chromatography using methanol as mobile phase (see Section 5.6.2, Experimental Part). The obtained fraction sets were submitted to a bioguided study in the p38α assay (see Table 5.13, Experimental Part) and the most active fractions with higher output yields, such as fractions G, H and I were further investigated. The selected fractions were subfractionated by flash chromatography, open column chromatography and analytical HPLC using methanol/acetonitrile and water as mobile phase (further details see Section 5.6.2, Experimental Part). The following compounds were isolated from the fractions: BS1 was isolated from fraction G; BS2, BS3 and BS4 were isolated from fraction H; and BS2 was isolated from fraction I.

Brugmansia suaveolens has been studied due to the presence of the alkaloids, as already mentioned in Section 1.2.3.4. The qualitative analysis of these alkaloids was performed by TLC (see Section 5.4.1, Experimental Part) by comparison of the ethanolic extract of *Brugmansia suaveolens* (BS) and the fraction sets (A-K) after Sephadex®LH-20 with the standards hyoscyamine and scopolamine. Figure 5.11 (Experimental Part) shows by means of this qualitative test that it was not possible to detect alkaloids.

3.1.2.2 Structural Elucidation

The chemical structures of the following compounds in *Brugmansia suaveolens* were elucidated by MS and NMR analysis. The absolute configuration of all characterized compounds was not studied. The known chemical structure was in accordance with the respectively literature.

3.1.2.2.1 BS4: Kaempferol 3-O-β-D-glucopyranosyl-(1$'''\rightarrow$2$''$) -O-α-L-arabinopyranoside

The subfractionation of the fraction H was carried out consecutively by flash chromatography, open column chromatography and analytical HPLC (see Section 5.6.2.2, Experimental Part), which yielded 3.2 mg of the compound BS4, which was identified as kaempferol 3-O-β-D-glucopyranosyl-(1$'''\rightarrow$ 2$''$)-O-α-L-arabinopyranoside[15]. This compound was isolated as a yellow amorphous powder and its chemical structure is shown in Figure 3.42. This structure was established on the basis of UV, IR, MS and NMR spectroscopic data.

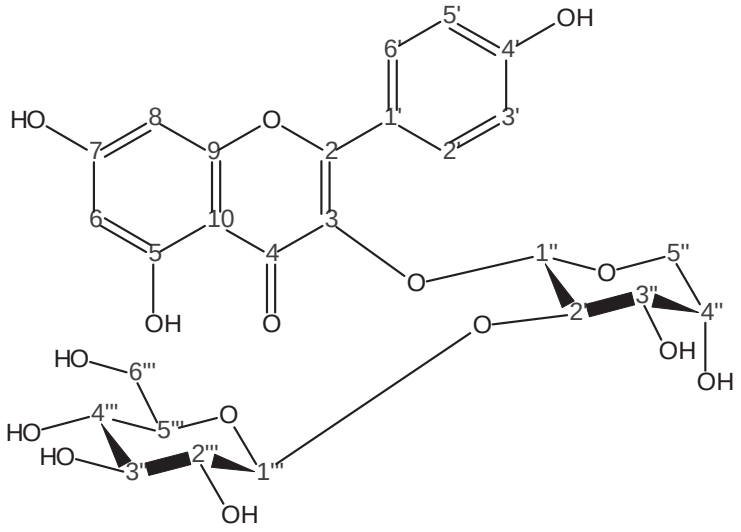

Figure 3.42: Chemical structure of BS4

The UV spectrum of BS4 (see Figure 3.43) exhibited two absorption maxima (in MeOH) at λ = 265 and 346 nm, which provided evidence to be in accordance with a 3,7-di-O-substituted flavonol skeleton [196]. The FTIR spectrum (see Figure 3.44) showed distinguishable absorption bands at: 3248.2, 2922.0, 1652.8, 1574.4, 1503.7, 1446.6, 1357.2, 1260.0, 1203.7, 1177.2, 1071.8, 1020.2, 805.5 cm^{-1}.

[15]IUPAC name: 5,7-dihydroxy-2-(4-hydroxyphenyl)-4-oxo-4H-chromen-3-yl 2-O-hexopyranosylpentopyranoside

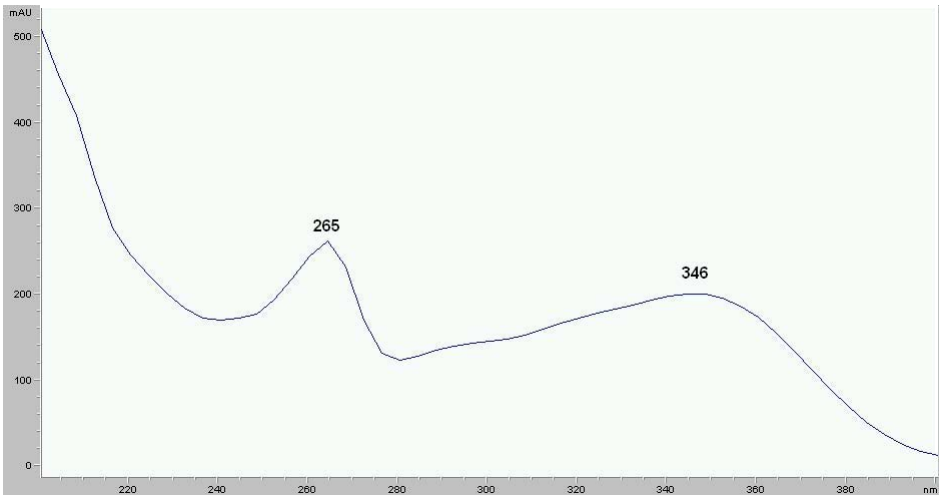

Figure 3.43: UV of the compound BS4

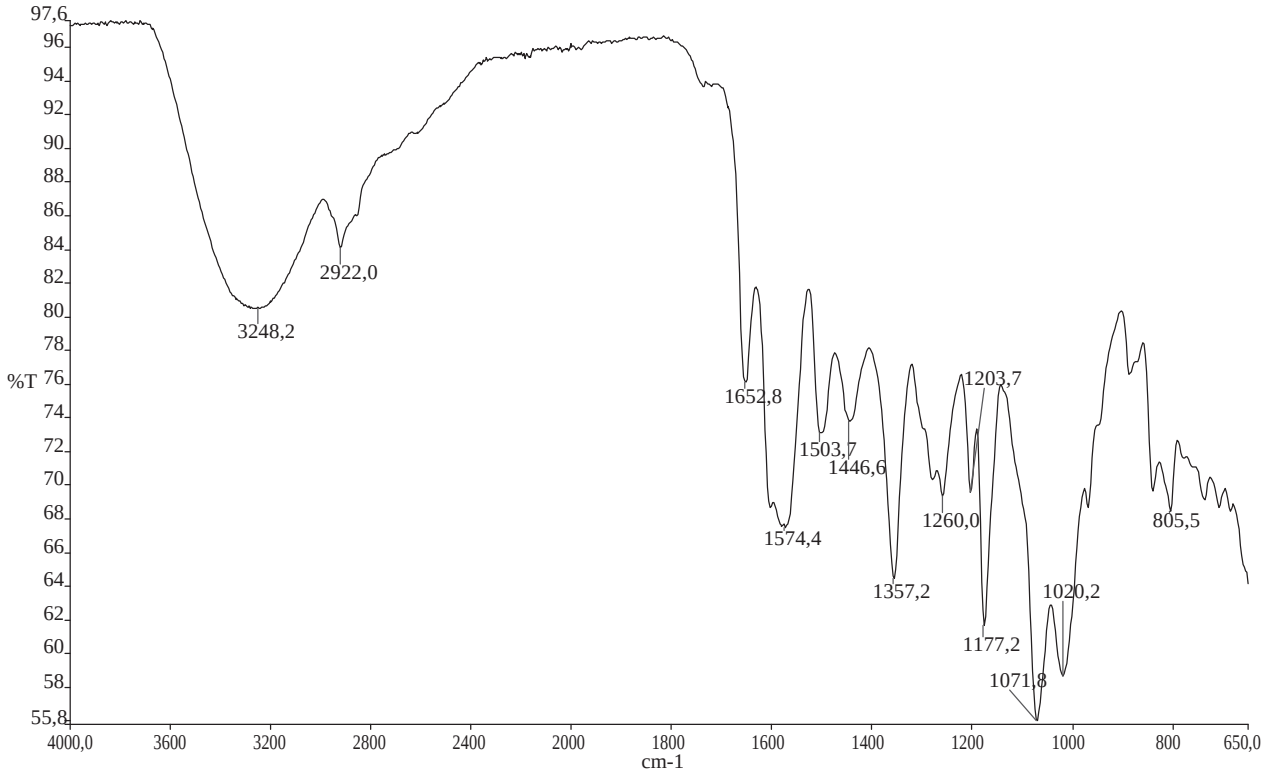

Figure 3.44: IR of the compound BS4

Useful structural information was supplied by mass spectrometry [200, 301, 63]. The ESI mass spectrum (see Figure 3.45) showed a quasimolecular positive ion peak[16] at *m/z* 603.1 $[M + Na]^+$ (54) and further ion peaks at *m/z*: 581.0 $[M + H]^+$ (52); 419.0 [M + H - glucose]$^+$ (43); 401.1 [M + H - glucose - H_2O]$^+$ (13); 287.2 [aglycone + H]$^+$ (100). The fragment ions at *m/z* = 419.0 and *m/z* = 287.2 (i.e., base peak) correspond to the loss of a hexose (162) and a pentosylhexose moieties (132 + 162), respectively. The ion at *m/z* = 287.2 indicated the occurrence of kaempferol as aglycone. The fragment [M + H - pentose]$^+$ is missing, which is a hint that the pentose is directly bound to the aglycone and that the glucose is linked as the second sugar moiety. The glucose fragment separates at first from the molecule during the ionization. On the basis of the molecular mass at *m/z* = 581.0 and the structural information obtained by NMR analysis, a molecular formula $C_{26}H_{28}O_{15}$ was assigned to compound BS4. The molecular mass was confirmed by high resolution FT-ICR-MS for $[M + Na]^+$ at *m/z* = 603.132636 (calculated mass for $C_{26}H_{28}O_{15}Na$ was 603.13204).

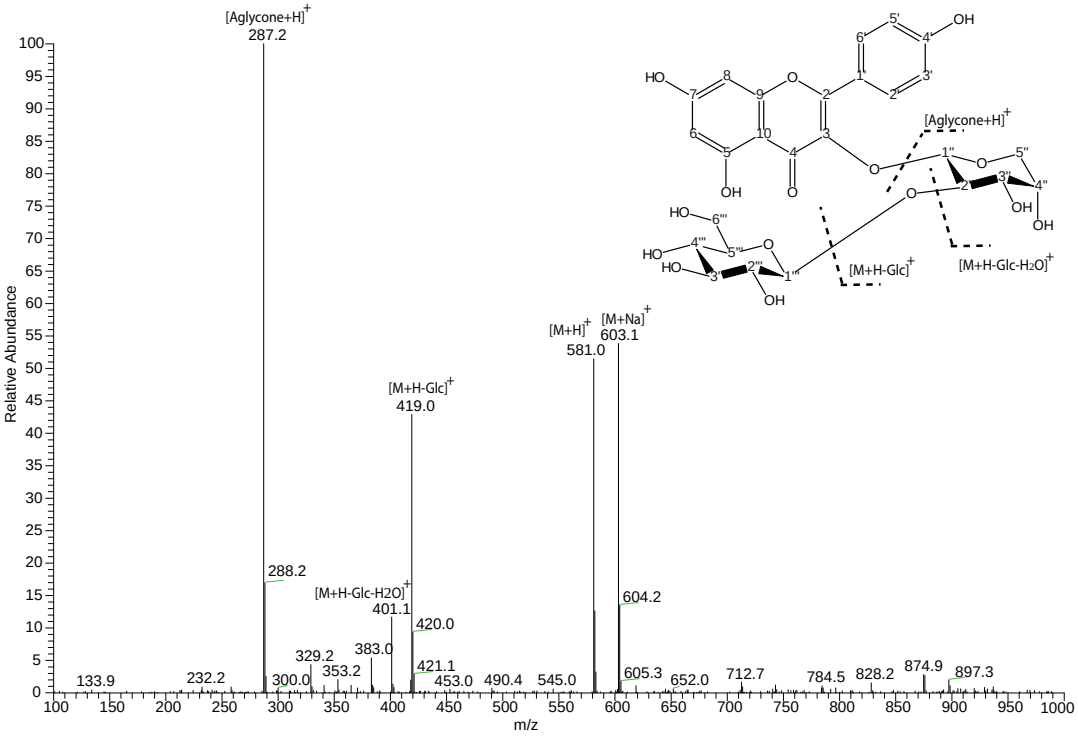

Figure 3.45: ESI-MS (positive mode) of the compound BS4

[16]In brackets the relative intensity in % of the ion peaks is shown.

The aromatic region of the ^{1}H-NMR (see Figure 3.46 and Table 3.5) showed two doublets signals at δ = 6.40 ppm and δ = 6.21 ppm and further two doublets at δ = 8.02 ppm and δ = 6.92 ppm (both d, J = 6 Hz), which indicate compound BS4 as a 5,7-dihydroxyflavonnol with a 1,4-disubtituted. In the upfield region, there are two anomeric signals due to the sugar units at 5.48 ppm and 4.55 ppm. Further nine protons have been identified in the upfield region due to the sugar units between δ = 3.2 ppm and δ = 4.4 ppm.

The ^{13}C-NMR spectrum (see Figure 3.47 and Table 3.5) showed 24 signals for 26 carbons. Between δ = 180 ppm and δ = 106 ppm, there are 13 signals for the 15 carbons of the kaempferol aglycone. Two of them (i.e., δ = 132.4 ppm and δ = 116.5 ppm) are represented by the same carbon signal through the symmetrical structure. The two signals at δ = 105.4 ppm and δ = 101.3 ppm represent the carbons of the sugar residues with the anomeric protons. The nine further signals are caused by the two sugar moieties between δ = 62.7 ppm and δ = 80.1 ppm. The DEPT-135 experiment (see Figure 3.48) determined two CH_2 groups at δ = 63.4 ppm and δ = 62.7 ppm and further 14 CH groups.

The H-H-COSY (see Figure 3.49 and Table 3.5) showed two meta-coupled doublets at δ = 6.40 ppm and 6.21 ppm. Additionally, an AA BB spin system (i.e., C-2 and C-5 , C-3 and C-6) was evident as two doublets at δ = 8.06 ppm and δ = 6.91 ppm. The values of the aromatic signals of both the ^{1}H- and ^{13}C-NMR spectra suggested the presence of kaempferol as the aglycone with two sugar units.

The coupling constant of the anomeric proton of the glucose (J = 6 Hz) was in accordance with a β-glycosidic linkage (i.e., β-D-glucopyranose), while the coupling constant of the anomeric proton of the pentose (J = 3 Hz) was in accordance with an α-glycosidic linkage (i.e., α-L-arabinopyranose). The H-H-COSY allowed to show the coupling between each protons of the sugar moieties as demonstrated in Figure 3.49 and in Table 3.5. The α-L-arabinopyranose exhibited the proton correlations: between H-1" (δ = 5.48 ppm) and H-2" (δ = 4.21 ppm); between H-2" and H-3" (δ = 3.96 ppm); and between H-4" (δ = 3.86 ppm) and H-5" (δ = 3.69 ppm). The β-D-glucopyranose presented the proton correlations: between H-1" (δ = 4.55 ppm) and H-2" (δ

= 3.25 ppm); between H-2" and H-3" (δ = 3.38 ppm); between H-4" (δ = 3.34 ppm) and H-5" (δ = 3.23 ppm δ = 3.73 ppm).

The HSQC experiment (see Figure 3.50) showed that the two signals at δ = 99.9 ppm and δ = 94.7 ppm were correlated to the proton signals at δ = 6.40 ppm (H-8) and δ = 6.21 ppm (H-6). The two carbon signals at δ = 132.4 ppm and δ = 116.5 ppm were also coupled with the two doublets of the 1,4-disubstituted aromatic moiety (B ring) at δ = 8.02 ppm and δ = 6.92 ppm, respectively.

In the HMBC experiment (see Figure 3.51 and Table 3.5), C-7 appeared at δ = 166.0 ppm and is coupled with H-8 (δ = 6.40 ppm). The signals C-5, C-9 and C-10 are also identified by HMBC long-range coupling. C-9 and C-10 (δ_{C9} = 159.0 ppm and δ_{C10} = 105.8 ppm) are coupled with H-8. C-10 and C-5 (δ_{C10} = 105.8 ppm and δ_{C5} = 161.6 ppm) show a correlation with H-6 (δ = 6.21 ppm). The carbons in the C-4 and C-2 position provide signals at δ_{C4} = 179.7 ppm and δ_{C2} = 158.5 ppm. C-2 is correlated with δ = 8.02 ppm (H-2 , H-6) and δ = 6.92 ppm (H-3 , H-5). Furthermore, the anomeric proton H-1" (δ = 5.48 ppm) is correlated with C-3 (δ_{C3} = 135.7 ppm) showing the coupling between the α-L-arabinopyranose and the aglycone kaempferol. Additionally, the coupling between the sugar units is shown by the correlation of the H-1" (δ = 4.55 ppm) of the β-D-glucopyranose with C-2"($\delta_{C2''}$ = 80.1 ppm) of the α-L-arabinopyranose. The HMBC experiment represented the following long-range correlations between ^{1}H and ^{13}C in α-L-arabinopyranose: between H-2" (δ = 4.21 ppm) and C-1" ($\delta_{C1'''}$ = 105.4 ppm); between H-4" (δ = 3.86 ppm) and C-5" ($\delta_{C5''}$ = 63.4 ppm); between H-5" (δ = 3.69 ppm) and C-1" ($\delta_{C1''}$ = 101.3 ppm) and C-3" ($\delta_{C3''}$ = 71.3 ppm). In β-D-glucopyranose, the HMBC experiment provided following long-range correlations between ^{1}H and ^{13}C: between H-2" (δ = 3.25 ppm) and C-1" ($\delta_{C1'''}$ = 105.4 ppm) and C-3" ($\delta_{C3'''}$ = 78.1 ppm) ; between both H-3" (δ = 3.38 ppm) and H-4" (δ = 3.34 ppm) with C-2" ($\delta_{C2'''}$ = 75.2 ppm); between H-5" (δ = 3.36 ppm) and C-4" ($\delta_{C4'''}$ = 71.4 ppm).

The chemical-shift values of the carbons of the sugar units were in agreement with those of a glucopyranose (i.e., β-D-glucopyranose) and an arabinopyranose (i.e., α-L-arabinopyranose) from the literature [169] (see Table 3.5). The assignment of the sugars to D- or L-series are based on the

literature [27]. Based on the MS, 1D- and 2D-NMR analysis, a kaempferol 3-O-β-D-glucopyranosyl-(1$'''\rightarrow$ 2$''$)-O-α-L-arabinopyranoside was identified as the compound BS4.

Table 3.5: Chemical shifts of BS4 and literature

Atom numbers	^{13}**C*** δ**/ppm**	^{13}**C**** δ**/ppm**	^{1}**H*** δ**/ppm (Mult., J(Hz), H)**	^{1}**H - ^{1}H COSY***	^{1}**H - ^{13}C HMBC***
2	158.5	-	-	-	-
3	135.7	-	-	-	-
4	179.7	-	-	-	-
5	161.6	-	-	-	-
6	99.9	-	6.21 (brs; 1H)	8	5, 8, 10
7	166.0	-	-	-	-
8	94.7	-	6.40 (brs; 1H)	6	6, 7, 9, 10
9	159.0	-	-	-	-
10	105.8	-	-	-	-
1$'$	122.6	-	-	-	-
2$'$	132.4	-	8.02 (d; 6 Hz; 1H)	3$'$, 5$'$	2, 4$'$, 6$'$
3$'$	116.5	-	6.92 (d; 6 Hz; 1H)	2$'$, 6$'$	2, 1$'$, 5$'$
4$'$	163.1	-	-	-	-
5$'$	116.5	-	6.92 (d; 6 Hz; 1H)	2$'$, 6$'$	2, 1$'$, 3$'$
6$'$	132.4	-	8.02 (d; 6 Hz; 1H)	3$'$, 5$'$	2, 2$'$, 4$'$
1$''$	101.3	100.9	5.48 (d; 3 Hz; 1H)	2$''$	3
2$''$	80.1	78.3	4.21 (dd; 6 Hz; 4 Hz; 1H)	1$''$, 3$''$	1$''$
3$''$	71.3	71.4	3.96 (dd; 6 Hz; 4 Hz; 1H)	2$''$	-
4$''$	66.6	66.3	3.86 (m; 1H)	5$''$	5$''$
5$''$	63.4	62.1	3.23 (m; 1H); 3.73 (m; 1H)	4$''$	1$''$, 3$''$
1$'''$	105.4	103.1	4.55 (d; 6 Hz; 1H)	2$'''$	2$''$
2$'''$	75.2	77.6	3.25 (d; 6 Hz; 1H)	1$'''$, 3$'''$	1$'''$, 3$'''$
3$'''$	78.1	79.4	3.38 (brs; 1H)	2$'''$	2$'''$
4$'''$	71.4	72.7	3.34 (brs; 1H)	5$'''$	2$'''$
5$'''$	78.0	78.2	3.36 (brs; 1H)	4$'''$	4$'''$
6$'''$	62.7	62.1	3.78-3.82 (m; 2H)	-	-

* In MeOH-d_4. ** Data from literature [169] in Pyridine-d_5.

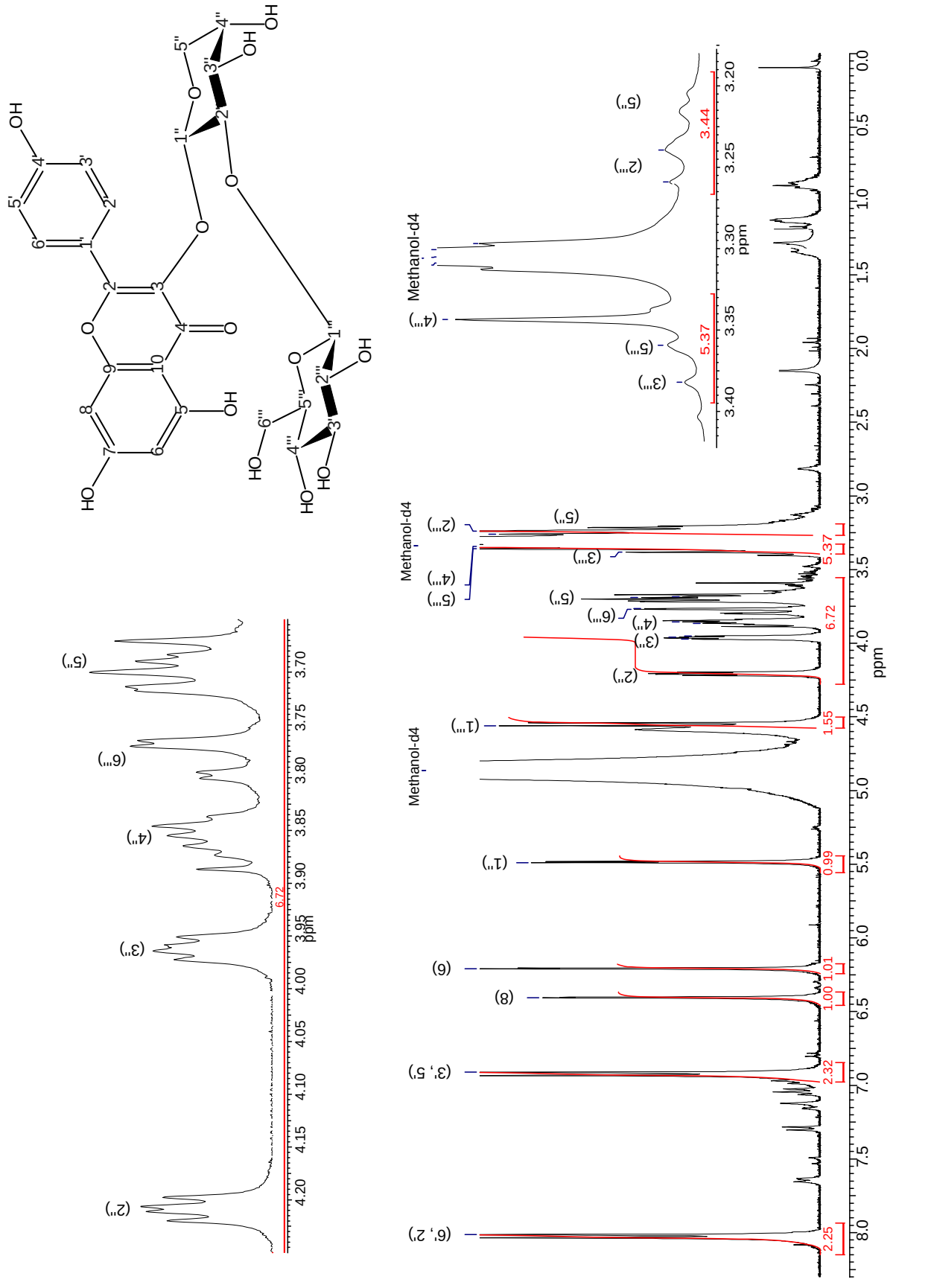

Figure 3.46: ^{1}H-NMR of BS4 (250 MHz, MeOH-d_4)

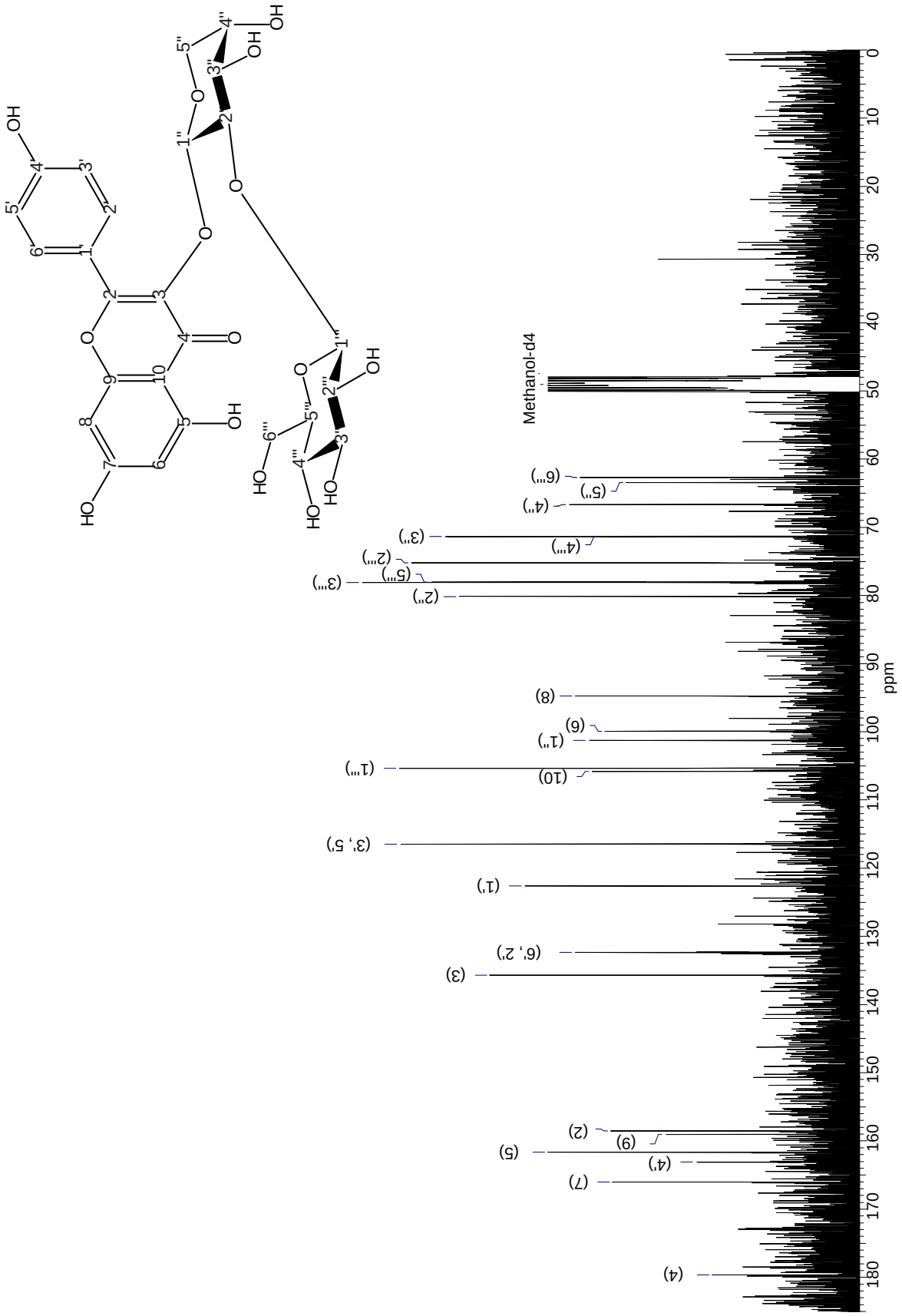

Figure 3.47: ^{13}C-NMR of BS4 (100 MHz, MeOH-d_4)

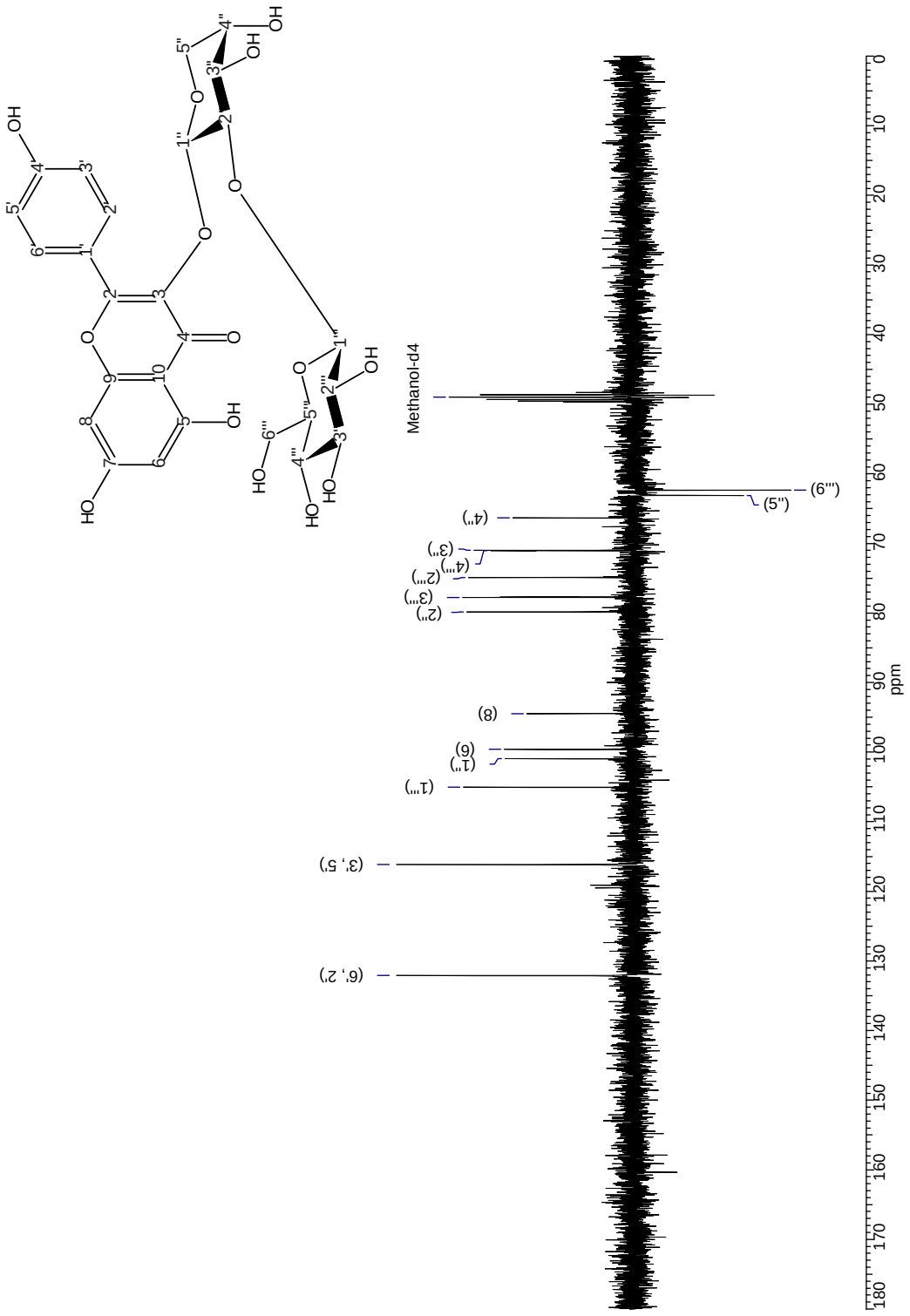

Figure 3.48: DEPT-135 of BS4 (100 MHz, MeOH-d_4)

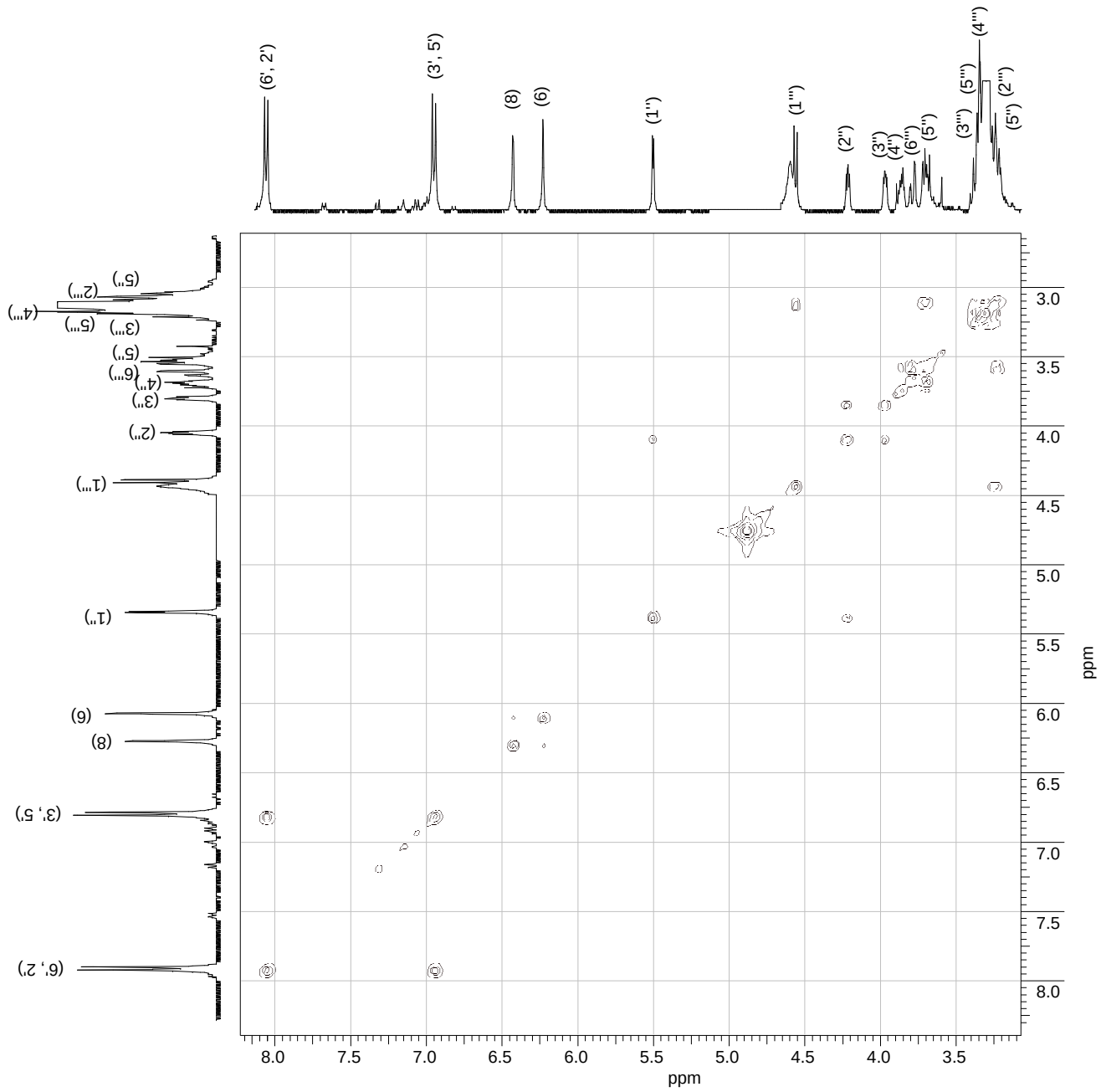

Figure 3.49: H-H-COSY of BS4 (600 MHz, MeOH-d_4)

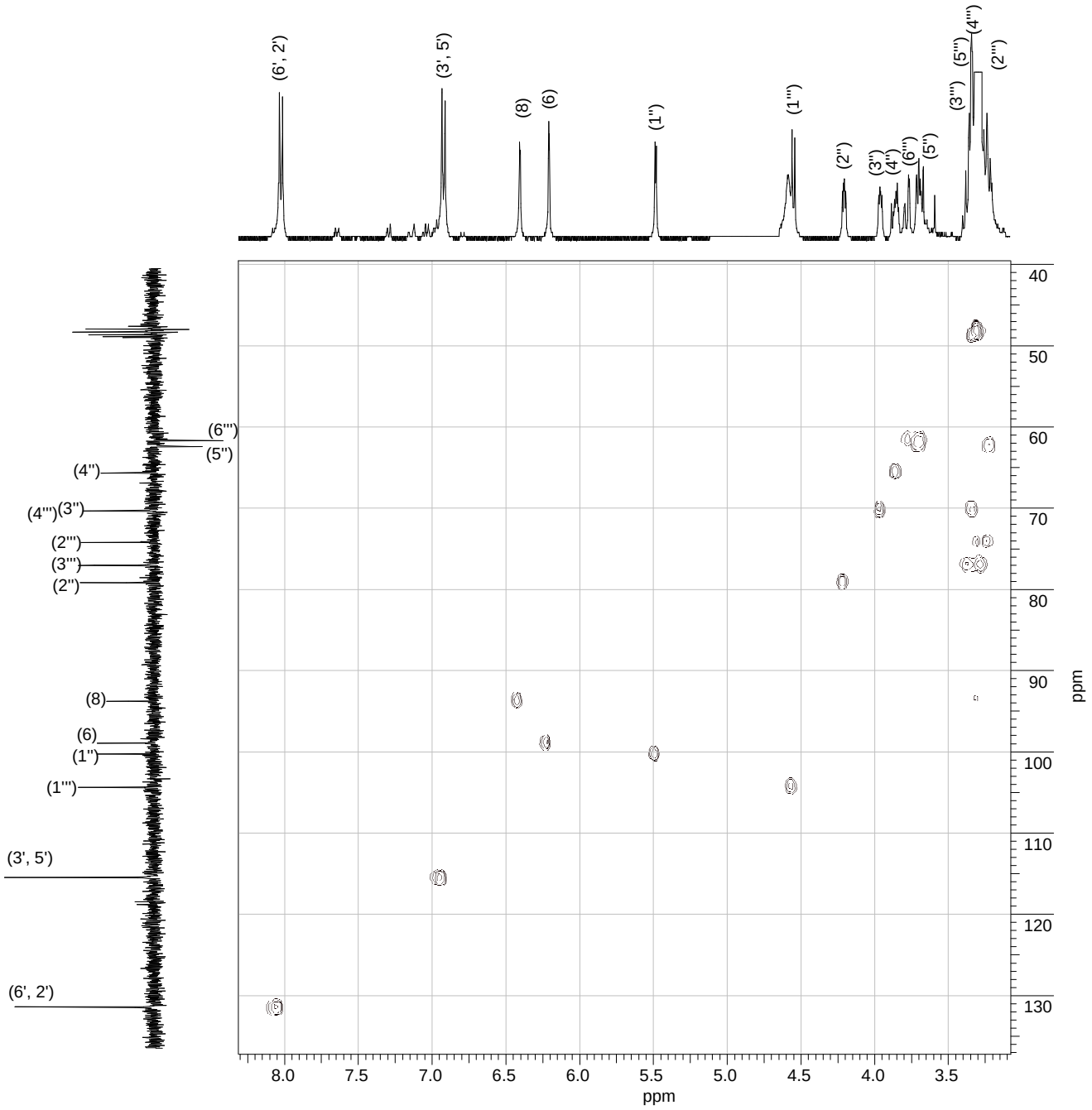

Figure 3.50: HSQC of BS4 (600 MHz, MeOH-d_4)

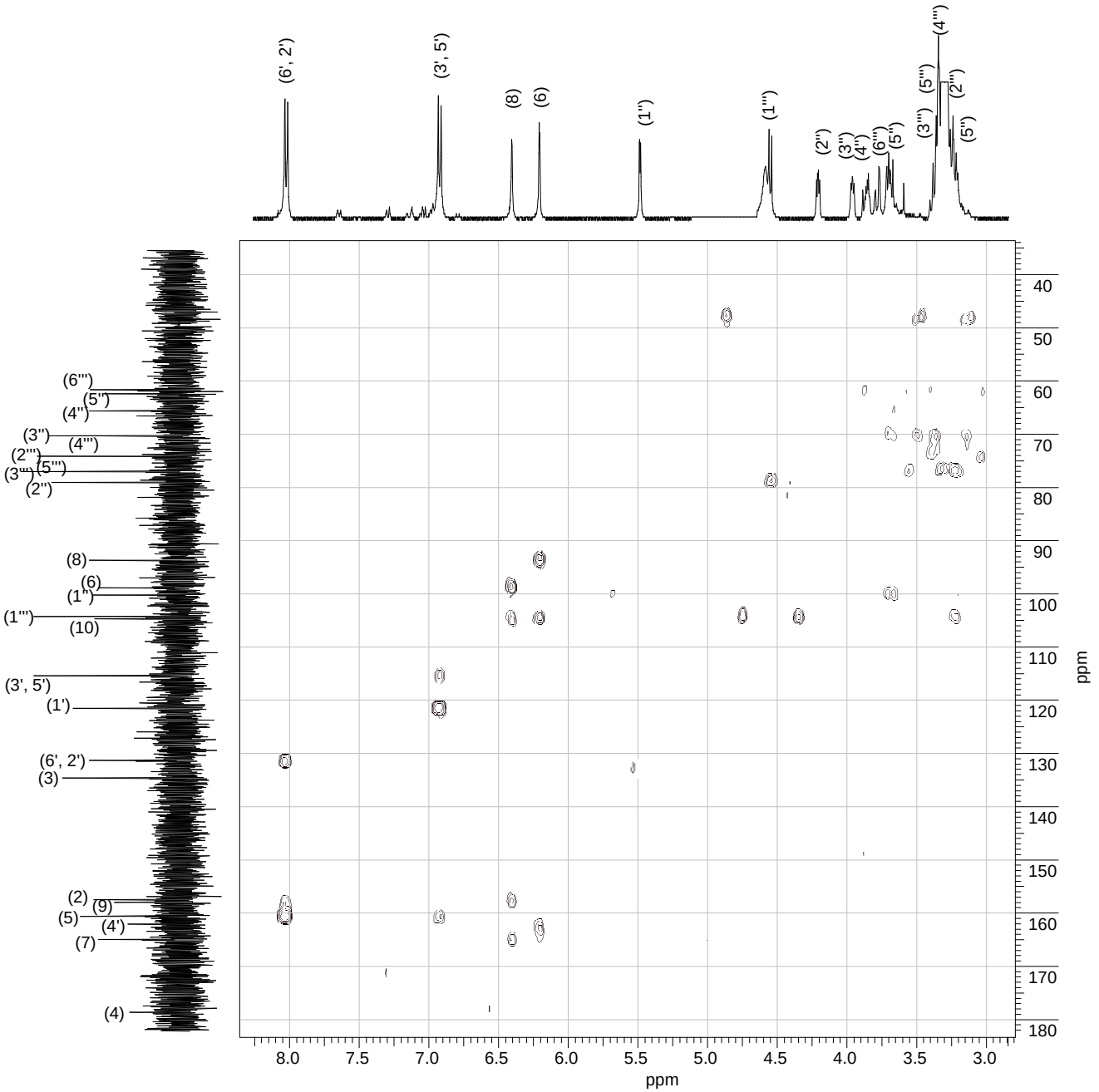

Figure 3.51: HMBC of BS4 (600 MHz, MeOH-d_4)

3.1.2.2.2 BS1: Kaempferol 3-O-β-D-glucopyranosyl-(1‴→2″) -O-α-L-arabinopyranoside-7-O-β-D-glucopyranoside

The subfractionation of the fraction G was performed consecutively by a sequence of two open column chromatography and analytical HPLC (see Section 5.6.2.2, Experimental Part) yielding 10.3 mg of the compound BS1, which was identified as kaempferol 3-O-β-D-glucopyranosyl--(1‴→2″)-O-α-L-arabinopyranoside-7-O-β-D-glucopyranoside[17]. This compound was isolated as a yellow amorphous powder with the chemical structure shown in Figure 3.52. This structure was established on the basis of UV, IR, MS and NMR spectroscopic data.

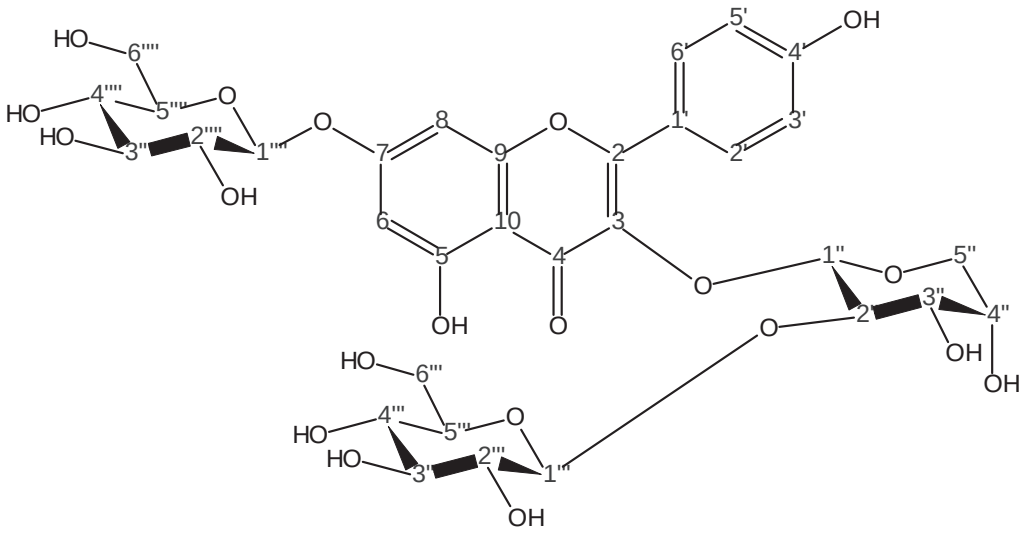

Figure 3.52: Chemical structure of the compound BS1

The UV spectrum of BS1 (see Figure 3.53) exhibited two absorption maxima (in MeOH) at λ = 265 and 345 nm, which provided evidence to be in accordance with a 3,7-di-O-substituted flavonol skeleton [196]. The FTIR spectrum (see Figure 3.54) showed distinguishable absorption bands at: 3365.6, 1653.8, 1605.3, 1557.9, 1493.3, 1351.1, 1307.3, 1280.1, 1199.0, 1182.2, 1118.9, 1064.0, 1039.9, 1017.0, 967.1, 887.1, 827.5, 786.0, 707.0 cm^{-1}.

[17] IUPAC name: 3-[(2-O-hexopyranosylpentopyranosyl)oxy]-5-hydroxy-2-(4-hydroxyphenyl)-4-oxo-4H-chromen-7-yl hexopyranoside

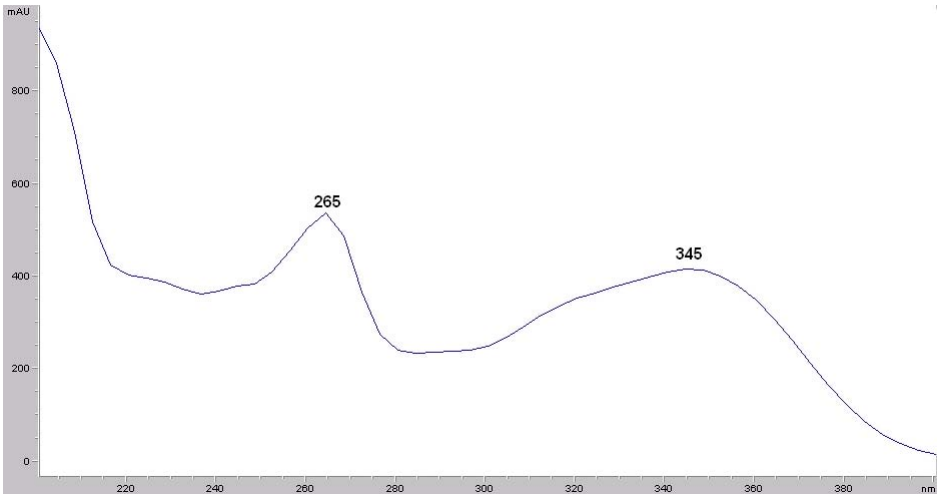

Figure 3.53: UV of the compound BS1

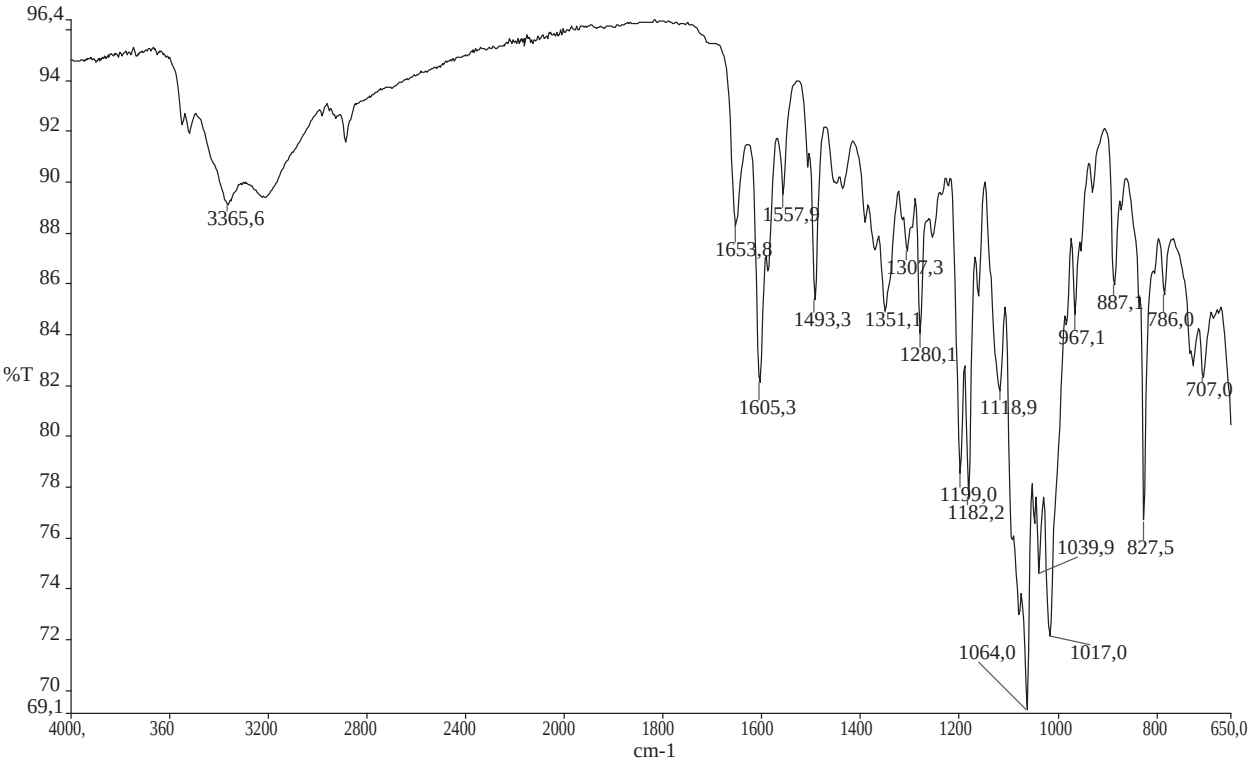

Figure 3.54: IR of the compound BS1

The ESI mass spectrum (see Figure 3.55) showed a quasimolecular positive ion peak[18] at *m/z* = 765.0 $[M + Na]^+$ (10), and further peaks at *m/z*: 742.8 $[M + H]^+$ (22); 580.9 $[M + H - glucose]^+$ (29); 448.8 $[M + H - arabinose - glucose]^+$ (100); 418.9 $[M + H - glucose - glucose]^+$ (15); 400.9 $[M + H - glucose - H_2O]^+$ (7); 287.1 $[aglycone + H]^+$ (82). The fragment ions at *m/z* = 580.9, 448.8 (i.e., base peak) and 418.9 correspond to the loss of a hexose (162), a pentosylhexose residue (132 + 162), and of two hexoses (162 + 162), respectively. On the basis of the molecular mass at *m/z* = 742.8 and the structural information obtained by NMR analysis, a molecular formula $C_{32}H_{38}O_{20}$ was assigned to compound BS1. The molecular mass was confirmed by high resolution FT-ICR mass spectrometry for $[M + Na]^+$ at *m/z* = 765.184176 (calculated mass for $C_{32}H_{38}O_{20}Na$ was 765.18486).

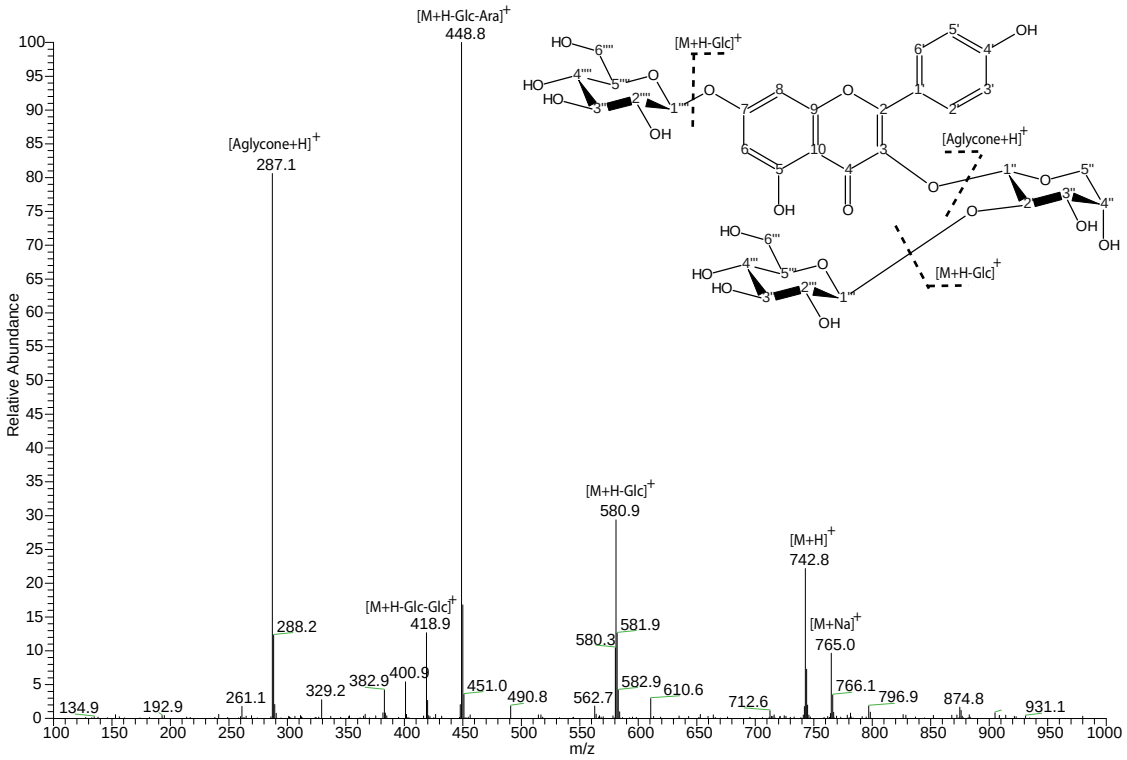

Figure 3.55: ESI-MS (positive mode) of the compound BS1

[18] In brackets, the relative intensity in % of the ion peaks is shown.

The NMR-spectra of BS1 are quite similar to those of BS4 (see Section 3.1.2.2.1). Additionally, in the middle region of the ^{1}H-NMR spectrum, one further anomeric signal due to sugar unit at δ = 5.07 ppm was identified.

The ^{13}C-NMR spectrum (see Figure 3.57 and Table 3.6) showed 30 signals for 32 carbons. The three signals at δ = 98.9 ppm, δ = 99.8 ppm and δ = 103.8 ppm can be assigned to anomeric carbons of the sugar units. The DEPT-135 experiment (see Figure 3.58) demonstrated three CH_2 groups at δ = 61.2 ppm, δ = 60.9 ppm and δ = 60.6 ppm and further 23 CH groups were identified.

The HSQC (see Figure 3.60) and the H-H-COSY experiments (see Figure 3.59 and Table 3.6) showed a similar spectra as that from BS4. The main difference is that BS1 has a possible third sugar unit. The values of the aromatic signals of both ^{1}H- and ^{13}C-NMR spectra suggested again the presence of a kaempferol as aglycone, however, with three sugar units (see Figure 3.61).

The coupling constant of the anomeric protons H-1'' and H-1'''' (both J = 6 Hz) of the glucoses were in accordance with a β-glycosidic linkage (i.e., β-D-glucopyranose), whereas the anomeric proton of the pentose (i.e., brs) was in accordance with an α-glycosidic linkage (i.e., α-L-arabinopyranose). The H-H-COSY showed the ^{1}H correlations for the second β-D-glucopyranose: between H-1'''' (δ = 5.07 ppm) and H-2'''' (δ = 3.25 ppm); between H-2'''' and H-3'''' (δ = 3.30 ppm); between H-4'''' (δ = 3.17 ppm) and H-5'''' (δ = 3.12 ppm); between H-5'''' and H-6'''' (δ = 3.70 ppm and δ = 3.43 ppm).

In the HMBC spectrum (see Figure 3.62 and Table 3.6), the anomeric proton H-1'''' (δ = 5.07 ppm) is correlated with C-7 (δ_{C7} = 162.9 ppm) showing the coupling between the β-D-glucopyranose with the aglycone kaempferol at C-7. Additionally, in this second β-D-glucopyranose, the following long-range correlations between ^{1}H and ^{13}C were observed in the HMBC experiment: between H-2'''' (δ = 3.25 ppm) and C-1'''' ($\delta_{C1''''}$ = 99.8 ppm); between H-3'''' (δ = 3.30 ppm) and C-2'''' ($\delta_{C2''''}$ = 73.6 ppm) and C-5'''' ($\delta_{C5''''}$ = 76.8 ppm).

The chemical-shift values of the carbons of the sugar units were in agreement with those of a glucopyranose (i.e., β-D-glucopyranose) and an arabinopyranose (i.e., α-L-arabinopyranose) from the literature [169] (see Table 3.6). The assignment of the sugars to D- or L-series is based on

the literature [27]. Based on the MS, 1D- and 2D-NMR analysis, a kaempferol 3-O-β-D-glucopyranosyl-(1$'''\rightarrow$2$''$)-O-α-L-arabinopyranoside-7-O-β-D-glucopyranoside was identified as the compound BS1.

Table 3.6: Chemical shifts of BS1

Atom numbers	^{13}**C*** δ**/ppm**	^{13}**C**** δ**/ppm**	^{1}**H*** δ**/ppm (Mult., J(Hz), H)**	^{1}**H - ^{1}H COSY***	^{1}**H - ^{13}C HMBC***
2	155.9	-	-	-	-
3	134.3	-	-	-	-
4	177.7	-	-	-	-
5	160.2	-	-	-	-
6	99.3	-	6.44 (brs; 1H)	8	5, 7, 8, 10
7	162.9	-	-	-	-
8	94.6	-	6.79 (brs; 1H)	6	6, 7, 9, 10
9	156.6	-	-	-	-
10	105.6	-	-	-	-
1$'$	120.3	-	-	-	-
2$'$	131.1	-	8.10 (d; 6 Hz; 1H)	3$'$, 5$'$	2, 4$'$, 6$'$
3$'$	115.4	-	6.91 (d; 6 Hz; 1H)	2$'$, 6$'$	1$'$, 4$'$, 5$'$
4$'$	160.2	-	-	-	-
5$'$	115.4	-	6.91 (d; 6 Hz; 1H)	2$'$, 6$'$	1$'$, 3$'$, 4$'$
6$'$	131.1	-	8.10 (d; 6 Hz; 1H)	3$'$, 5$'$	2, 2$'$, 4$'$
1$''$	98.9	100.9	5.61 (brs; 1H)	2$''$	3, 2$''$, 3$''$, 5$''$
2$''$	78.7	78.3	4.07 (brs; 1H)	1$''$, 3$''$	1$'''$
3$''$	68.7	71.4	3.86 (brs; 1H)	2$''$, 4$''$	-
4$''$	64.1	66.3	3.70 (m; 1H)	3$''$	3$''$
5$''$	61.2	62.1	3.07 (d; 6 Hz; 1H); 3.51 (m; 1H)	5$''$	3$''$
1$'''$	103.8	103.1	4.37 (d; 6 Hz; 1H)	2$'''$	2$''$, 3$''$
2$'''$	73.6	77.6	2.97 (m; 1H)	1$'''$, 3$'''$	1$'''$, 3$'''$
3$'''$	76.7	79.4	3.17 (m; 1H)	2$'''$	-
4$'''$	69.7	72.7	3.12 (d; 4 Hz; 1H)	3$'''$	3$'''$, 5$'''$, 6$'''$
5$'''$	77.1	78.2	3.43 (m; 1H)	6$'''$	-
6$'''$	60.9	62.1	3.59 (d; 11 Hz; 1H); 3.43 (m; 1H)	5$'''$	-
1$''''$	99.8	103.1	5.07 (d; 6 Hz; 1H)	2$''''$	7
2$''''$	73.1	77.6	3.25 (m; 1H)	1$''''$	1$''''$
3$''''$	76.4	79.4	3.30 (m; 1H)	2$''''$	2$''''$, 5$''''$
4$''''$	69.6	72.7	3.17 (m; 1H)	5$''''$	-
5$''''$	76.8	78.2	3.12 (d; 4 Hz; 1H)	6$''''$, 4$''''$	-
6$''''$	60.6	62.1	3.70 (m; 1H); 3.43 (m; 1H)	5$''''$, 6$''''$	-

* In DMSO-d_6. ** Data from literature [169] in Pyridine-d_5.

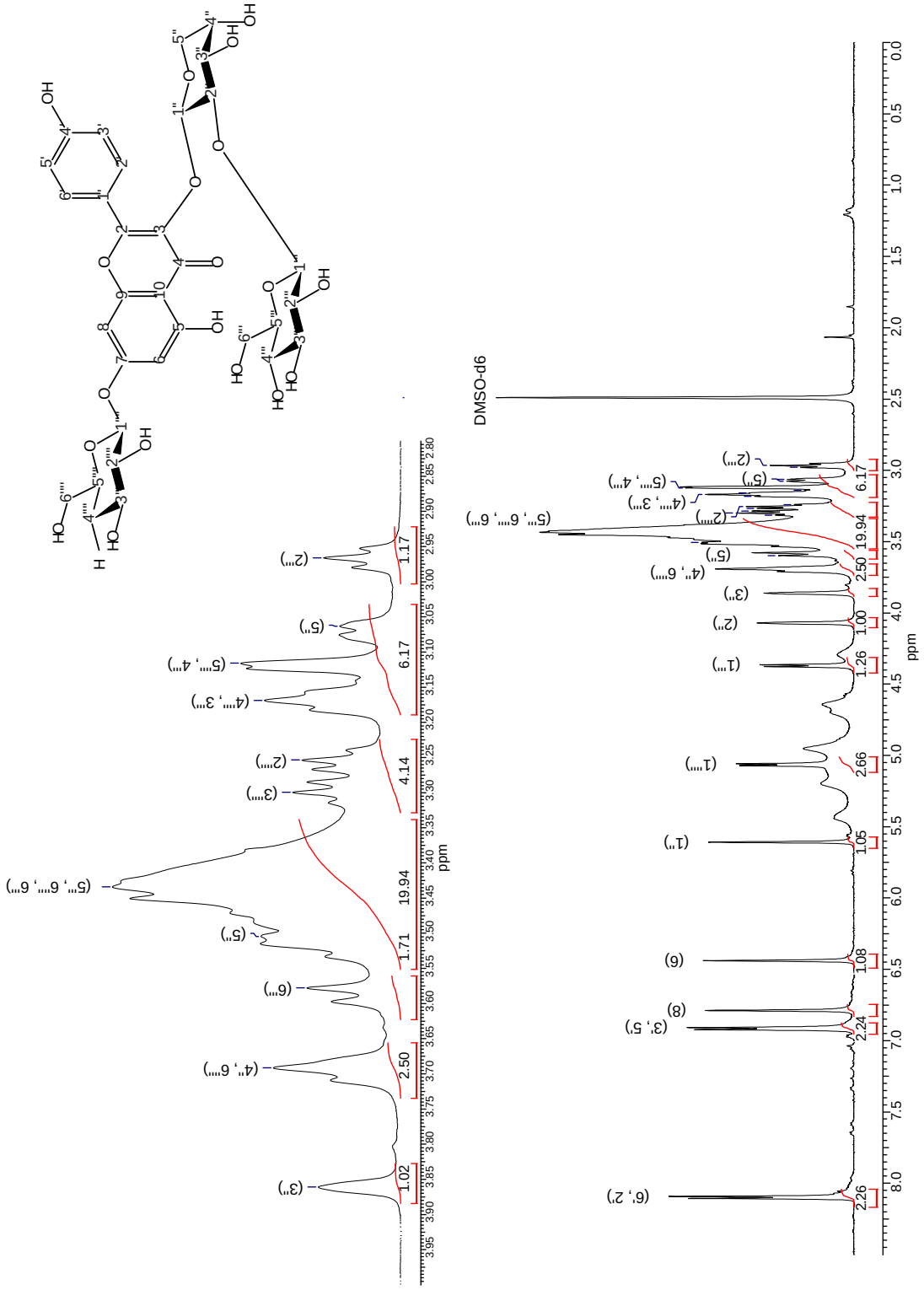

Figure 3.56: ^{1}H-NMR of BS1 (600 MHz, DMSO-d_6)

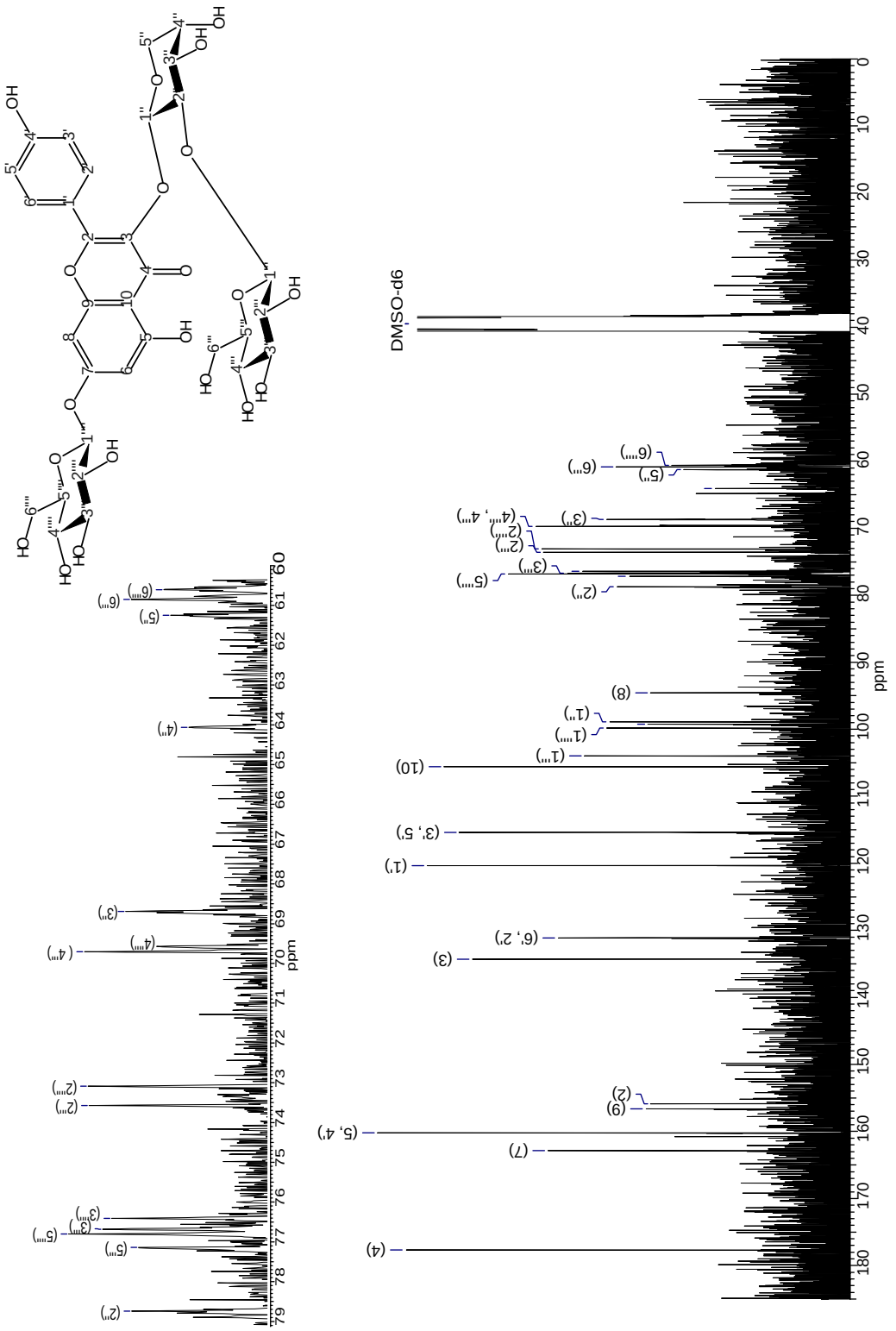

Figure 3.57: ^{13}C-NMR of BS1 (100 MHz, DMSO-d_6)

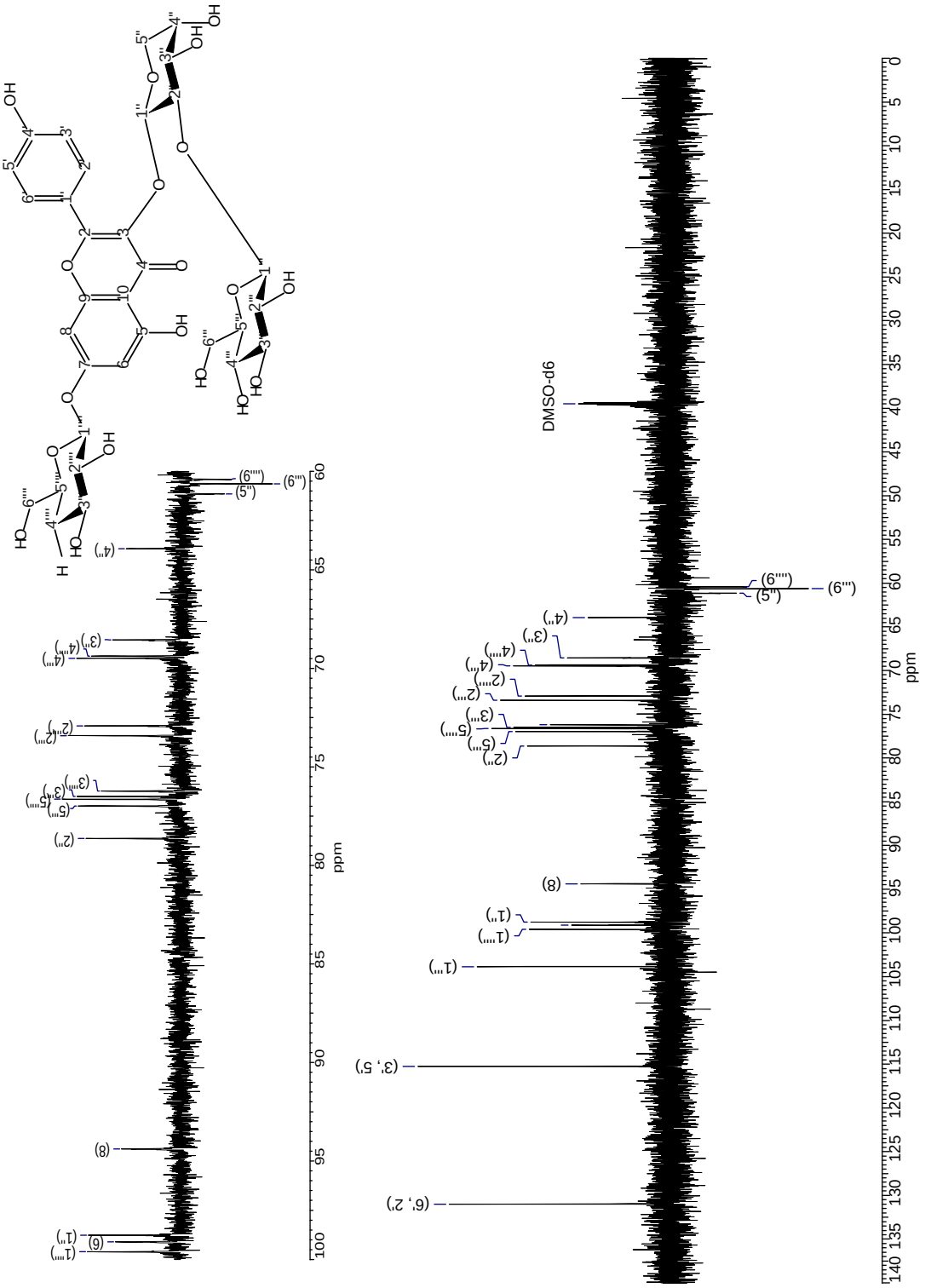

Figure 3.58: DEPT-135 of BS1 (100 MHz, DMSO-d_6)

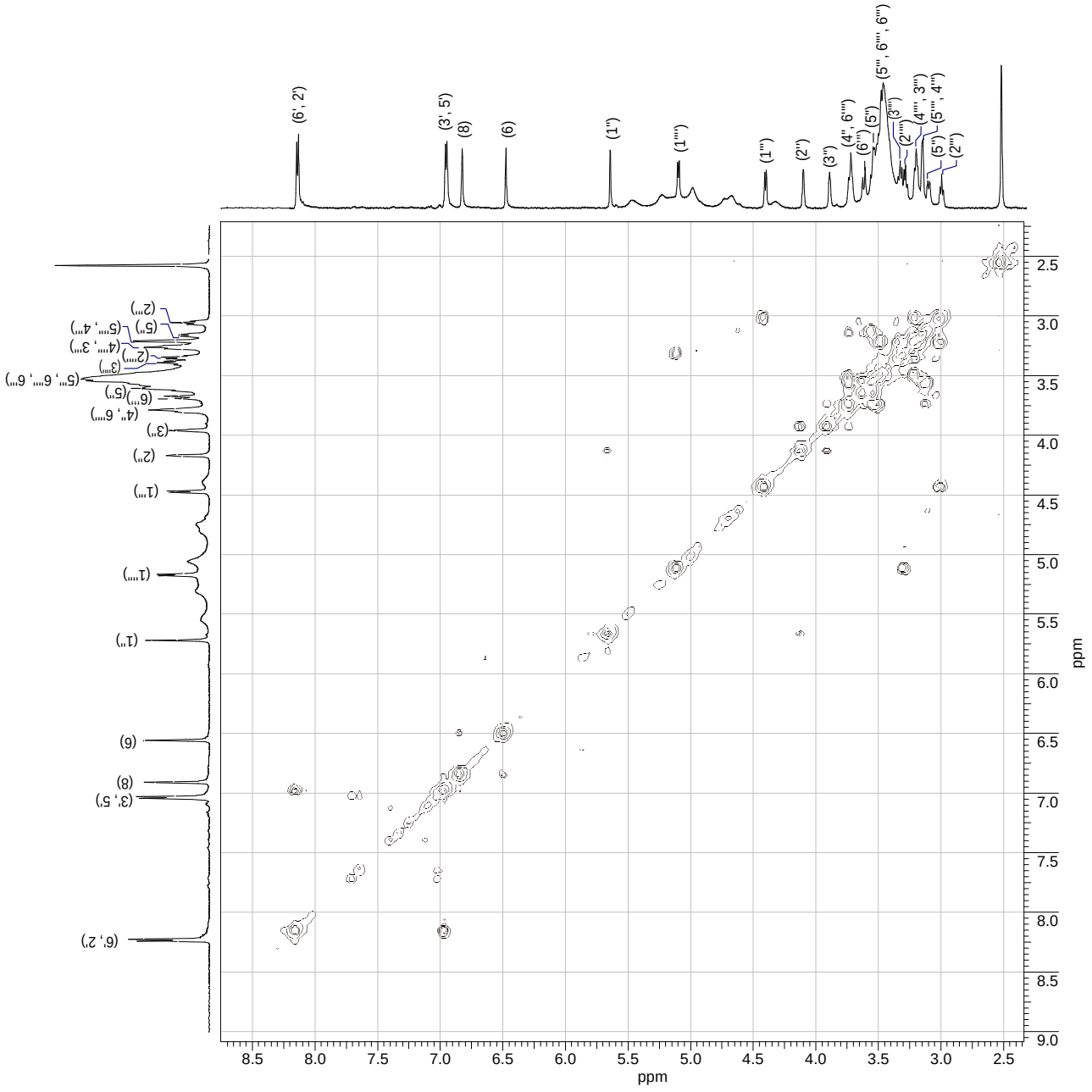

Figure 3.59: H-H-COSY of BS1 (600 MHz, DMSO-d_6)

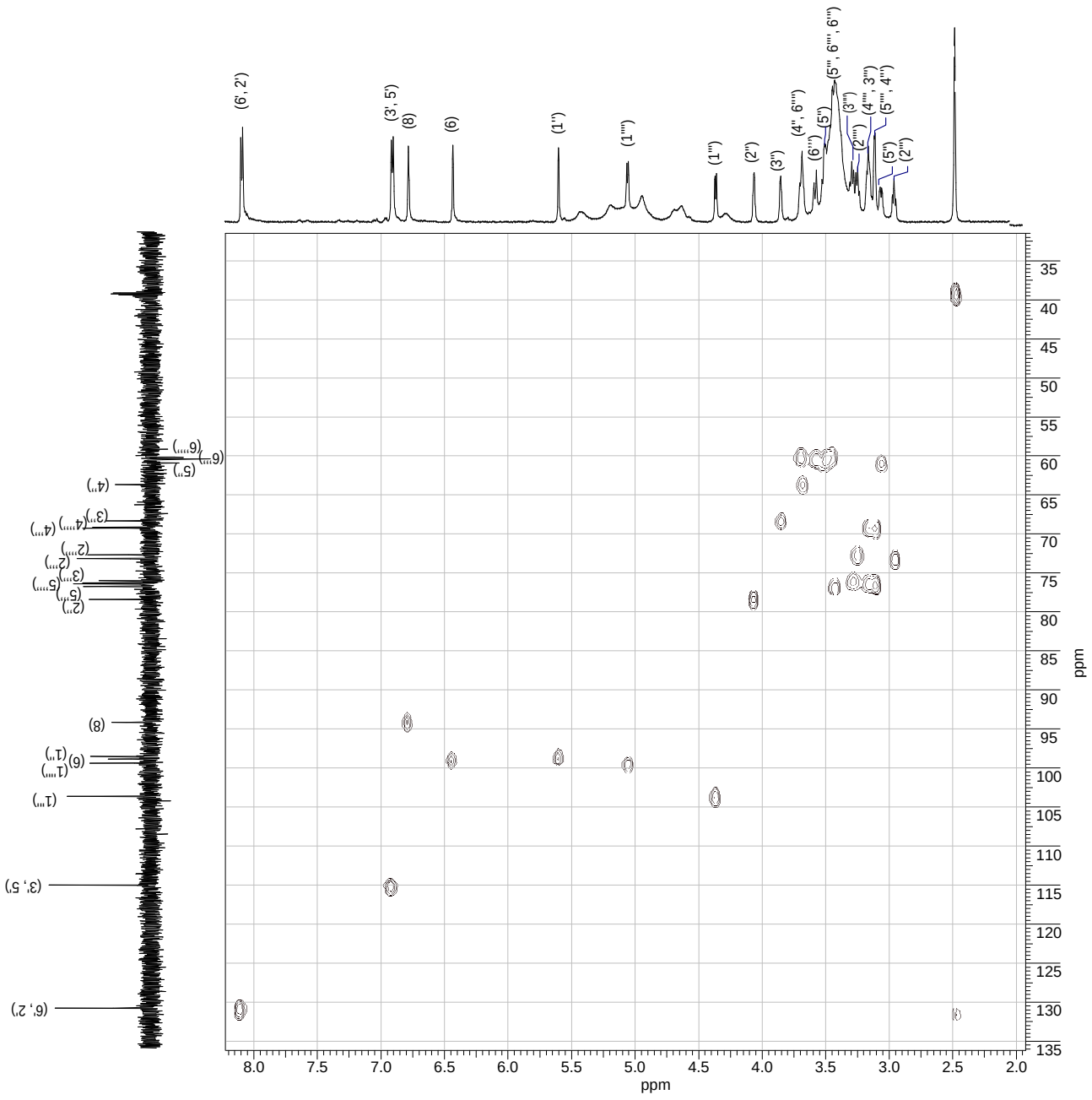

Figure 3.60: HSQC of BS1 (600 MHz, DMSO-d_6)

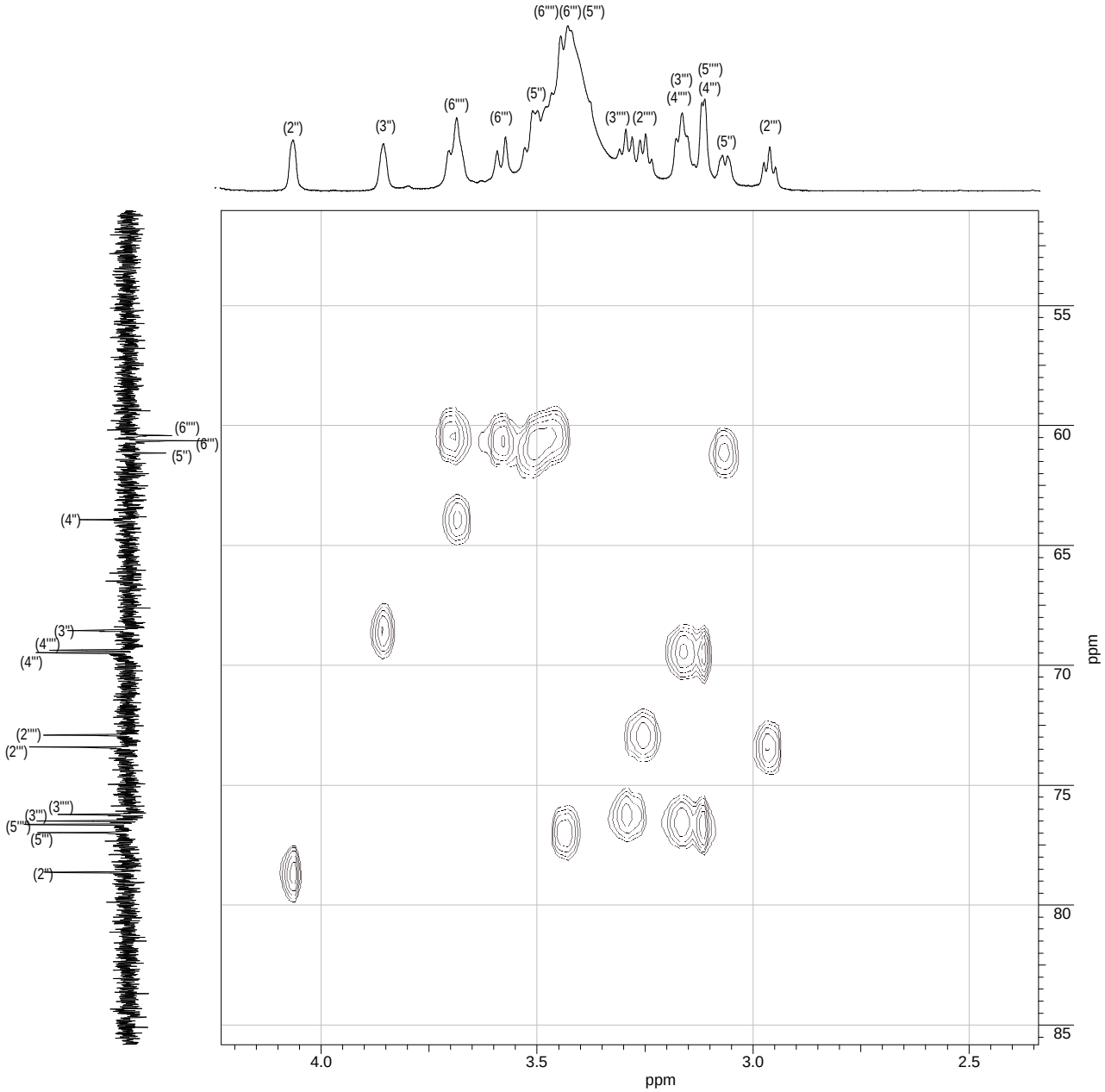

Figure 3.61: HSQC of BS1 sugar region (600 MHz, DMSO-d_6)

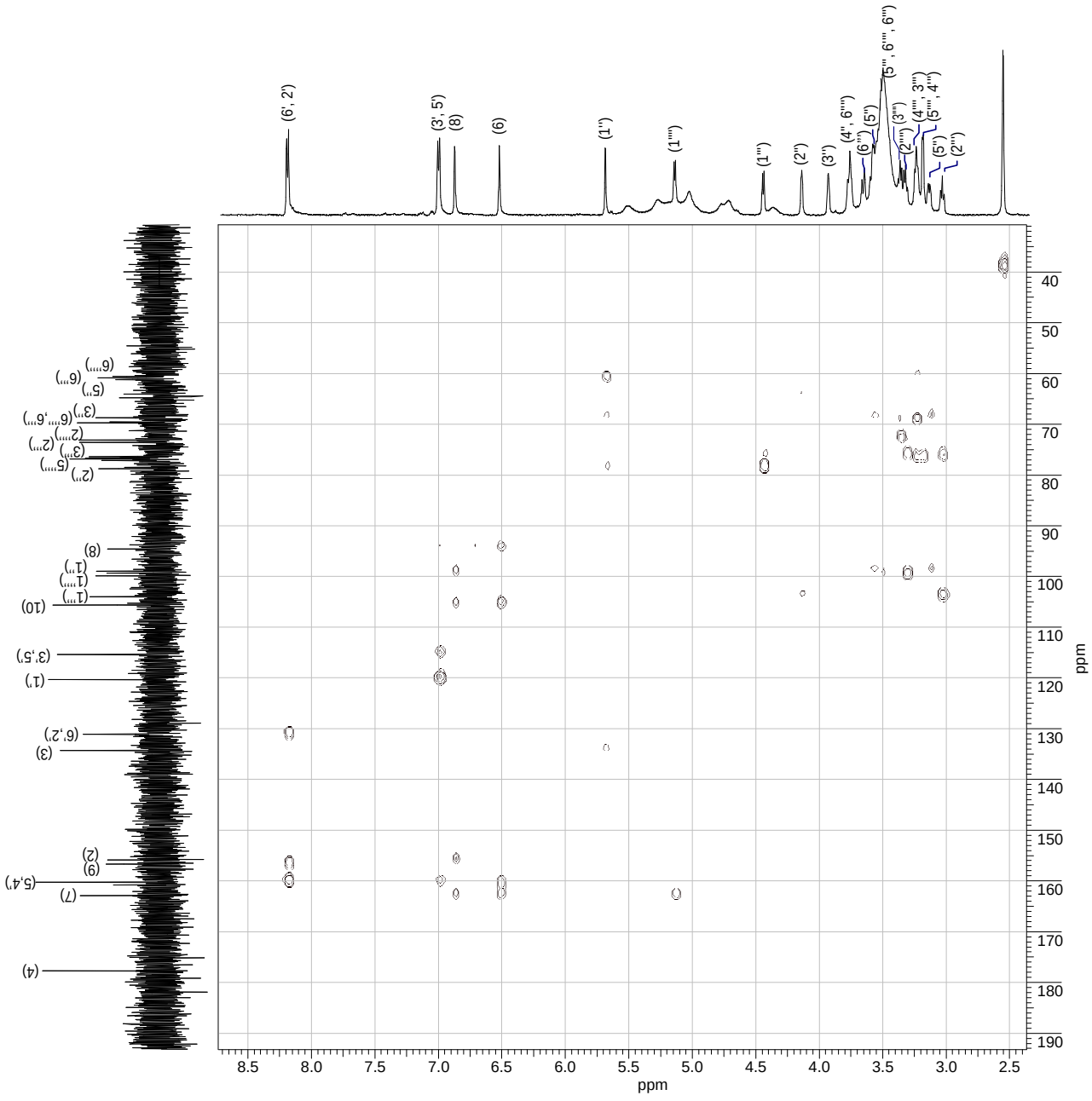

Figure 3.62: HMBC of BS1 (600 MHz, DMSO-d_6)

3.1.2.2.3 BS2: Kaempferol 3-O-β-D-[6$'''$-O-(3,4-dihydroxy-cinnamoyl)] -glucopyranosyl-(1$'''\rightarrow$2$''$)-O-α-L-arabinopyranoside-7-O-β-D-glucopyranoside

The subfractionation of the fractions H and I was performed consecutively by flash chromatography, open column chromatography and analytical HPLC (see Section 5.6.2.2, Experimental Part) yielding a total of 15.6 mg (11.1 mg from fraction H and 4.5 mg from fraction I) of the compound BS2, which was identified as kaempferol 3-O-β-D-[6$'''$-O-(3,4-dihydroxy-cinnamoyl)]-glucopyranosyl-(1$'''\rightarrow$2$''$)-O-α-L-arabinopyranoside-7-O-β-D-glucopyranoside[19]. This compound was obtained as a yellow amorphous powder and its chemical structure as shown in Figure 3.63. This structure was established on the basis of UV, IR, MS and NMR spectroscopic data.

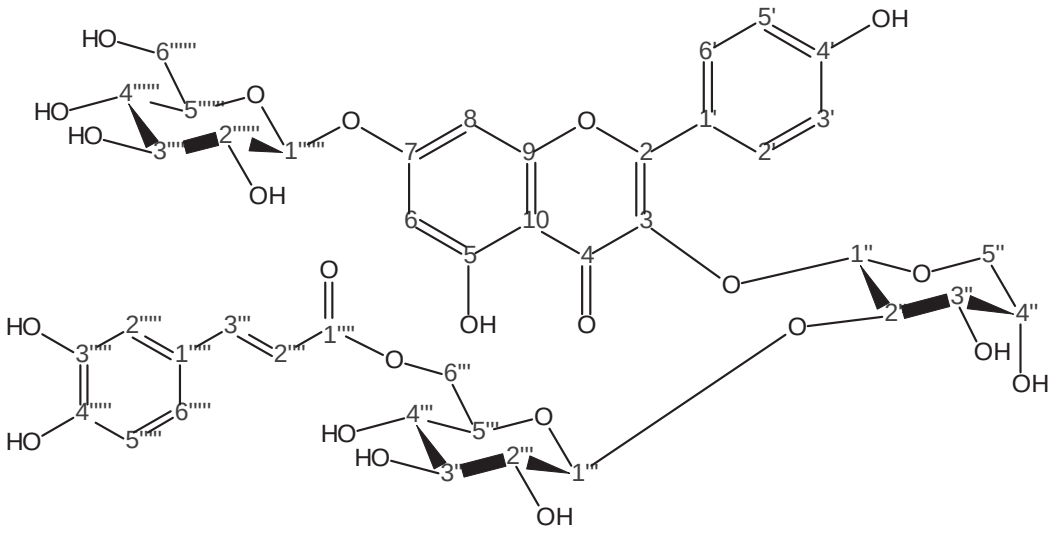

Figure 3.63: Chemical structure of BS2

The UV spectrum of BS2 (see Figure 3.64) exhibited two absorption maxima (in MeOH) at λ = 265 and 328 nm that provided evidences to be in accordance with a 3,7-di-O-substituted flavonol skeleton [196]. The FTIR spectrum (see Figure 3.65) showed distinguishable absorption bands at: 3309.5, 1651.9, 1598.2, 1491.0, 1346.1, 1260.6, 1178.3, 1072.4, 807.6 cm^{-1}.

[19]IUPAC name: 3-[(2-O-6-O-[(2E)-3-(3,4-dihydroxyphenyl)prop-2-enoyl]hexopyranosylpentopyranosyl)oxy]-5-hydroxy-2-(4-hydroxyphenyl)-4-oxo-4H-chromen-7-yl hexopyranoside

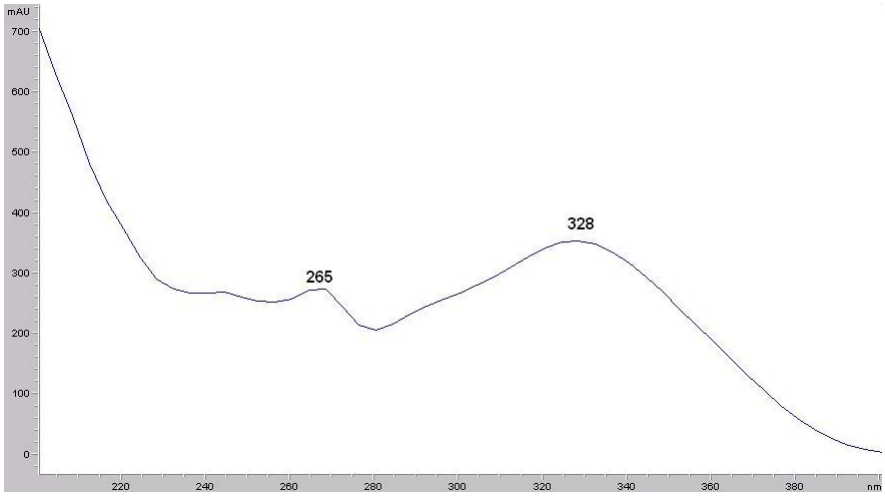

Figure 3.64: UV of BS2

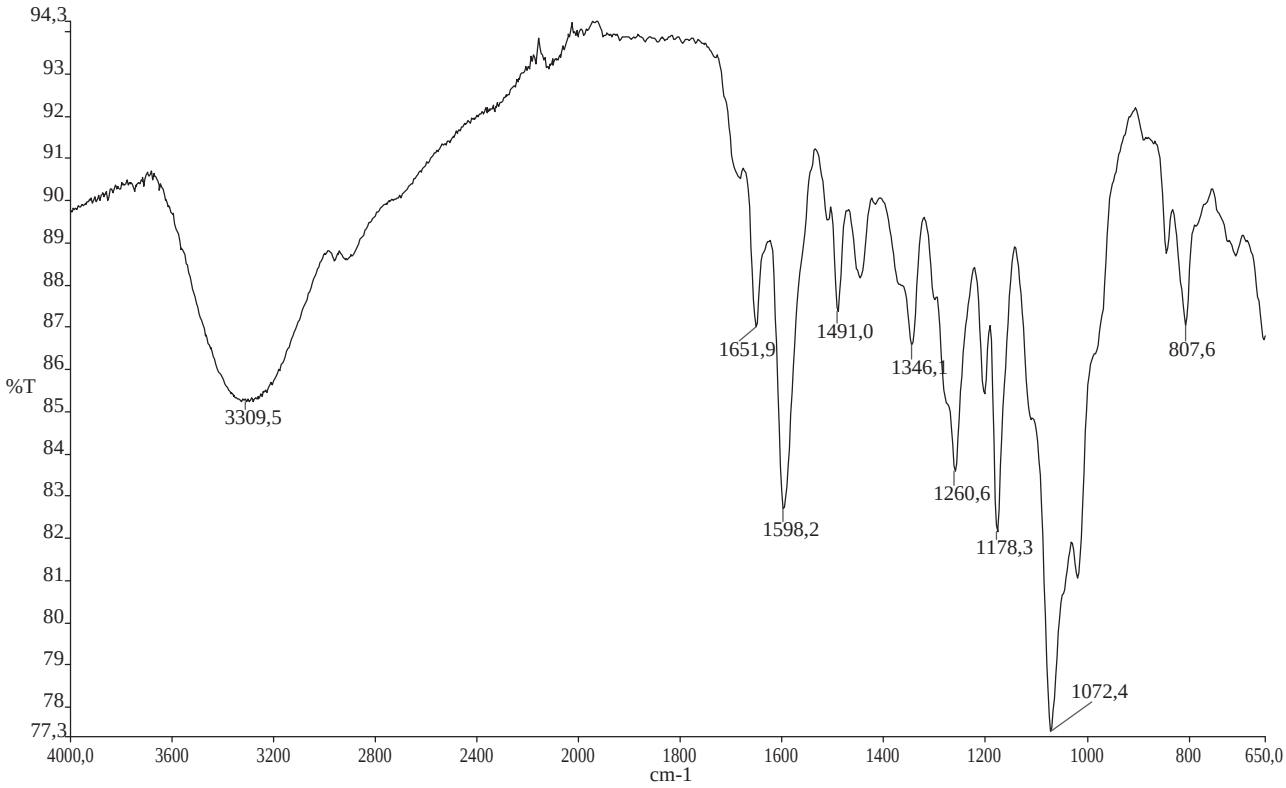

Figure 3.65: IR of the compound BS2

The ESI mass spectrum (see Figure 3.66) showed a quasimolecular positive ion peak[20] at *m/z* = 927.7 $[M + Na]^+$ (13), and further peaks at *m/z*: 904.8 $[M + H]^+$ (74); 742.9 [M + H - caffeic acid]$^+$ (21); 580.8 [M + H - caffeic acid - glucose]$^+$ (24); 448.9 [M + H - caffeic acid - arabinose - glucose]$^+$ (100); 418.8 [M + H - caffeic acid - glucose - glucose]$^+$ (7); 324.8 [caffeic acid + glucose - H_2O]$^+$ (8); 287.1 [aglycone + H]$^+$ (37); 162.9 [caffeic acid - OH]$^+$ (8). The fragment ions at *m/z* = 742.9, 580.8, 448.9 (i.e., base peak) and 418.8 correspond to the successive loss of caffeic acid (163), hexose residues (162) and pentose residues (132), respectively. Based on the molecular mass at *m/z* = 904.8 and the structural information obtained by NMR (following sentences) techniques, a molecular formula $C_{41}H_{44}O_{23}$ was assigned to BS2. The molecular mass was confirmed by the high resolution FT-ICR-MS for $[M + Na]^+$ at *m/z* = 927.215977 (calculated mass for $C_{41}H_{44}O_{23}Na$ was 927.21656).

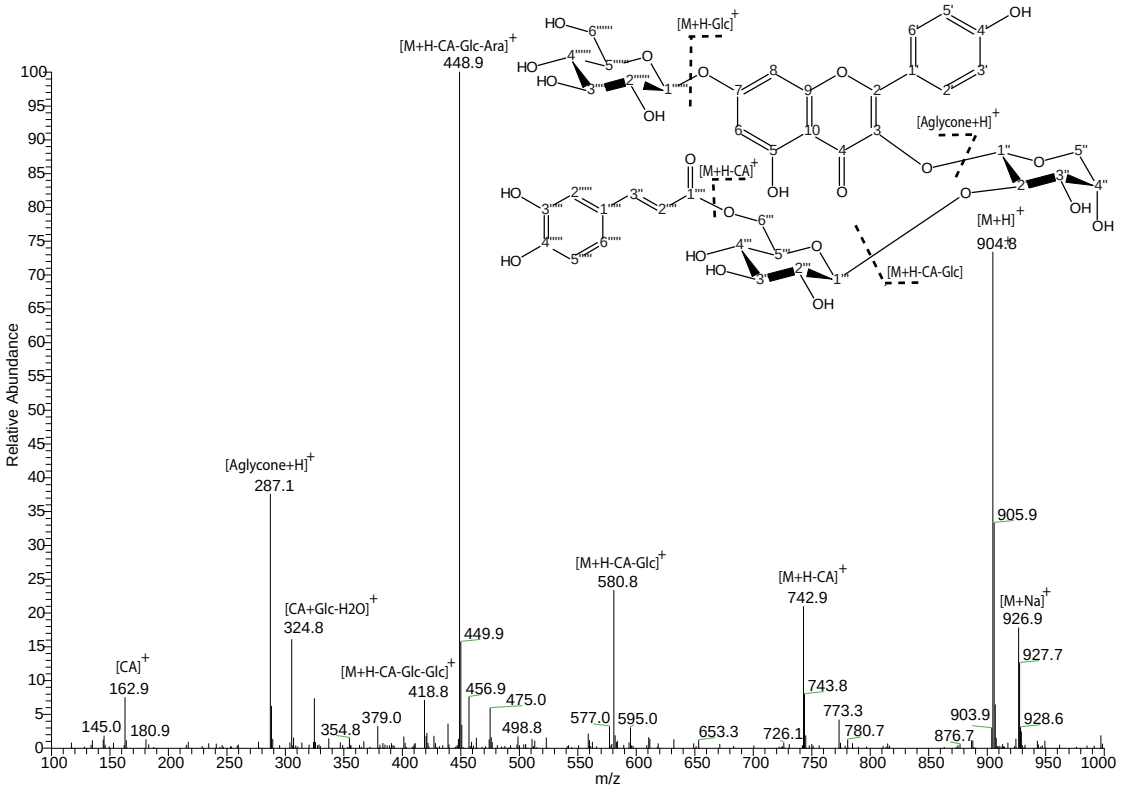

Figure 3.66: ESI-MS (positiv mode) of the compound BS2

[20]In brackets the relative intensity in % of the ion peaks is shown.

The NMR spectra of BS2 are quite similar to those of BS1 (see Section 3.1.2.2.2). The ^{1}H-NMR spectrum showed two singlets for the protons in the A ring (H-6 δ = 6.72 ppm and H-8 δ = 6.92 ppm) and two doublets (AA BB system) for the B ring (H-2 and H-6 δ = 8.44 ppm, H-3 and H-5 δ = 7.26 ppm), which are typical for a kaempferol aglycone. Additionally, in the aromatic region of the ^{1}H-NMR (see Figure 3.67 and Table 3.7), there are three further signals at δ = 7.12 ppm, δ = 7.40 ppm and δ = 6.95 ppm. Two new doublet signals at δ = 7.81 ppm and δ = 6.41 ppm are caused by the olefinic protons of the caffeic acid. Additionally, the ^{1}H-NMR spectrum showed the two protons for the H-6" methylene glycosyl, which shifted to the downfield at δ = 4.90-5.03 ppm and indicated an acylation on the C-6" position [81].

The ^{13}C-NMR (see Figure 3.68 and Table 3.7) showed 39 signals for 41 carbons. In addition to BS1, BS2 showed a signal at δ = 167.4 ppm, which is attributable to an additional carbonyl group and two de-shielded oxygen quaternary carbons at C-2"" (δ = 114.6 ppm) and C-3"" (δ = 145.6 ppm). Further six carbons were identified in the aromatic region: C-1"" (δ = 126.6 ppm), C-2"" (δ = 115.6 ppm), C-3"" (δ = 145.6 ppm), C-4"" (δ = 147.2 ppm), C-5"" (δ = 116.3 ppm), and C-6"" (δ = 121.8 ppm).

The HSQC (see Figure 3.70) and the H-H-COSY experiments (see Figure 3.69 and Table 3.7) exhibited also similar spectra to BS1. The main difference between BS1 and BS2 is the caffeic acid unit. Therefore, the values of the aromatic signals of both the ^{1}H- and ^{13}C-NMR spectra suggested again the presence of a kaempferol as aglycone with three sugar units, however, with an additional caffeic acid unit. The coupling constant of the anomeric protons H-1" and H-1"""" (both d, J = 6 Hz) of the glucoses were in accordance with a β-glycosidic linkage (i.e., β-D-glucopyranose) [169].

The HMBC experiment (see Figure 3.71 and Table 3.7) confirmed also the assignment for the caffeic acid to C-6" by a correlation between the C=O group (i.e., C-1"", δ = 167.4 ppm) of the caffeic acid and the H-6" (δ = 4.90-5.03 ppm). Furthermore, the signals H-2"" (δ = 6.41 ppm) and H-3"" (δ = 7.81 ppm) were correlated with the signal at δ = 167.4 ppm (C-1"") in the HMBC spectrum. Finally, the signals H-2"" (δ = 7.40 ppm) and H-6"" (δ = 6.95 ppm) were correlated

with the carbons at δ = 145.6 ppm (C-3””) and δ = 116.3 ppm (C-5””).

The chemical-shift values of the carbons of the sugar units were in agreement with those of a glucopyranose (i.e., β-D-glucopyranose) and an arabinopyranose (i.e., α-L-arabinopyranose) from the literature [169] (see Table 3.7). The assignment of the sugars to D- or L-series are based on the literature [27]. Based on the MS, 1D- and 2D-NMR analysis, a new kaempferol 3-O-β-D-[6$'''$-O-(3,4-dihydroxy-cinnamoyl)]-glucopyranosyl-(1$'''\rightarrow$2$''$)-O-α-L-arabinopyranoside-7-O-β-D-glucopyranoside was identified as the compound BS2.

Table 3.7: Chemical shifts of BS2

Atom numbers	^{13}**C*** δ**/ppm**	^{13}**C**** δ**/ppm**	^{1}**H*** δ**/ppm (Mult., J(Hz), H)**	^{1}**H - ^{1}H COSY***	^{1}**H - ^{13}C HMBC***
2	157.2	-	-	-	-
3	137.0	-	-	-	-
4	178.8	-	-	-	-
5	161.7	-	-	-	-
6	100.0	-	6.72 (brs; 1H)	8	7, 8, 9, 10
7	163.6	-	-	-	-
8	94.6	-	6.92 (brs; 1H)	6	4, 6, 9, 10
9	156.6	-	-	-	-
10	106.7	-	-	-	-
$1'$	121.8	-	-	-	-
$2'$	131.8	-	8.44 (d; 6 Hz; 1H)	$3'$, $5'$	2, 7, $3'$, $5'$, $6'$
$3'$	116.2	-	7.26 (d; 6 Hz; 1H)	$2'$, $6'$	2, 7, $2'$, $5'$, $6'$
$4'$	162.0	-	-	-	-
$5'$	116.2	-	7.26 (d; 6 Hz; 1H)	$2'$, $6'$	2, 7, $2'$, $3'$, $6'$
$6'$	131.8	-	8.44 (d; 6 Hz; 1H)	$3'$, $5'$	2, 7, $2'$, $3'$, $5'$
$1''$	100.4	100.9	6.41 (brs; 1H)	$2''$	$2''$, 3, $3''$, $5''$
$2''$	80.7	78.3	5.07 (brs; 1H)	$1''$, $3''$	$1''$, $4''$, $1'''$
$3''$	70.9	71.4	4.67 (brs; 1H)	$2''$, $4''$	-
$4''$	66.0	66.3	4.47 (m; 1H)	$5''$, $3''$	-
$5''$	62.1	62.1	4.38 (m; 1H); 4.56 (m; 1H)	$4''$, $5''$	$1''$
$1'''$	106.7	103.1	5.28 (d; 6 Hz; 1H)	$2'''$	-
$2'''$	75.1	77.6	4.12 (m; 1H)	$1'''$,$3'''$	$1'''$, $3'''$
$3'''$	78.1	79.4	4.05 (m; 1H)	$4'''$	$2'''$, $4'''$, $5'''$
$4'''$	70.9	72.7	4.15 (m; 1H)	$3'''$, $5'''$	-
$5'''$	75.4	78.2	4.05 (m; 1H)	$4'''$	$2'''$, $3'''$, $4'''$
$6'''$	63.9	62.1	4.90-5.03 (m; 2H)	$6'''$	$1''''$
$1''''$	167.4	-	-	-	-
$2''''$	114.6	-	6.41 (d; 12 Hz; 1H)	$3''''$	$1''''$, $1'''''$
$3''''$	145.6	-	7.81 (d; 12 Hz; 1H)	$2''''$	$1''''$, $2''''$, $6'''''$
$1'''''$	126.6	-	-	-	7
$2'''''$	115.6	-	7.40 (brs; 1H)	-	$1''''$, $3''''$, $5'''''$
$3'''''$	145.6	-	-	-	$5'''''$
$4'''''$	147.2	-	-	-	-
$5'''''$	116.3	-	7.12 (d; 6 Hz; 1H)	$6'''''$	-
$6'''''$	121.8	-	6.95 (brd; 6 Hz; 1H)	$5'''''$	$3''''$, $5'''''$
$1''''''$	101.3	103.1	5.78 (d; 6 Hz; 1H)	$2''''''$	-
$2''''''$	74.6	77.6	4.30 (m; 1H)	$1''''''$	$1''''''$, $3''''''$
$3''''''$	78.9	79.4	4.40 (m; 1H)	$3''''''$	$2''''''$, $4''''''$
$4''''''$	71.0	72.7	4.30 (m; 1H)	$2''''''$	-
$5''''''$	78.1	78.2	4.30 (m; 1H)	-	-
$6''''''$	63.4	62.1	3.71 (m; 1H); 4.50 (m; 1H)	$2''''''$, $3''''''$	-

* In Pyridine-d_5. ** Data from literature [169] in Pyridine-d_5.

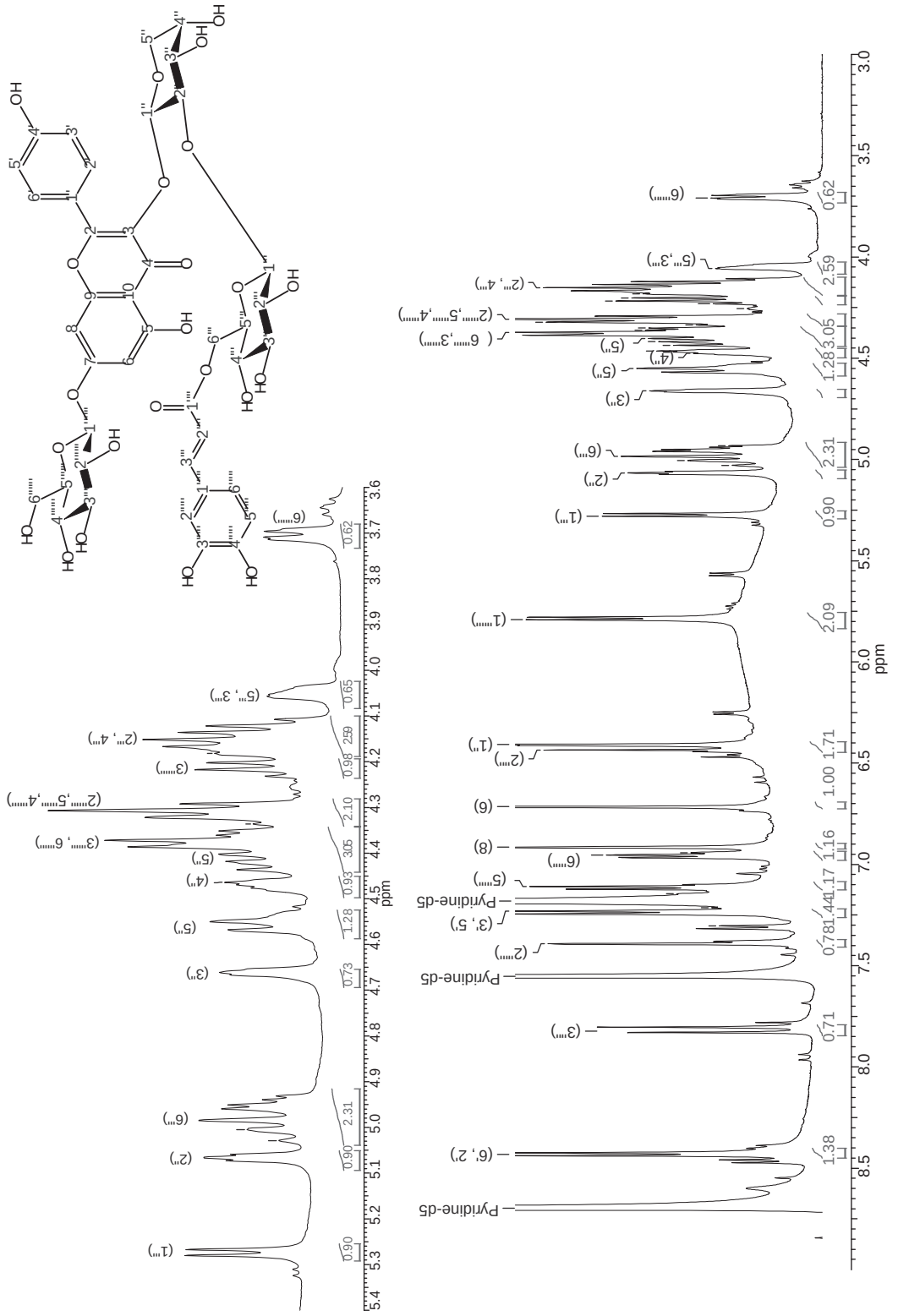

Figure 3.67: ^{1}H-NMR of BS2 (600 MHz, Pyridine-d_5)

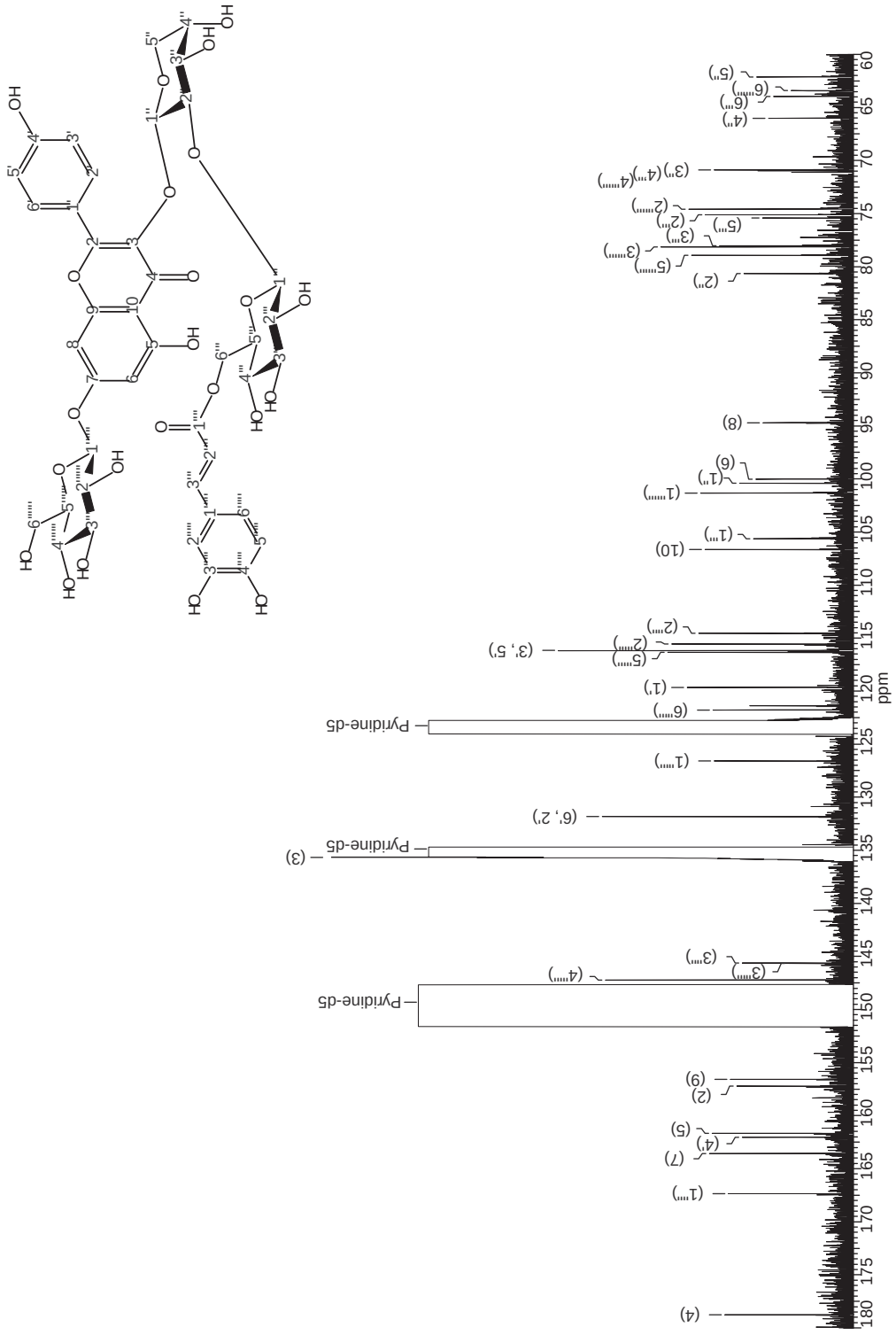

Figure 3.68: ^{13}C-NMR of BS2 (100 MHz, Pyridine-d_5)

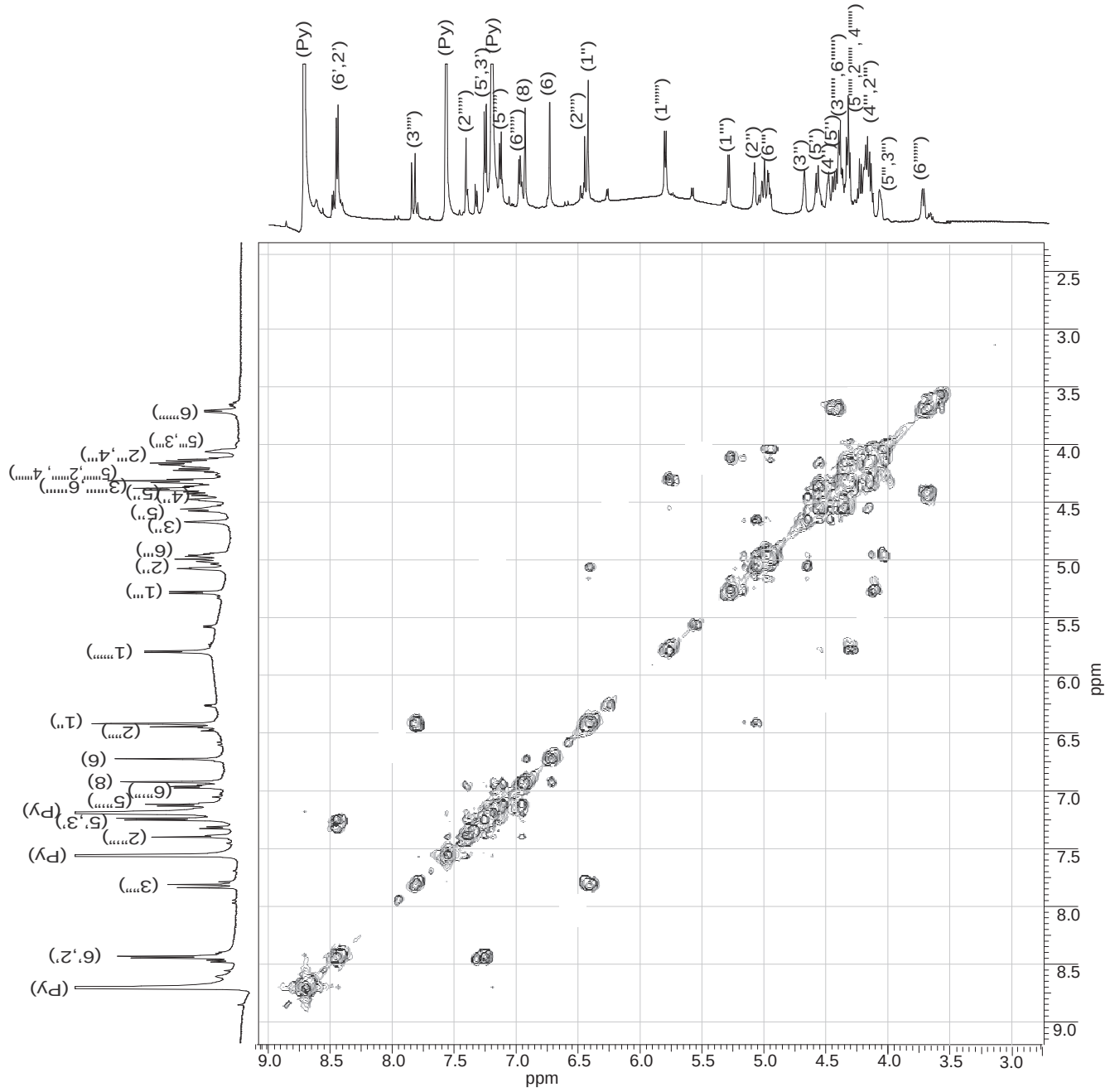

Figure 3.69: H-H-COSY of BS2 (600 MHz, Pyridine-d_5)

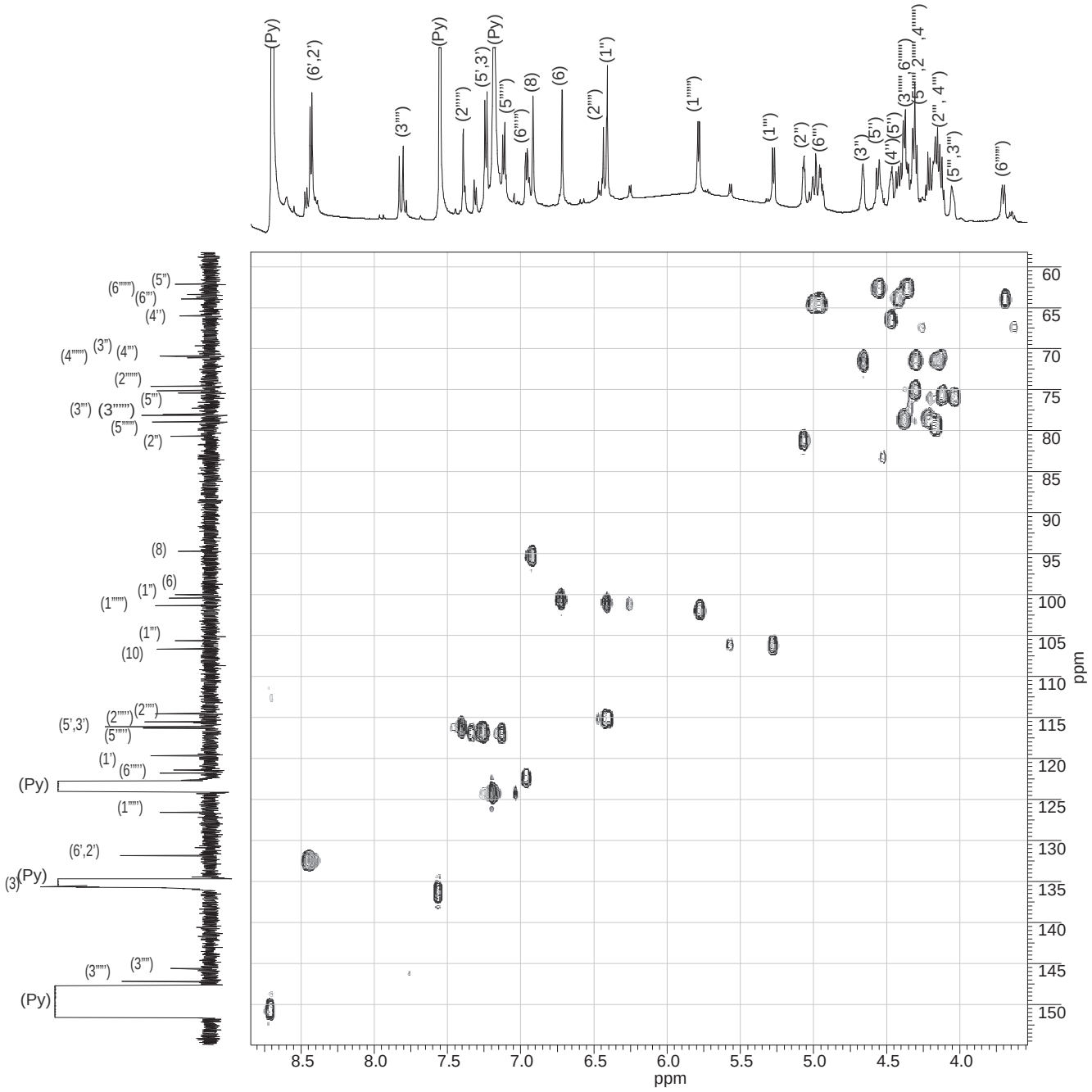

Figure 3.70: HSQC of BS2 (600 MHz, Pyridine-d_5)

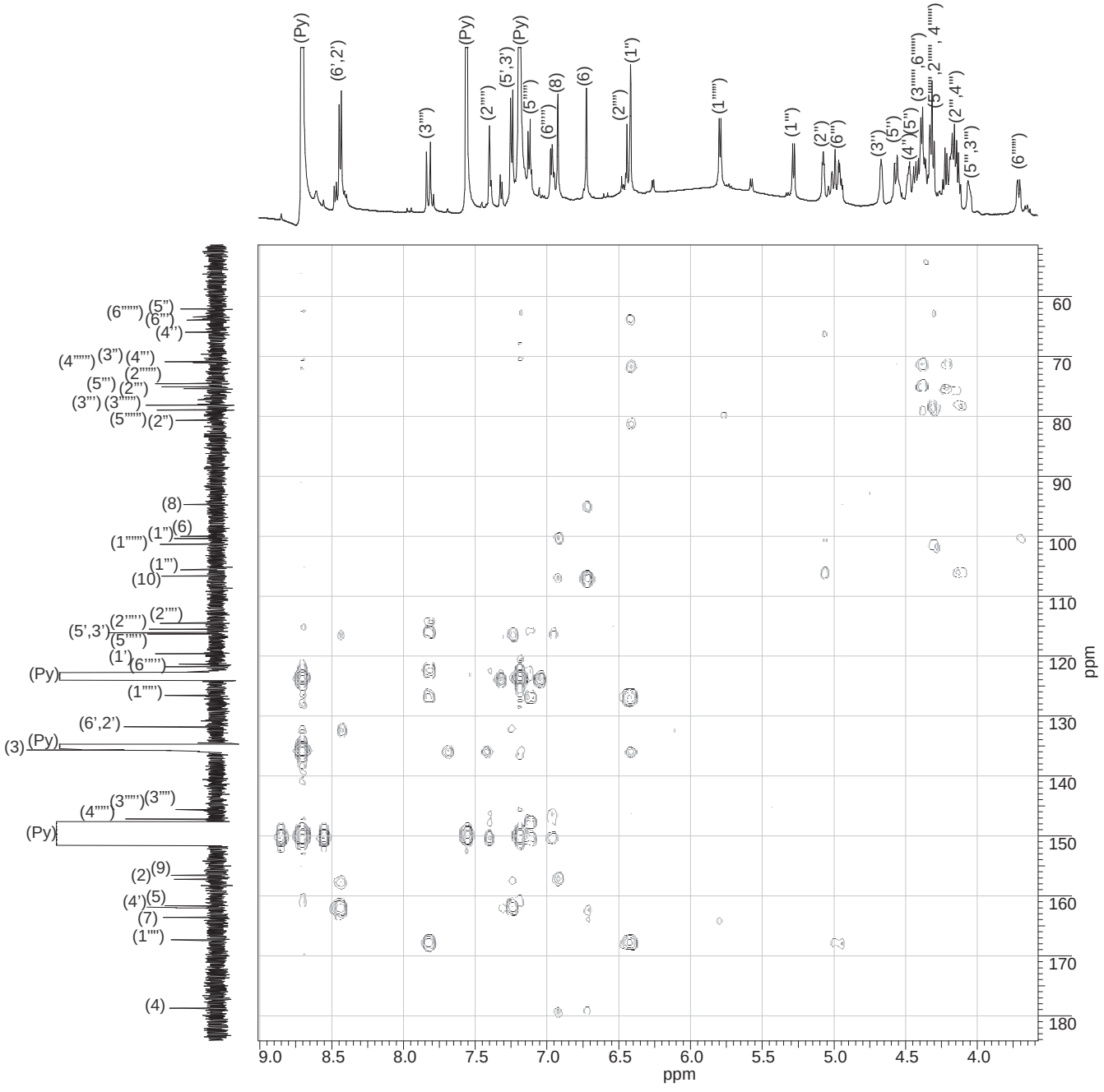

Figure 3.71: HMBC of BS2 (600 MHz, Pyridine-d_5)

3.1.2.2.4 BS3: Kaempferol 3-O-β-D-[2$'''$-O-(3,4-dihydroxy-cinnamoyl)] -glucopyranosyl-(1$'''\rightarrow$2$''$)-O-α-L- arabinopyranoside-7-O-β-D-glucopyranoside

The subfractionation of the fraction H was performed consecutively by flash chromatography, open column chromatography and analytical HPLC (see Section 5.6.2.2, Experimental Part), which yielded 3.5 mg of the compound BS3 and was identified as kaempferol 3-O-β-D-[2$'''$-O-(3,4-dihydroxy-cinnamoyl)]-glucopyranosyl-(1$'''\rightarrow$2$''$)-O-α-L-arabinopyranoside-7-O-β-D-glucopyranoside[21]. This compound was isolated as a yellow amorphous powder and its chemical structure is shown in Figure 3.72. The structural elucidation was established on the basis of UV, IR, MS and NMR spectroscopic data.

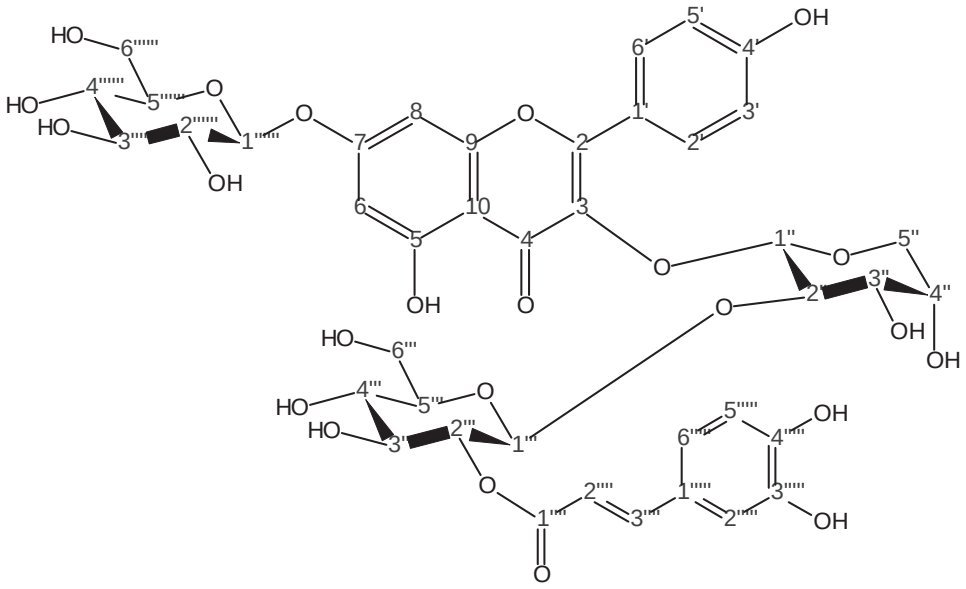

Figure 3.72: Chemical structure of the compound BS3

The UV spectrum of BS3 (see Figure 3.73) exhibited two absorption maxima (in MeOH) at λ = 265 and 330 nm that provided evidence to be in accordance with a 3,7-di-O-substituted flavonol skeleton [196]. The FTIR spectrum (see Figure 3.74) showed absorption bands at: 3263.2, 1586.6, 1491.2, 1448.8, 1348.1, 1259.1, 1203.4, 1177.5, 1118.5, 1071.2, 1021.7, 822.9, 764.0 cm^{-1}.

[21] IUPAC name: 3-[(2-O-2-O-[(2E)-3-(3,4-dihydroxyphenyl)prop-2-enoyl]hexopyranosylpentopyranosyl)oxy]-5-hydroxy-2-(4-hydroxyphenyl)-4-oxo-4H-chromen-7-yl hexopyranoside

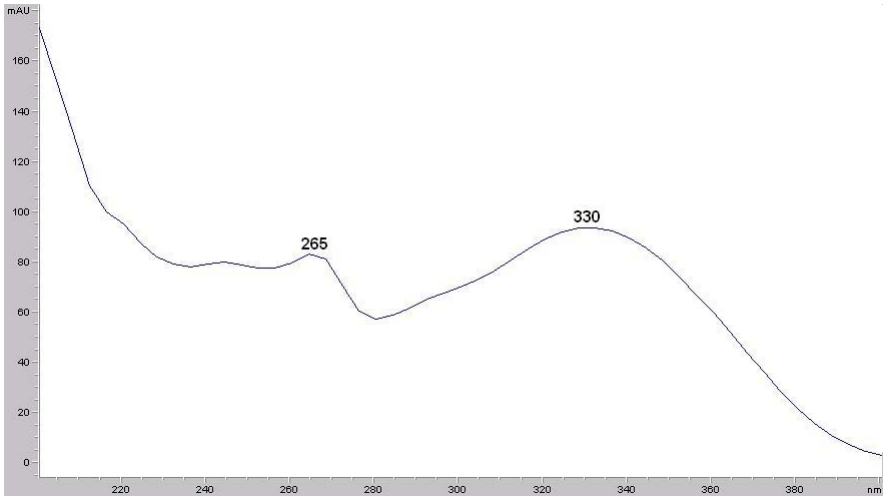

Figure 3.73: UV spectrum of BS3

Figure 3.74: IR of the compound BS3

The ESI mass spectrum (see Figure 3.75) showed a quasimolecular positive ion peak[22] at *m/z* = 927.1[M + Na]$^+$ (42), and further peaks at *m/z*: 904.9 [M + H]$^+$ (26); 742.9 [M + H - caffeic acid]$^+$ (10); 581.0 [M + H - caffeic acid - glucose]$^+$ (14); 448.9 [M + H - caffeic acid - arabinose - glucose]$^+$ (49); 419.1 [M + H - caffeic acid - glucose - glucose]$^+$ (6); 324.9 [caffeic acid + glucose - H_2O]$^+$ (25); 287.2 [aglycone + H]$^+$ (100); 162.9 [caffeic acid - OH]$^+$ (24). The fragment ions at *m/z* = 742.9, 581.0, 448.9 and 419.1 correspond to the successive loss of caffeic acid (163), hexose residues (162) and pentose residues (132), respectively. The base peak is characterized by the fragment *m/z* = 287.2 representing the aglycone. Based on the molecular mass at *m/z* = 904.9 and the structural information obtained by NMR analysis, the molecular formula $C_{41}H_{44}O_{23}$ was attributed to compound BS3, which was confirmed by the high resolution FT-ICR-MS for [M + Na]$^+$ at *m/z* = 927.216170 (calculated mass for $C_{41}H_{44}O_{23}Na$ was 927.21656).

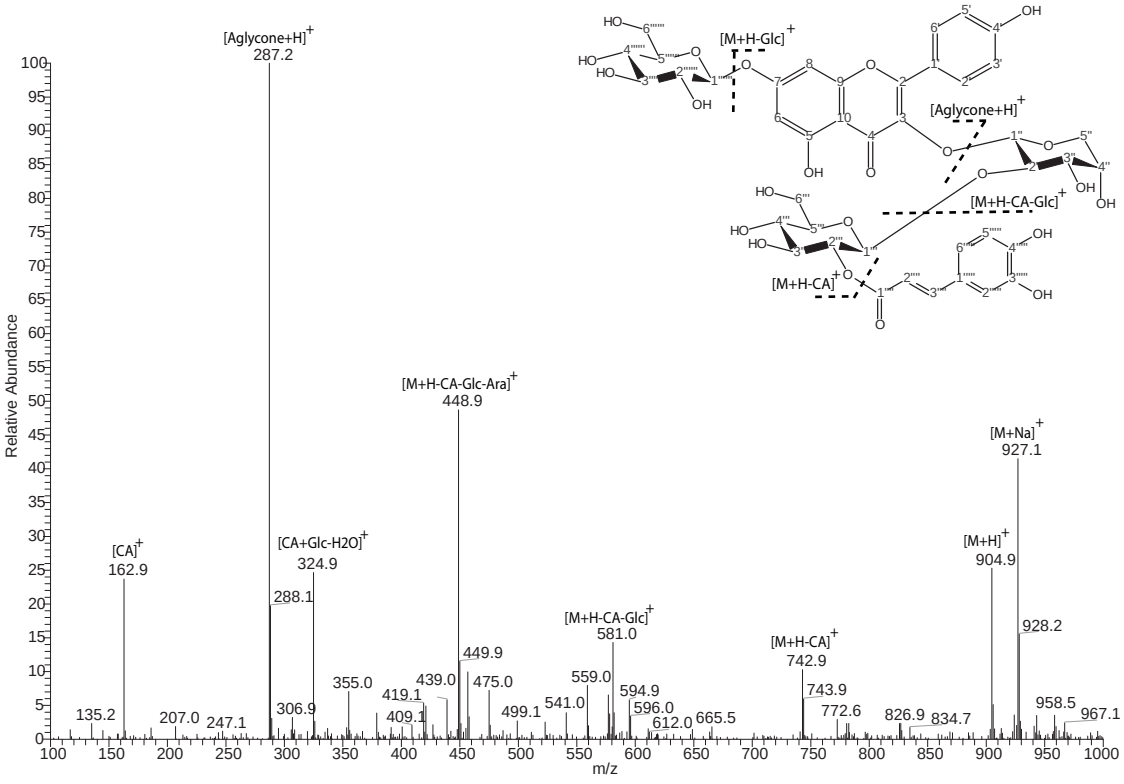

Figure 3.75: ESI-MS (positiv mode) of the compound BS3

[22]In brackets, the relative intensity in % of the ion peaks is shown.

The NMR-spectra of BS3 are quite similar to the ones of BS2 (see Section 3.1.2.2.3). The main difference between the compounds can be observed in the aromatic region of the ^{1}H-NMR spectrum (see Figure 3.76 and Table 3.8). Compared to the ^{1}H-NMR spectrum of BS2, the signals belonging to caffeic acid (i.e., aromatic ring δ = 7.07 ppm (H-2””), δ = 7.47 ppm (H-5””), δ = 7.07 ppm (H-6””), and olefinic protons δ = 6.25 (H-2””) and δ = 7.47 ppm (H-3””) are shifted to the high field region. Moreover, the ^{1}H-NMR spectrum showed one proton for the H-2” methylene glycosyl, which shifted downfield to δ = 4.60 ppm and confirmed the acylation at the C-2” position.

The ^{13}C-NMR spectrum (see Figure 3.77 and Table 3.8) exhibited 39 signals for 41 carbons. As well as BS2, BS3 showed a signal at δ = 165.6 ppm, which is attributable to an additional carbonyl group and two de-shielded oxygen quaternary carbon at δ = 113.9 ppm and δ = 145.0 ppm of the caffeic acid.

The HSQC (see Figure 3.80) and the H-H-COSY experiments (see Figure 3.79 and Table 3.8) showed similar spectra in comparison to BS2. Therefore, the values of the aromatic signals of both ^{1}H- and ^{13}C-NMR spectra suggested the presence of a kaempferol as aglycone with three sugar units, and a caffeic acid unit.

The HMBC experiment (see Figure 3.81 and Table 3.8) verified the assignment of the caffeic acid to C-2” by a correlation between the H-2” (δ = 4.60 ppm) and the C=O group (i.e., C-1””, δ = 165.6 ppm) of the caffeic acid.

The chemical-shift values of the carbons of the sugar units were in agreement with those of a glucopyranose (i.e., β-D-glucopyranose) and an arabinopyranose (i.e., α-L-arabinopyranose) from the literature [169] (see Table 3.7). The assignment of the sugars to D- or L-series are based on the literature [27]. Based on the MS, 1D- and 2D-NMR analysis, a new kaempferol 3-O-β-D-[2$'''$-O-(3,4-dihydroxy-cinnamoyl)]-glucopyranosyl-(1$'''\rightarrow$2$''$)-O-α-L-arabinopyranoside-7-O-β-D-glucopyranoside was identified as BS3.

Table 3.8: Chemical shifts of BS3

Atom numbers	^{13}**C*** δ**/ppm**	^{13}**C**** δ**/ppm**	^{1}**H*** **δ/ppm (Mult., J(Hz), H)**	^{1}**H - ^{1}H COSY***	^{1}**H - ^{13}C HMBC***
2	154.4	-	-	-	-
3	134.5	-	-	-	-
4	177.6	-	-	-	-
5	160.5	-	-	-	-
6	98.7	-	6.43 (brs; 1H)	-	-
7	162.9	-	-	-	-
8	94.0	-	6.76 (brs; 1H)	-	-
9	155.9	-	-	-	-
10	106.0	-	-	-	-
$1'$	121.2	-	-	-	-
$2'$	131.0	-	8.06 (d; 6 Hz; 1H)	$3'$, $5'$	$6'$
$3'$	115.4	-	6.81 (d; 6 Hz; 1H)	$2'$, $6'$	$5'$
$4'$	160.5	-	-	-	-
$5'$	115.4	-	6.81 (d; 6 Hz; 1H)	$2'$, $6'$	$3'$
$6'$	131.0	-	8.06 (d; 6 Hz; 1H)	$3'$, $5'$	$2'$
$1''$	98.7	100.9	5.58 (brs; 1H)	-	$2''$, 3, $3''$, $2'''$
$2''$	78.7	78.3	4.09 (brs; 1H)	$3''$	$1''$, $4''$, $3''$
$3''$	68.6	71.4	3.85 (brs; 1H)	$2''$, $4''$	-
$4''$	63.7	66.3	3.50 (m; 1H)	-	-
$5''$	60.6	62.1	3.00 (m; 1H); 3.50 (m; 1H)	$5''$	$1''$, $3''$, $4''$
$1'''$	101.5	103.1	4.68 (d; 6 Hz; 1H)	$2'''$	$2'''$
$2'''$	73.1	77.6	4.60 (d; 6 Hz; 1H)	$1'''$, $3'''$	$1'''$, $5'''$
$3'''$	73.6	79.4	3.48 (m; 1H)	-	$5'''$
$4'''$	69.5	72.7	3.25 (m; 1H)	-	-
$5'''$	76.4	78.2	3.30 (m; 1H)	-	-
$6'''$	60.3	62.1	3.50-3.70 (m; 2H)	$6'''$	$4'''$, $5'''$
$1''''$	165.6	-	-	-	-
$2''''$	113.9	-	6.25 (d; 12 Hz; 1H)	-	$1''''$, $1'''''$
$3''''$	145.0	-	7.47 (d; 12 Hz; 1H)	-	$1''''$, $2''''$, $6'''''$
$1'''''$	125.4	-	-	-	7
$2'''''$	114.9	-	7.07 (brs; 1H)	-	$4'''''$, $3'''''$, $5'''''$
$3'''''$	145.7	-	-	-	-
$4'''''$	148.7	-	-	-	-
$5'''''$	115.8	-	6.90 (d; 6 Hz; 1H)	-	-
$6'''''$	121.2	-	6.96 (brd; 6 Hz; 1H)	-	$3'''''$, $5'''''$
$1''''''$	99.8	103.1	5.06 (d; 6 Hz; 1H)	$2''''''$	7
$2''''''$	72.5	77.6	3.20 (m; 1H)	-	-
$3''''''$	76.8	79.4	3.28 (m; 1H)	-	-
$4''''''$	69.8	72.7	3.25 (m; 1H)	-	-
$5''''''$	77.1	78.2	3.40 (m; 1H)	-	$1''''''$
$6''''''$	60.3	62.1	3.50-3.70 (m; 2H)	$6''''''$	-

* In DMSO-d_6. ** Data from literature [169] in Pyridine-d_5.

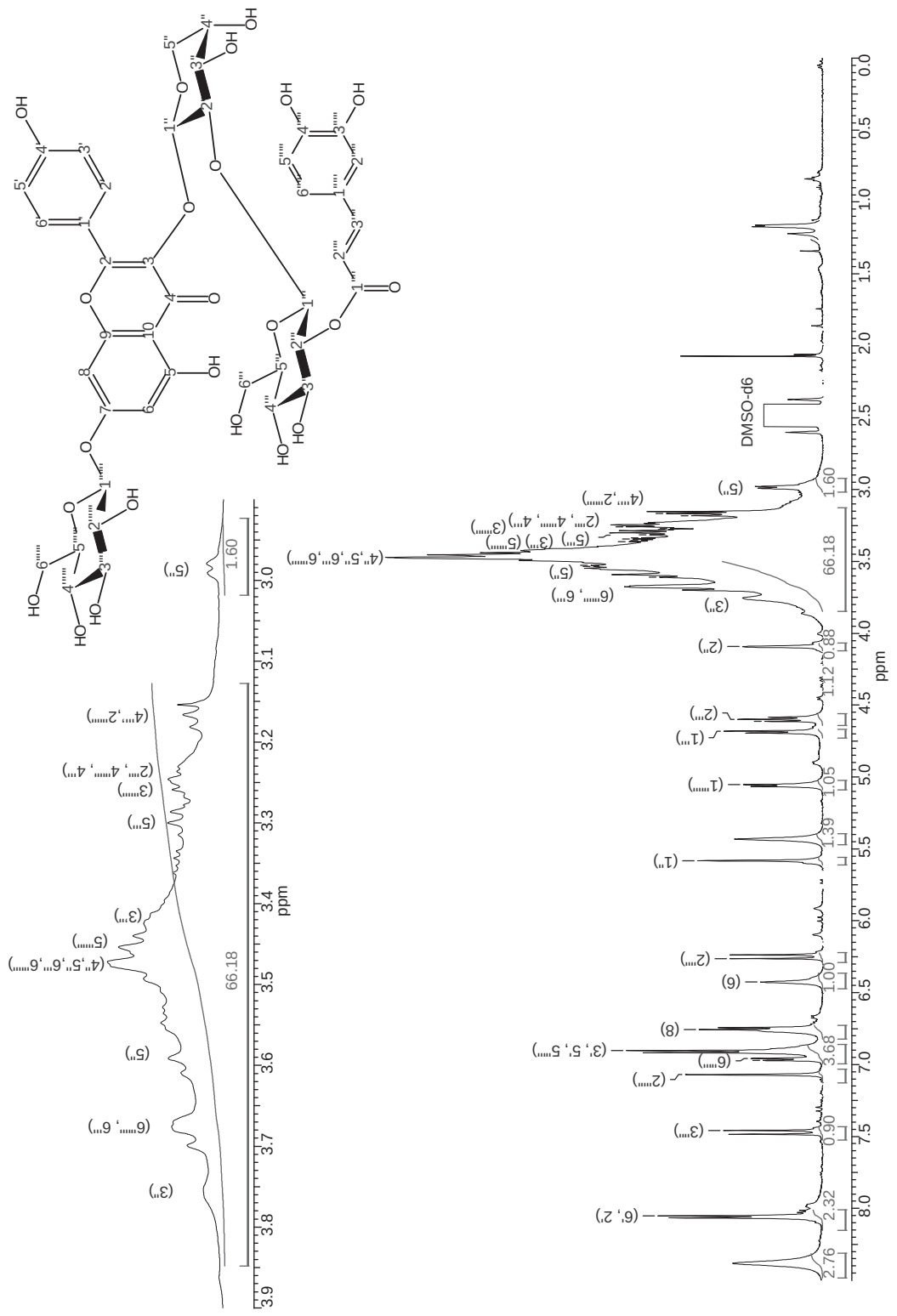

Figure 3.76: ^{1}H-NMR of BS3 (600 MHz, DMSO-d_6)

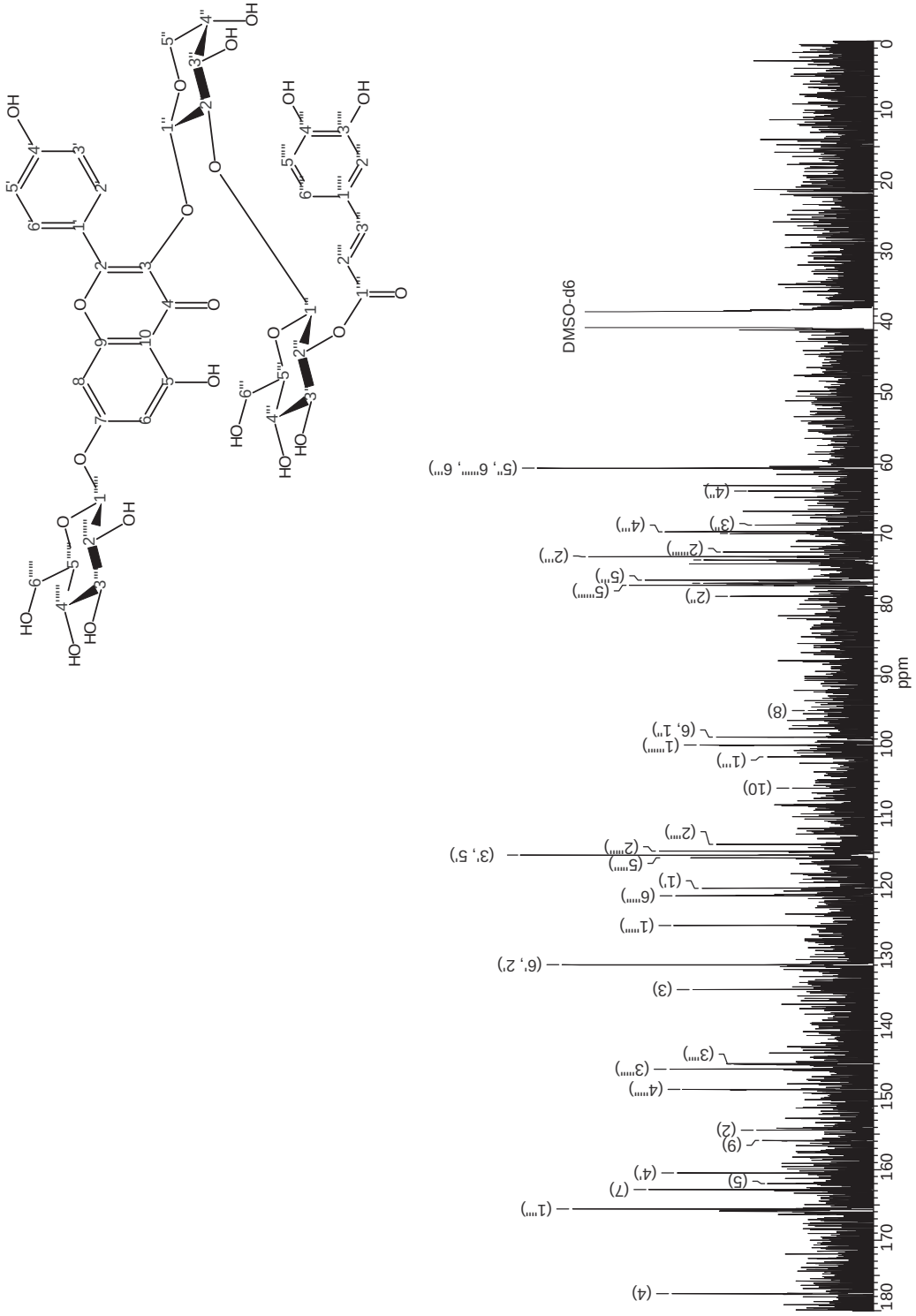

Figure 3.77: ^{13}C-NMR of BS3 (100 MHz, DMSO-d_6)

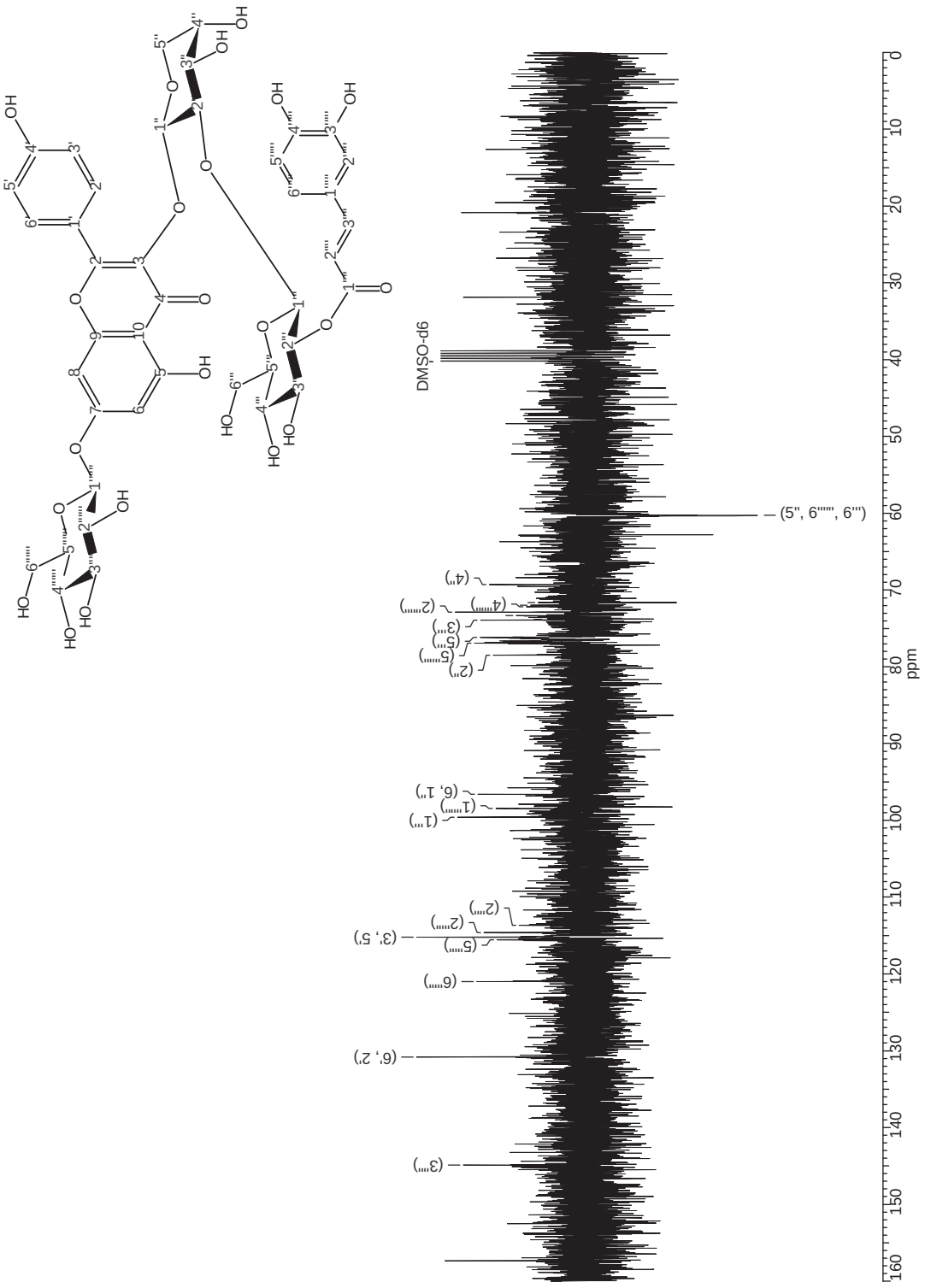

Figure 3.78: DEPT-135 of BS3 (100 MHz, DMSO-d_6)

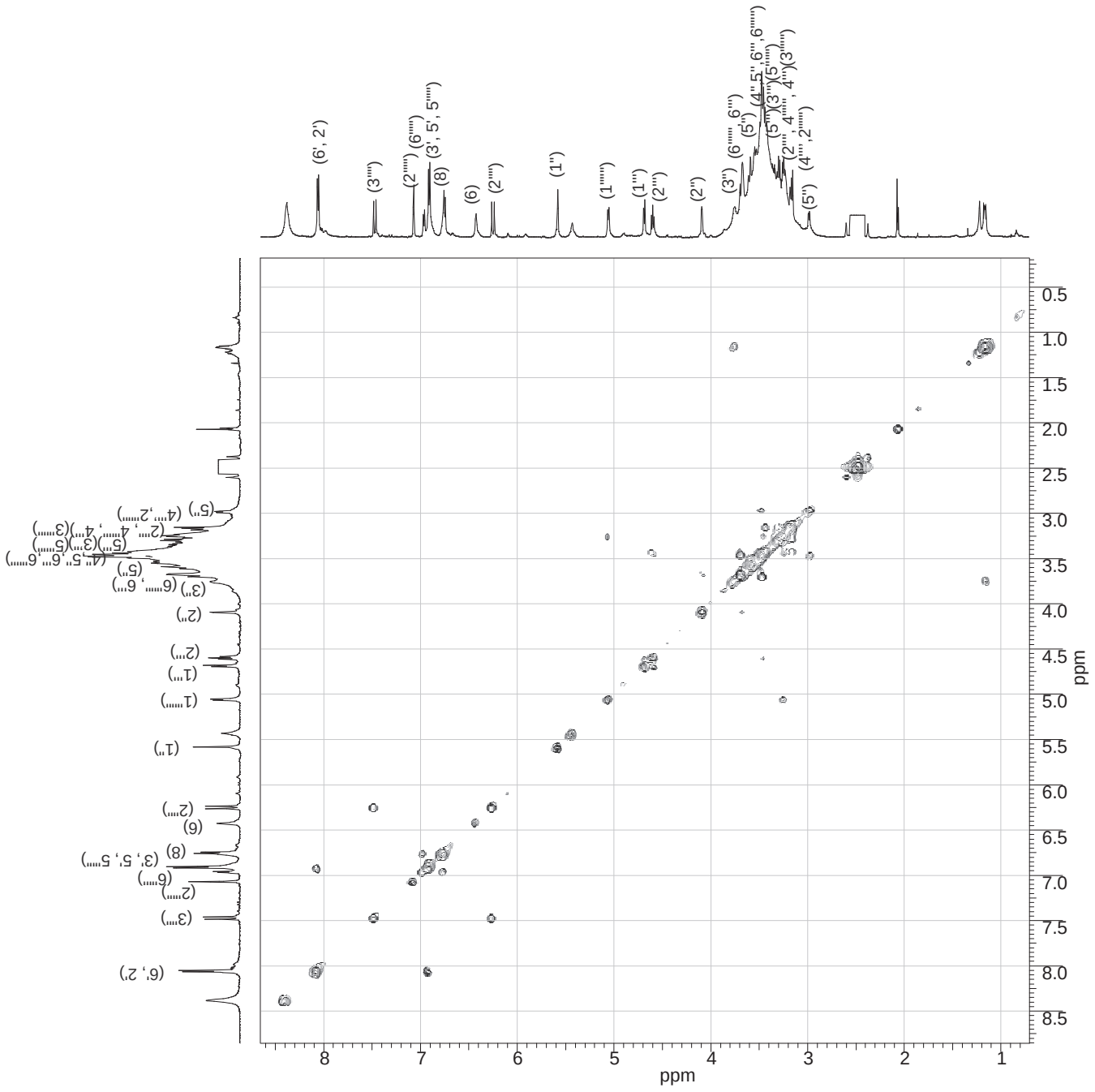

Figure 3.79: H-H-COSY of BS3 (600 MHz, DMSO-d_6)

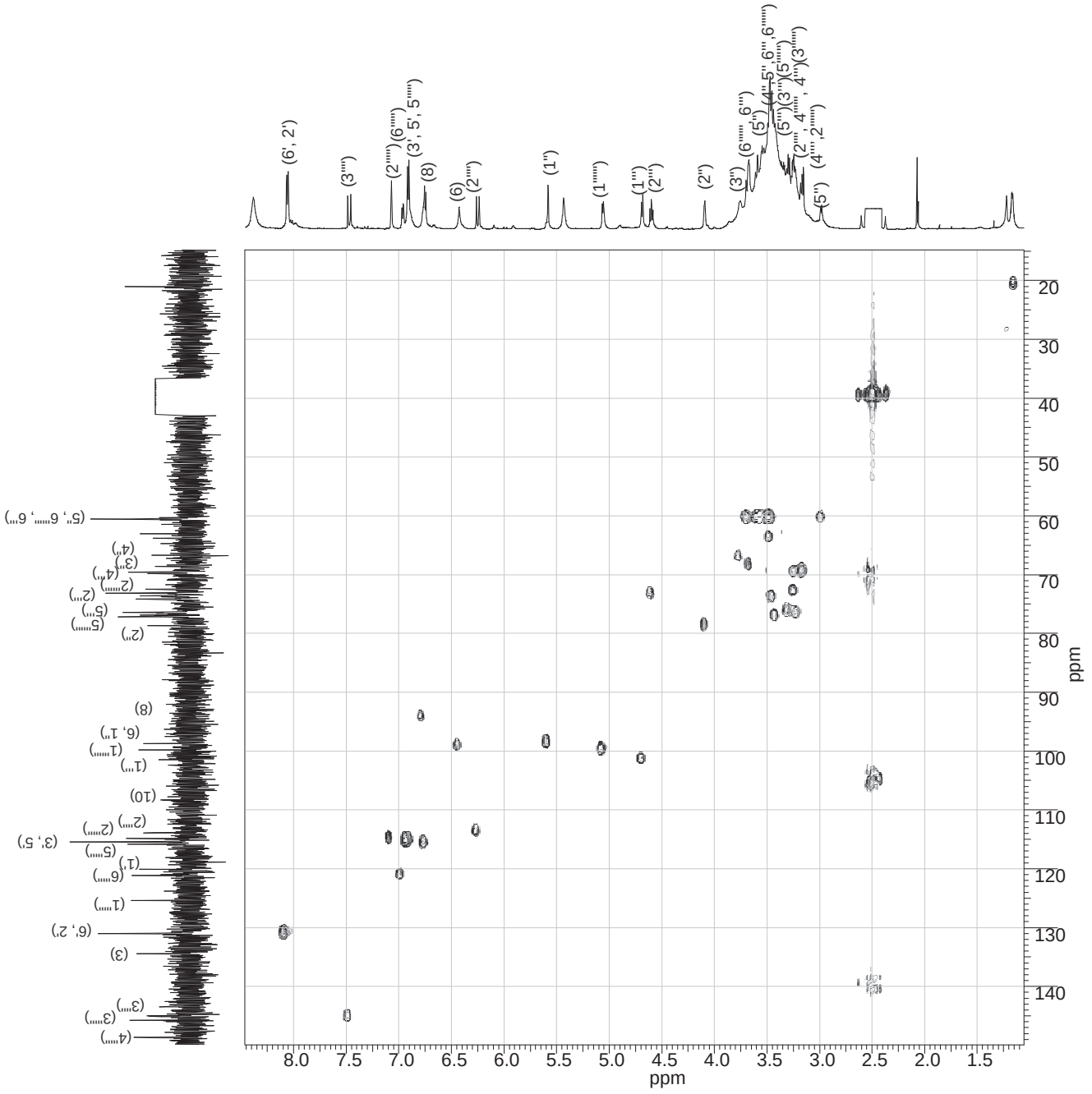

Figure 3.80: HSQC of BS3 (600 MHz, DMSO-d_6)

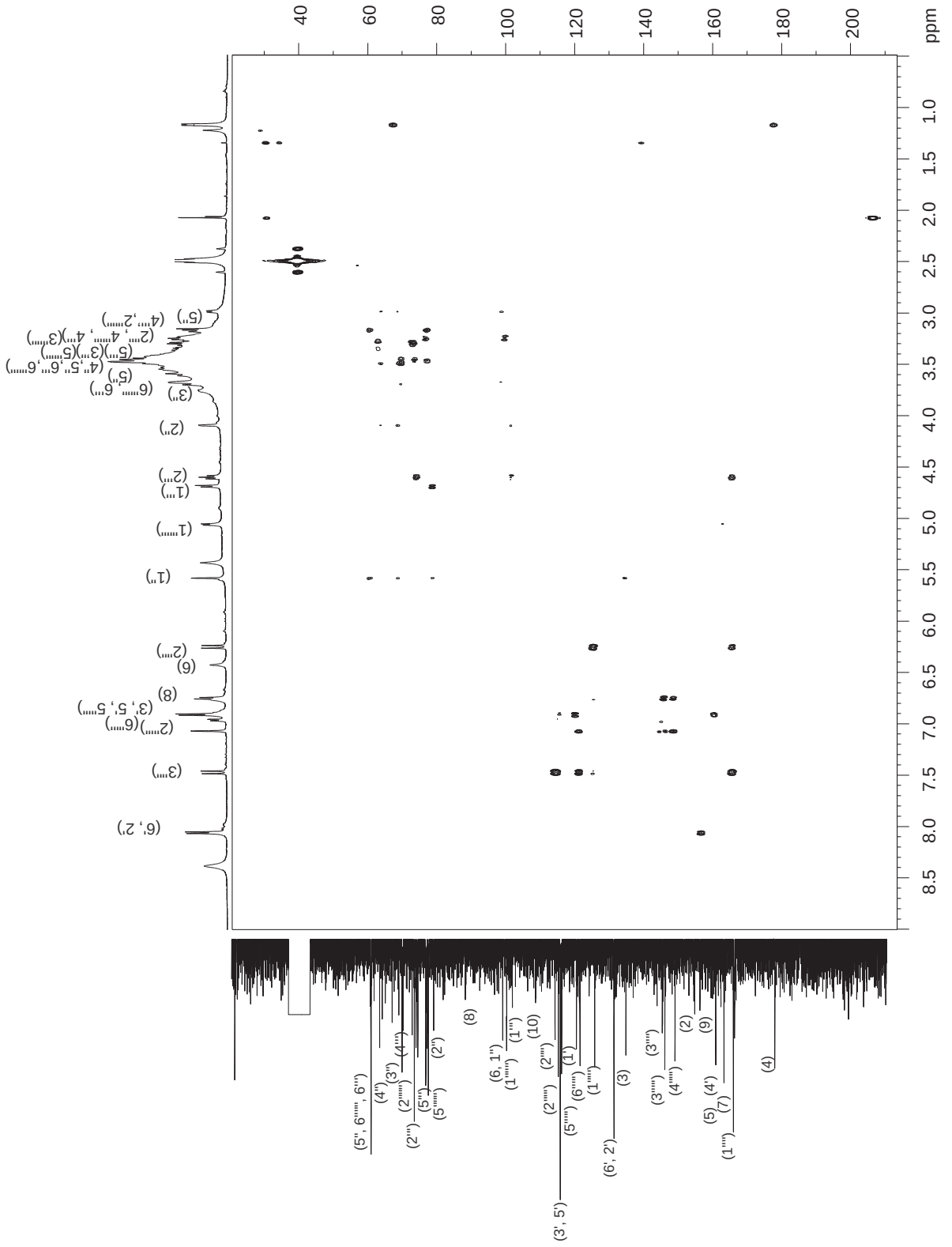

Figure 3.81: HMBC of BS3 (600 MHz, DMSO-d_6)

3.1.2.3 Discussion

In the previous sections, the phytochemical studies (i.e., MS and 1D and 2D NMR) revealed the presence of four flavonol glycosides in the ethanolic extract from the leaves of *Brugmansia suaveolens*. BS1 was assigned as kaempferol 3-O-β-D-glucopyranosyl-(1$'''\rightarrow$2$''$)-O-α-L-arabinopyranoside-7-O-β-D-glucopyranoside, BS2 as kaempferol 3-O-β-D-[6$'''$-O-(3,4-dihydroxy-cinnamoyl)]-glucopyranosyl-(1$'''\rightarrow$2$''$)-O-α-L-arabinopyranoside-7-O-β-D-glucopyranoside, BS3 as kaempferol 3-O-β-D-[2$'''$-O-(3,4-dihydroxy-cinnamoyl)]-glucopyranosyl-(1$'''\rightarrow$2$''$)-O-α-L-arabinopyranoside-7-O-β-D-glucopyranoside and BS4 as kaempferol 3-O-β-D-glucopyranosyl-(1$'''\rightarrow$ 2$''$)-O-α-L-arabinopyranoside. The compounds BS1, BS2, BS3 and BS4 were reported for the first time in nature. Figure 3.82 presents the HPLC chromatogram (Method HPLC-B, see Section 5.4.4, Experimental Part) of the ethanolic extract of *Brugmansia suaveolens* and its characterized compounds. Additionally, flavonol glycosides (i.e., kaempferol 3-O-α-L-arabinopyranoside and kaempferol 3-O-α-L-arabinopyranoside-7-O-β-D-glucopyranoside) have also been reported by Begum *et al.*, (2006) [27] in *B. suaveolens*.

Brugmansia suaveolens has mainly been studied due to the presence of alkaloids [84, 97, 10, 350]. However, the qualitative determination of alkaloids, which was carried out with the ethanolic extract, showed negative results. A reason that could explain this result might be the low concentration of alkaloids in the leaves of this plant. Alves *et al.*, (2007) [10] reported the occurrence of lower concentrations of alkaloids in the leaves and the highest concentrations were identified in the roots and in the flowers of *Brugmansia suaveolens*.

Concerning the biosynthesis of the aforementioned isolated compounds from *Brugmansia suaveolens*, a hypothetical pathway was proposed, as shown in Figure 3.83. As a first step, the kaempferol (Figure 3.83.A) is derived from a 4-hydroxycinnamoyl-CoA [80]. In the second step, the α-L-arabinopyranose group might be added to O-3 of kaempferol (Figure 3.83.B), which was already isolated from this plant by Begum *et al.*, (2006) [27]. Third step, β-D-glucopyranoses might be added to the O-7 of kaempferol (Figure 3.83.C was also already isolated from this plant by Be-

gum *et al.*, (2006) [27]) or to the O-2 of arabinose (Figure 3.83.D was isolated in this work). Fourth step, β-D-glucopyranoses might be added to the O-7 of kaempferol (Figure 3.83.D) or to the O-2 of arabinose (Figure 3.83.C) to produce the compounds BS1 (Figure 3.83.E). Fifth step, after the biosynthesis of the caffeic acid [237], the acylation might occur on the terminal glucosyl unit of the kaempferol 3,7-O-triglucoside to produce the compound BS2 (Figure 3.83.F). This acylation is very common at position C-6 [150] and has been described for some examples [105, 118, 140, 138, 50, 2]. However, the acylation at the position C-2 of the kaempferol 3,7-O-triglucoside producing the compound BS3 (Figure 3.83.G) is not a common transfer and has only been reported by Kellam *et al.*, (1993) [154] and by Tian *et al.*, (2007) [309]. Considering that the acylation at position C-6 occurs frequently in the nature compared to the acylation at the position C-2, one may speculate that the biosynthesis of compound BS2 might be produced before the biosynthesis of compound BS3. Based on this hypothesis, the possible biosynthesis of the compounds from *Brugmansia suaveolens* might follow: BS4 $\rightarrow$ BS1 $\rightarrow$ BS2 $\rightarrow$ BS3.

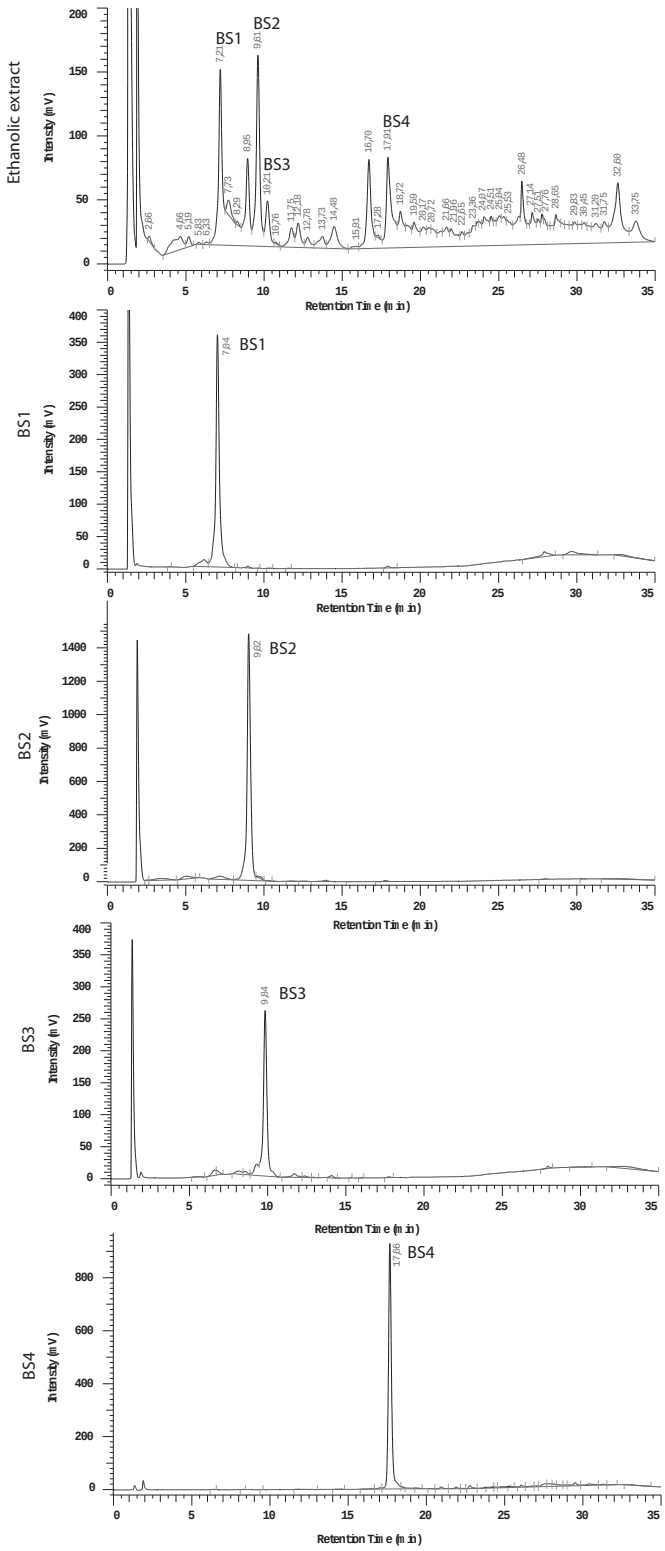

Figure 3.82: Representative HPLC chromatogram of the ethanolic extract of *Brugmansia suaveolens* and its isolated compounds (BS1), (BS2), (BS3), and (BS4) (Method HPLC-B with wavelength λ = 254 nm)

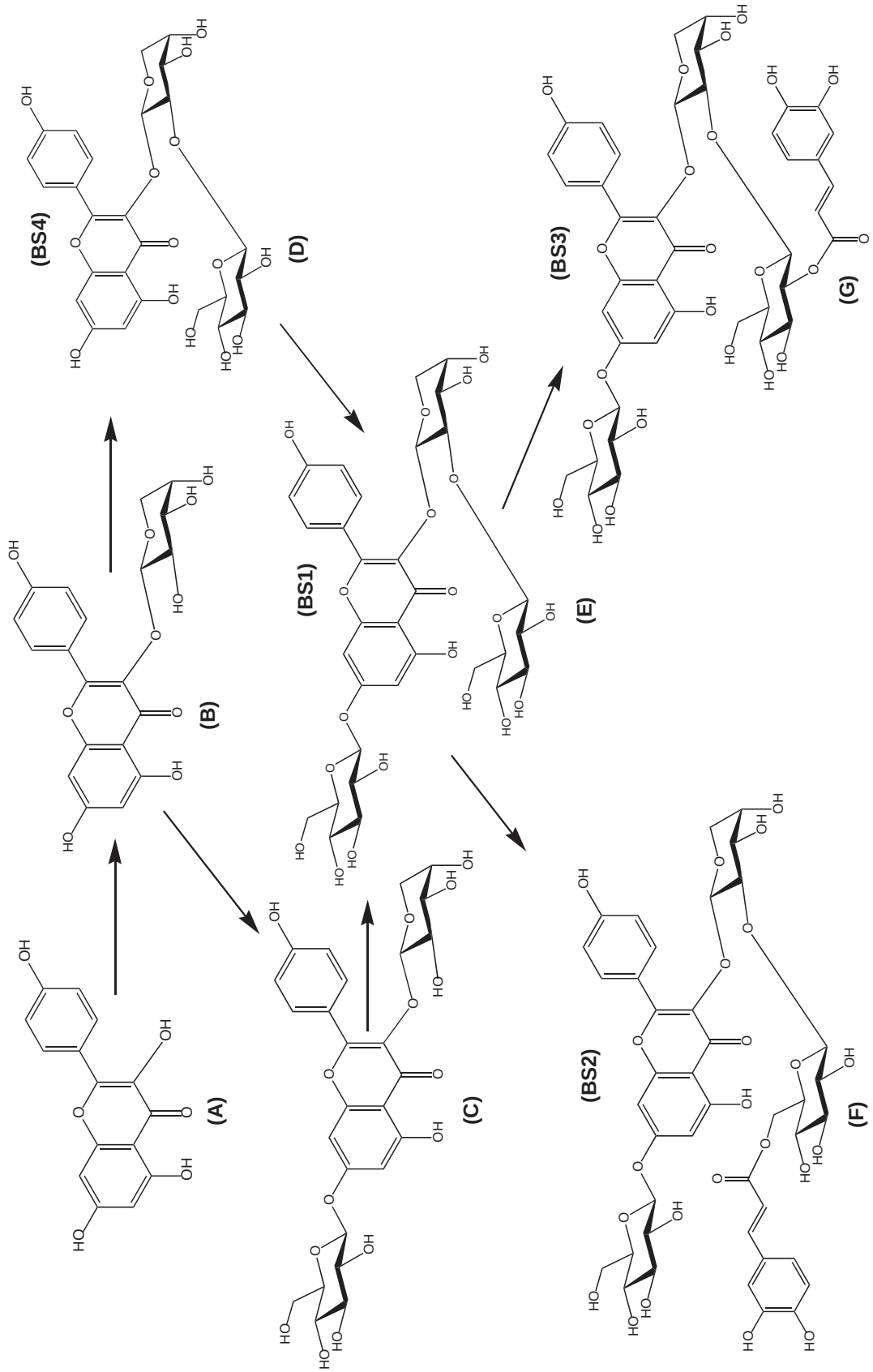

Figure 3.83: Proposed biosynthesis pathway of the isolated compounds BS1, BS2, BS3 and BS4 from *Brug-*
 mansia suaveolens

3.2 Biological Investigation and Discussion

The ethanolic extracts from the leaves of *Cordia americana* and *Brugmansia suaveolens* as well as their isolated compounds were evaluated using *in vitro* test systems, such as enzyme-linked immunosorbent assay (ELISA), which determines the inhibition of p38α and JNK3 in isolated enzyme assays. Moreover, docking studies were also performed in order to explain the possible binding modes of the most active isolated compounds at the ATP binding site of both enzymes. The activity of the plant extract and isolated compounds of *Cordia americana* were also studied for TNFα release in human whole blood assay. These assays[23] as well as the docking studies[24] were carried out in the Department of Pharmaceutical and Medicinal Chemistry at the University of Tübingen.

The 5-lipoxygenase assays were performed in cell free and in cell-based assays using isolated human PMNL. These assays[25] were carried out in the Department of Pharmaceutical Analytics at the University of Tübingen.

In cooperation with the Department of Pharmaceutical Biology and Biotechnology at the University of Freiburg, the NF-κB[26] activation was studied by means of the electrophoretic mobility shift assay (EMSA). The wound healing effects[27] were studied using the fibroblast scratch assay and finally cytotoxic effects of the plant extract were studied by the MTT (3-(4,5-dimethylthiazol-2-yl)-2,5-diphenyltetrazolium bromide) assay.

3.2.1 p38α MAPK

This section presents the results of the inhibition on p38α (see Section 5.7.1, Experimental Part) with regard to the ethanolic extracts of *Cordia americana*, *Brugmansia suaveolens* and their

[23] The MAPK (i.e., p38α and JNK3) and also the TNFα assays were carried out by Márcia Goettert and Katharina Bauer (by Prof. Dr. Laufer).
[24] The molecular modeling studies were carried out by Verena Schattel (by Prof. Dr. Laufer).
[25] 5-LO assays in cell free and isolated PMNL were carried out by Bianca Jazzar and Daniela Mueller (by Prof. Dr. Werz).
[26] The NF-κB assay was carried out by Cleber Schmidt (by Prof. Dr. Merfort).
[27] The MTT and fibroblast scratch assays were carried out by Márcio Fronza (by Prof. Dr. Merfort).

respective isolated constituents. The p38α enzyme phosphorylates ATF-2 and the amount of phosphorylated substrate reflects the enzyme activity in the assay.

Additionally, SB203580 (see Figure 5.13, Experimental Part) was used as reference compound. The most promising compounds were docked into the ATP binding site of p38α in order to explain the possible binding modes to the enzyme. The results were expressed in $IC_{50}\pm$SEM or in percentage of inhibition (%$\pm$SEM) for at least three experiments.

The reference compound pyridinylimidazol (SB203580) exhibited an inhibitory activity IC_{50} of 0.044$\pm$0.003 μM. These results are in agreement with the literature [104, 191, 287].

3.2.1.1 *Cordia americana*

The ethanolic extract presented an IC_{50} of 3.25$\pm$0.29 μg/mL.

Rosmarinic acid (CA1), the major compound quantified in the ethanolic extract (as shown in Section 5.6.1.3) presented an IC_{50} of 1.16$\pm$0.13 μg/mL (3.23$\pm$0.35 μM). As shown in Figure 3.84, the ethanolic extract presented a slighter lower inhibition than CA1.

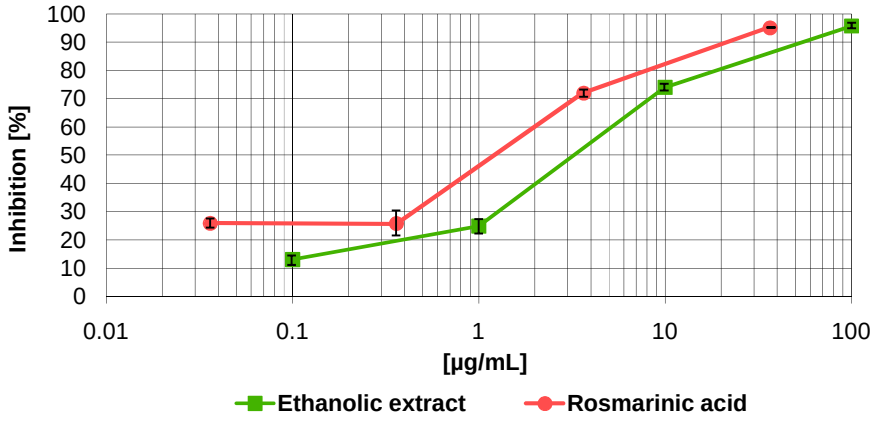

Figure 3.84: Inhibitory activity of the ethanolic extract of *Cordia americana* and rosmarinic acid on p38α

The docking results from different X-ray structures of p38α provided more than one possible binding mode for CA1 at the ATP binding site of the enzyme. As can be depicted from Figure 3.85 (states A and B), both docking results showed that the aromatic ring of the caffeic acid moiety is found in the so-called hydrophobic pocket I (i.e., selectivity pocket) in the entrance of the ATP

binding site. The state A shows that the hydroxy groups from the aromatic ring of the caffeic acid moiety build hydrogen bonds to the carbonyl group of the amino acid Glu71. However in state B, the two hydroxy groups on the C-3 and C-4 position of the caffeic acid make interactions with the amino group of the amino acid Lys53 by the building of a O$\cdots$H-N hydrogen bond, and with the carbonyl and amino group of the amino acid Asp168. Thus, for both docking results, the carboxylic acid moiety builds two hydrogen bonds O$\cdots$H-N to Met109, which lies in the hinge region. Finally, the second aromatic ring of the 2-hydroxypropanoic acid moiety is positioned in the front of the active site and builds two hydrogen bonds O-H$\cdots$O to Ser154 (state A and B).

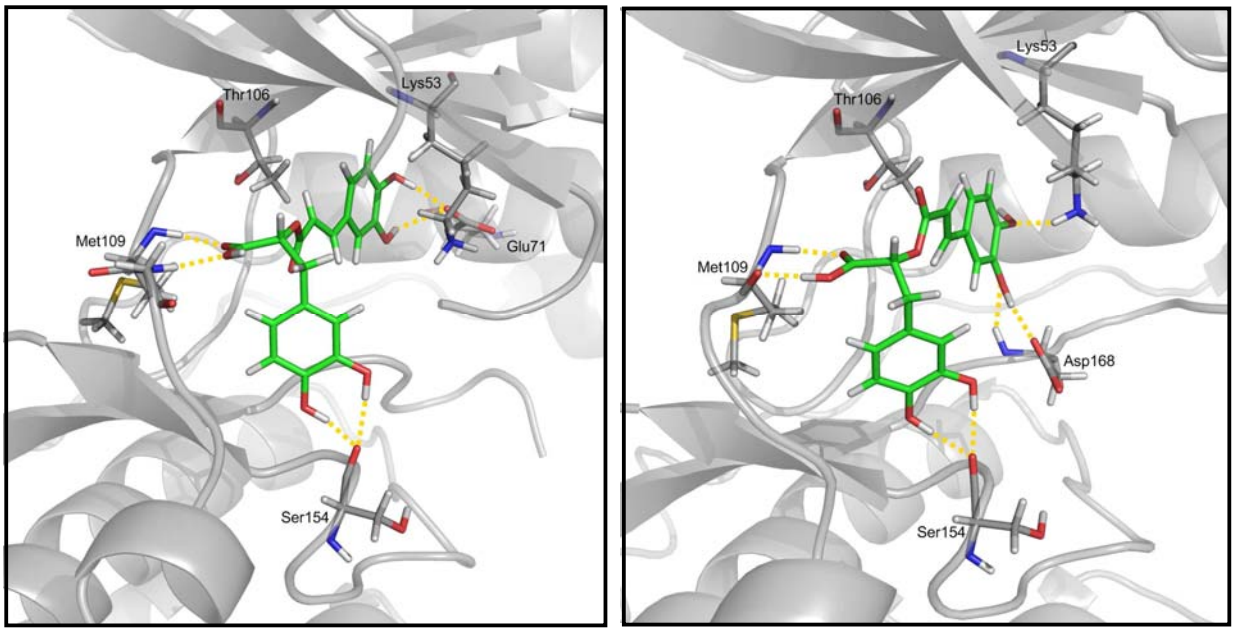

Figure 3.85: Possible binding modes for rosmarinic acid to the different X-ray structures of p38α: (A) PDB 2QD9 and (B) PDB 2ZAZ

Hagiwara *et al.*, (1988) [121] also discussed that the inhibitory potencies of phenolic compounds for serine/threonine kinases are closely correlated with the number of hydroxy residues. Up to now binding modes of flavonoids and phenolic inhibitors have been suggested for different protein kinases, but not for p38α. Jelić *et al.*, (2007) [147] proposed docking studies of CA1 in Fyn kinase. Beside the classical ATP binding site another additional binding site was proposed. In contrast, only docking positions at the ATP site were found. Major differences between Jelić *et*

al., (2007) [147] and this approach are: Fyn kinase is a non-receptor tyrosine kinase from the Src kinase family, whereas p38α is a serine/threonine kinase from the MAPK family. In addition, a homology model of the enzyme and docking was performed with FlexX and Gold software [147]. The current approach is based on X-ray structures of the p38α and the induced fit tool from Schrödinger software package [281] was used for docking.

CA1 was identified as the major compound with an amount of 8.44% in the ethanolic extract of the leaves of *Cordia americana*. However, the ethanolic extract from *Cordia americana* exhibited higher inhibition in comparison to the predominant constituent, as can be observed in Table 3.9. Thus, further compounds may contribute to the described biological effects.

Table 3.9: Biological effects of the ethanolic extract of *Cordia americana* and rosmarinic acid on p38α

	IC_{50} of the ethanolic extract (μg/mL)	**Content of CA1 (8.44%) in this amount of ethanolic extract (μg/mL)**	**IC_{50} of CA1 (μg/mL)**
p38α	3.25	0.27	1.16

CA1 is also the major constituent of lemon balm (*Melissa of cinalis*), a plant that has shown promising signs of therapeutic activity in patients with Alzheimer s diseases [146] and it is also used as a cough remedy [128, 318].

The rosmarinic acid ethyl ester (CA2) was studied and showed an IC_{50} of 5.10±0.43 μg/mL (13.13±1.1 μM). As observed in Figure 3.86, CA2 had a slight lower inhibition than the ethanolic extract and CA1.

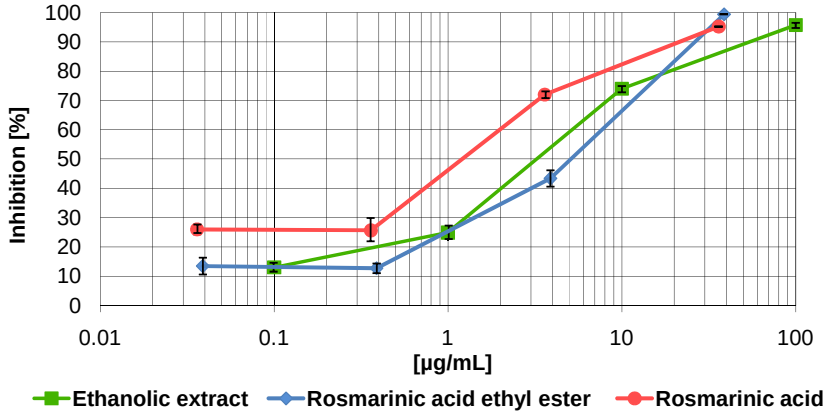

Figure 3.86: Inhibitory activity of the ethanolic extract of *C. americana*, rosmarinic acid ethyl ester and rosmarinic acid on p38α

Concerning the docking studies of CA2 at the ATP binding site of the kinase, it is possible to observe that the binding modes are similar as in CA1. As represented in Figure 3.87, the state A shows that both aromatic rings of CA2 bind and make interactions in the same position as the state A of CA1 (see Figure 3.85 (state A)). On one hand, in state B (see Figure 3.87), one hydroxy group of the aromatic ring of the 2-hydroxypropanoic acid moiety makes interactions with Asp168, and on the other hand, two hydroxy groups of the second aromatic ring of the caffeic acid interact with the carbonyl groups of both amino acids Asp112 and Ser154. Regarding the interactions in the hinge region, it is important to point out that the ester group might make weak or no interactions (state B) with Met109, which is probably reflected in a lower inhibition of the isolated CA2.

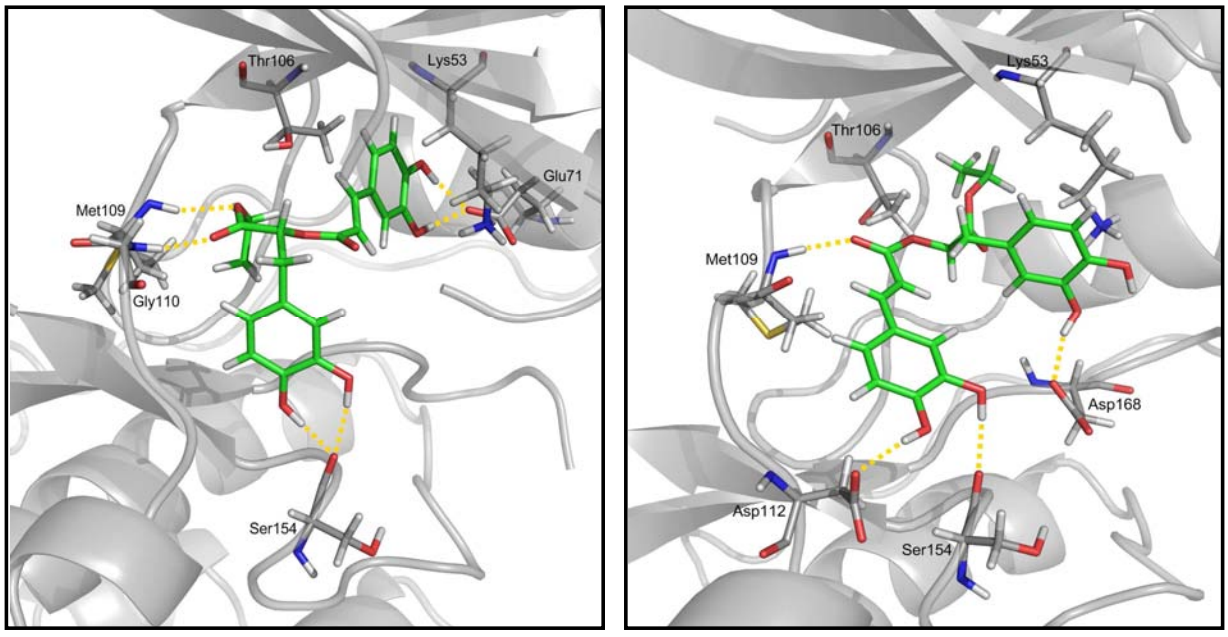

Figure 3.87: Possible binding modes for rosmarinic acid ethyl ester to the different X-ray structures of p38α: (A) PDB 2QD9 and (B) PDB 2ZAZ

The compounds 3-(3,4-dihydroxyphenyl)-2-hydroxypropanoic acid (CA3), rutin (CA4), quercitrin (CA5), and α-amyrin (CA8) were also evaluated on the p38α assay. As observed in Table 3.10, CA3 exhibited an IC_{50} of 4.28$\pm$1.97 μg/mL (21.64$\pm$8.9 μM). The flavonol glycosides CA5 and CA4 gave an IC_{50} of 12.59$\pm$0.52 μg/mL (28.08$\pm$1.17 μM) and 40.22$\pm$5.44 μg/mL (65.88$\pm$8.88 μM), respectively. Finally, the compound CA8 showed an IC_{50} of 15.25$\pm$1.36 μg/mL (35.75$\pm$3.18

μM). All these compounds showed a lower inhibition compared to the ethanolic extract, CA1 and CA2 (see Table 3.10).

The low inhibition of the phenolic compound CA3 might be due to the small structure size that probably do not allow enough interactions with the p38 binding pocket in order to produce an optimal inhibition. The inhibition of CA5 might be higher than CA4 due to the additional sugar moiety, which increases the size of the structure and its polarity and decreases the inhibition.

Table 3.10: Inhibition of the ethanolic extract of *Cordia americana* and characterized compounds on p38α

Compounds	**IC$_{50}$**
Ethanolic extract	3.25±0.29 μg/mL
Rosmarinic acid (CA1)	1.16±0.13 μg/mL (3.23±0.35 μM)
Rosmarinic acid ethyl ester (CA2)	5.10±0.43 μg/mL (13.13±1.1 μM)
3-(3,4-dihydroxyphenyl)-2-hydroxypropanoic acid (CA3)	4.28±1.97 μg/mL (21.64±8.9 μM)
Rutin (CA4)	40.22±5.44 μg/mL (65.88±8.88 μM)
Quercitrin (CA5)	12.59±0.52 μg/mL (28.08±1.17 μM)
α-amyrin (CA8)	15.25±1.36 μg/mL (35.75±3.18 μM)

3.2.1.2 *Brugmansia suaveolens*

The ethanolic extract of *Brugmansia suaveolens* and the isolated compounds were also evaluated targeting the inhibition on p38α. The isolated flavonol glycosides, which possessed as aglycone the kaempferol (Figure 3.88) and a caffeic acid moiety (i.e., BS2 and BS3) (Figure 3.89) were also tested, although they were not isolated from the plant extract. However, it was interesting to study their activity in order to understand better the inhibitory effects of the flavonol glycosides.

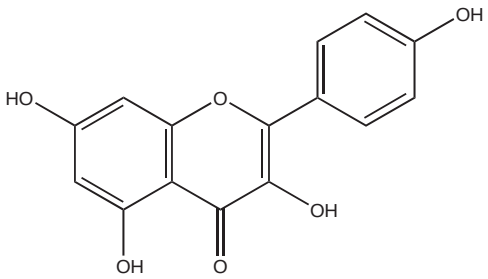

Figure 3.88: Kaempferol

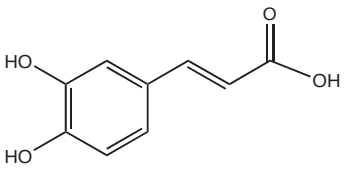

Figure 3.89: Caffeic acid

The ethanolic extract showed an IC_{50} of 1.21±0.02 μg/mL.

As observed in Table 3.11, the kaempferol 3-O-β-glucopyranosyl-(1→2)-O-α-L-arabinopyranoside (BS4) exhibited an IC_{50} of 26.80±1.78 μM (15.55±1.03 μg/mL) on p38α. The new compound kaempferol 3-O-β-glucopyranosyl-(1→2)-O-α-L-arabinopyranoside-7-O-β-glucopyranoside (BS1) showed an IC_{50} of 34.35±2.09 μM (25.51±1.55 μg/mL). The kaempferol 3-O-β-[6" -O-(3,4-dihydroxy-cinnamoyl)]-glucopyranosyl-(1→2)-O-α-L-arabinopyranoside-7-O-β-gluco- pyranoside (BS2) exhibited an IC_{50} of 25.73±3.63 μM (23.28±3.28 μg/mL) on p38α, as shown in Figure 3.90. On the other hand, no IC_{50}-value was obtained for the new kaempferol 3-O-β-[2" -O-(3,4-dihydroxy-cinnamoyl)]-glucopyranosyl-(1→2)-O-α-L-arabinopyranoside-7-O-β-glucopyranoside (BS3), whereas the highest inhibition of 41.39±3.75% was found at 100 μM (90.48 μg/mL). As can be observed, the acylation of the caffeic acid moiety at C-2" (i.e., BS3) might provoke a lower inhibition compared to the acylation of the caffeic acid moiety at C-6" (i.e., BS2).

In order to investigate, wether the aglycone kaempferol and the caffeic acid moiety contributed to the activity of the isolated flavonol glycosides, the corresponding reference compounds were also tested. Kaempferol inhibited p38α with an IC_{50} of 14.51±0.01 μM (4.15±0.01 μg/mL) and caffeic acid showed an IC_{50} of 50.40±8.29 μM (9.08±1.49 μg/ml), as shown in Table 3.11. Thus, it can be assumed that the kaempferol aglycone might contribute more than the caffeic acid moiety to the inhibition of the flavonol glycosides as well as to the ethanolic extract of *Brugmansia suaveolens* in the p38α. However, further non-characterized constituents might play a role in the effects of the plant extract.

Table 3.11: Inhibition of the ethanolic extract and isolated flavonol glycosides from *B. suaveolens* on p38α

Compounds	**IC_{50} / percentage of inhibition (%)**
Ethanolic extract	1.21±0.02 μg/mL
BS1	34.35±2.09 μM (25.51±1.55 μg/mL)
BS2	25.73±3.63 μM (23.28±3.28 μg/mL)
BS3	41.39±3.75% @ 100 μM (90.48 ±g/mL)
BS4	26.80±1.78 μM (15.55±1.03 μg/mL)
Kaempferol	14.51±0.01 μM (4.15±0.01 μg/mL)
Caffeic acid	50.40±8.29 μM (9.08±1.49 μg/ml)

Following these results, BS1-4 do not substantially contribute to the the activity of the extract, as can be observed in Figure 3.90. The flavonol glycosides from *Brugmansia suaveolens* (i.e., BS1, BS2, BS3 and BS4) might present low significantly activity due to the glycosylation.

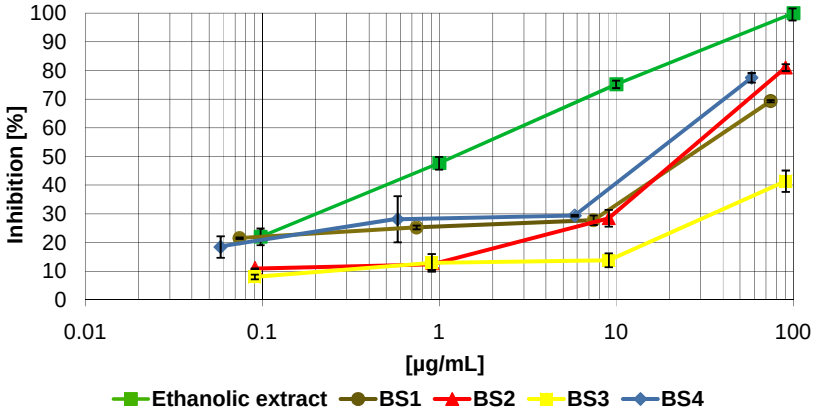

Figure 3.90: Inhibitory activity of the ethanolic extract of *Brugmansia suaveolens* and the isolated flavonol glycosides on p38α

Ferriola *et al.*, (1989) [92] have already suggested that the inhibitory potency on Protein Kinase C (PKC) by flavonols were reduced by glycosylation. This feature could be also observed with kaempferol, which has a higher inhibition on p38α than the isolated flavonol glycosides.

3.2.2 TNFα

p38α is also involved in the release of TNFα [282, 179, 176]. Further studies were carried out in order to evaluate the effects on release of TNFα with the ethanolic extract and the corresponding isolated compounds from *Cordia americana* using human whole blood by ELISA (see Section 5.7.3, Experimental Part). The isolated compounds from *Brugmansia suaveolens* were not tested in TNFα, because of their large molecular size and their polarity, which might hinder the diffusion across the cell membrane. All the values are expressed in $IC_{50}\pm$SEM or in percentage of inhibition at the highest tested concentration (%$\pm$SEM) from at least two experiments.

The pyridinylimidazole SB203580 was used as reference compound and exhibited an IC_{50} of 1.97$\pm$0.57 μM.

Table 3.12 shows the results of the ethanolic extract of *Cordia americana* and their respective compounds on TNFα release. The ethanolic extract moderately suppressed the release of TNFα, where the highest inhibition effect of 49.71$\pm$15.87% was achieved at 100 μg/mL. The major compound CA1 shows an inhibition of 36.75$\pm$1.54% tested in a concentration of 100 μM (36.03 μg/mL). Compared to CA1, the ethanolic extract presented a slightly lower activity. On the other hand, CA2 showed the highest inhibitory effect with an IC_{50} of 47.84$\pm$4.87 μM (18.58$\pm$1.89 μg/mL).

Table 3.12: Inhibition of ethanolic extract of *Cordia americana* and the characterized compounds on TNFα release

Compounds	**IC_{50} / percentage of inhibition (%)**
Ethanolic extract	49.71$\pm$15.87% @ 100 μg/mL
Rosmarinic acid (CA1)	36.75$\pm$1.54% @ 100 μM (36.03 μg/mL)
Rosmarinic acid ethyl ester (CA2)	47.84$\pm$4.87 μM (18.58$\pm$1.89 μg/mL)

It is important to point out that the inhibition effects of the compounds might be highly dependent of the donors of human blood. CA1 and CA2 have lower activity in the TNFα assay in comparison to the p38α on cell free assay. This might be probably explained due to the plasma protein binding, so that only a small amount of the inhibitor is absorbed by the cell.

As well as for the kinases assays (Section 3.2.1.1), the ethanolic extract exhibited a higher effect compared to CA1, since the ethanolic extract at 100 μg/mL, which contains 8.44% of CA1 (i.e., 8.44 μg/mL), resulted in 49.71% of inhibition. Therefore, one might suspect that the inhibitory properties of *Cordia americana* might be dependent mostly on CA1, but also on CA2.

3.2.3 JNK3 MAPK

In this assay, a non radioactive immunosorbent assay was used for measure the inhibitory effects of the ethanolic extracts of *Cordia americana* and *Brugmansia suaveolens* and the respective isolated compounds on JNK3. SP600125 was used as reference compound (see Figure 5.14, Experimental Part). The design of the JNK3 assay is similar to the p38α (see Section 5.7.2, Experimental Part). The results are expressed in $IC_{50}\pm$SEM or in percentage inhibition (%$\pm$SEM) for at least three experiments.

The anthrapyrazolone SP600125 correspond to an IC_{50} of 0.16$\pm$0.03 μM.

3.2.3.1 *Cordia americana*

The inhibitory activity of the ethanolic extract showed an IC_{50} of 12.01$\pm$0.01 μg/mL.

Rosmarinic acid (CA1) showed an IC_{50} of 12.91$\pm$0.55 μM (4.65$\pm$0.20 μg/mL). Figure 3.91 exhibited the inhibition of CA1 and the ethanolic extract, whose activity is slight lower than CA1.

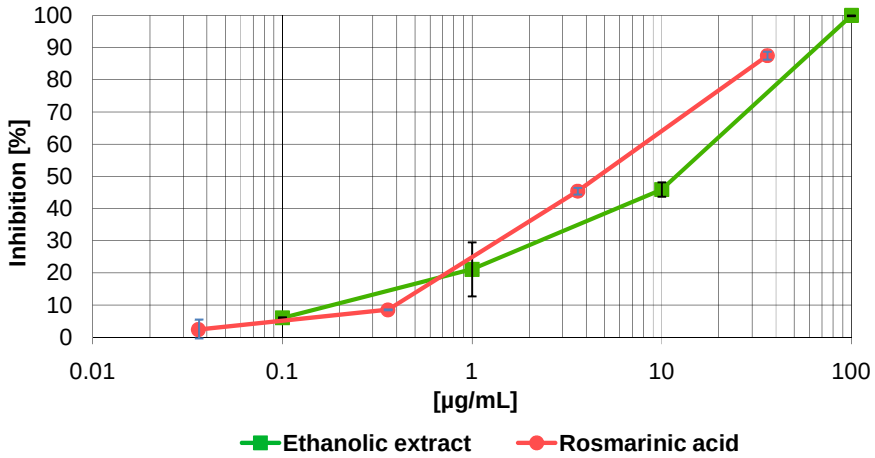

Figure 3.91: Inhibitory activity of the ethanolic extract of *Cordia americana* and rosmarinic acid on JNK3

Concerning the ATP binding site of p38α and JNK3, these MAPKs differ in the hydrophobic region II at two points [304]:

- In stead of Asp112 (p38α), there is an Asn115 in JNK3,
- In stead of Asn115 (p38α), there is a Gln155 in JNK3.

The docking results from different X-ray structures, referenced as PDB 3G9L (State A) and PDB 3FI3 (State B) provide also more than one possible binding mode for CA1 at the ATP binding site of JNK3. As shown in Figure 3.92 (PDB 3G9L and PDB 3FI3), both docking results demonstrate that the aromatic ring of the caffeic acid moiety is found in the so-called hydrophobic pocket I (i.e., selectivity pocket) in the entrance of the ATP binding site. The state A demonstrates that the hydroxy groups at the C-3 and C-4 position of the aromatic ring build hydrogen bonds to the carboxyl-group of the amino acid Glu111. However, in state B, the hydroxy group at the C-3 position makes interactions with the amino group of Lys93 (O$\cdots$H-N hydrogen bond) and with the carbonyl group of the amino acid Leu206 (O-H$\cdots$O hydrogen bond). The aromatic ring of the 2-hydroxypropanoic acid moiety is located in the hinge region in state A, whereas the two hydroxy groups build two hydrogen bonds to the carbonyl and amino group of Met149. In the state B, one hydroxy group makes interactions with Asp150 by the building of a O-H$\cdots$O hydrogen bond and with Gln155 by the building of a O$\cdots$H-N hydrogen bond. Finally, the carboxylic acid moiety builds in state A a hydrogen bond to the carbonyl-group of Asn152 (O-H$\cdots$O hydrogen bond), and in state B, it makes interactions with Met149 by the building of two hydrogen bonds to the carbonyl and amino group of Met149.

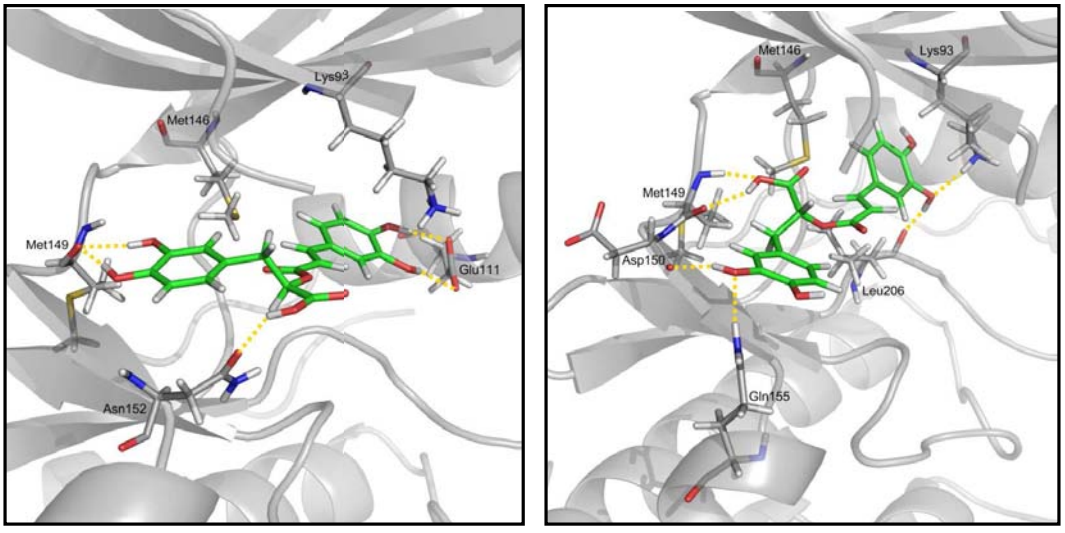

Figure 3.92: Possible binding modes for rosmarinic acid to the different X-ray structures of JNK3: (A) PDB 3G9L and (B) PDB 3FI3

The ethanolic extract from *Cordia americana* exhibited also higher inhibition in comparison to the predominant constituent CA1, as can be observed in Table 3.13. Thus, further compounds may contribute to the described biological effects.

Table 3.13: Biological effects of the ethanolic extract of *Cordia americana* and rosmarinic acid on JNK3

	IC_{50} of the ethanolic extract (μg/mL)	**Content of CA1 (8.44%) in this amount of ethanolic extract (μg/mL)**	**IC_{50} of CA1 (μg/mL)**
JNK3	12.01	1.01	4.65

The rosmarinic acid ethyl ester (CA2) inhibited JNK3 with an IC_{50} of 21.13±4.32 μM (8.21±1.68 μg/mL). From Figure 3.93 it can be depicted that CA2 has a slight higher inhibition than the ethanolic extract and a slight lower inhibition than CA1.

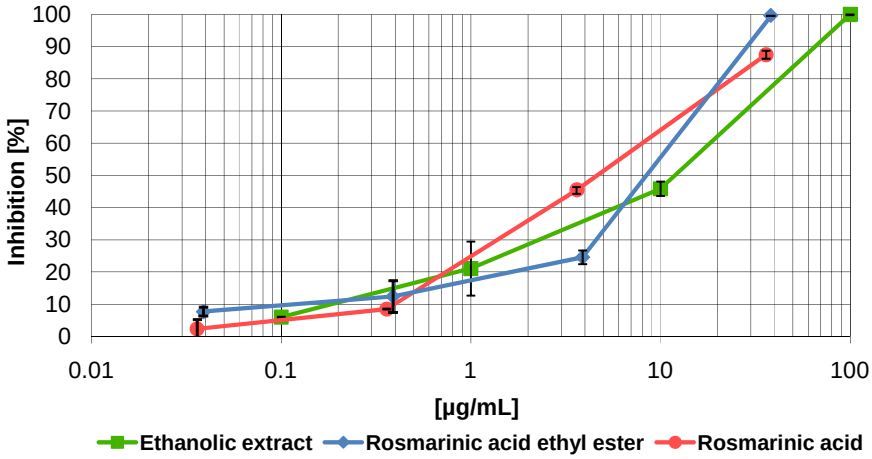

Figure 3.93: Inhibitory activity of the ethanolic extract of *Cordia americana*, rosmarinic acid ethyl ester and rosmarinic acid on JNK3

Concerning the docking studies of CA2 at the ATP binding site of JNK3 (Figure 3.94), it is possible to observe that the docking mode is similar in some aspects to CA1 in state A (Figure 3.91). In CA2, the hydroxy groups on the C-3 and C-4 position of the aromatic ring of 2-hydroxypropanoic acid build hydrogen bonds to the carboxyl-group of the amino acid Glu111 (O-H$\cdots$O hydrogen bond). The aromatic ring of the caffeic acid moiety is positioned in the hinge region. One of its hydroxy groups makes interactions with the carbonyl-group of Asp150 (O-H$\cdots$O hydrogen bond)

and with the amino-group of Met149 (N-H$\cdots$O hydrogen bond) and the second hydroxy group on position C-3 builds interactions with Asp150 by the building of a O-H$\cdots$O hydrogen bond and with the amino-group of Asn152 (O$\cdots$H-N hydrogen bond). This docking position shows no interaction between the ethyl ester moiety and any amino acid, which might explain the slightly lower inhibition compared to the CA1 on JNK3 assay.

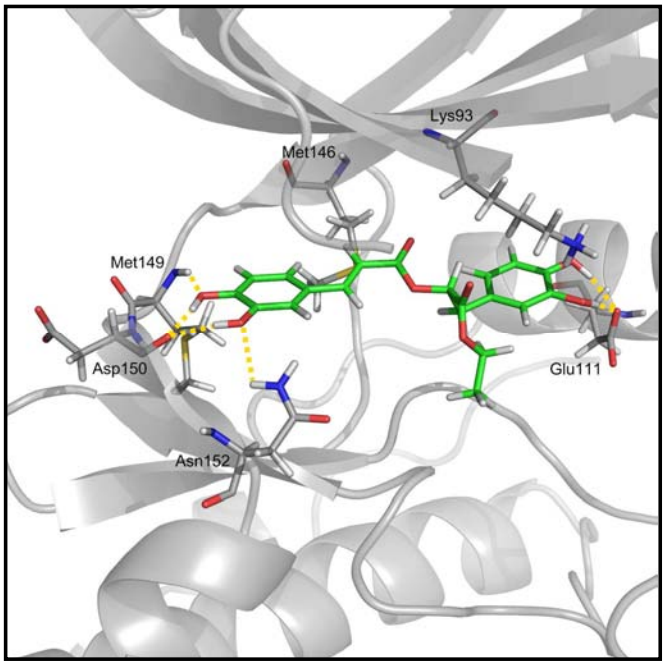

Figure 3.94: Possible binding mode for rosmarinic acid ethyl ester to the X-ray structure PDB 3G9L on JNK3

The compounds 3-(3,4-dihydroxyphenyl)-2-hydroxypropanoic acid (CA3), 3-O-β-glucoside of quercetin (CA5), rutin (CA4) and the pentacyclic triterpene α-amyrin (CA8) were also studied on the JNK3 assay. As demonstrated in Table 3.14, the CA5 showed an IC_{50} of 35.57$\pm$3.06 μM (15.95$\pm$1.37 μg/mL) and the CA8 an IC_{50} of 35.65$\pm$3.70 μM (15.21$\pm$1.58 μg/mL). On the other hand, the remaining compounds CA3 and CA4 presented lower inhibition with 35.5$\pm$2.67% at 150 μM (29.72 μg/mL) and 35.04$\pm$1.05% at 100 μM (61.05 μg/mL), respectively. All these compounds exibited lower effects compared to the ethanolic extract, CA1 and CA2 (see Table 3.14).

Table 3.14: Inhibition of the of the ethanolic extract of *Cordia americana* and characterized compounds on JNK3

Compounds	**IC_{50} / percentage inhibition (%)**
Ethanolic extract	12.01±0.01 μg/mL
Rosmarinic acid (CA1)	12.91±0.55 μM (4.65±0.20 μg/mL)
Rosmarinic acid ethyl ester (CA2)	21.13±4.32 μM (8.21±1.68 μg/mL)
3-(3,4-dihydroxyphenyl)-2-hydroxypropanoic acid (CA3)	35.5±2.67% @ 150 μM (29.72 μg/mL)
Rutin (CA4)	35.04±1.05% @ 100 μM (61.05 μg/mL)
Quercitrin (CA5)	35.57±3.06 μM (15.95±1.37 μg/mL)
α-amyrin (CA8)	35.65±3.70 μM (15.21±1.58 μg/mL)

The low inhibition of CA4 and CA5 might be explained due to the glycosylation which increases the size and polarity of the structure that might be not adequate to the small ATP binding pocket of JNK3.

3.2.3.2 *Brugmansia suaveolens*

The ethanolic extract of *Brugmansia suaveolens* and its respective isolated flavonol glycosides were also studied targeting the inhibition on JNK3. Furthermore, kaempferol that corresponds to the aglycone of the isolated compounds and the caffeic acid, which were not detected in the plant extract, were tested.

The ethanolic extract of *Brugmansia suaveolens* exhibited an IC_{50} of 20.76±0.18 μg/mL.

As can be observed in Table 3.15, none of the isolated flavonol glycosides showed relevant inhibition on JNK3 assay. This can mainly be explained due to the size of the compounds, since the ATP binding site of JNK3 is flat and small, which cannot accommodate larger inhibitors as the isolated ones.

Kaempferol inhibited the JNK3 with an IC_{50} of 17.77±0.38 μM (5.08±0.11 μg/mL) and caffeic acid exhibited lower inhibition of 18.80±1.49% at 100 μM (18.02 μg/mL), as shown in Table 3.15. Thus, it can be assumed that the kaempferol aglycone might contribute more than the caffeic acid to the inhibition of the ethanolic extract of *Brugmansia suaveolens* on JNK3. Moreover, further non-characterized compounds might explain the effects of the ethanolic extract of *Brugmansia suaveolens* on JNK3.

Table 3.15: Inhibition of ethanolic extract of *Brugmansia suaveolens* and the isolated flavonol glycosides on JNK3

Compounds	**IC_{50} / percentage inhibition (%)**
Ethanolic extract	20.76±0.18 μg/mL
BS1	13.5±1.62% @ 100 μM (74.26 μg/mL)
BS2	24.03±3.49% @ 100 μM (90.48 μg/mL)
BS3	33.4±0.80% @ 100 μM (90.48 μg/mL)
BS4	19.1±2.29% @100 μM (58.05 μg/mL)
Kaempferol	17.77±0.38 μM (5.08±0.11 μg/mL)
Caffeic acid	18.80±1.49% @ 100 μM (18.02 μg/mL)

Scapin *et al.*, (2003) [268] suggests also that small, flat and more hydrophobic inhibitors probably bind better to the JNK3 ATP binding site than to the more solvent exposed p38 cavity. Probably due to this feature, the isolated flavonol glycosides exhibited no considerable inhibitory effects on JNK3.

3.2.4 5-Lipoxygenase

The present section describes the results on the inhibition of 5-LO (see Section 5.7.4, Experimental Part), concerning the ethanolic extracts of *Cordia americana* and *Brugmansia suaveolens*, and their isolated compounds. The investigation on 5-LO inhibition was done in a cell-free assay using partially purified 5-LO. Moreover, the most active compounds were further tested in cell-based assay using human PMNL (polymorphonuclear leukocytes). BWA4C (see Figure 5.17, Experimental Part) was used as reference compound. All the values are expressed in IC_{50}±SEM or in percentage of inhibition (%±SEM) from at least two experiments.

3.2.4.1 Inhibition of 5-LO Activity in a Cell-free Assay

The reference compound BWA4C exhibited an IC_{50} of 0.3±0.01 μM.

3.2.4.1.1 *Cordia americana*

The ethanolic extract strongly suppressed 5-LO product formation with an IC_{50} of 0.69±0.27 μg/mL.

Rosmarinic acid (CA1) showed a similar inhibition compared to the ethanolic extract with an IC_{50} of 0.97±0.19 μg/mL (2.69±0.53 μM). The rosmarinic acid ethyl ester (CA2) efficiently suppressed 5-LO product formation with an IC_{50} of 0.15±0.01 μg/mL (0.38±0.03 μM). This compound showed a slightly higher inhibition than the ethanolic extract and CA1. Quercitrin (CA5) indicated an IC_{50} of 0.42±0.52 μg/mL (0.94±1.16 μM), that represents a slightly higher inhibition compared to the ethanolic extract and CA1, and slightly lower effect compared to CA2. These features are shown in Figure 3.95.

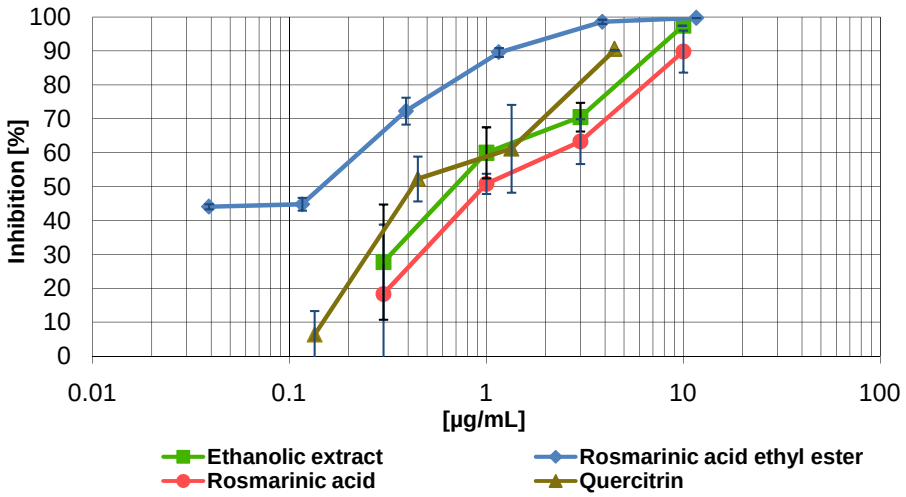

Figure 3.95: Inhibitory activity of the ethanolic extract of *Cordia americana*, rosmarinic acid, rosmarinic acid ethyl ester and quercitrin on 5-LO

As previously mentioned, CA1 presented an amount of 8.44% in the ethanolic extract of the leaves of *Cordia americana*. However, the ethanolic extract exhibited a slight higher effect compared to the isolated CA1, as can be observed in Table 3.16. Thus, further compounds may contribute to the described biological effects.

In general, phenolic acids and flavonoids are well known inhibitors of 5-LO product formation belonging to the class of redox-type 5-LO inhibitors. They act as antioxidants, and therefore, they

Table 3.16: Biological effects of the ethanolic extract of *Cordia americana* and rosmarinic acid on 5-LO

	IC_{50} of the ethanolic extract (μg/mL)	**Content of CA1 (8.44%) in this amount of ethanolic extract (μg/mL)**	**IC_{50} of CA1 (μg/mL)**
5-LO	0.69	0.0582	0.97

keep the active site-iron of 5-LO in the inactive ferrous state and uncouple the catalytic redox cycle of the enzyme. In case of CA1 and CA2, the presence of phenolic hydroxy groups might govern the potency on 5-LO inhibition. In particular, polyphenols active on 5-LO typically resemble fatty acid-like structures, with a carboxylic acid moiety or an acidic phenol core [330].

The compounds 3-(3,4-dihydroxyphenyl)-2- hydroxypropanoic acid (CA3) and rutin (CA4) were also investigated for the inhibition on the 5-LO product formation, as illustrated in Table 3.17. These compounds showed no notably activity.

Table 3.17: Inhibition of the isolated compounds from *Cordia americana* on 5-LO

Compounds	**Percentage of inhibition (%)**
3-(3,4-dihydroxyphenyl)-2-hydroxypropanoic acid (CA3)	14.96% @ 10 μM (1.98 μg/mL)
Rutin (CA4)	20.55% @ 10 μM (6.10 μg/mL)

3.2.4.1.2 *Brugmansia suaveolens*

The ethanolic extract of *Brugmansia suaveolens* and the respective isolated compounds were also evaluated targeting the inhibition on 5-LO product formation on cell-free assay. Furthermore, kaempferol, which corresponds to the aglycone of the flavonol glycosides and caffeic acid moiety (i.e., BS2 and BS3) were also studied.

The effect of the ethanolic extract resulted in a suppression of the 5-LO product formation with an IC_{50} of 5.42$\pm$5.16 μg/mL.

Table 3.18 exhibited the inhibitory effects of the isolated flavonol glycosides from *Brugmansia suaveolens*. Most of the new isolated compounds presented no significant activity on 5-LO product formation, with exception of BS3. The flavonol glycoside BS3 (kaempferol 3-O-β-[2" -O-(3,4-dihydroxy-cinnamoyl)]-glucopyranosyl-(1$\rightarrow$2)-O-α-L-arabinopyranoside-7-O-β-glucopyranoside) moderately inhibited the 5-LO product formation with an IC_{50} of 28.38$\pm$15.90 μM (25.68$\pm$14.38

μg/mL), but with a lower effect compared to the ethanolic extract. As it can also be observed in Table 3.18, the acylation of the caffeic acid moiety at C-2" (i.e., BS3) might allow a higher inhibition compared to the acylation at C-6" (i.e., BS2).

The ethanolic extract as well as BS3 exhibited the highest inhibitory effects, which are considered significantly (i.e., $IC_{50} < 50$ μM [330]) for blocking 5-LO product formation. However, the inhibition effects of the flavonol aglycones are generally superior over the corresponding glycosides [330], which can be supported by the inhibition of the kaempferol. Moreover, one may speculate that the aglycone kaempferol might contribute more than the caffeic acid to the inhibition of the flavonol glycosides as well as to the ethanolic extract in the 5-LO assay, as shown in Table 3.18.

Table 3.18: Inhibition of the ethanolic extract of *Brugmansia suaveolens* and the isolated flavonol glycosides on 5-LO

Compounds	**IC_{50} / percentage of inhibition (%)**
Ethanolic extract	5.42±5.16 μg/mL
BS1	$>$ 30 μM (22.29 μg/mL)
BS2	42.44±12.53% @ 30 μM (27.14 μg/mL)
BS3	28.38±15.90 μM (25.68±14.38 μg/mL)
BS4	25.69±4.01% @ 30 μM (17.41 μg/ml)
Kaempferol	0.72±0.27 μM (0.20±0.08 μg/mL)
Caffeic acid	26.48±11.23% at 30 μM (5.40 μg/mL)

3.2.4.2 Interference of 5-LO Activity in Cell-based Assay Using PMNL

The reference compound BWA4C exhibited an IC_{50} of 0.3±0.01 μM.

The plant extract of *Cordia americana* resulted in an IC_{50} of 8.67±0.80 μg/mL.

Rosmarinic acid ethyl ester (CA2) presented an IC_{50} of 0.66±0.04 μg/mL (1.69±0.11 μM), which is higher than the ethanolic extract, as shown in Figure 3.96. The activity of CA2 on 5-LO cell-based assay using human isolated PMNL, may be attributed to the relative hydrophobic character of the compound that probably affects the penetration in the cell.

Polymorphonuclear leukocytes are important effectors of the innate immune response and play a crucial role in the development of an inflammatory phenotype [160]. The differences between

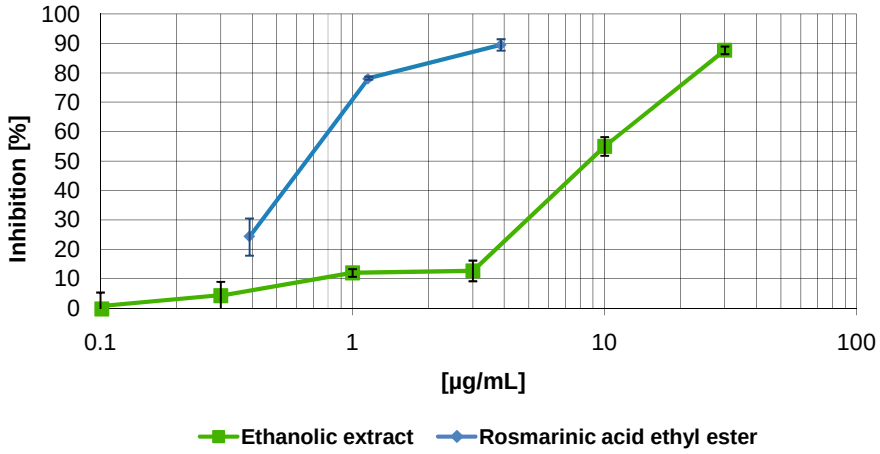

Figure 3.96: Inhibitory activity of the ethanolic extract of *Cordia americana* and rosmarinic acid ethyl ester on 5-LO (PMNL)

the effects on 5-LO product formation in cell free and cell based assays might be explained due to the limited availability of the inhibitor to penetrate in the cell, or due to plasma protein binding [244] and finally, by a possible competition with endogenous blood components such as fatty acids [293]. However, the ability of a compound to suppress leukotriene formation in isolated cells, like PMNLs, might reflect its efficacy *in vivo*.

3.2.5 Supplementary Assays for *Cordia americana*

In order to investigate in more details the anti-inflammatory and wound healing properties of the ethanolic extract of *Cordia americana* and its major compound rosmarinic acid (CA1), the NF-κB and scratch assays were also carried out.

3.2.5.1 NF-κB Assay

The influence of the ethanolic extract and CA1 on NF-κB activation (see Section 5.7.5, Experimental Part) were evaluated in the electrophoretic mobility shift assay (EMSA). As illustrated in Figure 3.97, the plant extract and CA1 showed a slightly NF-κB inhibition, around 17% at 50 μg/mL and 54 μM, respectively, after the evaluation against the positive control. Therefore, neither the ethanolic extract nor CA1 reduced NF-κB activation in Jurkat cells, indicating that inhibition

of TNFα seems to be independent from NF-κB DNA activation in Jurkat cells.

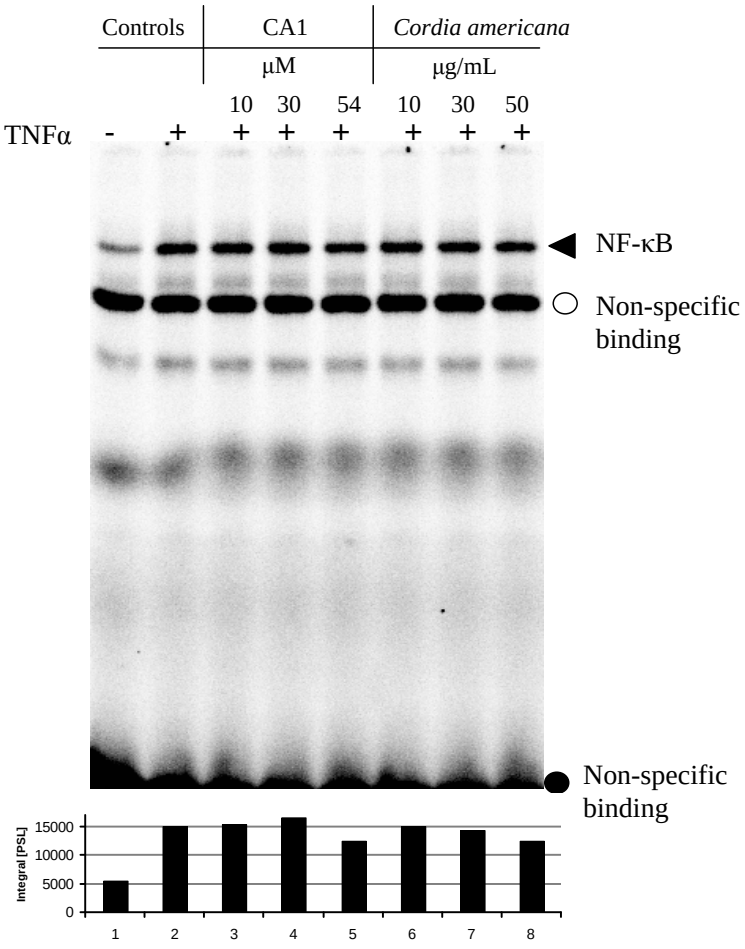

Figure 3.97: Inhibitory activity of the ethanolic extract of *Cordia americana* and rosmarinic acid on NF-κB

CA1 was proven to inhibit TNFα induced nuclear translocation of NF-κB in human dermal fibroblast by targeting IKK-β [182]. However in this study, neither the ethanolic extract nor CA1 reduced NF-κB activation in Jurkat cells indicating that inhibition of TNFα seems to be independent from NF-κB DNA activation in Jurkat cells.

3.2.5.2 Scratch Assay

Since the role of platelet derived growth factor (PDGF) in wound healing is well characterized, PDGF was taken as positive control in the fibroblasts scratch assay (see Section 5.7.6, Experimental Part). The effect of 2 ng/ml of PDGF increase the cell numbers around 62% after 12h of incubation. The results are expressed as percent of cell numbers in the wounded area compared to the control. Bars represent the mean±SEM of three experiments.

A concentration of 1 μg/mL of the ethanolic extract increased the proliferation and migration of fibroblasts by 19.8%. No concentration dependency was observed, probably due to the cytotoxic activity of the extract at higher concentrations. The effect of CA1 was also slight; at 10 μg/mL, the cell numbers enhanced to 11.8% (see Figure 3.98). In order to evaluate whether cytotoxic effects may have an impact on the results mentioned above, the MTT assay was carried out. At 50 μg/mL no significant citotoxicity was observed, however, at 100 μg/mL the plant extract reduced the cell viability to 41%, showing that inhibition on cell proliferation and migration at the highest tested concentration in the scratch assay is due to the cytotoxic effect of the extract.

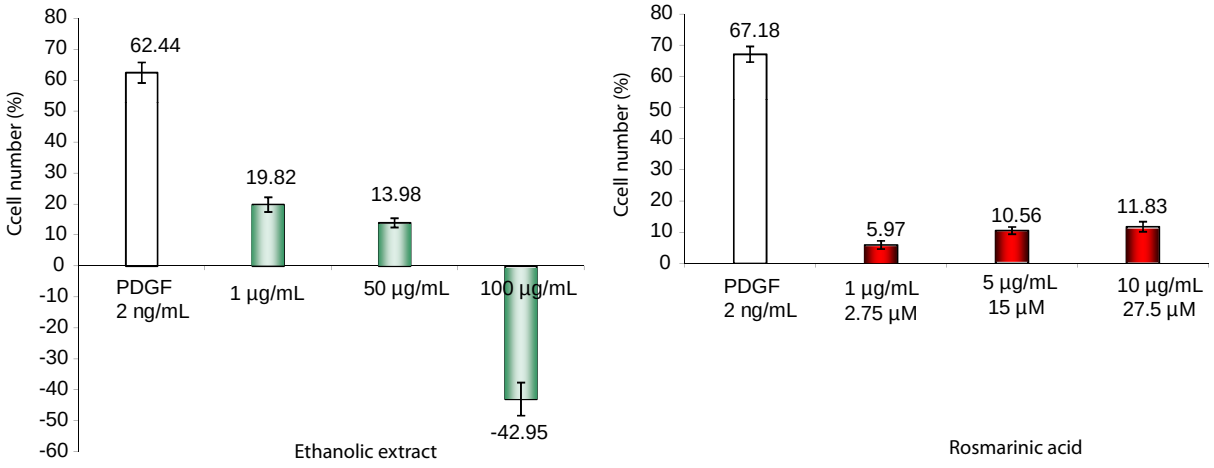

Figure 3.98: Effect of the ethanolic extract from *Cordia americana* and rosmarinic acid on the migration and proliferation of fibroblasts

Studies performed with the plant extract and its CA1 revealed only a very moderate activity in the reepithelialization phase, as shown in Table 3.19. The scratch assay has proven to be a convenient

and inexpensive method to give first insights on the proliferation and migration of fibroblasts into the damaged area, as demonstrated for the ethanolic extract of *Calendula of cinalis* (1 μg/mL), where an increasing effect of 60% was observed [100].

Table 3.19: Biological effect of the ethanolic extract of *Cordia americana* and rosmarinic acid on scratch assay

	Concentration of the plant extract (μg/mL)	**Content of CA1 (8.44%) in this amount of ethanolic extract (μg/mL)**	**Cell number compared to control (%)**	**Concentration of CA1 μg/mL)**	**Cell number compared to control (%)**
Scratch assay	1	0.084	19.8	1	6.0
	50	4.22	13.9	5	10.6
	100	8.44	-42.0	10	11.8

3.2.6 Summary of the Biological Activity

This section summarizes the biological activity of the characterized compounds of the investigated plants *Cordia americana* and *Brugmansia suaveolens*.

3.2.6.1 Rosmarinic Acid, Rosmarinic Acid Ethyl Ester and 3-(3,4-dihydroxyphenyl)-2-hydroxypropanoic acid

Rosmarinic acid (CA1) was isolated from many species of plants of the families Lamiaceae and Boraginaceae and was identified as one of the active components of several medicinal plants (e.g., *Salvia of cinallis*, *Mentha piperitam*, *Thymus vulgaris*, *Melissa of cinalis*, *Symphytum of cinale*) [237]. It has been shown to possess anti-inflammatory, antioxidative, antiviral as well as antibacterial activity in various *in vitro* assays [205, 238, 346, 234] and *in vivo* studies [348, 305]. Studies demonstrated inhibitory effects on 5 and 12-lipoxygenase and gene expression of cycloxygenase-2 [346, 247, 273]. Besides the antioxidative properties, CA1 acts as a potent antiviral agent *in vivo* against Japanese encephalitis virus by reducing the viral replication and secondary inflammation resulting from microglial activation [305]. Gao *et al.*, (2004) [107] and Hur *et al.*, (2004) [139] also showed neuroprotective effects for CA1 by inducing apoptosis.

Rosmarinic acid ethyl ester (CA2) showed hypotensive, antibacterial, anti-viral, anti-inflammatory, anti-tumor and hypoglycemic activities [327]. Choudhary *et al.*, (2005) [53] reported that CA2, isolated from *Lindelo a stylosa* (Boraginaceae), possesses antioxidant activity.

CA1 and CA2 have effects on the p56^{lck} SH2 domain (src homology-2 domain). The SH2 domain is a highly conserved non-catalytic module, consisting of 100 amino acids residues, and is found in many intracellular signal-transduction proteins. This domain recognizes phosphotyrosine, containing proteins with high affinity. Specific antagonist of the p56^{lck} SH2 domains can be developed as novel therapeutic agents to treat a broad range of human diseases such as cancer, autoimmune diseases, osteoporosis and chronic inflammatory disease [230]. CA1 exhibited a binding to the p56^{lck} SH2 domain with an IC_{50} of 24 μM, which was measured by an ELISA competitive assay. On the other hand, the CA2 showed a less potent binding affinity with an IC_{50} of 91$\pm$3 μM

in comparison with CA1, which can be explained by the presence of an ester group. Considering the structure-activity relationship (SAR) studies, all four hydroxyl groups from both compounds are essential for the interaction with p56^{lck} SH2 domain [230].

3-(3,4-dihydroxyphenyl)-2-hydroxypropanoic acid (CA3) (i.e.,danshenshu) has relaxing effects on 5-HT-precontracted coronary artery rings [349, 173] and in ischemic myocardial injury, which was proven in rats [342].

Psotová *et al.*, (2003) [247] studied the antioxidant activity of *Prunella vulgaris* and reported that the scavenging activity might be attributed due to the major isolated compounds CA1 and CA3. Baño *et al.*, (2003) [22] and Dapkevivius *et al.*, (2002) [67] attributed the antioxidant activity of CA1 due to the presence of two catechol structures, conjugated with a carboxylic acid group. In case of CA3, Chen and Ho (1997) [47] related the antioxidative activity to the hydroxyl groups.

3.2.6.2 β-Sitosterol and Campesterol

A variety of pharmacological properties are attributed to β-sitosterol (CA6), like antioxidant, anti-inflammatory, anti-carcinogenic and anti-atherogenic [303]. More specifically, CA6 blocks cholesterol absorption, resulting in lower serum cholesterol levels, and also prevents the oxidation of LDL cholesterol, whereby the risk of atherosclerosis is reduced. It has been used to treat prostate problems such as benign prostatic hypertrophy. Thus, it may reduce the growth of the prostate gland, as well as inhibiting colon cancer cells and altering membrane lipids [303]. CA6 had been reported to exhibit both antifungical and antibacterial activities against *Fusarium ssp.* and *Salmonella typhii*, respectively [158, 220].

There is an accumulating evidence that campesterol (CA7) exhibits chemoprotective effects against many cancers, including prostate [202], lung [271] and breast [19]. CA7 can inhibit endothelial cell proliferation and differentiation as well as neovascularization with no toxicity, suggesting that it could be an antiangiogenic candidate for the prevention and treatment of angiogenesis diseases [51]. However, finally further *in vivo* studies have to be carried out to confirm all these *in vitro* studies.

3.2.6.3 α- and β-Amyrin

The pentacyclic triterpene α-amyrin (CA8) and β-amyrin (CA9) were used to alleviate inflammatory symptoms [321] and is also reported to possess a wide range of activity against gram-positive and gram-negative bacteria. Vitor *et al.*, (2009) [321] showed that the anti-inflammatory effects of both compounds seem to be related to the local suppression of inflammatory cytokines and COX-2 levels, possibly via inhibition of NF-κB pathway, which were examinated on an experimental model of colitis in mice. Considering its biological effects, the mixture of compounds α- and β-amyrin presented antinociceptive properties [228].

3.2.6.4 Flavonol Glycosides

Flavonol glycosides play a special role in the protection of plants from ultraviolet damage [210] and in the excitation and coloring of plant fluorescence [296]. Plants usually glycosylate its secondary metabolites in order to enhance their solubility and improve sequestration into specific cellular compartments [132].

In nature, flavonoids exist almost as β-glycosides, although the 7 and 4 positions may also be glycosylated in some plants [96, 345]. Other classes of flavonoids are found mainly glycosylated in the position 7 [71]. The different structures of flavonoids significantly affect the absorption, metabolism, bioactivities, and the binding process with plasma proteins [323].

With respect to the structural differences of glycosides and aglycones, Amakura *et al.*, (2003) [11] reported that their differences in the activity may be described to the increasing molecular size and polarity and due to the transfer to the non-planar structure produced by the addition of sugars. Acylation and glycosylation of flavonoids also increase stability of the compound. On the other hand, flavonoid glycosides are generally hydrophilic and thus cannot be transported across membranes by passive diffusion. In case of hydrolysis by bacterial enzymes in the lower part of the intestine, the sugar moiety of flavonoid glycosides is cleaved, resulting in more lipophilic aglycones. These become permeable through the cell wall [345].

Rutin (CA4) has anti-inflammatory [286] and anti-tumour [41] effects and showed also activity against hemoglobin oxidation [119]. Moreover, rutin can reduce capillary fragility, swelling and has been used in the treatment of venous insufficiency (varicose veins, haemorrhoids, diabetic vascular disease, and diabetic retinopathy), and for improving micro-vascular blood flow (pain, tired legs, night cramps, and restless legs) [3]. CA4 also demonstrated antioxidant effects on malonaldehyde formation from ethyl arachidonate.

Quercitrin (CA5), the 3-O-β-glucoside of quercetin, is a flavonol glycoside, which shows antileishmanial (*in vitro*) [219] and antioxidant activities [235].

4 Summary

In Brazil, the medicinal plants *Cordia americana* and *Brugmansia suaveolens* have been used to treat inflammations and wounds in folk medicine. However, the effective compounds responsible for the biological effects of these plants are widely unknown. Therefore, both plants were investigated in this dissertation and the conclusions and scientific contributions are summarized:

- Bioguided fractionation, based on p38α MAPK assay, was carried out with the fraction sets of the ethanolic extract of *Cordia americana* and revealed five groups that were submitted to successive subfractionation. The phytochemical studies (i.e., MS, 1D and 2D NMR) allowed the identification of flavonols (rutin and quercitrin), phytosterols (campesterol and β-sitosterol), triterpenoids (α- and β-amyrin) and phenolic acids (3-(3,4-dihydroxyphenyl)-2-hydroxypropanoic acid, rosmarinic acid and rosmarinic acid ethyl ester).

- All the aforementioned compounds were identified for the first time in *Cordia americana*, and 3-(3,4-dihydroxyphenyl)-2-hydroxypropanoic acid and rosmarinic acid ethyl ester were described for the first time for the genus *Cordia*.

- HPLC analysis revealed rosmarinic acid as the major compound in the ethanolic extract of *Cordia americana*. Therefore, a quantification method was developed and a content of 8.44% of rosmarinic acid in the dried leaves of *Cordia americana* was detected, which is so far the highest concentration found in Boraginaceaes species.

- Concerning the biological effects, the ethanolic extract of *Cordia americana* as well as rosmarinic acid and rosmarinic acid ethyl ester exhibited the highest inhibitory effects on the

pro-inflammatory mediators p38α and JNK3. 5-LO product formation was strongly inhibited by the ethanolic extract, rosmarinic acid, quercitrin and rosmarinic acid ethyl ester. The latter exhibited the highest inhibitory effects and was also tested in cell-based assay using isolated human PMNL, presenting also high inhibition. The major compound and rosmarinic acid ethyl ester have a lower activity in the TNFα assay in comparison to the p38α on cell free assay. The NF-κB activation in Jurkat cells was not reduced neither by the ethanolic extract nor rosmarinic acid. Finally, slight effects were observed in the impact on fibroblasts migration and proliferation in the scratch assay. In conclusion, the ethanolic extract from *Cordia americana* exhibited higher inhibition in comparison with the predominant and other isolated compounds. Hence, although rosmarinic acid is the major constituent, further secondary metabolites may contribute to the described biological effects.

- The molecular modeling studies on the ATP binding site of p38α and JNK3 suggested that the inhibitory effects of the bioactive compounds rosmarinic acid and rosmarinic acid ethyl ester correlate with the hydroxylation and with the number of hydrogen bonds formed.

- Altogether the biological results targeting different aspects of inflammation and wound healing processes contribute to explain the traditional use of the plant. This work demonstrated for the first time pharmacological effects of *Cordia americana*, providing evidences for a substantial role of rosmarinic acid as the major key player.

- The phytochemical investigations on *Brugmansia suaveolens* revealed four new flavonol glycosides (see Figure 4.1), namely, kaempferol 3-O-β-D-glucopyranosyl-(1$'''\rightarrow$2$''$)-O-α-L-arabinopyranoside-7-O-β-D-glucopyranoside (BS1), kaempferol 3-O-β-D-[6$'''$-O-(3,4-dihydroxy-cinnamoyl)]-glucopyranosyl-(1$'''\rightarrow$2$''$)-O-α-L-arabinopyranoside-7-O-β-D-glucopyranoside (BS2), kaempferol 3-O-β-D-[2$'''$-O-(3,4-dihydroxy-cinnamoyl)]-glucopyranosyl--(1$'''\rightarrow$2$''$)-O-α-L-arabinopyranoside-7-O-β-D-glucopyranoside (BS3), and kaempferol 3-O-β-D-glucopyranosyl-(1$'''\rightarrow$ 2$''$)-O-α-L-arabinopyranoside (BS4).

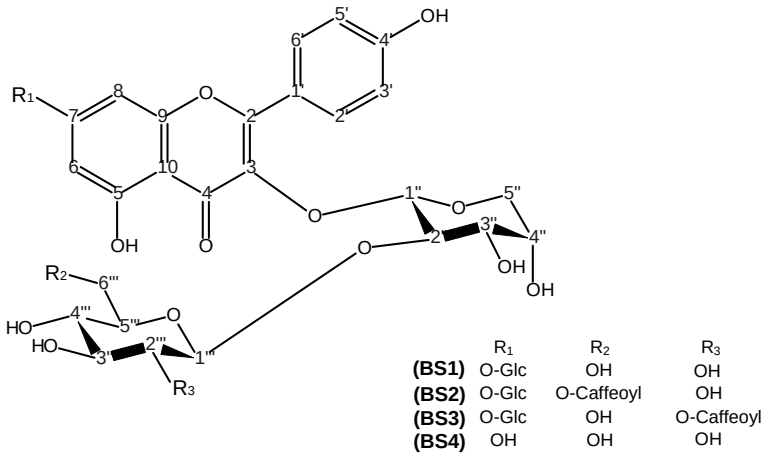

Figure 4.1: Isolated flavonol glycosides from the ethanolic extract of *Brugmansia suaveolens*

- The biological studies on p38α, JNK3 as well as 5-LO with the ethanolic extract of *Brugmansia suaveolens* and the isolated flavonol glycosides exhibited moderate inhibitory effects. The inhibition of the flavonol glycosides (i.e., BS1, BS2, BS3 and BS4) are probably due to the kaempferol aglycone that presented also a moderate inhibition in the assays. Thus, the difference in the activity might be influenced by the glycosylation, which increases the molecular size and the polarity of the compounds. Therefore, it can be assumed that the plant extract contains other secondary metabolites that were not identified, but they might also contribute to the overall biological activity of the ethanolic extract from *Brugmansia suaveolens*.

- A biosynthesis pathway was hypothesized for the isolated flavonol glycosides from *Brugmansia suaveolens*, considering that the acylation at position C-6$'''$ (BS2) occurs frequently and is widely known compared to the acylation at the position C-2$'''$ (BS3). One may speculate that the biosynthesis of compound BS2 might be produced before BS3. Based on this hypothesis, the possible biosynthesis pathway might follow: BS4 $\rightarrow$ BS1 $\rightarrow$ BS2 $\rightarrow$ BS3.

5 Experimental Part

This chapter presents the materials and methods applied in this work. More specifically, it describes in details the plant material and the methods for: plant extraction, isolation, quantification, chromatography, spectroscopy and biological assays.

5.1 Plant Material

The leaves from *Cordia americana* and from *Brugmansia suaveolens* were collected in the region of Santa Maria, Rio Grande do Sul, Brazil in October 2007 and January 2008, respectively. *Cordia americana* was authenticated by the botanist Solon J. Longhi and *Brugmansia suaveolens* by Gilberto Zanetti. Voucher specimens of both plants are deposited in the herbarium of the Department of Biology at the Santa Maria University, Brazil, under the reference number SMDB12308 (*Cordia americana*) and SMDB12520 (*Brugmansia suaveolens*).

5.2 Chemicals, Reagents and Materials

Table 5.1: Chemicals, reagents and materials

Material	Manufacturer
Acetone p.a	Sigma-Aldrich, Germany
Acetonitrile HPLC grade	Merck, Germany
Diethylamine p.a	Sigma-Aldrich, Germany
Dimethylsulfoxide-d_6	Euriso-Top Germany
Ethylacetate p.a	Sigma-Aldrich, Germany
Formic Acid p.a	Sigma-Aldrich, Germany
Methanol-d_4	Euriso-Top, Germany
Methanol HPLC grade	Merck, Germany
Methanol p.a	Brenntag Chemiepartner, Germany
p-Anisaldehyd 97%	Acros Organics, Belgien
Pyridine-d_5	Sigma-Aldrich, Germany
Sephadex®LH-20 (Bead size 25-100 μ)	Sigma-Aldrich, Germany
Sulfuric acid (95-97%) p.a	Sigma-Aldrich, Germany
Toluen p.a	VWR International, Germany
α-amyrin	Extrasynthese, France
Rosmarinic acid	Synthesized at University of Tübingen, Germany
Quercitrin	Carl Roth, Germany
Kaempferol	Extrasynthese, France
Caffeic acid	Carl Roth, Germany
Hiosciamin	Carl Roth, Germany
Scopolamin	Carl Roth, Germany
RP-18 LiChroprep RP-18 (25-40 μm)	Merck, Germany
Fluorescent tagged SiO_2 60 F_{254}	Merck, Germany
Fluorescent tagged RP-18 F_{254}	Merck, Germany

5.3 Instruments

Table 5.2: Instruments

Instruments	Manufacturer
Hairdryer	Siemens, Germany
Fraction collector	FRS Mini Manuel, Germany
Milli-Q Water	Millipore Purification System, USA
Liofilizator	Finn-Aqua Lyovac GT2, Germany
Millipore-Water System (MilliQ Plus)	Billerica, MA, USA
Rotavapor	Büchi, Germany
Ice machine	Wessamat Flake Line, Germany
Cabinet dryer	WTB Binder , Germany
Photo Camera Desaga UV/VIS	Sarsted-Gruppe, Germany
Balance	Kern Sohn, Germany

5.4 Chromatographic and Spectroscopic Methods

5.4.1 Thin Layer Chromatography (TLC)

Thin layer chromatography was used to control each fraction after separation procedures.

An amount of 5 μL up to 30 μL was manually applied for TLC plates in a band-shaped of 1 cm. The TLC plates were dried with a hair-dryer and run 8 cm using one of the methods (TLC-A), (TLC-B) or (TLC-C). After that, plates were dried again and analyzed under white light, short-wave (λ = 254 nm) and long-wave (λ = 366 nm). Additionally, plates were derivatized using the anisaldehyde-sulfuric reagent. Finally, plates were photographed for documentation using the Photo Camera Desaga UV/VIS system.

5.4.1.1 TLC Method for *Cordia americana*

- Method TLC-A:
  - Mobile phase: ethyl acetate:methanol:water (77:15:8)
  - Plate: Silica gel 60 F_{254}
  - Anisaldehyde-sulfuric reagent: 10 mL of sulfuric acid was carefully added to an ice-cooled mixture of 170 mL methanol and 20 mL of acetic acid. To this solution, 1 mL anisaldehyde was added. The plate was immersed in the reagent for 1 sec then heated at 100 °C for 2-5 minutes.
  - Examination: white light, UV λ = 366 nm.

5.4.1.2 TLC Methods for *Brugmansia suaveolens*

- Method TLC-B:
  - Mobile phase: toluene:methanol:diethylamine (8:1:1)
  - Plate: Silica gel 60 F_{254}

  - Anisaldehyde-sulfuric reagent: see Section 5.4.1.1
  - Examination: white light

- Method TLC-C
  - Mobile phase: water:methanol(1:1)
  - Plate: reverse phase RP-18 F_{254}
  - Anisaldehyde-sulfuric reagent: see Section 5.4.1.1
  - Examination: white light

- Method TLC-D:
  - Mobile phase: toluene:methanol:diethylamine (8:1:1)
  - Plate: Silica gel 60 F_{254}
  - Dragendorff s reagent: solution A: 0.85 g of basic bismuth nitrate was dissolved in 10 mL acetic acid and 40 mL water under heating; solution B: 8 g potassium iodide was dissolved in 30 mL water. Just before spraying, 1 mL of each solution was mixed with 4 mL of acetic acid and 20 mL of water.
  - Examination: white light

5.4.2 Column Chromatography

5.4.2.1 Sephadex®LH-20

A total amount of 300 g of Sephadex®LH-20 was dissolved with 1,250 mL of methanol split in three Erlenmeyer flasks. The solution was reposed for 12 h in order to expand. After that, the solution was applied in the open column (i.e., 80 cm long and 6 cm diameter) avoiding the formation of bubbles. The open column with Sephadex®LH-20 was reposed for 12 h in order to form a homogeneous and tight packing.

Before separation of the plant extract, the solvent was moved, keeping 1 cm of methanol over the top of the stationary phase. Finally, the plant extract was applied into the column and fractions were collected with a manual fraction collector.

5.4.2.2 Open Column Chromatography (OC)

A column with 25 cm long and 1 cm diameter was used and at each reaction tube 2 mL was collected. The following methods were used:

- Method OC-A: water:methanol (1:1)
- Method OC-B: water:methanol (2:1)

5.4.3 Flash Chromatography (FC)

- LaFlash System, FC 204 Fraction Collector (VWR International GmbH)
- UV-Filterphotometer with 200, 220, 254 and 280 nm (Labomatic Instruments AG)
- Pre-column with 10 cm length and 2 cm diameter
- Column with 20 cm length and 3 cm diameter

Table 5.3: Method FLASH-A

Time (minutes)	Water	Methanol	Flow rate (mL/min)
0.00	90	10	10
5.00	90	10	10
50.00	0	100	10

Table 5.4: Method FLASH-B

Time (minutes)	Water	Methanol	Flow rate (mL/min)
0.00	90	10	10
5.00	90	10	10
60.00	0	100	10

Table 5.5: Method FLASH-C

Time (minutes)	Water	Methanol	Flow rate (mL/min)
0.00	90	10	10
5.00	90	10	10
80.00	0	100	10

Table 5.6: Method FLASH-D

Time (minutes)	Water	Methanol	Flow rate (mL/min)
0.00	90	10	10
5.00	90	10	10
100.00	0	100	10

5.4.4 High Pressure Liquid Chromatography (HPLC)

- Merck-Hitachi HPLC;
- Organizer with Auto Injection (20 μL), Interface Module D-7000, Pump L-7100, UV/VIS Detector 7420;
- Column LiChrospher RP-18 (5 m, 100 x 2 mm).

Table 5.7: Method HPLC-A

Time (minutes)	**ACN:H_2O 90:10 +0.1% FA**	**ACN+0.1% FA**	**Flow rate (mL/min)**
0.0	95.0	5.0	0.5
10.0	80.0	20.0	0.5
17.0	75.0	25.0	0.5
25.0	65.0	35.0	0.5
35.0	55.0	45.0	0.5
40.0	75.0	25.0	0.5
50.0	95.0	5.0	0.5

Table 5.8: Method HPLC-B

Time (minutes)	**ACN/H_2O 90:10 +0.1% FA**	**ACN**	**Flow rate (mL/min)**
0.0	95.0	5.0	0.8
4.0	90.0	10.0	0.8
12.0	85.0	15.0	0.8
20.0	60.0	40.0	0.8
25.0	0.0	100.0	0.8
30.0	0.0	100.0	0.8
35.0	95.0	5.0	0.8

Table 5.9: Method HPLC-C

Time (minutes)	**H_2O 100+0.1% FA**	**ACN+0.1% FA**	**Flow rate (mL/min)**
0.0	95.0	5.0	0.8
5.0	90.0	10.0	0.8
13.0	85.0	15.0	0.8
15.0	95.0	5.0	0.8

Table 5.10: Method HPLC-D

Time (minutes)	**H_2O 100+0.1% FA**	**ACN**	**Flow rate (mL/min)**
0.0	85.0	15.0	0.5
20.0	50.0	50.0	0.5
21.0	0.0	100.0	0.5
25.0	0.0	100.0	0.5

5.4.5 UV-Visible Spectroscopy

- HPLC-DAD Hewlett Packard HP 1090
- Column Specification: ZORBAX Eclipse XDB-C8 (4.6 x 150 mm, 5 μm)
- Pump: Merck Hitachi (Darmstadt)
- Software: Shimazdu Client Server 7.2.1 SPI

5.4.6 Fourier Transform-Infrared Spectroscopy (FT-IR)

- Perkin Elmer Spectrum One (ATR Technology)
- Software: Graph Server v 1.60

5.4.7 Mass Spectroscopy

5.4.7.1 Gas Chromatography-Mass Spectrometry (GC-MS)

- **Method GC-MS**[1]:
- GC-MS System (Agilent 6890 series) with natural compound library (NIST MS Search Program version 1.7A);
- Capillar-column Rtx-1 MS (Fa. Restek; 25 m; 0.25 mm diameter; 0.25 μm Film Thickness-Dimethylsiloxane; Carrier Gas: Helium);
- Agilent 5973 Network Mass Selective Detector;
- Injector 7683 Series;

[1] GC-MS was performed by C. Schmidt at the Department of Pharmaceutical Biology and Biotechnology, University of Freiburg.

- Conditions: Initial temperature: 120 °C; Ramp 1 (10 min): 250 °C; Ramp 2 (10 min): 270 °C; Run time: 35 min.; Flow rate of 1.0 mL/min;
- Inlet: Split mode; 11.6 PSI; Flow: 14.1 mL/min; Split ratio: 10:1

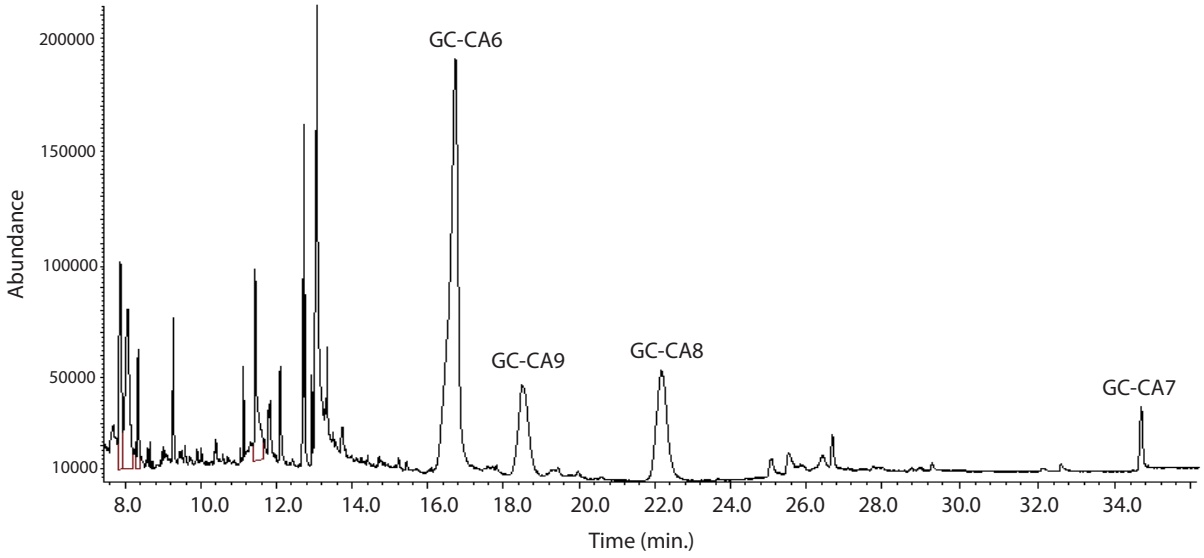

Figure 5.1: GC-MS of fraction E from *Cordia americana* (Method GC-MS)

5.4.7.2 Electron Ionization Mass Spectrometry (EI-MS)

- TSQ70 Mass Spectroscopies, Thermo Finnigan;
- Capillary Temperature: 200 °C;
- Evaporation Temperature: 30-300 °C;
- Ionization Energie: 45 and 70 V.

5.4.7.3 Electrospray Ionisation-Mass Spectrometry (ESI-MS)

- Thermo (Finningan) Surveyor MS Pump;
- Thermo (Finningan) LCQ Duon Ion Trap;

- DCM1000 (Degaser), P4000 (Pump), AS 3000 (Autosampler), UV 6000 LP (DAD 200-400 nm), Column Grom SIL 120 ODS-5 ST, 3 μm, 150 x 2 mm;
- Software: Xcalibur Home page version 1.3;
- Ionization: Positive/Electrospray (ESI);
- Sprayvoltage: 4.5 kV;
- Capillary Temperature: 250 °C;
- Sheath Gas Flow Rate: 60 (ARB);
- Aux Gas Flow Rate: 5 (ARB);
- Collision Gas: Argon;
- Detection: Full Scan 50-1000 m/z, Product Ion Scan.

Time (minutes)	ACN:H_2O 90:10 +0.1% FA	ACN+0.1% FA	Flow rate (mL/min)
0.00	100	0	0.2
3.00	100	0	0.2
25.0	5	95	0.2
30.0	5	95	0.2
31.0	100	0	0.2
35.0	100	0	0.2

Table 5.11: Method LC-DAD

5.4.7.4 Fourier-Transform-Ion Cyclotron Resonance Mass-Spectrometry (FT-ICR-MS)

High-resolution mass spectrometry (FT-ICR-MS) was determined using an APEX II FT-ICR mass spectrometer instrument from Bruker. The ionization was performed by electrospray ionization (ESI). The mass spectra were expressed as a mass to charge ratio (m/z).

5.4.8 Nuclear Magnetic Resonance Spectroscopy (NMR)

Cordia americana

For the structural elucidation of the isolated compounds of this plant, the following NMR 1D (^{1}H, ^{13}C and DEPT-135) and 2D (H-H-COSY) were carried out using the following instruments: Bruker Avance ARX-250; (Bruker S.A., Wissembourg, France); Bruker Avance DMX-400; (Bruker S.A., Wissembourg, France).

Brugmansia suaveolens

In order to elucidate the isolated compounds of this plant, the 1D (^{1}H, ^{13}C and DEPT-135) and 2D NMR (H-H-COSY, HSQC, HMBC) were carried out with: Bruker AMX 600.13 MHz Spectrometer; Magnetic field strength of 14.1 Tesla; Micro-probe was an inverse ^{1}H/^{13}C micro volume flow probe with 1.5 μL active detection configuration in solenoids (Protasis Corp., Marlboro, MA, USA); Bruker Avance ARX-250; (Bruker S.A., Wissembourg, France).

5.5 Plant Extraction Methods for the Biological Screening Phase

For the biological screening phase, the selected parts of the plants were dried, grounded and extracted using soxhlet, ultrasound or maceration. The soxhlet extraction was performed with 25 g of plant material, using at first n-hexane (250 mL), and after drying, ethanol (250 mL). 10 g were taken for the ultrasound extraction using n-hexane (100 mL), followed by ethanol (100 mL). The maceration process was carried out with 438.5 g of *Sedum dendroideum* and 329.5 g of *Kalanchoe tubi ora*. Each solvent was applied twice directly to the grounded plant material during 16 days changing the solvent each 8 days. Firstly, hexane was used for 16 days, followed by ethanol with the same material for another 16 days. Extraction was exhaustively carried out in each case. The solvents were removed under vacuum at 40 °C. Finally, extracts were lyophilised. Figure 5.2 depicts the extraction procedures.

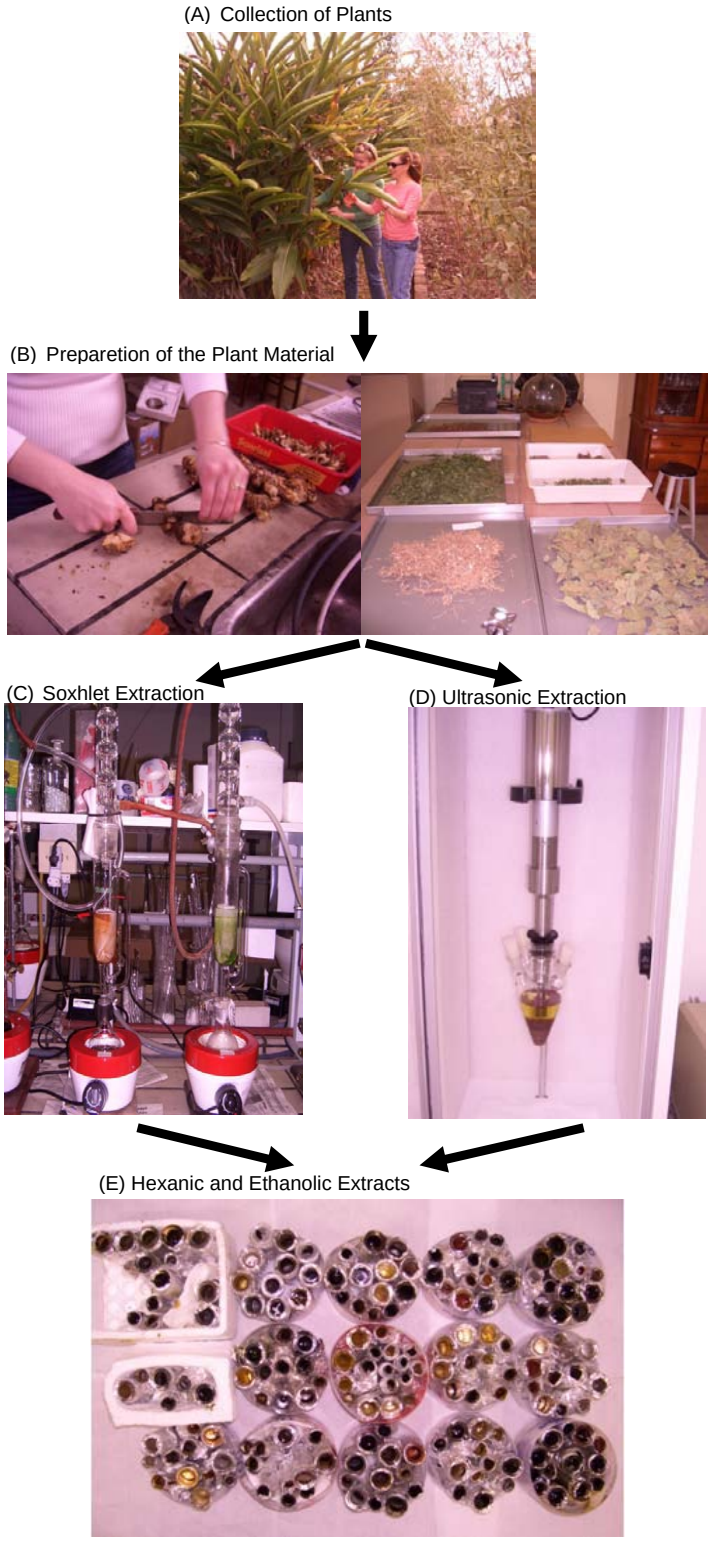

Figure 5.2: Plant extraction flow

5.6 Extraction and Isolation Methods

5.6.1 *Cordia americana*

The air-dried and powdered leaves (1140.94 g) of *Cordia americana* were exhaustively extracted with ethanol in a soxhlet apparatus. The resulting ethanolic extract was concentrated under vacuum at 40 °C and finally lyophilisated to yield 227.7 g of extract, that is, 19.90% of the original powdered leaves. The ethanolic extract was defatted resulting in 219.6 g.

The defatting process was carried out by dissolving the ethanolic extract of *Cordia americana* in methanol. This solution was left for 48 h in the refrigerator at -20 °C. After that, it was filtered, evaporated and lyophilisated.

In the next step, as shown in Figure 5.3, an amount of 6.0 g of the defatted ethanolic extract was diluted in 20 mL of methanol. This solution was subjected to column chromatography using Sephadex®LH-20 (see Section 5.4.2.1) and 100% methanol as mobile phase, with a flow rate of 1.0 mL/min. The fractions were collected in reaction tubes with 10 mL resulting in a total of 282 tubes. After TLC control with Method TLC-A (see Section 5.4.1.1) for detection, the tubes with a similar composition were combined and 16 fractions (A-P) were obtained, as shown in Figure 5.4. The yield of each fraction is shown in Table 5.12.

The fraction sets were investigated for the inhibition on p38α assay (see Section 5.7.1) in a concentration of 30 μg/mL. Additionally, HPLC analysis of the ethanolic extract in different wave lengths (see Figure 5.5) revealed the presence of a major peak and a few secondary peaks. Thus, the criteria to choose the fractions for further subfractionation was based on:

- inhibitory activity considering the results on p38α assay (bioguided investigation);
- major and secondary HPLC peaks;
- yields of fraction sets.

Therefore, the fractions E, F, G, H, I and K were further studied.

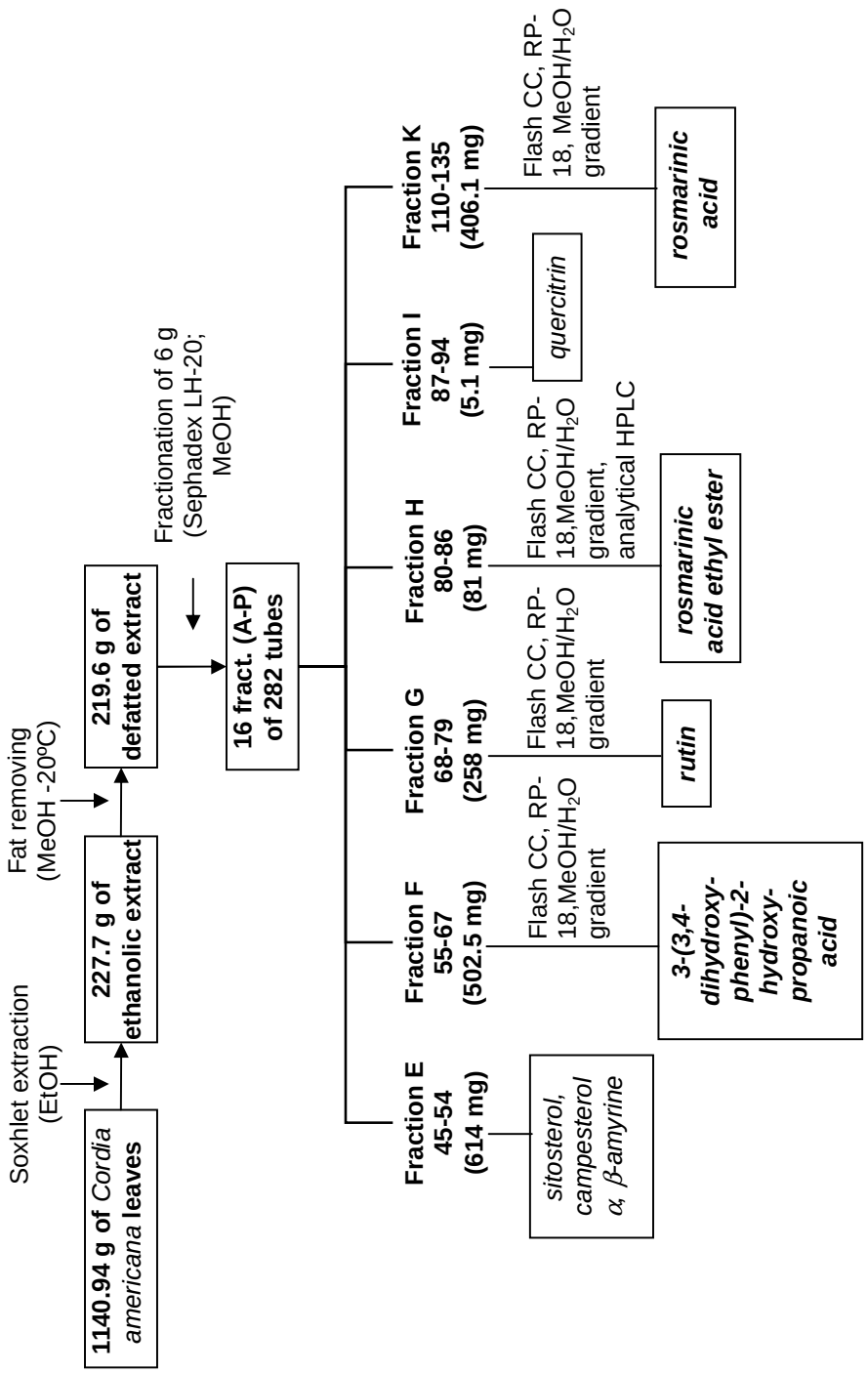

Figure 5.3: Extraction and isolation of compounds from the ethanolic extract of the leaves of *Cordia americana*. Cursive letters: compounds identified from the fractions; Bold letters: isolated compounds

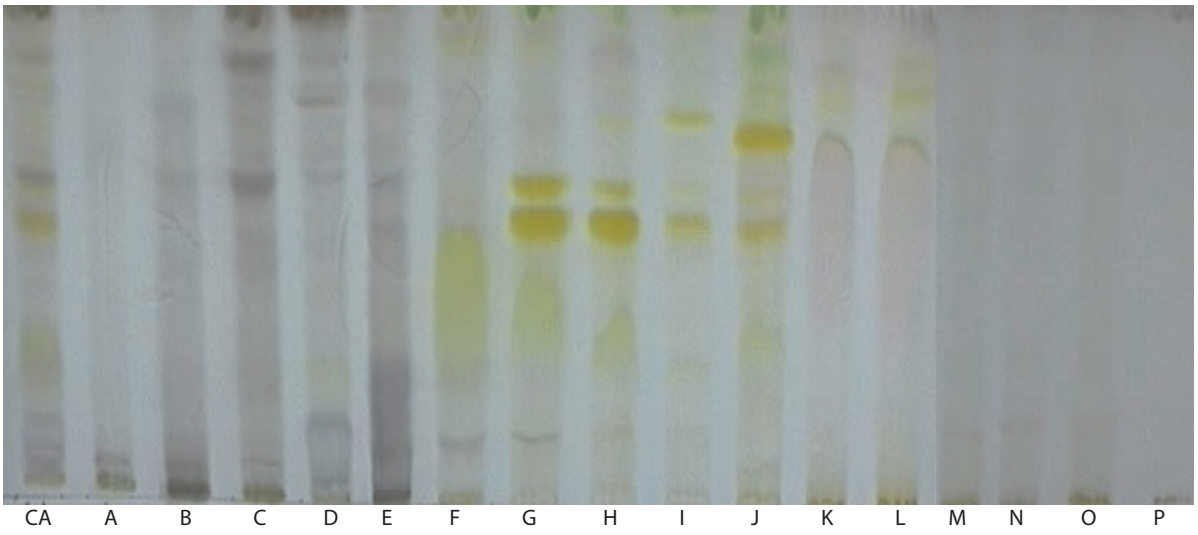

Figure 5.4: TLC of *Cordia americana* fractions (A-P) (Method TLC-A, see Section 5.4.1.1)

Table 5.12: p38α inhibition and yield of the fraction sets of *Cordia americana*

Fractions	**p38α inhibition (%) at 30 μg/mL**	**Yield (mg)**
A	76.17	72.5
B	77.93	188.6
C	87.13	590.6
D	89.15	866.2
E	82.23	614.0
F	90.11	502.5
G	93.78	258.0
H	95.59	81.0
I	95.10	5.1
J	79.96	207.70
K	89.47	406.1
L	87.53	458.7
M	65.61	127.0
N	65.16	119.1
O	41.76	98.6
P	29.12	12.3

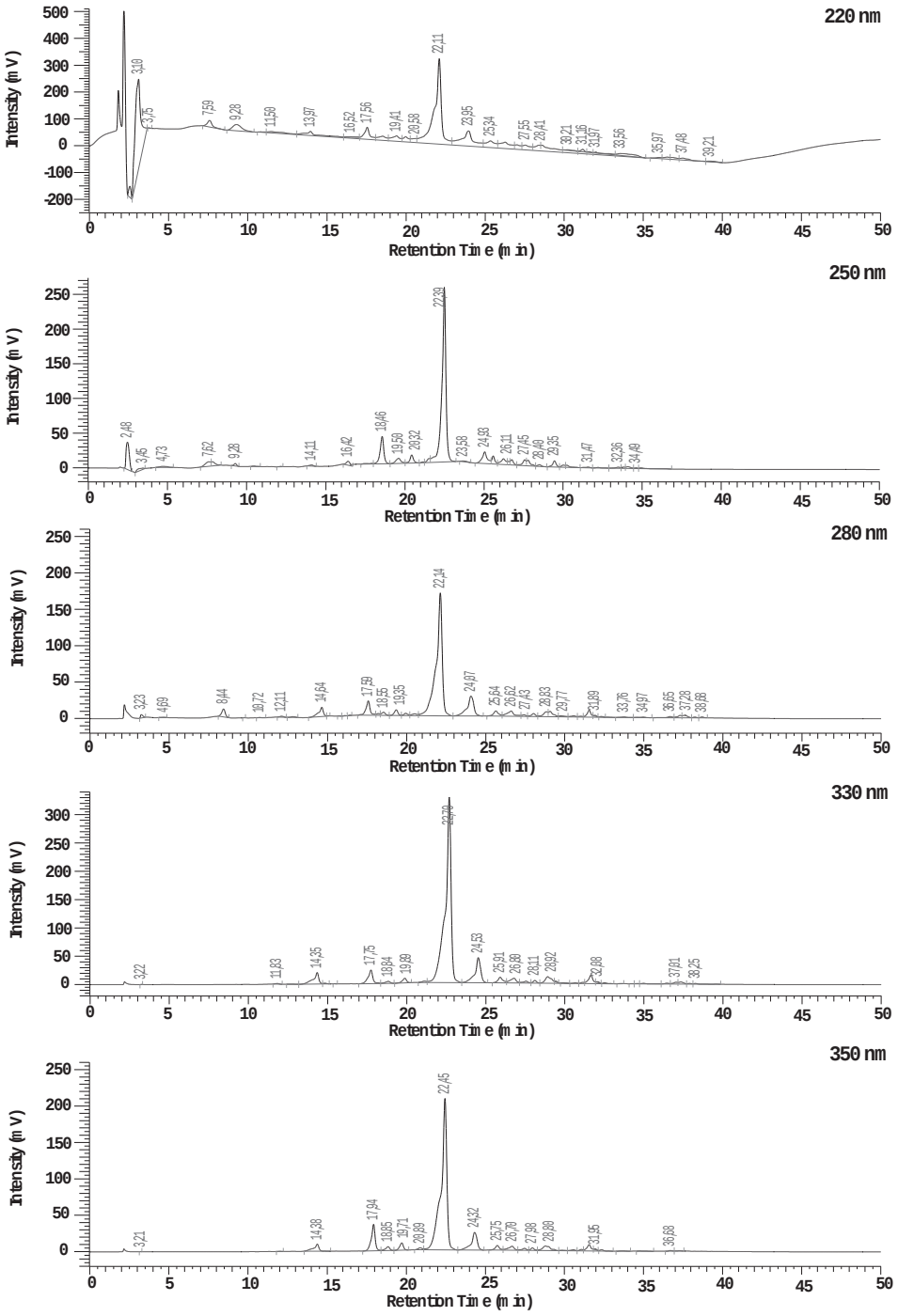

Figure 5.5: Representative analytical HPLC of the ethanolic extract of *Cordia americana* in different wave lengths (Method HPLC-A, see Section 5.4.4)

5.6.1.1 Isolation of Compounds

The following procedures were carried out in order to isolate the compounds from the plant extract:

- **Rosmarinic acid (CA1)**: Parts of the active fraction K (100 mg) were subfractionated by flash chromatography (Method FLASH-A, Section 5.4.3) over a RP-18 (25-40 μm) column using methanol-water as mobile phase with a linear gradient starting at 10% methanol to 100% within 50 min and a flow rate of 10 mL/min. This process provided 81 fractions, whereas 5 of them yielded the isolation of rosmarinic acid (12 mg) with a purity of 98.81%.

- **Rosmarinic acid ethyl ester (CA2)**: Separation of fraction H (81 mg) with methanol-water as eluate with a linear gradient starting at 10% methanol to 100% within 50 min (Method FLASH-A, Section 5.4.3) followed by a further purification in the analytical HPLC (Method HPLC-D, Section 5.4.4), which yielded the isolation of rosmarinic acid ethyl ester (3.3 mg) with a purity of 95.70%.

- **3-(3,4-dihydroxyphenyl)-2-hydroxypropanoic acid (CA3)**: Parts of fraction F (101 mg) were subfractionated by methanol-water as mobile phase with a linear gradient of 10% methanol to 100% within 80 min (Method FLASH-B, Section 5.4.3) and 5 mg of 3-(3,4-dihydroxyphenyl)-2-hydroxypropanoic acid (syn. danshensu) were obtained with a purity of 93.26%.

- **Rutin (CA4)**: Fraction G (120.04 mg) were subfractionated by methanol-water with a linear gradient from 10% methanol to 100% over 100 min (Method FLASH-C, Section 5.4.3) to provide rutin (15 mg) with a purity of 94.72%.

5.6.1.2 Characterization of the Compounds

The isolated as well as the identified compounds showed the following characteristic features:

- **Rosmarinic Acid (CA1)**
  - Molecular formula: $C_{18}H_{16}O_8$
  - Molecular mass: M = 360.08 g/mol
  - Retention factor (Method TLC-A): R_f = 0.63
  - Coloring (Method TLC-A): absorption at 254 nm; light blue at 366 nm; light gray after derivatisation with anisaldehyde-sulfuric reagent
  - Retention time (Method HPLC-A): t_R = 12.91 min
  - UV absorption maximum (in MeOH): see Section 3.1.1.2.5 (Results)
  - IR Spectroscopy: see Section 3.1.1.2.5 (Results)
  - MS data (ESI-MS, positive mode): m/z = 361.0 (39), 162.9 (100)
  - MS data (ESI-MS, negative mode): see Section 3.1.1.2.5 (Results)
  - High resolution FT-ICR-MS: see Section 3.1.1.2.5 (Results)
  - NMR data: see Section 3.1.1.2.5 (Results)
- **Rosmarinic Acid Ethyl Ester (CA2)**
  - Molecular formula: $C_{20}H_{20}O_8$
  - Molecular mass: M = 388.12 g/mol
  - Retention factor (Method TLC-A): R_f = 0.88
  - Coloring (Method TLC-A): absorption at 254 nm; light blue at 366 nm; light gray after derivatisation with anisaldehyde-sulfuric reagent
  - Retention time (Method HPLC-A): t_R = 15.68 min
  - MS data (ESI-MS, positive mode) (relative intensity %): m/z = 389.1 (19), 287.1 (10), 180.9 (35), 163.0 (100)
  - MS data (ESI-MS, negative mode): see Section 3.1.1.2.7 (Results)

- High resolution FT-ICR-MS: see Section 3.1.1.2.7 (Results)
- NMR data: see Section 3.1.1.2.7 (Results)

- **3-(3,4-dihydroxyphenyl)-2-hydroxypropanoic acid (CA3)**
  - Molecular formula: $C_9H_{10}O_5$
  - Molecular mass: M = 198.1 g/mol
  - Retention factor (Method TLC-A): R_f = 0.44
  - Coloring (Method TLC-A): no absorption at 254 nm; blue at 366 nm; beige after derivatisation with anisaldehyde-sulfuric reagent
  - Retention time (Method HPLC-A): t_R = 4.01 min
  - MS data (EI-MS): see Section 3.1.1.2.1 (Results)
  - NMR data: see Section 3.1.1.2.1 (Results)

- **Rutin (CA4)**
  - Molecular formula: $C_{27}H_{30}O_{16}$
  - Molecular mass: M = 610.15 g/mol
  - Retention factor (Method TLC-A): R_f = 0.54
  - Coloring (Method TLC-A): absorption at 254 nm; dark blue at 366 nm; yellow after derivatisation with anisaldehyde-sulfuric reagent
  - Retention time (Method HPLC-A): t_R = 10.93 min
  - UV absorption maximum (in MeOH): see Section 3.1.1.2.4 (Results)
  - IR Spectroscopy: see Section 3.1.1.2.4 (Results)
  - MS data (ESI-MS, positive mode): see Section 3.1.1.2.4 (Results)
  - MS data (ESI-MS, negative mode): m/z = 610.2 (41), 609.1 (100), 301.1 (10), 147.2 (5)

  - High resolution FT-ICR-MS: see Section 3.1.1.2.4 (Results)
  - NMR data: see Section 3.1.1.2.4 (Results)

- **Quercitrin (CA5)**
  - Molecular formula: $C_{21}H_{20}O_{11}$
  - Molecular mass: M = 448.10 g/mol
  - Retention factor (Method TLC-A): R_f = 0.60
  - Coloring (Method TLC-A): absorption at 254 nm; dark blue at 366 nm; orange after derivatisation with anisaldehyde-sulfuric acid reagent
  - Retention time (Method HPLC-A): t_R = 12.02 min
  - MS data (ESI-MS, positive mode): m/z = 471.0 (100), 488.8 (5), 303.2 (98), 173.1 (10)
  - MS data (ESI-MS, negative mode): see Section 3.1.1.2.5 (Results)

- **β-sitosterol (CA6)**
  - Molecular formula: $C_{29}H_{50}O_1$
  - Molecular mass: M = 414.38 g/mol
  - Retention time (Method GC-MS, see Section 5.4.7.1): t_R = 16.7 min
  - MS data (GC-MS): see Section 3.1.1.2.6 (Results)

- **Campesterol (CA7)**
  - Molecular formula: $C_{28}H_{48}O_1$
  - Molecular mass: M = 400.37 g/mol
  - Retention time (Method GC-MS, see Section 5.4.7.1): t_R = 34.8 min
  - Fragmentation mass (GC-MS): see Section 3.1.1.2.7 (Results)

- **α-amyrin (CA8)**

  - Molecular formula: $C_{30}H_{50}O_1$
  - Molecular mass: M = 426.38 g/mol
  - Retention time (Method GC-MS, see Section 5.4.7.1): t_R = 22.2 min
  - Fragmentation mass (GC-MS): see Section 3.1.1.2.8 (Results)

- **β-amyrin (CA9)**
  - Molecular formula: $C_{30}H_{50}O_1$
  - Molecular mass: M = 426.38 g/mol
  - Retention time (Method GC-MS, see Section 5.4.7.1): t_R = 18.7 min
  - Fragmentation mass (GC-MS): see Section 3.1.1.2.9 (Results)

5.6.1.3 Quanti cation Method

Mobile phase (A): water-acetonitrile-formic acid (90:10:0.1) and mobile phase (B): acetonitrile-formic acid (0.1%) with a linear gradient starting from 0% (B) and ending with 95%; flow rate 0.5 mL/min; injection volume 20 μL; detection wavelength 330 nm. This wavelength was choosen, because the compound shows here its UV maxima. All chromatographic operations were carried out at room temperature (RT). Within the concentration range of 1-100 μg/mL, the relationship between the peak area of rosmarinic acid was linear with a regression equation y = 59784.x-73460 (see Figure 5.6). The linearity of the calibration curve was verified by the correlation coefficient (r^2 = 0.9998). Each measurement was repeated three times. A concentration of 1.0 mg/mL of the ethanolic extract was used to calculate the amount of rosmarinic acid in the extract of *Cordia americana*.

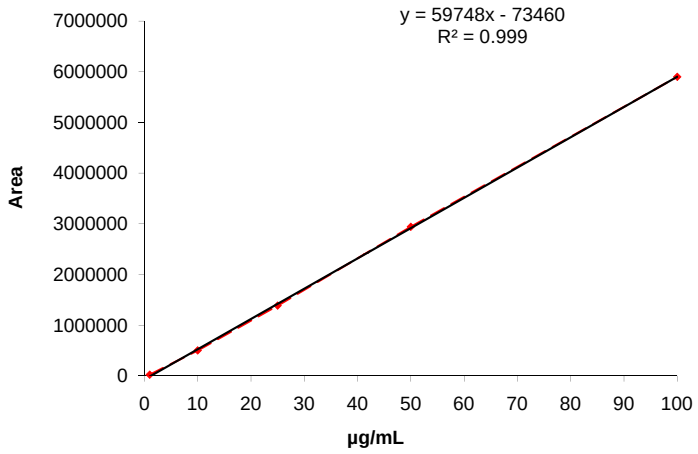

Figure 5.6: Calibration curve of rosmarinic acid

5.6.2 *Brugmansia suaveolens*

The air-dried and powdered leaves (1087.0 g) of *Brugmansia suaveolens* were exhaustively extracted with ethanol in a Soxhlet apparatus. The resulting EtOH extract was concentrated under vacuum at 40 °C and finally lyophilized to yield 359.94 g of extract, that is, 33.11% of the original powdered leaves. The plant extract was defatted affording 344.82 g.

The defatting process was carried out by dissolving the ethanolic extract of *Brugmansia suaveolens* in methanol. This solution was left for 48 h in the refrigerator at -20 °C. After that, it was filtered, evaporated and lyophilisated.

In the next step, as shown in Figure 5.7, an amount of 6.18 g of the defatted ethanolic extract was subjected to column chromatography using Sephadex®LH-20 and 100% methanol as mobile phase with a flow rate of 1.0 mL/min. A total of 300 tubes with 10 mL each were collected and controlled by TLC using silica gel with toluene-methanol-diethylamine (8:1:1) (i.e., Method TLC-B, Figure 5.8) and RP-18 with methanol-water (1:1) (i.e., Method TLC-C, Figure 5.9) and anisaldehyde-sulfuric for detection. The fractions with a similar profile were combined and yielded 11 fractions (A-K). The yield of each fraction is shown in Table 5.13. Furthermore, HPLC analysis of the ethanolic extract in different wave lenghts (see Figure 5.10) revealed the presence of four major

peaks and other secondary peaks. The criteria to choose the fractions for further subfractionation was the same as for the extract of *Cordia americana* (see Section 5.6.1). Thus, the fractions G, H and I from *Brugmansia suaveolens* were investigated.

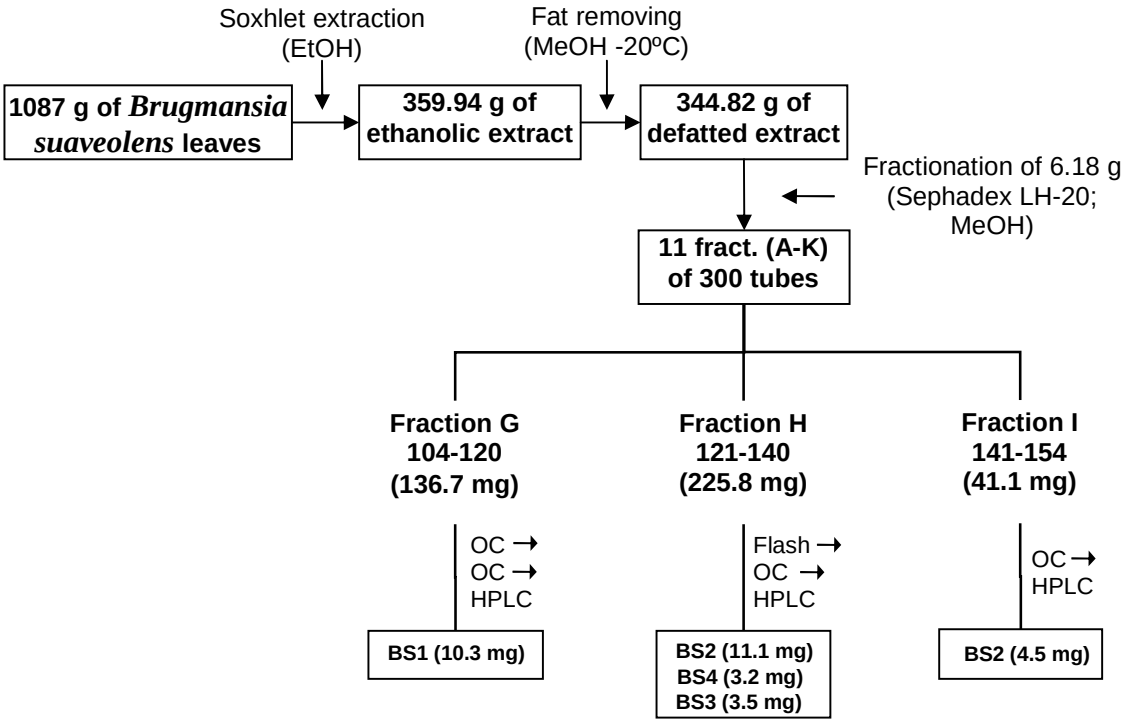

Figure 5.7: Extraction and isolation of compounds from the ethanolic extract of the leaves of *Brugmansia suaveolens*

Table 5.13: p38α inhibition and yield of the fraction sets of *Brugmansia suaveolens*

Fractions	**p38α inhibition (%) at 30 μg/mL**	**Yield (mg)**
A	46.71	127.1
B	47.39	268.8
C	54.85	459.7
D	38.33	697.7
E	50.49	1464.1
F	39.04	125.9
G	67.78	136.7
H	84.49	225.8
I	88.48	41.1
J	82.28	108.4
K	64.67	189.6

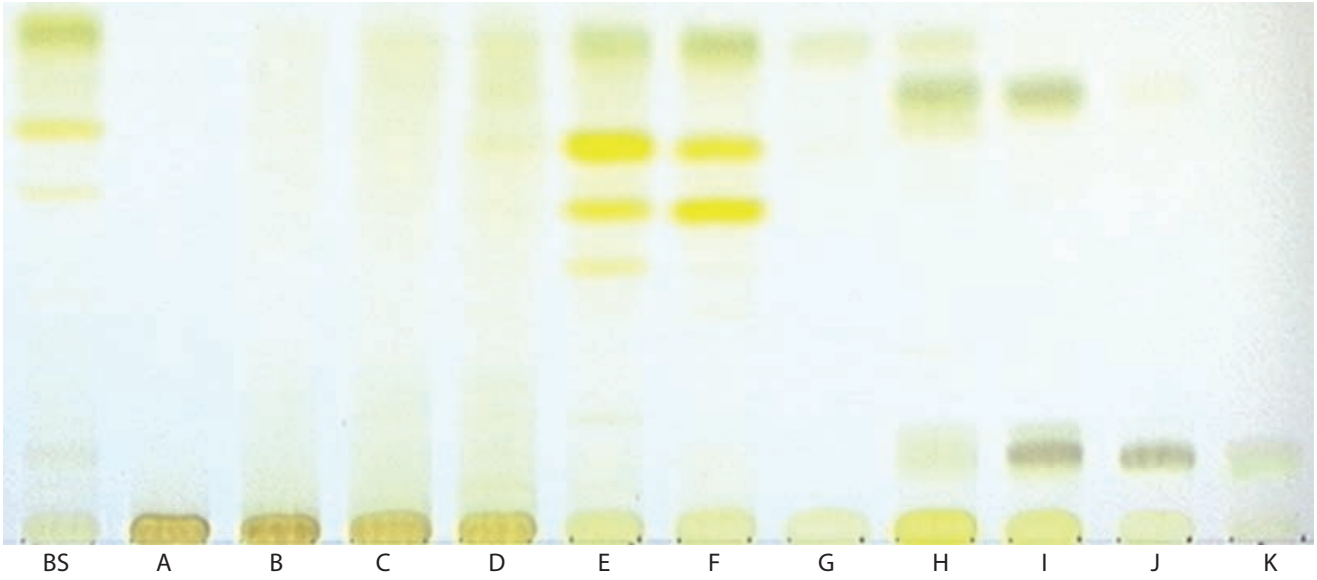

Figure 5.8: TLC of *Brugmansia suaveolens* fraction (A-K) (Method TLC-B, see Section 5.4.1.2)

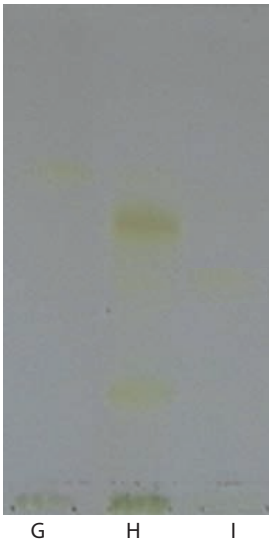

Figure 5.9: TLC of *Brugmansia suaveolens* fraction (G-I) (Method TLC-C, see Section 5.4.1.2)

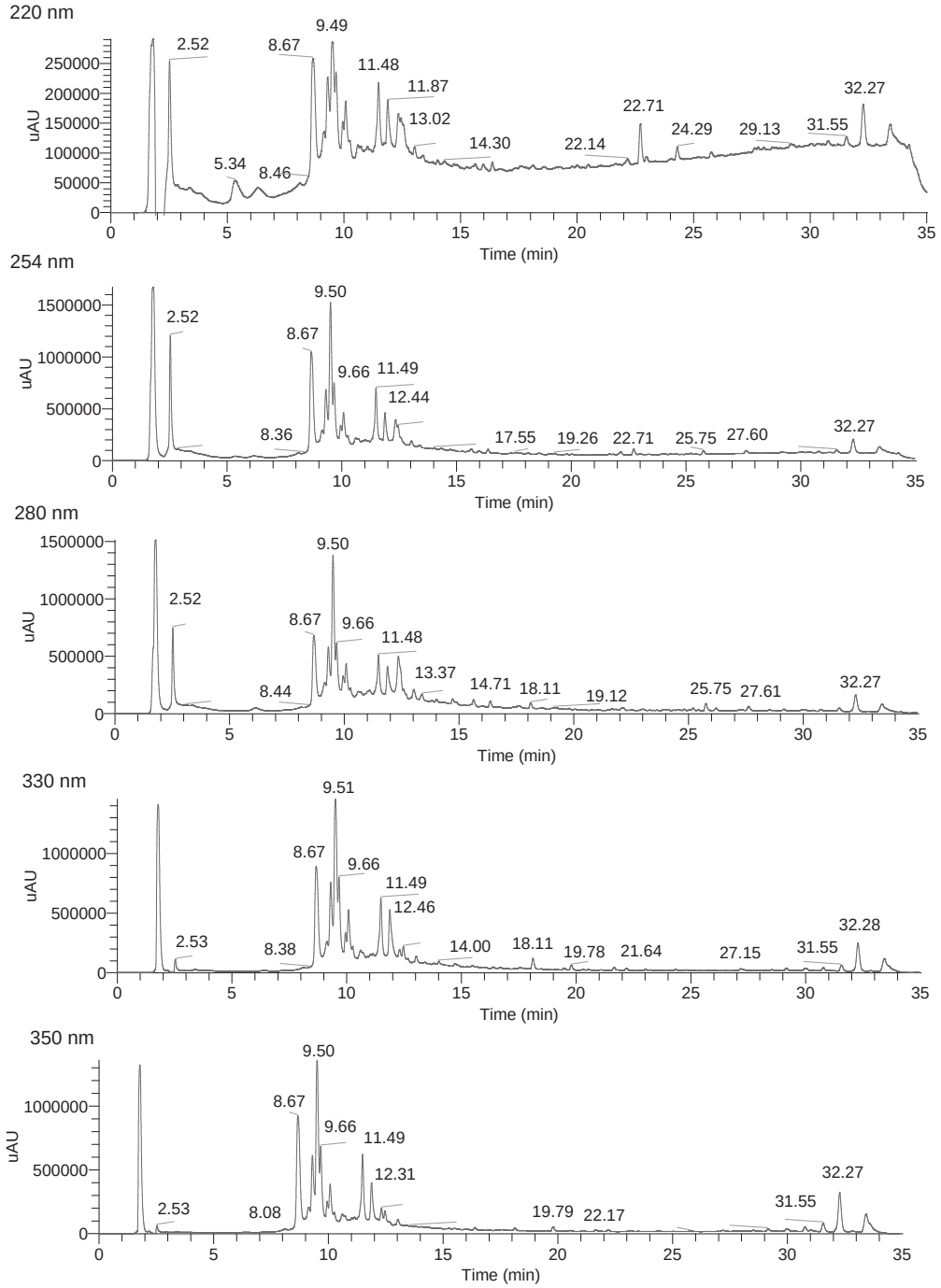

Figure 5.10: Representative HPLC chromatogram of the ethanolic extract of *Brugmansia suaveolens* in different wave lengths (Method LC-DAD)

5.6.2.1 Qualitative Analysis for Alkaloids

In order to examine the presence of alkaloids in the plant extract, the ethanolic extract, the fraction sets (A-K), and the alkaloids hyoscyamine and scopolamine were evaluated by means of TLC using the Method TLC-D (see Section 5.4.1, Experimental Part). Figure 5.11 shows that the aforementioned alkaloids cannot be detected in the ethanolic extract as well as in the fraction sets.

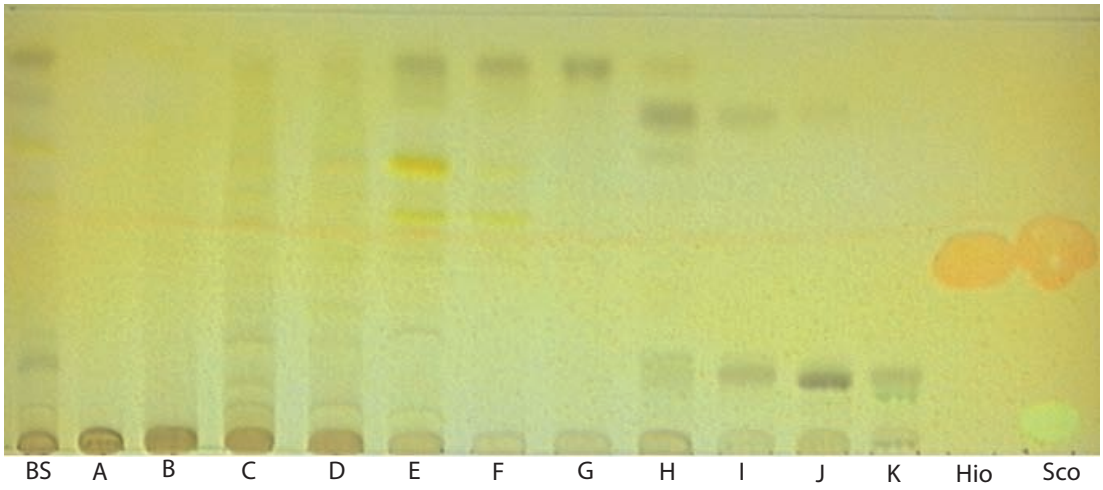

Figure 5.11: TLC analysis for alkaloids in the ethanolic extract of *Brugmansia suaveolens* (Method TLC-D)

5.6.2.2 Isolation of Compounds

The following procedures were carried out in order to isolate the compounds from the plant extract:

- **BS1**: Part of fraction G (80 mg) was subfractionated by open column chromatography (OC) using methanol:water (1:1) as eluent (Method OC-A, Section 5.4.2.2). A subfraction set was again fractionated by OC with methanol:water (1:2) (Method OC-B, Section 5.4.2.2) and then applied to HPLC (Method HPLC-C, Section 5.4.4) affording 10.3 mg of compound BS1 with a purity of 91.2%.
- **BS2**: Fraction I (41.1 mg) was subfractionated by OC using methanol:water (1:1) as eluent (Method OC-A, Section 5.4.2.2) and subsequently separated by HPLC resulting in 4.5 mg

of compound BS2 (Method HPLC-C, Section 5.4.4). Parts of fraction H (100 mg) were subfractionated by flash chromatography with methanol:water as mobile phase with a linear gradient starting from 10% methanol to 100% within 60 minutes (Method FLASH-D, Section 5.4.3). A subfraction set (25.2 mg) was applied to HPLC (Method HPLC-C, Section 5.4.4) affording 11.1 mg of compound BS2 with a purity of 93.2%.

- **BS3**: From the aforementioned fraction H, the subfraction (35.2 mg) was applied to HPLC affording 3.5 mg (Method HPLC-C, Section 5.4.4) of compound BS3 with a purity of 91.0%.

- **BS4**: Additionally from the fraction H (100 mg) one subfraction (47.8 mg) was further separated by OC using methanol:water (1:1) as mobile phase (Method OC-A, Section 5.4.2.2) yielding 3.2 mg of compound BS4 with a purity of 90.1%.

5.6.2.3 Characterization of the Compounds

The elucidated compounds from *Brugmansia suaveolens* had the following characteristic features:

- **BS1**
  - Molecular formula: $C_{26}H_{28}O_{15}$
  - Molecular mass: M = 742.2 g/mol
  - Retention factor (Method-TLC-C): R_f = 0.65
  - Coloring (Method-TLC-C): absorption at 254 nm; dark blue at 366 nm; yellow after derivatisation with anisaldehyde-sulfuric reagent
  - Retention time (Method-HPLC-B): t_R = 7.21 min
  - UV absorption maximum (in MeOH): see Section 3.1.2.2.2 (Results)
  - IR Spectroscopy: see Section 3.1.2.2.2 (Results)
  - MS data (ESI-MS, positive mode): see Section 3.1.2.2.2 (Results)

- MS data (ESI-MS, negative mode): m/z = 742.2 (51), 741.0 (100), 579.1 (19), 446.1 (8), 283.4 (5)
- High resolution FT-ICR-MS: see Section 3.1.2.2.2 (Results)
- NMR data: see Section 3.1.2.2.2 (Results)

- **BS2**
  - Molecular formula: $C_{41}H_{44}O_{23}$
  - Molecular mass: M = 904.2 g/mol
  - Retention factor (Method-TLC-C): R_f = 0.61
  - Coloring (Method-TLC-C): absorption at 254 nm; dark blue at 366 nm; yellow after derivatisation with anisaldehyde-sulfuric reagent
  - Retention time (Method-HPLC-B): t_R = 9.61 min
  - UV absorption maximum (in MeOH): see Section 3.1.2.2.3 (Results)
  - IR Spectroscopy: see Section 3.1.2.2.3 (Results)
  - MS data (ESI-MS, positive mode): see Section 3.1.2.2.3 (Results)
  - MS data (ESI-MS, negative mode): m/z = 904.1 (40), 903.1 (100), 741.1 (31), 579.1 (3), 447.1 (2), 284.0 (2)
  - High resolution FT-ICR-MS: see Section 3.1.2.2.3 (Results)
  - NMR data: see Section 3.1.2.2.3 (Results)

- **BS3**
  - Molecular formula: $C_{41}H_{44}O_{23}$
  - Molecular mass: M = 904.2 g/mol
  - Retention factor (Method-TLC-C): R_f = 0.51

- Coloring (Method-TLC-C): absorption at 254 nm; dark blue at 366 nm; yellow after derivatisation with anisaldehyde-sulfuric reagent
- Retention time (Method-HPLC-B): t_R = 10.21 min
- UV absorption maximum (in MeOH): see Section 3.1.2.2.4 (Results)
- IR Spectroscopy: see Section 3.1.2.2.4 (Results)
- MS data (ESI-MS, positive mode): see Section 3.1.2.2.4 (Results)
- MS data (ESI-MS, negative mode): m/z = 904.2 (41), 903.1 (100), 741.1 (32), 579.0 (3), 287.1 (2)
- High resolution FT-ICR-MS: see Section 3.1.2.2.4 (Results)
- NMR data: see Section 3.1.2.2.4 (Results)

• **BS4**

- Molecular formula: $C_{26}H_{28}O_{15}$
- Molecular mass: M = 580.14 g/mol
- Retention factor (Method-TLC-C): R_f = 0.40
- Coloring (Method-TLC-C): absorption at 254 nm; dark blue at 366 nm; orange after derivatisation with anisaldehyde-sulfuric reagent
- Retention time (Method-HPLC-B): t_R = 17.91 min
- UV absorption maximum (in MeOH): see Section 3.1.2.2.1 (Results)
- IR Spectroscopy: see Section 3.1.2.2.1 (Results)
- MS data (ESI-MS, positive mode): see Section 3.1.2.2.1 (Results)
- MS data (ESI-MS, negative mode): m/z = 580.3 (25), 579.2 (100), 285.1 (3)
- High resolution FT-ICR-MS: see Section 3.1.2.2.1 (Results)
- NMR data: see Section 3.1.2.2.1 (Results)

5.7 Biological Assays

In order to characterize the anti-inflammatory activity and the wound healing properties of the ethanolic extracts of *Cordia americana* and *Brugmansia suaveolens* and their isolated compounds, the following bioassays were carried out.

5.7.1 p38α MAPK Assay

This assay evaluates the inhibitory effect of a potential p38α inhibitor using the phosphorylation of the kinase substrate ATF-2. Its amount reflects the enzyme activity. The assay was developed by Forrer *et al.*, (1998) [95] and further optimized in the department by Greim and Thuma [179].

The ethanolic extracts as well as the isolated compounds were tested according to the *in vitro* enzyme-linked immunossorbent assay, described in Laufer *et al.*, (2005) [179]. The concentration, used in the test were 100, 10, 1 and 0.1 μM for the natural compounds and 100, 10, 1 and 0.1 μg/mL for the plant extracts. The ethanolic extracts as well as the isolated compounds were tested three times. The ATP concentration in this assay was 100 μM. There are two antibodies in this assay: the primary antibody (phospho-ATF-2(Thr69/71)-antibody) that detects dual phosphorylated ATF-2 at (Thr69/71) and acts as antigen for the second AP-conjugated secondary antibody (anti-rabbit IgG-AP-Antibody) that dephosphorylates 4-nitrophenylphosphate in order to allow the 4-nitrophenyl to be detected photometrically at a wavelength of 405 nm. This ELISA-based p38α assay consists of the following steps (see Figure 5.12):

1. Coating the wells of the microtiter plates with the kinase substrate ATF-2 and than incubation for 90 min in 37 °C;

2. Blocking of the free binding sites with blocking buffer which includes TBS (Tris Buffered Saline), BSA, sodium azide and tween 20;

3. Addition of kinase reaction mixture which contains ATP as co-substrate, different phosphatase inhibitors, p38α and the test compounds. In the incubation period (1 h), ATP and

the test compounds compete for the binding pocket of the p38α. If ATP binds in the binding pocket, than phosphorylation of ATF-2 occurs in the amino acids Thr69/71, however, if the potential inhibitor binds in the ATP-binding pocket, then the phosphorylation of ATF-2 is inhibited.

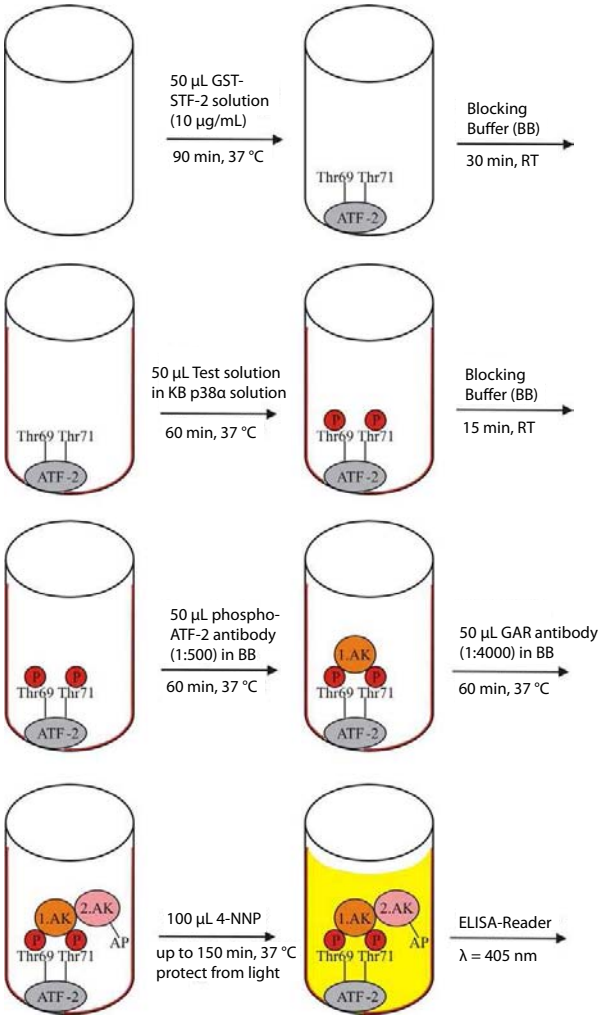

Figure 5.12: Scheme of the p38α assay [161]

4. Addition of primary antibody (phospho-ATF-2(Thr69/71)-antibody) which recognizes specific double phosphorylated ATF-2 and binds to the substrate.

5. Addition of the secondary antibody (anti-rabbit IgG-AP-antibody) conjugated with alkaline phosphatase. This antibody binds specific to the primary antibody.

6. Finally, 4-nitrophenylphosphate (4-NPP) is added, which is dephosphorylated by the second antibody bound to the alkaline phosphatase. The chromophore 4-nitrophenyl can be detected and quantified by a microplate reader at a wavelength of 405 nm.

In addition, stimulation controls and non-specific binding (NSB) were also tested in the polystyrene plate. The stimulation control contained only ATP and activated p38α without inhibitor. After the addition of the antibodies and the 4-NPP, the value of the maximum of phosphorylation can be determined. In order to obtain the value of NSB, the kinase buffer without p38α and inhibitor was used. If there was no kinase in these wells, it means that no phosphorylation of ATF-2 has occurred and, therefore, no color can be observed. For the evaluation of the inhibition rate, the NSB value is subtracted from all samples and also from the stimulation control.

The relative inhibition is calculated by the following equation:

$$RelativeInhibition[\%] = 100 - \frac{OD_{Comp}}{OD_{Stim}} * 100 \tag{5.1}$$

OD_{Comp}: Mean of the optical density in 3 wells of the corresponding compounds.

OD_{Stim}: Mean of the optical density in the non-inhibited stimulation controls.

Subsequently, the IC_{50} values were determined. The IC_{50} value is defined as the inhibitory concentration by which 50% of the enzyme activity is inhibited. It can be graphically constructed by interpolation of the semi-logarithmic plot of the inhibition [%] on the inhibitor concentration [log c]. The straight line joining points intersect the 50% inhibition in the IC_{50} value corresponding to the concentration.

On each plate, the reference compound SB203580 (see Figure 5.13) was also tested in the concentration of 10, 1, 0.1 and 0.01 μM.

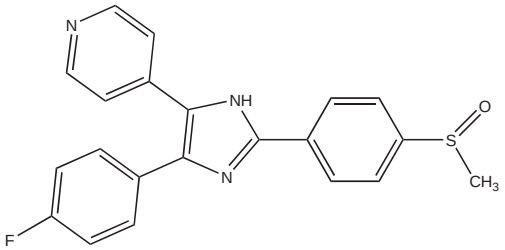

Figure 5.13: p38α reference compound SB203580

5.7.2 JNK3 MAPK Assay

A non radioactive immunosorbent assay was used for the measurement of the inhibition of the plant extracts and their isolated compounds on JNK3. The JNK3 assay is similar to the p38α (Section 5.7.1), except for the concentration of ATP, which is 1 μM and the incubation time that is reduced to 45 minutes. The reference compound, used in the test, was SP600125 (see Figure 5.14) in the concentration of 10, 1, 0.1 and 0.01 μM. The isolated compounds were tested in a concentration 100, 10, 1 and 0.1 μM, and in addition, the ethanolic extract in a concentration of 0.1, 1, 10 and 100 μg/mL. The experiments were carried out three times.

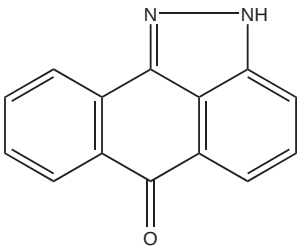

Figure 5.14: JNK3 reference compound SP600125

5.7.3 TNFα Release Assay

The ethanolic extract and isolated compounds from *Cordia americana* were tested in human whole blood assay, in order to evaluate the inhibition of TNFα release. In the whole blood assay, some factors such as solubility, plasma protein binding, and penetration of the compounds play a essential role. Therefore, some compounds which had good inhibition values in the kinase assays, could be less effectively in the whole blood assay. In this test system, the TNFα concentration is indirectly determined by an ELISA test, in which the whole blood is stimulated by a LPS [98].

The inhibitors are first dissolved in Cremophor®-EL/ethanol in a concentration of 10 mM for the isolated compounds and 100 μg/mL for the plant extract. From the stock solution, the first two dilutions are produced with DPBS-Gentamicin and subsequent dilutions are done with 1% Cremophor®-EL/ethanol. The isolated compounds and the plant extract were tested in concentrations of 100, 10, 1 and 0.1 μM and 100, 10, 1 and 0.1 μg/mL, respectively. For the reference compound SB203580 (see Figure 5.13), the concentration was 10, 1, 0.1 and 0.01 μM. Each test compound was tested twice, with blood of two different donors. Samples and reference compounds were diluted again with blood and lipopolysaccharide (LPS) (see Figure 5.15).

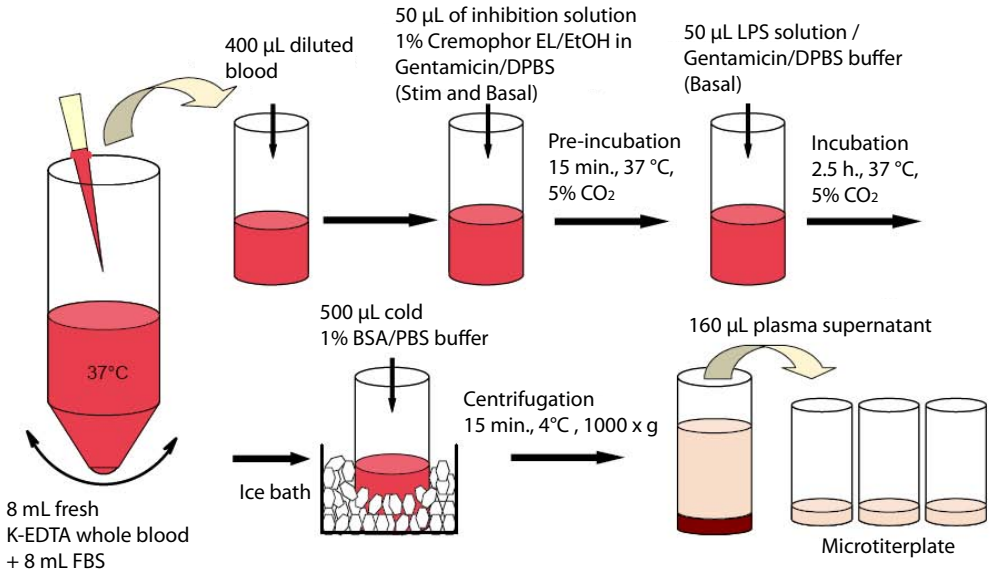

Figure 5.15: Stimulation of cytokine release by human whole blood diluted 1:2 in LPS [188]

The blood is initially 1:1 diluted with fetal bovine serum (FBS) followed by the incubation with the test compounds for 15 min in the CO_2 cabinet (37 °C, 5% CO_2 saturation, 100% of humidity). Then, by adding LPS, the cytokine release is stimulated and the solution is incubated again (2.5 hours, 5% of CO_2 saturation, 100% of humidity). After incubation, the reaction is stopped by adding a 1% ice-cold BSA (bovine serum albumin) buffer. The cellular components are centrifugated. The concentration of the proinflammatory TNFα is determined from the supernatant (plasma) by ELISA (Figure 5.16).

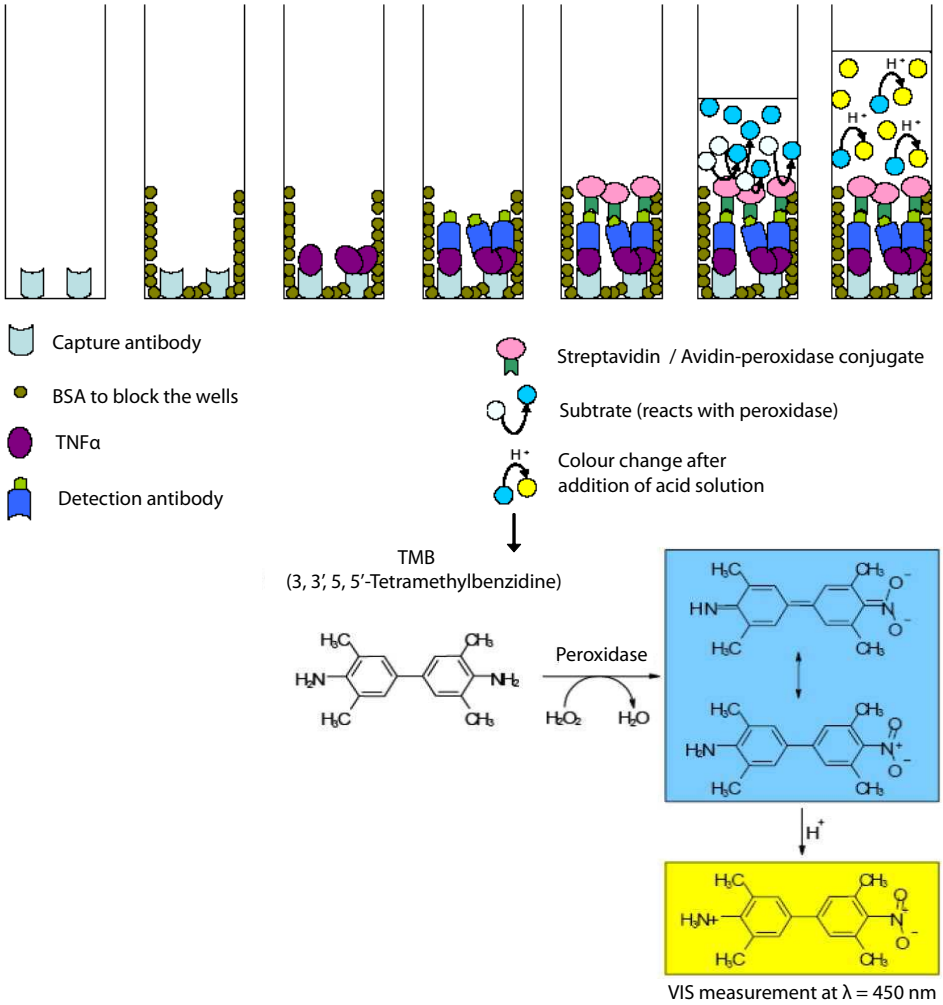

Figure 5.16: Scheme of the Cytokine-ELISA assay for the determination of TNFα release [161]

For the ELISA, the supernatant is diluted with a special diluent (TNFα Diluent, Beckman Coulter). The plate is first coated with the primary antibody (capture antibody; TNFα: murine-human

antibody) and the free binding sites are blocked with BSA. 100 μL of plasma are added to a standard series of TNFα and incubated for 2 hours at RT. During this time, the cytokines bind to the primary antibody. Subsequently, the addition of the second antibody occurs (detection antibody; biotinylated anti-human TNFα antibody) and is incubated for two hours again. An enzym-reagent is added consisting of streptavidin (TNFα-Merrettich-Peroxidase-Conjugated). Streptavidin binds to the biotin rest of the second antibody. After addition of the substrate solution of 3,3 ,5,5 - tetramethylbenzidine (TMB) and hydrogen peroxide, a blue color is formed by the oxidation of one of the two amino groups of TMB. After 30 minutes, the enzyme reaction is stopped with 1 M sulfuric acid. This leads to a protonation of the remaining amino group and to a bathochromic shift indicating by a yellow color. The detection is carried out by an ELISA reader at 450 nm.

The inhibition rate of the cytokine release is calculated using the following equation:

$$RelativeInhibition[\%] = 100 - \frac{C_{Comp} - C_{Basal}}{C_{Stim} - C_{Basal}} * 100 \tag{5.2}$$

C_{Comp}: concentration of cytokines in wells with test compound.

C_{Basal}: concentration of cytokines in wells with test compound and without LPS.

C_{Stim}: mean of the cytokine concentration in the stimulation control.

5.7.4 5-Lipoxygenase Assay

5.7.4.1 Determination of 5-LO Product Formation in Cell-free Assays

Escherichia coli (*E.coli*) MV1190 was transformed with pT3-5-LO plasmid and recombinant 5-LO protein was expressed as described in [94]. In brief, *E.coli* was harvested and lysed by incubation in 50 mM triethanolamine/HCl, pH = 8.0, 5 mM EDTA, soybean trypsin inhibitor (60 μg/mL), 1 mM phenylmethylsulphonyl fluoride and lysozyme (500 μg/mL), homogenized by sonication (3 x 15 sec) and centrifuged at 19,000 x g for 15 min. Proteins including 5-LO were precipitated with 50% saturated ammonium sulfate during stirring on ice for 60 min. The precipitate was collected by centrifugation at 16,000 x g for 25 min and the pellet was resuspended in 20 mL PBS containing 1 mM EDTA and 1 mM PMSF. After centrifugation at 100,000 x g for 70 min at 4 °C, the 100,000 x g supernatant was applied to an ATP-agarose column (Sigma A2767), and the column was eluted as described previously [94].

For activity assays, partially purified 5-LO was resuspended in 1 mL PBS, pH = 7.4 containing 1 mM EDTA, and 1 mM ATP was added. Samples were preincubated with the test compounds for 10 min at 4 °C, prewarmed for 30 s at 37 °C, and then 2 mM $CaCl_2$ and 20 μM arachidonic acid were added to start 5-LO product formation. The reaction was stopped after 10 min at 37 °C by addition of 1 mL ice cold methanol and the formed metabolites were analyzed by HPLC as described [331].

5-LO products include LTB_4 isomers and 5(S)-hydro(pero)xy-6-trans-8,11,14-cis-eicosatetraenoic acid (5-H(p)ETE). The ethanolic extract of *Cordia americana* was tested at concentration of 10, 3, 1 and 0.1 μg/mL and its compounds at 10, 3, 1 and 0.1 μM. The ethanolic extract of *Brugmansia suaveolens* was determined at concentrations of 3 and 30 μg/mL and its compounds at 3 and 30 μM for at least two experiments. Finally, the reference compound BWA4C (see Figure 5.17) was also tested at a concentration of 3 μM.

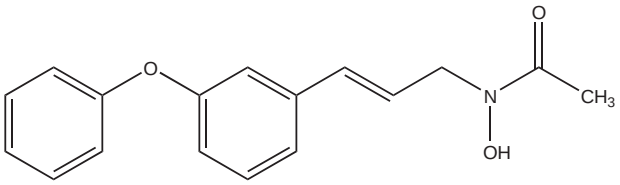

Figure 5.17: 5-LO reference compound BWA4C

5.7.4.2 Isolation of Human PMNL from Venous Blood

Human PMNL (polymorphonuclear leukocytes) were freshly isolated from buffy coats obtained from the Blood Center of the University Hospital Tübingen (Germany). In brief, venous blood from healthy donors was taken and leukocyte concentrates were prepared by centrifugation at 4,000 g for 20 min at RT. Buffy coats were diluted 1:1 (V:V) with phosphate buffered saline pH = 7.4 (PBS) and then with ice-cold 5% dextran (w/v in PBS) in a ratio of 4:5 (V:V), for 45 min. After dextran sedimentation, neutrophils were immediately isolated by centrifugation at 1,000 g, 10 min, RT (Heraeus sepatech, Varifuge 3.0, Hanau , Germany) on Nycoprep cushions, and hypotonic lysis of erythrocytes as described [331]. PMNL (106 cells/mL; purity $>$ 96-97%) were finally resuspended in PBS plus 1 mg/mL glucose (PG buffer) or in PG buffer plus 1 mM $CaCl_2$ (PGC buffer) as indicated.

5.7.4.3 Determination of 5-LO Product Formation in Cell-based Assays Using Isolated Human PMNL

For determination of cellular 5-LO product formation, 5 x 10^6 freshly isolated PMNL in 1 mL PGC buffer with or without bovine serum albumin (BSA) was pre-incubated with test compounds or with vehicle (DMSO) for 10 min at 37 °C, as indicated. 5-LO product formation was started by addition of A23187 (2.5 μM) with or without 20 μM AA. The reaction was stopped after 10 min with 1 mL of methanol and then 30 μL of 1 N HCl, 200 ng PGB1 and 500 μL of PBS were added. Formed 5-lipoxygenase metabolites were extracted and analyzed by HPLC as described [329]. 5-Lipoxygenase product formation includes leukotriene B4 and its all-trans isomers and

5(S)- H(P)ETE. Cysteinyl leukotrienes C4, D4 and E4 were not detected, and oxidation products of leukotriene B4 were not determined. The ethanolic extract of *Cordia americana* was tested based at the concentrations of 0.1, 0.3, 1, 3, 10 and 30 μg/mL and CA2 at 1, 3 an 10 μM for at least two experiments.

5.7.5 NF-κB Electrophoretic Mobility Shift Assay (EMSA)

Jurkat T cells were maintained in RPMI 1640 medium, supplemented with 10% fetal calf serum, 100 IU/mL penicillin and 100 g/mL streptomycin (all Gibco-BRL, Groningen, Netherlands).

Total cell extracts from Jurkat T cells were prepared as previously described [159]. In contrast to the previous study, NF-κB oligonucleotide (Promega) was labeled using [γ^{-33}P] dATP (3000 Ci/mmol; Amersham) and a T4 nucleotide kinase (New England Biolabs). The ethanolic extract was tested at the concentrations of 10, 30 and 50 μg/mL and rosmarinic acid of 10, 30, 54 μM, for at least two experiments.

5.7.6 Fibroblast Scratch Assay

Scratch assay was performed, as previously described [100]. In detail: Swiss 3T3 albino mouse fibroblasts were cultured in Dulbecco s modified Eagle s medium (DMEM), supplemented with 10% fetal calf serum, 100 IU/mL penicillin and 100 g/mL streptomycin and maintained at 37 °C in a humidified, 5% CO_2 environment (all Gibco-BRL, Groningen, Netherlands).

Swiss 3T3 albino mouse fibroblasts were grown in a confluent cell monolayer on coverslips into 24-well plates. The coverslips were precoated with collagen type I (40 μg/mL) for 2 h at 37 °C, before seeding the cells. Then the cells were cultured to nearly confluent monolayers and thereafter a linear wound was generated in the monolayer with a sterile 100 μL plastic pipette tip. The medium was changed in order to remove scraped cells. DMEM medium with dimethyl sulfoxid (0.25%), platelet derived growth factor (2 ng/mL), ethanolic extract (1, 50 and 100 μg/mL) and rosmarinic acid (1, 5, 10 μg/mL) were added to a set of 3 coverslips per dose and incubated for

12 h at 37 °C with 5% CO_2. The cells were fixed with 4% paraformaldehyde for 15 minutes and stained with 4 ,6-diamino-2-phenylindole (DAPI) overnight. Three representative images from each coverslip of the scratched areas under each condition were photographed to estimate the relative migration and proliferation of the cells. The effect of 1, 50 and 100 μg/mL of ethanolic extract of *Cordia americana*, and 1, 5 and 10 μg/mL of CA1, were assayed on fibroblast scratched monolayers. The experiments were carried out in triplicate.

5.7.7 MTT Assay

The cytotoxic activity was studied using the MTT colorimetric assay as previously described by [216]. For all samples and controls, 4 mL of a suspension of Jurkat cells (2.5 x 10^5 cells/mL) were used. The ethanolic extract (10 mg/mL DMSO) were tested in independent assays at concentrations of 50 and 100 μg/mL. Parthenolide (100 μM) was used as positive control and DMSO 1% (V:V) as negative control. All plates were incubated at 37 °C, 5% CO_2, during 24 hours. After incubation, 1.5 mL of MTT (0.5% in sterile PBS) was added to each plate, followed by additional 2 hours incubation in 5% CO_2 at 37 °C. The volume of each plate was transferred to tubes and centrifugated at 5,000 rpm for 10 min at 4 °C. The supernatant was discarded and the cells were resuspended with 1 mL of extraction solution buffer (20% SDS, 50% DMF). After overnight incubation (5% CO_2 at 37 °C), the absorbance of each sample and controls was measured at λ = 595 nm and the percentual of inhibition was calculated. Jurkat cells were treated for 24 h at a concentration of 50 and 100 μg/mL of the ethanolic extract of *Cordia americana*.

5.8 Computer Program

The following programs and databases have been used during the execution of the present work: ChemDraw Ultra 8, Scifinder Scholar 2007, ACDLabs 5.07, LaFlash System 1.1.

5.9 Statistical Analysis

Statistical evaluation was carried out with Origin Scientific Graphing and Analysis Software, and Microsoft Office Excel 2007.

5.10 Docking

The molecular modeling studies, that is, the visualization and building of the 3D-structures of the ligands were done with Maestro (version 8.5) from Schrödinger [280]. Docking studies were performed with Induced Fit docking protocol from Schrödinger [281]. The figures which showed the different docking positions to the ATP binding site were prepared with PyMol [77].

Bibliography

[1] Abadleh, M. M. M., 2009. Diarylisoxazoles as lead for the design and synthesis of protein kinase inhibitors. Ph.D. thesis, University of Tübingen.

[2] Abdallah, O. M., Kamel, M. S., Mohamed, M. H., 1994. Phenylpropanoid glycosides for *Prunus ssiori*. Phytochemistry 37, 1689–1692.

[3] Abou-Donia, A. H., Toaima, S. M., Hammoda, H. M., Shawky, E., 2006. Determination of rutin in *Amaryllis belladonna* L. flowers by HPTLC and spectrophotometry. Chromatographia 64, 109–112.

[4] Afzal, M., Obuekwe, C., Shuaib, N., Barakat, H., 2004. Photosynthetic pigment profile of *Cordia myxa* L. and its potential in folklore medicinal application. Food, Agriculture & Environment 2, 114–120.

[5] Agnihotri, V. K., Srivastava, S. D., Srivastava, S. K., Pitre, S., Rusia, K., 1987. Constiuents of *Cordia obliqua* as potential anti-inflammatory agents. Indian Journal of Pharmaceutical Sciencies 49, 66–69.

[6] Akhtar, A. H., Ahmad, K. U., 1995. Anti-ulcerogenic evaluation of the methanolic extracts of some indigenous medicinal plants of Pakistan in aspirin-ulcerated rats. Journal of Ethnopharmacology 46, 1–6.

[7] Al-Awadi, F. M., Srikumar, T. S., Anim, J. T., Khan, I., 2001. Antiinflammatory effects of *Cordia myxa* fruit on experimentally induced colitis in rats. Nutrition 17, 391–396.

[8] Albert, D., Zndorf, I., Dingermann, T., Mller, W. E., Steinhilber, D., Werz, O., 2002. Hyperforin is a dual inhibitor of cyclooxygenase-1 and 5-lipoxygenase. Biochemical Pharmacology 64, 1767–1775.

[9] Allard, J. B., Brock, T. G., 2005. Structural organization of the regulatory domain of human 5-lipoxygenase. Current Protein and Peptide Science 6, 125–131.

[10] Alves, M. N., Sartoratto, A., Trigo, J. R., 2007. Scopolamine in *Brugmansia suaveolens* (Solanaceae): Defense, allocation, costs, and induced response. Journal of Chemical Ecology 33, 297–309.

[11] Amakura, Y., Tsutsumi, T., Nakamura, M., Kitagawa, H., Fujino, J., Sasaki, K., Toyoda, M., Yoshida, T., Maitani, T., 2003. Activation of the aryl hydrocarbon receptor by some vegetable constituents determined using in vitro reporter gene assay. Biological & Pharmaceutical Bulletin 26, 532–539.

[12] Anthony, S. J., Zuchowski, W., Setzer, W. N., 2009. Composition of the floral essential oil of *Brugmansia suaveolens*. Records of Natural Products 3, 76–81.

[13] Anvisa, 2005. Farmacopéia Brasileira ganha reconhecimento da Europa.
URL `http://www.anvisa.gov.br/`

[14] ANVISA, 2009. Farmacopéia Brasileira.
URL `http://www.anvisa.gov.br/hotsite/farmacopeia/index.htm`

[15] Arbour, N., Naniche, D., Homann, D., Davis, R. J., Flavell, R. A., Oldstone, M. B., 2002. C-jun NH2-terminal kinase (JNK)1 and JNK2 signalling pathways have divergent roles in CD8+ T cell- mediated antiviral immunity. Journal of Experimental Medicine 195, 801–810.

[16] Arend, W. P., 2001. The innate immune system in rheumatoid arthritis. Arthritis and Rheumatism 44, 2224–2234.

[17] Ashworth, A., Nakielny, S., Cohen, P., Marshall, C., 1996. The amino acid sequence of a mammalian MAP kinase kinase. Journal of Biological Chemistry 271, 27696–27700.

[18] Atkins, C. M., Selcher, J. C., Petraitis, J. J., Trzaskos, J. M., Sweatt, J. D., 1998. The MAPK cascade is required for mammalian asscociative learning. Nature Neuroscience 1, 602– 609.

[19] Awad, A. B., Fink, C. S., 2000. Phytosterols as anticancer dietary components: evidence and mechanism of action. Journal of Nutrition 130, 2127–2130.

[20] Baldwin, A. S., 2001. The transcription factor NF-κB and human disease. Journal of Clinical Investigation 107, 36.

[21] Balkwill, F., 2000. TNF is here to stay! Immunology Today 21, 470–471.

[22] Bano, J. M., Lorente, J., Castillo, J., Garca-Benavente, O., Rio, J. A., Ortuno, A., Quirin, K. W., Gerard, D., 2003. Phenolic diterpenes, flavones, and rosmarinic acid distribution during the development of leaves, flowers, stems, and roots of *Rosmarinus of cinalis*. Antioxidant activity. Agricultural and Food Chemistry 51, 4247–4253.

[23] Baron, D., 1995. Cytokine: Ihre Biologie und klinische Anwendung. Pharmazeutische Zeitung 25, 9–20.

[24] Barr, R. K., Bogoyevitch, M. A., 2001. The c-jun N-terminal protein kinase family of mitogen-activated protein kinases (JNK MAPK). International Journal of Biochemistry and Cell Biology 33, 1047–1063.

[25] Baud, V., Karin, M., 2001. Signal transduction by tumor necrosis factor and its relatives. Trends in Cell Biology 11, 372–377.

[26] Bayeux, M., Fernandes, A., Foglio, M., Carvalho, J., 2002. Evaluation of the antiedematogenic activity of artemetin isolated from *Cordia curassavica*. Brazilian Journal of Medical and Biological Research 35, 1229–1232.

[27] Begum, S., Sahai, M., Fujimoto, Y., Asai, K., Schneider, K., Nicholson, G., Suessmuth, R., 2006. A new kaempferol diglycoside from *Datura suaveolens* Humb. & Bonpl. ex. Willd. Natural Product Research 20, 1231–1236.

[28] Bellon, S., Fitzgibbon, M. J., Fox, T., Hsiao, H. M., Wilson, K. P., 1999. The structure of phosphorylated p38γ is monomeric and reveals a conserved activation-loop conformation. Structure 9, 1057–1065.

[29] Bhatt, D., Chang, J.-I., Hiraokan, N., 2004. *In vitro* propagation and storage of *Brugmansia versicolor* lagerheim. Plant Biotechnology 21, 237–241.

[30] Boldt, S., Kolch, W., 2004. Targeting MAPK signalling: Prometheus *re or Pandora s* Box? Current Pharmaceutical Design 10, 1885–1905.

[31] Bonvini, P., Zorzi, E., Mussolin, L., Monaco, G., Pigazzi, M., Basso, G., Rosolen, A., 2009. The effect of the cyclin-dependent kinase inhibitor flavopiridol on anaplastic large cell lymphoma cells and relationship with NPM-ALK kinase expression and activity. Haematologica 94, 944–955.

[32] Boulton, T. G., Yancopoulos, G. D., Gregory, J. S., Slaughter, C., Moomaw, C., Hsu, J., Cobb, M. H., 1990. An insulin-stimulated protein kinase similar to yeast kinases involved in cell cycle control. Science 249, 64–67.

[33] Bozyczko-Coyne, D., OKane, T. M., Wu, Z. L., Dobrzanski, P., Murthy, S., Vaught, J. L., Scott, R. W., 2001. CEP-1347/KT-7515, an inhibitor of SAPK/JNK pathway activation, promotes survival and blocks multiple events associated with AB-induced cortical neuron apoptosis. Journal of Neurochemistry 77, 849–863.

[34] Brambilla, R., Gnesutta, N., Minichiello, L., White, G., Roylance, A. J., Herron, C. E., Ramsey, M., Wolfer, D. P., Cestari, V., Rossi-Arnaud, C., Grant, S. G., Chapman, P. F., Lipp, H. P., Sturani, E., Klein, R., 1997. A role for the Ras signalling pathway in synaptic transmission and long- term memory. Nature 390, 281–286.

[35] Brancho, D., Tanaka, N., Jaeschke, A., Ventura, J.-J., Kelkar, N., Tanaka, Y., Kyuuma, M., Takeshita, T., Flavell, R. A., Davis, R. J., 2003. Mechanism of p38 MAP kinase activation *in vivo*. Genes and Development 17, 1969–1978.

[36] Calixto, J. B., 2005. Twenty-five years of research on medicinal plants in Latin America: A personal view. Journal of Ethnopharmacology 100, 131–134.

[37] Calixto, J. B., Otuki, M. F., Santos, A. R., 2003. Anti-inflammatory compounds of plant origin. Part I. Action on arachidonic acid pathway, nitric oxide and nuclear factor kappa B (NF-κB). Planta Medica 69, 973–983, pMID: 14735432.

[38] Capasso, A., Feo, V. D., Simone, F. D., Sorrentino, L., 1997. Activity-directed isolation of spasmolytic (anti-cholinergic) alkaloids from *Brugmansia arborea* (L.) Lagerheim. Pharmaceutical Biology 35, 43–48.

[39] Cardillo, A. B., Alvarez, A. M. O., Lopez, A. C., Lozano, M. E. V., Talou, J. R., Giulietti, A. M., 2009. Anisodamine production from natural sources: Seedlings and hairy root cultures of Argentinean and Colombian *Brugmansia candida* plants. Planta Med 76, 402–405.

[40] Cardillo, A. B., Talou, J. R., Giulietti, A. M., 2008. Expression of *Brugmansia candida* hyoscyamine 6 beta-hydroxylase gene in *Saccharomyces cerevisiae* and its potential use as biocatalyst. Microbial Cell Factories 7, 7–17.

[41] Carlo, G. D., Mascolo, N., Izzo, A. A., Capasso, F., 1999. Flavonoids: Old and new aspects of a class of natural therapeutic drugs. Life Sciences 65, 337–353.

[42] Carrizo, C. N., Pitta-Alvareza, S. I., Koganb, M. J., Giulietti, A. M., Tomaro, M. L., 2001. Occurrence of cadaverine in hairy roots of *Brugmansia candida*. Phytochemistry 57, 759–763.

[43] CEBRID, 2006. Anti-colinérgicos. CENTRO BRASILEIRO DE INFORMAÇÕES SOBRE DROGAS PSICOTRÓPICAS.
URL `http://bvsms.saude.gov.br/bvs/folder/`

[44] CellSignal, 2008. MAPK signaling cascades.
URL `http://www.cellsignal.com/`

[45] Chang, H. Y., Yang, X., 2000. Proteases for cell suicide: Function and regulation of caspases. Microbiology and Molecular Biology Reviews 64, 821–846.

[46] Chang, L., Karin, M., 2001. Mammalian MAP kinase signalling cascades. Nature 410, 37–40.

[47] Chen, J. H., Ho, C.-T., 1997. Antioxidant activities of caffeic acid and its related hydroxycinnamic acid compounds. Journal of Agricultural and Food Chemistry 45, 2374–2378.

[48] Chen, Z., Gibson, T. B., Robinson, F., Silvestro, L., Pearson, G., e Xu, B., Wright, A., Vanderbilt, C., Cobb, M. H., 2001. MAP Kinases. Chemical Reviews 101, 2449–2476.

[49] Cheng, H. P., Wei, S., Wei, L. P., Verkhratsky, A., 2006. Calcium signaling in physiology and pathophysiology. Acta Pharmacologica Sinica 27, 767–772.

[50] Chiang, H.-C., Lo, Y. J., Lu, F.-J., 1994. Xanthine oxidase inhibitors from the leaves of *Alsophila spinulosa*. Journal of Enzyme Inhibition and Medicinal Chemistry 8, 61–71.

[51] Choi, J. M., Lee, E. O., Lee, H. J., Kim, K. H., Ahn, K. S., Shim, B. S., Kim, N. I., Song, M. C., Baek, N. I., Kim, S. H., 2007. Identification of campesterol from *Chrysanthemum coronarium* L. and its antiangiogenic activities. Phytotherapy Research 10, 954–959.

[52] Chomarat, P., Vannier, E., Dechanet, J., Rissoan, M. C., Banchereau, J., Dinarello, C. A., Miossec, P., 1995. Balance of IL-1 receptor antagonist/IL-1b in rheumatoid synovium and its regulation by IL-4 and IL-10. Journal of Immunology 154, 1432–1439.

[53] Choudhary, M. I., Begum, A., Abbaskhan, A., Ajaz, A., ur Rehman, S., ur Rahman, A., 2005. Phenyl polypropanoids from *Lindelo a stylosa*. Chemical & Pharmaceutical Bulletin 53, 1469–1471.

[54] Choy, E. H., Panayi, G. S., 2001. Cytokine pathways and joint inflammation in rheumatoid arthritis. New England Journal of Medicine 344, 907–916.

[55] Clerk, A., H.Sugden, P., 1999. Activation of protein kinase cascades in the heart by hypertrophic G protein-coupled receptor agonists. American Journal of Cardiology 83, 64H–69H.

[56] Cobb, M. H., Goldsmith, E. J., 1995. How MAP kinases are regulated. Journal of Biological Chemistry 25, 14843–14846.

[57] Cole, J., Tsou, R., Wallace, K., Gibran, N., Isik, F., 2001. Early gene expression profile of human skin to injury using high-density cDNA microarrays. Wound Repair and Regeneration 9, 360–370.

[58] Conze, D., Krahl, T., Kennedy, N., Weiss, L., Lumsden, J., Hess, P., Flavel, R. A., Le, G. G., Davis, R. J., Rincon, M., 2002. C-jun NH(2)-terminal kinase (JNK)1 and JNK2 have distinct roles in CD8 (+) T cell activation. Journal of Experimental Medicine 195, 811–823.

[59] Correa, M. P., 1952. Dicionário das Plantas Úteis do Brasil e das Exóticas Cultivadas. Imprensa Nacional.

[60] Crews, C. M., Alessandrini, A., Erikson, R. L., 1992. The primary structure of MEK, a protein kinase that phosphorylates the ERK gene product. Science 258, 478–480.

[61] Crow, F. W., Tomer, K. B., Looker, J. H., Gross, M. L., 1986. Fast atom bombardment and tandem mass spectrometry for structure determination of steroid and flavonoid glycosides. Analytical Biochemistry 155, 286–307.

[62] Cuenda, A., Cohen, P., Buée-Scherrer, V., Goeder, M., 1997. Activation of stress-activated protein kinase-3 (SAPK3) by cytokines and cellular stresses is mediated via SAPKK3 (MKK6); comparison of the specificities of SAPK3 and SAPK2 (RK/p38). The EMBO Journal 16, 295–305.

[63] Cuyckens, F., Claeys, M., 2004. Mass spectrometry in the structural analysis of flavonoids. Journal of Mass Spectrometry 39, 1–15.

[64] da Silva, S. A. S., Rodrigues, M. S. L., de Ftima Agra, M., da Cunhaa, E. V. L., Barbosa-Filhoa, J. M., da Silva, M. S., 2004. Flavonoids from *Cordia globosa*. Biochemical Systematics and Ecology 32, 359–361.

[65] Dambach, D. M., 2005. Potential adverse effects associated with inhibition of p38α/β MAP kinases. Current Topics in Medicinal Chemistry 5, 929–939.

[66] Danese, S., Semeraro, S., Armuzzi, A., Papa, A., Gasbarrini, A., 2006. Biological therapies for inflammatory bowel disease: Research drives clinics. Mini-Reviews in Medicinal Chemistry 6, 771–784.

[67] Dapkevicius, A., van Beek, T. A., Lelyveld, G. P., van Veldhuizen, A., de Groot, A., Linssen, J. P. H., Venskutonis, R., 2002. Isolation and structure elucidation of radical scavengers from *Thymus vulgaris* leaves. Journal of Natural Products 65, 892–896.

[68] Davidson, A., Diamond, B., 2001. Autoimune diseases. New England journal of Medicine 345, 340–350.

[69] Davies, G., Fataftah, A., Radwan, A., Raffauf, R. F., Ghabbour, E. A., Jansen, S. A., 1997. Isolation of humic acid from the terrestrial plant *Brugmansia sanguinea*. Science of The Total Environment 201, 79–87.

[70] Davis, R. J., 2000. Signal transduction by the JNK group of MAP kinases. Cell 103, 239–252.

[71] Day, A. J., DuPont, M. S., Ridley, S., Rhodes, M., Rhodes, M. J., Morgan, M. R., Williamson, G., 1998. Deglycosylation of flavonoid and isoflavonoid glycosides by human small intestine and liver beta-glucosidase activity. FEBS Letters 436, 71–75.

[72] Dayer, J.-M., Bresnihan, B., 2002. Targeting interleukin-1 in the treatment of rheumatoid arthritis. Arthritis and Rheumatism 46, 574–578.

[73] de Carvalho, P., Rodriguesa, R., Sawayaa, A., Marquesb, M., Shimizu, M., 2004. Chemical composition and antimicrobial activity of the essential oil of *Cordia verbenacea* D.C. Journal of Ethnopharmacology 95, 297–301.

[74] de Carvalho, P. E. R., 2004. Guajuvira - *Patagonula americana*. Tech. rep., Embrapa.

[75] de las Heras, B., Hortelano, S., 2009. Molecular basis of the anti-inflammatory effects of terpenoids. Inflammation & Allergy - Drug Targets 8, 28–39.

[76] de Menezes, J. A., Lemos, T., Pessoa, O., Braz-Filho, R., Montenegro, R., Wilke, D., Costa-Lotufo, L., Pessoa, C., de Moraes, M., Silveira, E., 2005. A cytotoxic meroterpenoid benzoquinone from roots of *Cordia globosa*. Planta Medica 71, 54–8.

[77] DeLano, W. L., 01 2002. The PyMol Molecular Graphics System. DeLano Scientific, san Carlos, CA, USA.
URL `http://www.pymol.org`

[78] Derijard, B., Hibi, M., Wu, I. H., Barret, T., Su, B., Deng, T., Karin, M., Davis, R. J., 1994. JNK1: A protein kinase stimulated by UV light and Ha-Ras that binds and phosphorylates the c-Jun activation domain. Cell 76, 1025–1037.

[79] Detzel, A., Wink, M., 1993. Attraction, deterrence or intoxication of bees (*Apis mellifera*) by plant allelochemicals. Chemoecology 4, 8–18.

[80] Dewick, P., 2001. Medicinal Natural Products: A Biosynthetic Approach. Wiley & Sons, West Sussex, England.

[81] El-Sayed, N., Omara, N., Yousef, A., Farag, A., Mabry, T., 2001. Kaempferol triosides from *Reseda muricata*. Phytochemistry 57, 575–578.

[82] Englisch, J. D., Sweatt, J. D., 1996. Activation of p42 mitogen-activated protein kinase in hippocampal lon term potentiation. Journal of Biological Chemistry 271, 24329–24332.

[83] Estus, S., Zaks, W. J., Freemann, R. S., Gruda, M., Bravo, R., Johnson, E. M., 1994. Altered gene expression in neurons during programmed cell death: Identification of c-jun as necessary for neuronal apoptosis. Journal of Cell Biology 127, 1717–1727.

[84] Evans, W., Lampard, J., 1972. Alkaloids of *Datura suaveolens*. Phytochemistry 11, 3293–3298.

[85] Evans, W. C., Major, V. A., 1968. The alkaloids of the genus *Datura*, section *Brugmansia*. Part IV. New alkaloids of *Datura sanguinea* R. and P. Chemical Society C: Organic articles, 2775–2778.

[86] Fabian, M. A., Biggs, W. H., Treiber, D. K., Atteridge, C. E., Azimioara, M. D., Benedetti, M. G., Carter, T. A., Ciceri, P., Edeen, P. T., Floyd, M., Ford, J. M., Galvin, M., Gerlach, J. L., Grotzfeld, R. M., Herrgard, S., Insko, D. E., Insko, M. A., Lai, A. G., Lelias, J.-M., Mehta, S. A., Milanov, Z. V., Velasco, A. M., Wodicka, L. M., Patel, H. K., Zarrinkar, P. P., Lockhart, D. J., 2005. A small molecule-kinase interaction map for clinical kinase inhibitors. Nature Biotechnology 23, 329–336.

[87] Fathiazada, F., Delazara, A., Amiria, R., Sarkerb, S. D., 2006. Extraction of flavonoids and quantification of rutin from waste *Tobacco* leaves. Iranian Journal of Pharmaceutical Research 3, 222–227.

[88] Feisst, C., Franke, L., Appendino, G., Werz, O., 2005. Identification of molecular targets of the oligomeric nonprenylated acylphloroglucinols from *Myrtus communis* and their implication as anti-inflammatory compounds. Journal of Pharmacology and Experimental Therapeutics 315, 389–396.

[89] Feo, V. D., 2003. Ethnomedical field study in northern Peruvian Andes with particular reference to divination practices. Journal of Ethnopharmacology 85, 243–256.

[90] Ferrari, F., Monache, F. D., Compagnone, R., Oliveri, M. C., 1997. Chemical constituents of *Cordia dentata* flowers. Fitoterapia 68, 88.

[91] Ferrel, J. E., 1996. Tripping the switch fantastic: How a protein kinase cascade can convert graded inputs into switch-like outputs. Trends in Biochemistry Science 21, 460–466.

[92] Ferriola, C. P., Cody, V., Middleton, J. E., 1989. Protein kinase C inhibition by plant flavonoids. Biochemical Pharmacology 38, 1617–1624.

[93] Ficarra, R., Ficarra, P., Tommasini, S., Calabro, M. L., Ragusa, S., Barbera, R., Rapisarda, A., 1995. Leaf extracts of some *Cordia* species: Analgesic and anti-inflammatory activities as well as their chromatographic analysis. Pharmacology 50, 245–256.

[94] Fischer, L., Szellas, D., Radmark, O., Steinhilber, D., Werz, O., 2003. Phosphorylation and stimulus-dependent inhibition of cellular 5-lipoxygenase activity by non-redox-type inhibitors. FASEB Journal 17, 949–951.

[95] Forrer, P., Tamaskovic, R., Jaussi, R., 1998. Enzyme-linked immunosorbent assay for measurement of JNK, ERK, and p38 kinase activities. Journal of Biological Chemistry 379, 1101–1111.

[96] Fossen, T., Pedersen, A. T., Andersen, O. M., 1998. Flavonoids from red onion (*Allium cepa*). Phytochemistry 47, 281–285.

[97] Freitas, A. V. L., Trigo, J. R., Junior, K. S. B., Witte, L., Hartmann, T., Barata, L. E. S., 1996. Tropane and pyrrolizidine alkaloids in the ithomiines *Placidula euryanassa* and *Miraleria cymothoe* (Lepidoptera: Nymphalidae). Chemoecology 7, 61–67.

[98] Friedrichs, A., 2005. Optimierung eines Vollblut-Testsystems zur Evaluirung von Hemmstoffen der Zytokin-Freisetzung. Master s thesis, Universität Tübingen.

[99] Frödin, M., Sekine, N., Roche, E., Filloux, C., Prentki, M., Wollheim, C. B., Obberghen, E. J. V., 1995. Glucose, other secretagogues, and nerve growth factor stimulate mitogen-activated protein kinase in the insulin-secreting beta-cell line, INS-1. Journal of Biological Chemistry 270, 7882–7889.

[100] Fronza, M., Heinzmann, B., Hamburger, M., Laufer, S., Merfort, I., 2009. Determination of the wound healing effect of *Calendula extracts using the scratch assay with 3T3 broblasts*. Journal of Ethnopharmacology 126, 463–467.

[101] Fun, C., Svendsen, A. B., 1990. The essential oil of *Cordia cylindrostachya* Roem. & Schult. grown on Aruba. Journal of Essential Oil Research 2, 209–210.

[102] Funk, C. D., 2001. Prostaglandins and leukotrienes: Advances in eicosanoid biology. Science 294, 1871–1875.

[103] Gadotti, V. M., Schmeling, L. O., Machado, C., Liz, F. H., Filho, V. C., Meyre-Silva, C., Santos, A. R., 2005. Antinociceptive action of the extract and the flavonoid quercitrin isolated from *Bauhinia microstachya* leaves. Journal of Pharmacy and Pharmacology 57, 1345–1351.

[104] Gallagher, T. F., Seibel, G. L., Kassis, S., Laydon, J. T., Blumenthal, M. J., Lee, J. C., Lee, D., Boehm, J. C., Fier-Thompson, S. M., Abt, J. W., Soreson, M. E., Smietana, J. M., Hall, R. F., Garigipati, R. S., Bender, P. E., Erhard, K. F., Krog, A. J., Hofmann, G. A., Sheldrake, P. L., McDonnell, P. C., Kumar, S., Young, P. R., Adams, J. L., 1997. Regulation of stress-induced cytokine production by pyridinylimidazoles inhibition of CSBP kinase. Bioorganic & Medicinal Chemistry 5, 49–64.

[105] Gallo, M. B. C., Rocha, W. C., da Cunha, U. S., Diogo, F., da Silva, F. C., Vieira, P. C., Vendramim, J. D., Fernandes, J. B., da Silva, M. F., Batista-Pereira, L. G., 2006. Bioactivity of extracts and isolated compounds from *Vitex polygama* (Verbenaceae) and *Siphoneugena densi ora* (Myrtaceae) against *Spodoptera frugiperda* (Lepidoptera: Noctuidae). Pest Management Science 62, 1072–1081.

[106] Gálvez, J., 1996. Application of natural products in experimental models of intestinal inflammation in rats. Methods & Findings in Experimental & Clinical Pharmacology 18, 7–10.

[107] Gao, L. P., Wei, H. L., Zhao, H. S., Xiao, S. Y., Zheng, R. L., 60. Antiapoptotic and antioxidant effects of rosmarinic acid in astrocytes. Pharmazie 2005, 62–65.

[108] Garay, M., Gaarde, W., Monia, B. P., Nero, P., Cioffi, C. L., 2000. Inhibiton of hipoxia/reoxygenation-induced apoptosis by an antisense oligonucleotide targeted to JNK1 in human kidney cells. Biochemical Pharmacology 59, 1033–1043.

[109] Garcia-Pilneres, A. J., 2003. Contribution to the elucidation of the anti-inflammatory activity of sesquiterpene lactones. Ph.D. thesis, Albert-Ludwigs-Universitt Freiburg.

[110] Garc´a-Pilneres, A. J., Castro, V., Mora, G., Schmidt, T. J., Strunck, E., Pahl, H. L., Merfort, I., 2001. Cysteine 38 in p65/NF-κB plays a crucial role in DNA binding inhibition by sesquiterpene lactones. Journal of Biologic Chemistry 276, 39713–39720.

[111] Gearan, T., Castilho, O. A., Schwarzchild, M. A., 2001. The parkinsonian neurotoxin, MPP+ induces phosphorylated c-Jun in dopaminergic neurons of mesencephalic cultures. Parkinsonism & Related Disorders 8, 19–22.

[112] Geitmann, A., Hudak, J., Vennigerholz, F., Walles, B., 1995. Immunogold localization of pectin and callose in pollen grains and pollen tubes of *Brugmansia suaveolens* - Implications for the self-incompatibility reaction. Journal of Plant Physiology 147, 225–235.

[113] Geller, F., Schmidt, C., Göttert, M., Fronza, M., Schattel, V., Heinzmann, B., Werz, O., Flores, E., Merfort, I., Laufer, S., 2010. Identification of rosmarinic acid as the major active constituent in *Cordia americana*. Journal of Ethnopharmacology 128, 561–566.

[114] Ghose, A. K., Herbertz, T., Pippin, D. A., Salvino, J. M., Mallamo, J. P., 2008. Knowledge based prediction of ligand binding modes and rational inhibitor design for kinase drug discovery. Journal of Medicinal Chemistry 51, 5149–5171.

[115] Goedert, M., Cuenda, A., Craxton, M., Jakes, R., Cohen, P., 1997. Activation of the novel stress-activated protein kinase SAPK4 by cytokines and cellular stresses is mediated by SKK3 (MKK6); comparison of its substrate specificity with that of other SAP kinases. The EMBO Journal 16, 3563 – 3571.

[116] Goldstein, D. M., Kuglstatter, A., Lou, Y., Soth., M. J., 2009. Selective p38α inhibitors clinically evaluated for the treatment of chronic inflammatory disorders. Journal of Medicinal Chemistry 53, 2345–2353.

[117] Gottschling, M., 2003. Phylogenetic analysis of selected Boraginales. Ph.D. thesis, Freien Universität Berlin.

[118] Gouda, Y. G., Abdel-Baky, A. M., Mohamed, K. M., Darwish, F. M., R. Kasai, K. Y., 2006. Phenylpropanoid and phenylethanoid derivatives from *Kigelia pinnata* dc. fruits. Journal of Natural Products 20, 935–939.

[119] Grinberg, L. N., Rachmilewitz, E. A., Newmark, H., 1994. Protective effects of rutin against hemoglobin oxidation. Biochemical Pharmacology 48, 643–649.

[120] Gum, R. J., Mclaughlin, M. M., Kumar, S., Wang, Z., Bower, M. J., Lee, J. C., Adams, J. L., Livi, G. P., Goldsmith, E. J., Young, P. R., 1998. Acquisition of sensitivity of stress-activated protein kinases to the inhibitor, SB 203580, by alteration of one or more amino acids within the ATP binding pocket. Journal of Biological Chemistry 273, 15605– 15610.

[121] Hagiwara, M., Inoue, S., Tanaka, T., Nunoki, K., Ito, M., Hidaka, H., 1998. Differential effects of flavonoids as inhibitors of tyrosine protein kinases and serine/threonine protein kinases. Biochemical Pharmacology 37, 2987–2992.

[122] Hale, K. K., Trollinger, D., Rihanek, M., Manthey, C. L., 1999. Differential expression and activation of p38 mitogen-activated protein kinase α, β, γ and δ in inflammatory cell lineages. Journal of Immunology 162, 4246– 4252.

[123] Ham, J., Babij, C., Whitfield, J., Pfarr, C. M., Lallemand, D., Yaniv, M., Rubin, L. L., 1995. A c-jun dominant negative mutant protects sympathetic neurons against programmed cell death. Neuron 14, 927– 939.

[124] Hammarberg, T., Provost, P., Presson, B., Radmark, O., 2000. The N-terminal domain of 5-lipoxygenase binds calcium and mediates calcium stimulation of enzyme activity. Journal of Biological Chemistry 275, 38787–38793.

[125] Han, Z., Boyle, D. L., Chang, L., Bennett, B., Karin, M., Yang, L., Manning, A. M., Firestein, G. S., 2001. c-Jun N-terminal kinase is required for metalloproteinase expression and joint destruction in inflammatory arthritis. Journal of Clinical Investigation 108, 73–81.

[126] Han, Z., Chang, L., Yamanishi, Y., Karin, M., Firestein, G. S., 2002. Joint damage and inflammation in c-jun N-terminal kinase 2 knockout mice with passive murine collagen-induced arthritis. Arthritis & Rheumatism 46, 818– 823.

[127] Hanks, S. K., Hunter, T., 1995. Protein kinases 6. The eukaryotic protein kinase superfamily: kinase (catalytic) domain structure and classification. Journal of the Federation of American Societies for Experimental Biology 8, 576–596.

[128] Hansel, R., Keller, K., Rimpler., H., Schneider, G., 1993. Hagers Handbuch der Pharmazeutischen Praxis: Drogen E-O. Springer Verlag.

[129] Havelius, U., Asman, P., 2002. Accidental mydriasis from exposure to Angel s trumpet (*Datura suaveolens*). Acta Ophthalmologica Scandinavica 80, 332–335.

[130] He, H., Li, H. L., Lin, A., Gottlieb, R. A., 1999. Activation of JNK pathway is important for cardiomyocyte death in response to stimulated ischemia. Cell Death & Differentiation 6, 987– 991.

[131] Hegnauer, R., Hegnauer, M., 2001. Chemotaxonomie der Pflanzen: Band 3: Dicotyledoneae. Birkhäuser Basel.

[132] Heldt, H. W., Piechulla, B., 1999. Pflanzen-biochemie. Spektrum Akademischer Verlag.

[133] Hemak, J., Gale, D., Brock, T. G., 2002. Structural characterization of the catalytic domain of the human 5-lipoxygenase enzyme. Journal of Molecular Modeling 8, 102–112.

[134] Herlaar, E., Brown, Z., 1999. p38 MAPK signalling cascades in inflammatory disease. Molecular Medicine Today 5, 439– 447.

[135] Hirosumi, J. G., Chang, L., Goerguen, C. Z., Uysal, K. T., Maeda, K., Karin, M., Hotamisligil, G. S., 2002. A central role of JNK in obesity and insulin resistance. Nature 420, 333–336.

[136] HMDB, 2006. 3-(3,4-Dihydroxyphenyl)lactic acid (HMDB03503).
URL `http://www.hmdb.ca/metabolites/HMDB03503`

[137] Holm, M., Lehmann, F., Laufer, S., 2008. Medicinal chemistry and molecular inhibitor mechanism of tyrosine kinase inhibitors. Pharmazie in unserer Zeit 37, 382–392.

[138] Hosny, M., 1998. Secoiridoid glucosides from *Fraxinus oxycarba*. Phytochemistry 47, 1569–1576.

[139] Hur, Y.-G., Yun, Y., Won, J., 2004. Rosmarinic acid induces $p56^{lck}$-dependent apoptosis in Jukart and pheripheral T cells via mitochondrial pathway independent from Fas/Fas ligand interaction. Journal of Immunology 172, 79–87.

[140] Hussein, S. A. M., Ayoub, N. A., Nawwar, M. A. M., 2003. Caffeoyl sugar esters and an ellagitannin from *Rubus sanctus*. Phytochemistry 63, 905–911.

[141] Hwang, B. Y., Lee, J. H., Koo, T. H., Kim, H. S., Hong, Y. S., Ro, J. S., Lee, K. S., Lee, J. J., 2001. Kaurane diterpenes from *Isodon japonicus* inhibit nitric oxide and prostaglandin E2 production and NF-κB activation in LPS-stimulated macrophage RAW264.7 cells. Planta Med 67, 406–410.

[142] Ikeda, I., Konno, R., Shimizu, T., Ide, T., Takahashi, N., Kawada, T., Nagao, K., Inoue, N., Yanagita, T., Hamada, T., Morinaga, Y., Tomoyori, H., Imaizumi, K., Suzuki, K., 2006. Campest-5-en-3-one, an oxidized derivative of campesterol, activates PPAR, promotes energy consumption and reduces visceral fat deposition in rats. Biochimica et Biophysica Acta 1760, 800–807.

[143] Ioset, J.-R., Marstona, A., Guptab, M. P., Hostettmanna, K., 1998. Antifungal and larvicidal meroterpenoid naphthoquinones and a naphthoxirene from the roots of *Cordia linnael*. Phytochemistry 47, 729–734.

[144] Isbister, G. K., Oakley, P., Dawson, A. H., Whyte, I. M., 2003. Presumed Angels trumpet (Brugmansia) poisoning: Clinical effects and epidemiology. Emergency Medicine 15, 376–382.

[145] Isomaki, P., Punnonen, J., 1997. Pro and anti-inflammatory cytokines in rheumatoid arthritis. Annals of Medicine 29, 499–507.

[146] Iuvone, T., Filippis, D. D., Esposito, G., D Amico, A., Izzo, A. A., 2006. The spice sage and its active ingredient rosmarinic acid protect PC12 cells from amyloid-beta peptide-induced neurotoxicity. Journal of Pharmacology and Experimental Therapeutics 317, 1143–1149.

[147] Jelić, D., Mildner, B., Kostrun, S., Nujić, K., Verbanac, D., Cÿulić, O., R. Antolović Brandt, W., 2007. Homology modeling of human Fyn kinase structure: discovery of rosmarinic acid as a new Fyn Kinase inhibitor and in silico study of its possible binding modes. Journal of Medicinal Chemistry 50, 1090–1100.

[148] Jiang, Y., Gra, H., Zhao, M., New, L. G., Gu, J., Feng, L. L., Dipadova, F., Ulevitch, R. J., Han, J. H., 1997. Characterization of the structure and function of the fourth member of p38 group of mitogen-activated protein kinases. Journal of Biological Chemistry 272, 30122–30128.

[149] Johnson, G. L., Lapadat, R., 2002. Mitogen-activated protein kinase pathways mediated by ERK, JNK, and p38 protein kinases. Science 298, 1911–1912.

[150] Jourdan, P. S., Mansell, R. L., 1982. Isolation and partial characterization of three glucosyl transferases involved in the biosynthesis of flavonol triglucosides in *Pisum sativum* L. Arch. Biochemical and Biophysical Research Communications 213, 434–443.

[151] Kaminska, B., 2005. MAPK signalling pathway as molecular targets for anti-inflammatory therapy from molecular mechanisms to therapeutic benefits. Biochimica et Biophysica Acta 1754, 253– 262.

[152] Karin, M., Ben-Neriah, Y., 2000. Phosphorylation meets ubiquitination: The control of NF-κB activity. Annual Review of Immunology 18, 621–663.

[153] Karin, M., Lin, A., 2002. NF-κB at the crossroads of life and death. Nature Immunology 3, 221–227.

[154] Kellam, S. J., Mitchell, K. A., Blunt, J. W., Clark, B. M., Munro, M. H. G., Walker, J. R. L., 1993. Phenylpropanoid glycoside esters: leucine aminopeptidase inhibitors from *Hebe stricta* var. atkinsonii. Natural Product Letters 2, 87–94.

[155] Khan, W. A., Blobe, G. C., Hannum, Y. A., 1995. Arachidonic acid and free fatty acids as a second messengers and the role of protein kinase C. Cell Signal 7, 171–184.

[156] Khanna, D., Sethi, G., Ahn, K. S., Pandey, M. K., Kunnumakkara, A. B., Sung, B., Aggarwal, A., Aggarwal, B. B., 2007. Natural products as a gold mine for arthritis treatment. Current Opinion in Pharmacology 7, 344–351.

[157] Khoo, S., Cobb, M. H., 1997. Activation of mitogen-activating protein kinase by glucose is not required for insulin secretion. National Academy of Sciencies 94, 5599– 5604.

[158] Kiprono, P. C., Kaberia, F., Keriko, J. M., Karanja, J. N., 2000. The in vitro anti-fungal and anti-bacterial activities of beta-sitosterol from *Senecio lyratus* (Asteraceae). Zeitschrift fr Natürforschung C 55, 485–488.

[159] Klaas, C. A., Wagner, G., Laufer, S., Sosa, S., Della, L. R., Bomme, U., Pahl, H. L., Merfort, I., 2002. Studies on the anti-inflammatory activity of phytopharmaceuticals prepared from Arnica flowers. Planta Medica 68, 385–391.

[160] Koberle, A., 2009. Identification and characterization of microsomal prostaglandin E2 synthase-1 inhibitors. Ph.D. thesis, University of Tübingen.

[161] Koch, P. R. G., 2009. Design, synthese und biologische testung von 2-alkylsulfanyl-5-pyridinylimidazolen, pyridinylimidazol-2-onen, pyridinylchinoxalinen und pyridinylpyridopyrazinen als neuartige hemmstoffe der p38α map kinase. Ph.D. thesis, University of Tübingen.

[162] Kopp, E., Ghosh, S., 1994. Inhibition of NF-kappa B by sodium salicylate and aspirin. Science 265, 956–959.

[163] Korb, A., Tohidast-Akrad, M., Cetin, E., Axmann, R., Smolen, J., Schett, G., 2006. Differential tissue expression and activation of p38 MAPK alpha, beta, gamma and delta in rheumatoid arthritis. Arthritis & Rheumatism 54, 2745– 2756.

[164] Körbes, C. V., 1995. Manual de Plantas Medicinais. ASSESOAR.

[165] Kosako, H., Gotoh, Y., Matsuda, S., Ishikawa, M., Nishida, E., 1992. Xenopus MAP Kinase activator is serine/threonine/tyrosine kinase activated by threonine phosphorylation. EMBO Journal 11, 2903– 2908.

[166] Kroll, D. J., 2001. Concerns and needs for research in herbal supplement pharmacotherapy and safety. Journal of Herbal Pharmacotherapy 1, 3–23.

[167] Kumar, S., Boehm, J., Lee, J. C., 2003. p38 MAP kinases: key signalling molecules as therapeutic targets for inflammatory diseases. Nature Reviews Drug Discovery 9, 717–726.

[168] Kuppast, I. J., Nayak, P. V., 2006. Wound healing activity of *Cordia dichotoma* Forst. f. fruits. Natural Product Radiance 5, 103–107.

[169] Kuroda, M., Mimaki, Y., Ori, K., Sakagami, H., Sashida, Y., 2004. 27-Norlanostane glycosides from the bulbs of *Muscari paradoxum*. Journal of Natural Products 67, 2099–2103.

[170] Kurylowicz, A., Nauman, J., 2008. The role of nuclear factor-κB in the development of autoimmune diseases: a link between genes and environment. Acta Biochimica Polonica 55, 629–647.

[171] Kyriakis, J. M., Avruch, J., 2001. Mammalian mitogen-activated protein kinase signal transduction pathways activated by stress and inflammation. Physiological Reviews 81, 807–869.

[172] Kyriakis, J. M., Banerjee, P., Nikolakaki, E., Dai, T., Rubie, E. A., andJ. Avruch, M. A., Woodgett, J. R., 1994. The stress-activated protein kinase subfamily of c-Jun kinases. Nature 369, 156–160.

[173] Lam, F. F. Y., Yeung, J. H. K., Chan, K. M., Or, P. M. Y., 2007. Relaxant effects of danshen aqueous extract and its constituent danshensu on rat coronary artery are mediated by inhibition of calcium channels. Vascular Pharmacology 46, 271–277.

[174] Lansdown, A. B., 2002. Calcium: A potential central regulator in wound healing in the skin. Wound Repair Regen 10, 271–285.

[175] Laufer, S., Gay, S., Brune, K., 2007. Rheumatische Erkrankungen und Entzndung. Georg Thieme Verlag Stuttgart.

[176] Laufer, S., Greim, C., Bertsche, T., 2002. A in vitro screening assay for the detection of inhibitors of proinflammatory cytokine synthesis: a useful tool for the development of new antiarthritic and disease modifying drugs. Osteoarthritis and Cartilage 10, 961–967.

[177] Laufer, S., Merfort, I., Heinzmann, B., Bittencourt, C. F., 2005. Identifizierung und Charakterisierung aktiver Inhaltstoffe brasilianischer Arzneipflanzen. Projektantrag.

[178] Laufer, S., Striegel, H., Neher, K., Patent EP6945[2000017192], 1999. Preparation of 2-aralkylthioimidazoles and related compounds as antiinflammatories.

[179] Laufer, S., Thuma, S., Peifer, C., Greim, C., Herweh, Y., Albrecht, A., Dehner, F., 2005. An immunosorbent, nonradioactive p38 MAP Kinase assay comparable to standard radioactive liquid-phase assays. Analytical Biochemistry 344, 135–137.

[180] Laufer, S. A., Zimmermann, W., Ruff, K. J., 2004. Tetrasubstituted imidazole inhibitors of cytokine release: Probing substituents in the N-1 position. Journal of Medicinal Chemistry 47, 6311–6325.

[181] Lawler, S., Fleming, Y., Goedert, M., Cohen, P., 1998. Synergistic activation of SAPK1/JNK1 by two kinases *in vitro*. Current Biology 8, 1387–1390.

[182] Lee, J., Jung, E., Kim, Y., Lee, J., Park, J., Hong, S., Hyun, C.-G., Park, D., Kim, Y. S., 2006. Rosmarinic acid as a downstream inhibitor of IKKβ in TNF-α-induced upregulation of CCL11 and CCR3. British Journal of Pharmacology 148, 366–375.

[183] Lee, J. C., Kassis, S., Kumar, S., Badger, A., Adams, J. L., 1999. p38 mitogen-activated protein kinase inhibitors-mechanisms and therapeutic potentials. Pharmacology & Therapeutics 82, 389– 397.

[184] Lee, J. C., Laydon, J. T., McDonnell, P. C., Gallagher, T. F., Kumar, S., Green, D., McNulty, D., Blumenthal, M. J., Heys, J. R., Landvatter, S. W., 1994. A protein kinase involved in the regulation of inflammatory cytokine biosynthesis. Nature 372, 739– 746.

[185] Lee, J. H., Koo, T. H., Hwang, B. Y., Lee, J. J., 2002. Kaurane diterpene, kamebakaurin, inhibits NF-κB by directly targeting the DNA-binding activity of p50 and blocks the expression of antiapoptotic NF-κB target genes. Journal of Biological Chemistry 277, 18411–18420.

[186] Leiper, L. J., Walczysko, P., Kucerova, R., Ou, J., Shanley, L. J., Lawson, D., Forrester, J. V., McCaig, C. D., Zhao, M., Collinson, J. M., 2006. The roles of calcium signaling and ERK1 2 phosphorylation in a Pax6^{+-} mouse model of epithelial wound-healing delay. BMC Biology 16, 4–27.

[187] Liao, J. J. L., 2007. Molecular recognition of protein kinase binding pockets for design of potent and selective kinase inhibitors. Journal of Medical Chemistry 50, 409–424.

[188] Liedtke, A. J., 2008. Synthese, Analytik und biologische Testung von tri- und tetrasubstituierten Imidazolen als ATP-kompetitive Hemmstoffe der p38 MAP Kinase: Optimierung von Wechselwirkungen mit der Hydrophoben Enzymregion II. Ph.D. thesis, University of Tübingen.

[189] Lindenmeyer, M. T., 2004. Untersuchungen zum molekularen Wirkmechanismus der antiinflamatorischen Aktivität von Sesquiterpenlactonen. Ph.D. thesis, Albert-Ludwigs-Universität Freiburg.

[190] Linsenmaier, S., 2006. Entwicklung und Optimierung von in vitro Testverfahren zur Evaluierung von Hemmstoffen der p38α MAP Kinase und JNK3. Ph.D. thesis, University of Tübingen.

[191] Liverton, N. J., Butcher, J. W., Claiborne, C. F., Claremon, D. A., Libby, B. E., Nguyen, K. T., Pitzenberger, S. M., Selnick, H. G., Smith, G. R., Tebben, A., Vacca, J. P., Varga, S. L., Agarwal, L., Dancheck, K., Forsyth, A. J., Fletcher, D. S., Frantz, B., Hanlon, W. A., Harper, C. F., Hofsess, S. J., Kostura, M., Lin, J., Luell, S., O Neill, E. A., Orevillo, C. J., Pang, M., Parsons, J., Rolando, A., Sahly, Y., Visco, D. M., O Keefe, S. J., 1999. Design and synthesis of potent, selective, and orally bioavailable tetrasubstituted imidazole inhibitors of p38 mitogen-activated protein kinase. Journal of Medicinal Chemistry 42, 2180–2190.

[192] LoGrasso, P. V., Frantz, B., Rolando, A. M., OKeefe, S. J., Hermes, J. D., ONeill, E. A., 1997. Kinetic mechanism for p38 MAP kinase. Biochemistry 36, 10422– 10427.

[193] Loppnow, H., 2001. Cytokines: Classification, receptors, mechanisms of action. Internisten Berlin 42, 13–27.

[194] Lorenzi, H., 1998. Árvores Brasileiras, Manual de Identificacao e Cultivo de Plantas Arbóreas Nativas do Brasil. Vol. 1. Plantarum.

[195] Luo, Y., Umegaki, H., Wang, X., Abe, R., Roth, G. S., 1998. Dopamine induces apoptosis through on oxidation-involved SAPK/JNK activation pathway. Journal of Biological Chemistry 273, 3756– 3764.

[196] Mabry, T. J., Markham, K. R., Thomass, M. B., 1970. The systematic identification of flavonoids. Springer, Heidelberg.

[197] Makarov, S. S., 2000. NF-kappaB as a therapeutic target in chronic inflammation: recent advances. Molecular Medicine Today 6, 441–448.

[198] Mann, J., 1994. Murder, Magic, and Medicine. Oxford University Press.

[199] Manning, G., Whyte, D. B., Martinez, R., Hunter, T., Sudarsanam, S., 2002. The protein kinase complement of the human genome. Science 298, 1912– 1934.

[200] March, R. E., Miao, X.-S., Metcalfe, C. D., 2004. A fragmentation study of a flavone triglycoside, kaempferol-3-O-robinoside-7-O-rhamnoside. Rapid Communications in Mass Spectrometry 18, 931–934.

[201] Matsusea, I. T., Limb, Y. A., Hattorib, M., Correac, M., Gupta, M. P., 1998. A search for anti-viral properties in Panamanian medicinal plants: The effects on HIV and its essential enzymes. Journal of Ethnopharmacology 64, 15–22.

[202] McCann, S. E., Ambrosone, C. B., Moysich, K. B., Brasure, J., Marshall, J. R., Freudenheim, J. L., Wilkinson, G. S., Graham, S., 2005. Intakes of selected nutrients, foods, and phytochemicals and pro-state cancer risk in western New York. Nutrition and Cancer 53, 33–41.

[203] McInnes, I. B., Schett, G., 2007. Cytokines in the pathogenesis of rheumatoid arthritis. Nature Reviews 7, 429–442.

[204] Medeiros, R., Passos, G., Vitor, C., Koepp, J., Mazzuco, T., Pianowski, L., Campos, M., Calixto, J., 2007. Effect of two active compounds obtained from the essential oil of *Cordia verbenacea* on the acute inflammatory responses elicited by LPS in the rat paw. British Journal of Pharmacology 151, 618–627.

[205] Mehrabani, M., Ghassemi, N., Sajjadi, E., Ghannadi, A. R., Shams-Ardakani, M. R., 2005. Main phenolic compound of petals of *Echium amoenum* Fish. and C.A. Mey, a famous medicinal plant of Iran. Daru (Journal of Faculty of Pharmacy) 13, 65–69.

[206] Menezes, J. E. S. A., Lemos, T. L. G., Silveira, E. R., Braz-Filho, R., Braz, O. D. L. P. J., 2001. Trichotomol, a new cadinenediol from *Cordia trichotoma*. Journal of the Brazilian Chemical Society 12, 787–790.

[207] Mentz, L. A., Lutzemberger, L. C., Schenkel, E. P., 1997. Da flora medicinal do Rio Grande do Sul: Notas sobre a Obra de D Avila (1910). Caderno de Farmácia 13, 25–48.

[208] Merfort, I., 2003. Arnika: Neue Erkenntnisse zum Wirkungsmechanismus einer traditionellen Heilpflanze. Forschende Komplementrmedizin und klassische Naturheilkunde 10 (Suppl. 1), 45–48.

[209] Merfort, I., Heinzmann, B., Flores, E., Bittencourt, C., Schmidt, C., Geller, F., Goettert, M., Laufer, S., 2007. Biological active compounds from Brazilian traditional medicinal plants. Poster at 3. Deutsch-Brasilianisches Symposium.

[210] Middleton, E. M., Teramura, A. H., 1993. The role of flavonol glycosides and carotenoids in protecting soybean from ultraviolet-b damage. Plant Physiology 103, 741–752.

[211] Miklos, E. J., Botz, L., Horvath, G., Farkas, A., Dezso, G., Szabo, L. G., 2001. Atropine and scopolamine in leaf and flower of *Datura arborea* L. International Journal of Horticultural Science Hungary 72, 61–64.

[212] Miralles, J., Noba, K., Bassene, E., 1989. Chimiotaxonomie des Borraginaceae: Composition en acides gras et stérols des feuilles de quelques espéces appartenant aux genres *Cordia et Heliotropium*. Herba hungarica 2, 7–12.

[213] Moir, M., Thomson, R., 1973. A new cinnamaldehyde from *Patagonula americana*. Phytochemistry 12, 2501– 2503.

[214] Moir, M., Thomson, R. H., 1973. Naturally occurring quinones. Part XXIII. Cordiachromes from *Patagonula americana* L. Journal of the Chemical Society Perkin Transactions 1, 1556 – 1561.

[215] Montes, M., Tagieva, N. E., Heveker, N., Nahmias, C., Baleux, F., Trautmann, A., 2000. SDF-1-induced activation of ERK enhances HIV-1 expreession. European Cytokine Network 11, 470–477.

[216] Mosmann, T., 1983. Rapid colorimetric assay for cellular growth and survival: application to proliferation and cytotoxicity assays. Journal of Immunological Methods 65, 55–63.

[217] Murata, T., Watahiki, M., Tanaka, Y., Miyase, T., Yoshizaki, F., 2010. Hyaluronidase inhibitors from Takuran, *Lycopus lucidus*. Chemical & Pharmaceutical Bulletin 58, 394–397.

[218] Muthusamy, V., Piva, T., 2010. The UV response of the skin: a review of the MAPK, NF-κB and TNF-α signal transduction pathways. Archives of Dermatological Research 302, 5– 17.

[219] Muzitano, M. F., Tinoco, L. W., Guette, C., Kaiser, C. R., Rossi-Bergmann, B., Costa, S. S., 2006. The antileishmanial activity assessment of unsual flavonoids from *Kalanchoe pinnata*. Phytochemistry 67, 2071–2077.

[220] Mwangi, E. S. K., Keriko, J. M., Machocho, A. K., Wanyonyi, A. W., H. M. Malebo, S. C. C., Tarus, P. K., 2010. Antiprotozoal activity and cytotoxicity of metabolites from leaves of *Teclea trichocarpa*. Journal of Medicinal Plants Research 4, 726–731.

[221] Nakamura, N., Kojima, S., Lim, Y. A., Meselhy, M. R., Hattori, M., Gupta, M. P., Correa, M., 1997. Dammarane-type triterpenes from *Cordia spinescens*. Phytochemistry 46, 1139–1141.

[222] Nath, P., Eynott, P., Leung, S., Adcock, I. M., Bennett, B. L., Chung, K. F., 2005. Potential role of c- jun NH2- terminal kinase in allergic airway inflammation and remodelling: Effects of SP600125. European Journal of Pharmacology 506, 273– 283.

[223] Nathan, C., 2002. Points of control in inflammation. Nature 420, 846–852.

[224] Nencini, C., Cavallo, F., Bruni, G., Capasso, A., Feo, V. D., Martinob, L. D., Giorgia, G., Micheli, L., 2006. Affinity of *Iresine herbstii* and *Brugmansia arborea* extracts on different cerebral receptors. Journal of Ethnopharmacology 105, 352–357.

[225] Oliveira, R. B., Godoy, S. A. P., Costa, F. B., 2003. Plantas Tóxicas - Conhecimento e Prevencão de Acidentes. Holos.

[226] Olmstead, R., Bohs, L., 2007. A summary of molecular systematic research in Solanaceae: 1982-2006. In: ISHS Acta Horticulturae. No. 745. pp. 255–268.

[227] Otto, I. M., Raabe, T., Rennefahrt, U. E., Bork, P., Rapp, U. R., Kerkhoff, E., 2000. The p150-Spir protein provides a link between c-Jun N-terminal kinase function and actin reorganization. Current Biology 10, 345–348.

[228] Otuki, M. F., Ferreira, J., Lima, F. V., Meyre-Silva, C., Malheiros, A., Muller, L. A., Cani, G. S., Santos, A. R. S., Yunes, R. A., Calixto, J. B., 2005. Antinociceptive properties of mixture of alpha-amyrin and beta-amyrin triterpenes: Evidence for participation of protein kinase C and protein kinase a pathways. Journal of Pharmacology and Experimental Therapeutics 313, 310–318.

[229] Palladino, M., Bahjat, F. R., Theodorakis, E. A., Moldawer, L. L., 2003. Anti-TNF-α therapies: The next generation. Nature Reviews/ Drug Discovery 2, 736–746.

[230] Park, S.-H., Oh, H.-S., Kang, M.-A., Cho, H., Prasad, J. B., Won, J., Leeb, K.-H., 2007. The structure-activity relationship of the series of non-peptide small antagonists for p56lck SH2 domain. Bioorganic & Medicinal Chemistry 15, 3938–3950.

[231] Parker, A. G., Peraza, G. G., Sena, J., Silva, E. S., Soares, M. C., Furlong, M. R. V. E. B., Muccillo-Baisch, A. L., 2007. Antinociceptive effects of the aqueous extract of *Brugmansia suaveolens* flowers in mice. Biological Research For Nursing 8, 234–239.

[232] Patwardhan, B., January 2009. Drug discovery and development: Traditional medicine and ethnopharmacology perspectives. [Online available] http://www.scitopics.com/.

[233] Payne, M., Rossomando, A. J., Martino, P., Erickson, A. K., Her, J.-H., Shabanowitz, J., Donald F. Hunt, M. J. W., Sturgill, T. W., 1991. Identification of the regulatory phosphorylation sites in pp42/mitogen-activated protein kinase (MAP kinase). The EMBO Journal 10, 885–892.

[234] Peake, P. W., Pussell, B. A., Martyn, P., Timmermans, V., Charlesworth, J. A., 1991. The inhibitory effect of rosmarinic acid on complement involves the C5 convertase. International Journal of Immunopharmacology 13, 853–857.

[235] Peng, L. Z. F., Strack, D., Baumert, A., Subramaniam, R., Goh, N. K., Chia, T. F., Tan, S. N., Chia, L. S., 2003. Antioxidant flavonoids from leaves of *Polygonum hydropiper*. Phytochemistry 62, 219–228.

[236] Peters-Golden, M., Henderson, W. R., 2007. Leukotrienes. New England Journal of Medicine 357, 1841–1854.

[237] Petersen, M., Abdullah, Y., Benner, J., Eberle, D., Gehlen, K., Hücherig, S., Janiak, V., Kim, K. H., Sander, M., Weitzel, C., Wolters, S., 2009. Evolution of rosmarinic acid biosynthesis. Phytochemistry 70, 1663–1679.

[238] Petersen, M., Simmonds, M., 2003. Rosmarinic acid. Phytochemistry 62, 121–125.

[239] Phan, T. T., Hughes, M. A., Cherry, G. W., 2001. Effects of an aqueous extract from the leaves of *Chromolaena odorata* (Eupolin) on the proliferation of human keratinocytes and on their migration in an in vitro model of reepithelialization. Wound Repais and Regeneration 9, 305–313.

[240] Phillips, K. M., Ruggio, D. M., Ashraf-Khorassani, M., 2005. Phytosterol composition of nuts and seeds commonly consumed in the United States. Journal of Agricultural and Food Chemistry 53, 9436–9445.

[241] Pickering, J., October 2010. Discover Live.
URL `http://www.discoverlife.org`

[242] PittaAlvarez, S. I., Spollansky, T. C., Giulietti, A. M., 2000. The influence of different biotic and abiotic elicitors on the production and profile of tropane alkaloids in hairy root cultures of *Brugmansia candida*. Enzyme and Microbial Technology 26, 252–258.

[243] Pleschka, S., Wolff, T., Ehrhardt, C., Hobom, G., Planz, O., Rapp, U., 2001. Influenza virus propagation is impaired by inhibition of the Raf/MEK/ERK signalling cascade. Nature Cell Biology 3, 301–305.

[244] Poeckel, D., Greiner, C., Verhoff, M., Rau, O., Tausch, L., Hrnig, C., Steinhilber, D., Schubert-Zsilavecz, M., Werz, O., 2008. Carnosic acid and carnosol potently inhibit human 5-lipoxygenase and suppress pro-inflammatory responses of stimulated human polymorphonuclear leukocytes. Biochemical Pharmacology 76, 91–97.

[245] Pombo, C. M., Bonventre, J. V., Avruch, J., R.Woodgett, J., Kyriakis, J. M., Force, T., 1994. The stress-activated protein kinases are major c-jun amino-terminal kinases activated by ischemia and reperfusion. Journal of Biological Chemistry 269, 26546– 26551.

[246] Preissel, U., Preissel, H.-G., 2002. Brugmansia and Datura: Angel s Trumpets and Thorn Apples. Firefly Books.

[247] Psotová, J., Kolár, M., Sousek, J., Svagera, Z., Vicar, J., Ulrichová, J., 2003. Biological activities of *Prunella vulgaris* extract. Phytotherapy Research 9, 1082–1087.

[248] Qi, M., Elion, E., 2005. MAP Kinase pathways. Journal of Cell Science 118, 3569–3572.

[249] Qiao, C., Zhao, L., Jiang, S., Song, P., 2007. Separation and determination of water soluble active components in *Salvia miltiorrhiza* Bunge and its pharmaceutical preparations by capillary zone electrophoresis with Diode Array Detection. Liquid Chromatography & Related Technologies 30, 2819 – 2833.

[250] Radmark, O., Werz, O., Steinhilber, D., Samuelsson, B., 2007. 5-lipoxygenase: Regulation of expression and enzyme activity. Trends in Biochemical Sciences 32, 332–341.

[251] Raffauf, R. F., 1996. Plant alkaloids: A guide to their discovery and distribution. CRC.

[252] Ranzato, E., Patrone, M., Mazzucco, L., Burlando., B., 2008. Platelet lysate stimulates wound repair of HaCaT keratinocytes. Britsh Journal of Dermatology 159, 537–545.

[253] Rapisarda, A., Ficarra, R., Tommasin, S., Caldbro, M. L., Hungsa, S., 1992. *Cordia francisci*, *Cordia martinicensis*, *Cordia myxa*, *Cordia serratifolia* and *Culmfolia* leaves as new source of routin: analgesic and anti-inflammatory activity. Plant Medica 42, 643.

[254] Rapisarda, A., Ragusa, S., de Pasquale, A., 1993. Hepatotoxic effect of the leaves of some *Cordia species*. In: ISHS Acta Horticulturae.

[255] Rapoport, M., Ferreira, A., 2000. PD98059 prevents neurite degeneration induced by fibrillar beta-amyloid in mature hippocampal neurons. Journal of Neurochemistry 74, 125–133.

[256] Rates, S., 2000. Plants as source of drugs. Toxicon 39, 603–613.

[257] Rhen, T., Cidlowski, J. A., 2005. Antiinflammatory action of glucocorticoids - New mechanisms for old drugs. The New England Journal of Medicine 353, 1711–1723.

[258] Rincon, M., Flavell, R. A., Davis, R. J., 2001. Signal transduction by MAP kinases in T lymphocytes. Oncogene 20, 2490–2497.

[259] Rincon, M., Whitmarsh, A., Yang, D. D., Weiss, L., Derijard, B., Jayaraj, P., David, R. J., Flavel, R. A., 1998. The JNK pathway regulates the in vivo deletion of immature CD4+ CD8+ thymocytes. Journal of Experimental Medicice 188, 1817– 1830.

[260] Rishton, G. M., 2008. Natural products as a robust source of new drugs and drug leads: Past successes and present day issues. The American Journal of Cardiology 101, S43 – S49.
URL `http://www.sciencedirect.com/science/article/B6T10-4SGDVDK-C/2/077a46fa7444569517a59f99d8c4209e`

[261] Roux, P. P., Blenis, J., 2004. ERK and p38 MAPK-activated protein kinases: a family of protein kinases with diverse biological functions. Microbiology and Molecular Biology Reviews 68, 320–344.

[262] Sabapathy, K., Hu, Y., Kallunki, T., Schreiber, M., David, J. P., Jochum, W., Wagner, E. F., karin, M., 1999. JNK2 is required for efficient T-cell activation and apoptosis but not for normal lymphocyte development. Current Biology 9, 116–125.

[263] Saccani, S., Pantano, S., Natoli, G., 2002. p38 dependent marking of inflammatory genes for increased NF-$kappa$B recruitment. Nature Immunology 3, 69–75.

[264] Safayhi, H., Mack, T., Sabieraj, J., Anazodo, M. I., Subramanian, L. R., Ammon, H. T., 1992. Boswellic acids: Novel, specific, nonredox inhibitors of 5-lipoxygenase. Journal of Pharmacology and Experimental Therapeutics 261, 1143–1146.

[265] Sailer, E. R., Schweizer, S., Boden, S. E., Ammon, H. P. T., H.Safayhi, 1998. Characterization of acetyl-11-keto-b-boswellic acid and arachidonate-binding regulatory site of 5-lipoxygenase using photoaffinity labeling. European Journal of Biochemistry 256, 364–368.

[266] Sakita, M., Vallilo, M., 1990. Estudos fitoqu´micos preliminares em espécies florestais do Parque Estadual do Morro do Diabo. Revista do Instituto Florestal 2, 215–226.

[267] Saklatvala, J., 2004. The p38 MAP kinase pathway as a therapeutic target in inflammatory disease. Current Opinion in Pharmacology 4, 372–377.

[268] Scapin, G., Patel, S. B., Lisnock, J., Becker, J. W., LoGrasso, P. V., 2003. The structure of JNK3 in complex with small molecule inhibitors: Structural basis for potency and selectivity. Chemistry & Biology 10, 705–712.

[269] Scarpati, M. L., Oriente, G., 1958. Isolamento e costituzione dell acido rosmarinico (dal *Rosmarinus off.*). Rice Science 28, 2329–2333.

[270] Scett, G., Zwerina, J., Firestein, G., 2008. The p38 mitogen-activated protein kinase (MAPK) pathway in reumathoid arthritis. Annals of the Rheumatic Diseases 67, 909– 916.

[271] Schabath, M. B., Hernandez, L. M., Wu, X., Pillow, P. C., Spitz, M. R., 2005. Dietary phytoestrogens and lung cancer risk. Journal of the American Medical Association 294, 1493–1504.

[272] Schaeffer, H. J., Weber, M. J., 1999. Mitogen-activated protein kinases: Specific messages from ubiquitous messengers. Molecular and Cellular Biology 19, 2435– 2444.

[273] Scheckel, K. A., Degner, S. C., Romagnolo, D. F., 2008. Rosmarinic acid antagonizes activator protein-1-dependent activation of cyclooxygenase-2 expression in human cancer and nonmalignant cell lines. Journal of Nutrition 138, 2098–2105.

[274] Schett, G., Tohidast-Akrad, M., Smolen, J. S., Schimid, B. J., Steiner, C. W., Bitzan, P., Zenz, P., Redlich, K., Xu, Q., Steiner, G., 2000. Activation, differentiall localization and regulation of the stress-activated protein kinases, extracellular signal regulated kinase, c-Jun N-terminal kinase, and p38 mitogen-activated protein kinase, in synovial tissue and cells in rheumatoid arthritis. Arthritis & Rheumatism 43, 2501– 2512.

[275] Schieven, G. L., 2005. The biology of p38 kinase: A central role in inflammation. Current Topics in Medicinal Chemistry 5, 921– 928.

[276] Schindler, J. F., Monahan, J. B., Smith, W. G., 2007. p38 pathway kinases as anti-inflammatoy drug targets. Journal of Dental Research 86, 800– 811.

[277] Schmidt, C., Fronza, M., Goettert, M., Geller, F., Luik, S., Flores, E. M. M., Zanetti, C. B. G. D., Heinzmann, B. M., Laufer, S., Merfort, I., 2009. Biological studies on Brazilian plants used in wound healing. Journal of Ethnopharmacology 122, 523–532.

[278] Schneider, I., Bucar, F., 2005. Lipoxygenase inhibitors from natural plant sources. Part 2: Medicinal plants with inhibitory activity on arachidonate 12-lipoxygenase, 15-lipoxygenase and leukotriene receptor antagonists. Phytotherapy research 19, 263–272.

[279] Schorr, K., 2005. *Smallanthus sonchifolius* (Asteraceae): estudo fitoqu´mico, controle de qualidade e ensaios biológicos. Ph.D. thesis, Universidade de São Paulo.

[280] Schrödinger, 2008. Maestro, version 8.5. LLC, New York, NY.

[281] Schrödinger, 2008. Induced Fit Docking Protocol; Glide version 5.0. Prime version 1.7. LLC, New York, NY.

[282] Schwenger, P., Alpert, D., Skolnik, E., Vilcek, J., 1998. Activation of p38 mitogen activated protein kinase by sodium salicylate leads to inhibition of tumor necrosis factor-induced IkappaB alpha phosphorylation and degradation. Molecular and Cellular Biology 18, 7884.

[283] Sebold, D. F., 2003. Levantamento etnobotânico de plantas de uso medicinal no munic´pio de Campo Bom, Rio Grande do Sul, Brasil. Master s thesis, Universidade Federal do Rio Grande do Sul, 107 p.

[284] Seger, R., Seger, D., Lozeman, F. J., Ahn, N. G., Graves, L. M., Campbell, J. S., Ericsson, L., Harrylock, M., Jensen, A. M., Krebs, E. G., 1992. Human T-cell mitogen-activated protein kinase kinases are related to yeast signal transduction kinases. The Journal of Biological Chemistry 267, 25628– 25631.

[285] Sekula, B. C., Nes, W. R., 1980. The identification of cholesterol and other steroids in *Euphorbia pulcherimma*. Phytochemistry 19, 1509–1512.

[286] Selloum, L., Bouriche, H., Tigrine, C., Boudoukh, C., 2003. Anti-inflammatory effect of rutin on rat paw oedema, and on neutrophils chemotaxis and degranulation. Experimental and Toxicologic Pathology 54, 313–318.

[287] Semones, M., Feng, Y., Johnson, N., Adams, J. L., Winkler, J., Hansbury, M., 2007. Pyridinylimidazole inhibitors of Tie2 kinase. Bioorganic & Medicinal Chemistry Letters 17, 4756–4760.

[288] Senderowicz, A. M., 1999. Flavopiridol: The first cyclin-dependent kinase inhibitor in human clinical trials. Investigational New Drugs 17, 313–320.

[289] Serhan, C. N., Chiang, N., Dyke, T. E. V., 2008. Resolving inflammation: Dual anti-inflammatory and pro-resolution lipid mediators. Nature Reviews Immunology 8, 349–361.

[290] Sertié, J., Woisky, R., Wiezel, G., Rodrigues, M., 2005. Pharmacological assay of *Cordia verbenacea* V: Oral and topical anti-inflammatory activity, analgesic effect and fetus toxicity of a crude leaf extract. Phytomedicine 12, 338–344.

[291] Shakhov, A. N., Collart, M. A., Vassalli, P., Nedospasov, A., Jongeneel, C. V., 1990. kB-Type enhancers are involved in lipopolysaccharide-mediated transcriptional activation of the tumor necrosis factor a gene in primary macrophages. Journal of Experimental Medicine 171, 35–47.

[292] Siedle, B., Hrenn, A., Merfort, I., 2007. Natural compounds as inhibitors of human neutrophil elastase. Planta Medica 73, 401–420.

[293] Siemoneit, U., 2009. Anti-inflammatory actions of boswellic acids: Identification and critical evaluation of molecular targets and signaling pathways. Ph.D. thesis, University of Tübingen.

[294] Simoes, C. M. O., Mentz, L. A., Schenkel, E. P., Irgang, B. E., Stehmann, J. R., 1986. Plantas da medicina popular no Rio Grande do Sul/Medicinal plants in Rio Grande do Sul. Universidade Federal do Rio Grande do Sul.

[295] Sluss, H. K., Barret, T., Derijard, B., Davis, R. J., 1994. Signal transduction by tumor necrosis factor mediated by JNK protein kinases. Molecular and Cellular Biology 14, 8376– 8384.

[296] Smith, G. J., Markham, K. R., 1998. Tautomerism of flavonol glucosides: relevance to plant UV protection and flower colour. Journal of Photochemistry and Photobiology A: Chemistry 118, 99–105.

[297] Smith, L., 1970. Boragináceas. Tech. rep., Itaja: Herbrio Barbosa Rodrigues.

[298] Soberman, R. J., Christmas, P., 2003. The organization and consequences of eicosanoid signaling. Journal of Clinical Investigation 111, 1107–1113.

[299] Steele, V. E., Holmes, C. A., Hawk, E. T., Kopelovich, L., Lubet, R. A., Crowell, J. A., Sigman, C. C., Kelloff, G. J., 1999. Lipoxygenease inhibitors as potential cancer chemopreventives. Cancer Epidemiology, Biomarkers & Prevention 8, 467–483.

[300] Steinhilber, D., 1999. 5-lipoxygenase: a target for antiinflammatory drugs revisited. Current Medicinal Chemistry 6, 69–83.

[301] Stobiecki, M., 2000. Application of mass spectrometry for identification and structural studies of favonoid glycosides. Phytochemistry 54, 237–256.

[302] Stobiecki, M., Malosse, C., Kerhoas, L., Wojlaszek, P., Einhorn, J., 1999. Detection of isoflavonoids and their glycosides by liquid chromatography/electrospray ionization mass spectrometry in root extracts of lupin (*Lupinus albus*). Phytochemical Analysis 10, 198 – 207.

[303] Sudhamalla, B., Gokara, M., Ahalawat, N., Amooru, D. G., Subramanyam, R., 2010. Molecular dynamic/simulation and binding studies of β-sitosterol with human serum albumin and its biological relevance. Journal of Physical Chemistry 114, 9054–9062.

[304] Swahn, B. M., Huerta, F., Kallin, E., Malmstroem, J., Weigelt, T., Viklund, J., Womack, P., Xue, Y., Oehberg, L., 2005. Design and synthesis of 6-anilinoindazoles as selective inhibitors of c-Jun N-terminal kinase-3. Bioorganic & Medicinal Chemistry Letters 15, 5095–5099.

[305] Swarup, V., Ghosh, J., Ghosh, S., Saxena, A., Basu, A., 2007. Anti-viral and anti-inflammatory effects of rosmarinic acid in an experimental murine model of *Japanese encephalitis*. Antimicrobial Agents and Chemotherapy 51, 3367–3370.

[306] Taroda, N., Gibbs, P., 1987. Studies on the genus *Cordia* L. Boraginaceae in Brazil. An outline taxonomic revision of subgenus *Myxa Taroda*. Hoehnea 14, 31–52.

[307] Terrazul, 2006. O Brasil e a Convencão sobre Diversidade Biológica.
URL `http://www.terrazul.m2014.net/spip.php?article277`

[308] Thirupathi, K., Kumar, S., Raju, V., Ravikumar, B., Krishna, D., G.K.Mohan, 2008. A review of medicinal plants of the genus Cordia: Their chemistry and pharmacological uses. Journal of Natural Remedies 8, 1–10.

[309] Tian, X.-Y., Wang, Y.-H., Liu, H.-Y., Yu, S.-S., Fang, W.-S., 2007. On the chemical constituents of *Dipsacus asper*. Chemical & Pharmaceutical Bulletin 12, 1677–1681.

[310] Ticlia, F. K., Hagea, L. I., Cambraia, R. S., Pereira, P. S., Magro, A. J., Fontes, M. R., Stábelid, R. G., Giglioe, J. R., Franca, S. C., Soares, A. M., 2005. Rosmarinic acid, a new snake venom phospholipase A2 inhibitor from *Cordia verbenacea* (Boraginaceae): Antiserum action potentiation and molecular interaction. Toxicon 46, 318–327.

[311] Tong, L., Pav, S., White, D. M., Rogers, S., Crane, K. M., Cywin, C. L., Brown, M. L., Pargellis, C. A., 1997. A highly specific inhibitor of human p38 MAP kinase binds in the ATP pocket. Nature Structural Biology 4, 311– 316.

[312] Tóth, J., Mrlianová, M., Tekelóvá, D., Korenová, M., 2003. Rosmarinic acid: an important phenolic active compound of Lemon Balm (*Melissa of cinalis* L.). Acta Facultatis Pharmaceuticae Universitas Comenianae 3, 139–145.

[313] Tournier, C., Dong, C., Turner, T. K., Jones, S. N., Flavell, R. A., Davis, R. J., 2001. MKK7 is an essential component of the JNK signal transduction pathway activated by proinflammatory cytokines. Genes & Development 15, 1419–1426.

[314] Traxler, P., Furet, P., 1999. Strategies toward the design of novel and selective proteins tyrosine kinase inhibitors. Pharmacology & Therapeutics 82, 195– 206.

[315] Trompezinski, S., Denis, A., Schmitt, D., Viac, J., 2003. Comparative effects of polyphenols from green tea (EGCG) and soybean (genistein) on VEGF and IL-8 release from normal human keratinocytes stimulated with the proinflammatory cytokine TNF alpha. Archives of Dermatological Research 295, 112–116.

[316] Troy, C. M., Rabacchi, S. A., Xu, Z., Maroney, A. C., Connors, T. J., Shelanski, M. L., Greene, L. A., 2001. Beta-amyloid-induced neuronal apoptosis requires c-Jun N-terminal kinase activation. Journal of Neurochemistry 77, 157– 164.

[317] Trusheva, B., Popova, M., Bankova, V., Simova, S., Marcucci, M. C., Miorin, P. L., da Rocha Pasin, F., Tsvetkova, I., 2006. Bioactive constituents of Brazilian red propolis. Evidence-based on Complementary and Alternative Medicine 3, 249–254.

[318] Trute, A., Nahrstedt, A., 1996. Separation of rosmarinic acid enantiomers by three different chromatographic methods (HPLC, CE, GC) and the determination of rosmarinic acid in *Hedera helix* L. Phytochemical Analysis 7, 204 –208.

[319] Vaudano, E., Rosenblad, C., Bjorklund, A., 2001. Injury induced c-jun expression and phosphorylation in the dopaminergicnigral neurons of the rat: correlation with neuronal death and modulation by glial-cell-line-derived neurotrophic factor. European Journal of Neuroscience 13, 1–14.

[320] Velde, V. V., Lavie, D., Zelnik, R., Matida, A. K., Panizza, S., 1982. Cordialin A and B, two new triterpenes from *Cordia verbenacea* DC. Journal of the Chemical Society Perkin Transactions 1, 2697 – 2700.

[321] Vitor, C. E., Figueiredo, C. P., Hara, D. B., Bento, A. F., Mazzuco, T. L., Calixto, J. B., 2009. Therapeutic action and underlying mechanisms of a combination of two pentacyclic triterpenes, alfa and beta-amyrin, in a mouse model of colitis. British Journal of Pharmacology 157, 1034–1044.

[322] Wada, T., Nakagawa, K., Watanabe, T., Nishitai, G., Seo, J., Kishimoto, H., Kitagava, D., Sasaki, T., Penninger, J. M., Nishina, H., 2001. Impaired synergistic activation of stress-activated protein kinase SAPK/JNK in mouse embryonic stem cells lacking SEK1/MKK4: different contribution of SEK2/MKK7 isoforms to the synergic activation. Journal of Biological Chemistry 276, 30892–30897.

[323] Walle, T., 2004. Absorption and metabolism of flavonoids. Free Radical Biology & Medicine 36, 829–837.

[324] Wang, Y., Ohtani, K., Kasai, R., Yamasaki, K., 1996. Flavonol glycosides and phenolics from leaves of *Cordia dichotoma*. Natural Medicines 50, 367.

[325] Wang, Y., Su, B., Sah, V. P., Brown, J. H., Han, J., Chien, K. R., 1999. Cardiac hipertrophy induced by mitogen-activated protein kinase kinase 7, a specific activator for c-jun NH2-terminal kinase in ventricular muscle cells. Journal of Biological Chemistry 6, 987– 991.

[326] Wang, Z., Canagarajah, B. J., Boehm, J. C., Kassis, S., Cobb, M. H., Young, P. R., Abdel-Meguid, S., Adams, J. L., Goldsmith, E. J., 1998. Structural basis of inhibitor selectivity in MAP kinases. Structure 6, 1117–1128.

[327] Wang, Z. J., Zhao, Y. Y., Wang, B., AI, T. M., Chen, Y. Y., 2000. Depsides from *Prunella vulgaris*. Chinese Chemical Letters 11, 997–1000.

[328] Werner, S., Grose, R., 2003. Regulation of wound healing by growth factors and cytokines. Physiological Reviews 83, 835–870.

[329] Werz, O., 2002. 5-lipoxygenase: Cellular biology and molecular pharmacology. Current Drugs Targets-Inflammation & Allergy 1, 23–44.

[330] Werz, O., 2007. Inhibition of 5-lipoxygenase product synthesis by natural compounds of plant origin. Planta Medica 73, 1331–1357.

[331] Werz, O., Burkert, E., Samuelsson, B., Radmark, O., Steinhilber, D., 2002. Activation of 5-lipoxygenase by cell stress is calcium independent in human polymorphonuclear leukocytes. Blood 99, 1044–1052.

[332] Werz, O., Klemm, J., Samuelsson, B., Radmark, O., 2000. 5-lipoxygenase is phosphorylated by p38 kinase-dependent MAPKAP kinases. Proceedings of the National Academy of Sciences 97, 5261–5266.

[333] Werz, O., Steinhilber, D., 2005. Development of 5-lipoxygenase inhibitors-lessons from cellular enzyme regulation. Biochemical Pharmacology 70, 327–333.

[334] Werz, O., Tretiakova, I., Michel, A., Ulke-Lemee, A., Horning, M., Franke, L., 2005. Caspase-mediated degradation of human 5-lipoxygenase in β lymphocytic cells. Proceedings of the National Academy of Sciences 102, 13164–13169.

[335] Weston, C. R., Davis, R. J., 2002. The JNK signal transduction pathway. Current Opinion in Genetics & Development 12, 14–21.

[336] Westra, J., Limburg, P. C., 2006. p38 mitogen-activated protein kinase (MAPK) in rheumatoid artthritis. Mini-Reviews in Medicinal Chemistry 6, 867– 874.

[337] Wettasinghe, M., Shahidi, F., Amarowicz, R., Abou-Zaid, M. M., 2001. Phenolic acids in defatted seeds of borage (*Borago of cinalis* L.). Food Chemistry 75, 49–56.

[338] Wilson, K. P., Fitzgibbon, M. J., Caron, P. R., Griffith, J. P., Chen, W., McCaffrey, P. G., Chambers, S. P., Su, M. S. S., 1996. Crystal structure of p38 mitogen-activated protein kinase. Journal of Biological Chemistry 271, 27696– 27700.

[339] Wilson, K. P., McCaffrey, P. G., Hsiao, K., Pazhinisamy, S., Galullo, V., Bemis, G. W., Fitzgibbon, M. J., Caron, P. R., Murcko, M. A., Su, M. S. S., 1997. The structural basis for the specificity of pyridinylimidazole inhibitors of p38 MAPK. Chemistry & Biology 4, 423– 431.

[340] Woo, E.-R., Piao, M. S., 2004. Antioxidative constituents from *Lycopus lucidus*. Archives of Pharmacal Research 27, 173–176.

[341] Wu, J., Harrison, J. K., Vincent, L. A., Haystead, C., Haystead, T. A., Michel, H., Hunt, D. F., Lynch, K. R., Sturgill, T. W., 1993. Molecular structure of a protein-tyrosine/threonine kinase activating p42 mitogen-activated protein (MAP) kinase: MAP kinase kinase. Proceedings of the National Academy of Sciences 90, 173–177.

[342] Wu, L., Qiao, H., Lib, Y., Li, L., 2007. Protective roles of puerarin and Danshensu on acute ischemic myocardial injury in rats. Phytomedicine 14, 652–658.

[343] Xia, X. G., Harding, T., Weller, M., Bieneman, A., Uney, J. B., Schulz, J. B., 2001. Gene transfer of the JNK interacting protein-1 protects dopaminergic neurons in the MPTP model of Parkinsons disease. Proceedings of the National Academy of Sciences of the United States of America 98, 10433– 10438.

[344] Xia, Z., Dickens, M., Raingeaud, J., Davis, R. J., Grenberg, M. E., 1995. Opposing effects of ERK and JNK-p38 MAP kinases on apoptosis. Science 270, 1326– 1331.

[345] Xiao, J., Cao, H., Wang, Y., Zhao, J., Wei, X., 2009. Glycosylation of dietary flavonoids decreases the affinities for plasma protein. Journal of Agricultural and Food Chemistry 57, 6642–6648.

[346] Yamamoto, H., Sakakibar, J., Nagatsu, A., Sekiya, K., 1998. Inhibitors of arachidonate lipoxygenase from defatted *Perilla seed*. Journal of Agricultural and Food Chemistry 46, 862–865.

[347] Yokot, T., Nomur2, T., Nakayama, M., 1997. Identification of brassinosteroids that appear to be derived from campesterol and cholesterol in tomato shoots. Plant and Cell Physiology 38, 1291–1294.

[348] Youn, J., Lee, K.-H., Won, J., Huh, S.-J., Yun, H.-S., Cho, W.-G., Paik, D.-J., 2003. Beneficial effects of rosmarinic acid on suppression of collagen induced arthritis. Journal of Rheumatology 6, 1203–1207.

[349] Yuan, J.-C., Han, G.-Z., Yao, J.-H., Li, L., Yuan, J., Su, C.-Y., 2006. Simultaneous determination of danshensu, protocatechuic acid, protocatechuic aldehyde and salvinolic acid B in plasma of *Salvia miltiorrhiza* injection. Asian Journal of Pharmacodynamics and Pharmacokinetics 6, 231–234.

[350] Zayed, R., Wink, M., 2004. Induction of tropane alkaloid formation in transformed root cultures of *Brugmansia suaveolens* (Solanaceae). Zeitschrift fr Naturforschung 59, 863–867.

[351] Zee, K. J. V., Kohno, T., Fischer, E., Rock, C. S., Moldawer, L. L., Lowry, S. F., 1992. Tumor necrosis factor soluble receptors circulate during experimental and clinical inflammation and can protect against excessive tumor necrosis factor α *in vitro* and *in vivo*. Proceedings of the National Academy of Sciences 89, 4845– 4849.

[352] Zhu, M., Fu, Y., 2010. The complicated role of NF-κB in T-cell selection. Cellular and Molecular Immunology 7, 89–93.

[353] Zu, Y., Qi, J., Gilchrist, A., Fernandez, G. A., Vazquez-Abad, D., Kreutzer, D. L., Huang, C.-K., Shaafi, R. I., 1998. p38 mitogen-activated protein kinase activation is required for human neutrophil function triggered by TNF-α or FMLP stimulation. Journal of Immunology 160, 1982–1989.